

285

# AIRCRAFT PROPELLER DESIGN

BY

FRED E. WEICK, B.S.

*Aeronautical Engineer, Langley Memorial Aeronautical Laboratory,  
National Advisory Committee for Aeronautics; Member,  
Society of Automotive Engineers*

FIRST EDITION  
ELEVENTH IMPRESSION

McGRAW-HILL BOOK COMPANY, Inc.

NEW YORK AND LONDON

1930

7539

430

COPYRIGHT, 1930, BY THE  
MCGRAW-HILL BOOK COMPANY, INC.

PRINTED IN THE UNITED STATES OF AMERICA

*All rights reserved. This book, or  
parts thereof, may not be reproduced  
in any form without permission of  
the publishers.*



## PREFACE

Great strides have been made in propeller design during the past decade, and it is the object of this book to collect in one volume the important experimental, theoretical, and practical developments and to present them in a simple, usable manner. The various factors have been considered not only from the point of view of propeller performance and efficiency but also directly in terms of the effect on airplane performance.

It is hoped that the work brings out clearly the dominating influence which the airplane and engine designers have on the propulsive efficiency obtained, due to their control of the conditions under which the propeller must operate. In this connection it is thought that certain chapters, such as that on the desirability of gearing, should be of at least as great interest to airplane designers as to propeller designers.

The writer has spent the past several years in experimenting with and designing propellers, which is his justification for attempting this work. His first work of this nature was as propeller designer for the Bureau of Aeronautics, Navy Department. He was then transferred to the staff of the National Advisory Committee for Aeronautics, where he was in charge of the Twenty Foot Propeller Research Tunnel. Following this, as chief engineer of the Hamilton Aero Manufacturing Company, he had an opportunity to apply practically the experimental results and to check them by means of flight tests. He has been particularly fortunate in regard to this work in that, being engaged in research work on the staff of the National Advisory Committee for Aeronautics, experimental results were available to him as soon as the tests were completed. This has given him an opportunity to include the latest developments, and in this connection the friendly attitude of the N.A.C.A. officials has been of great help.

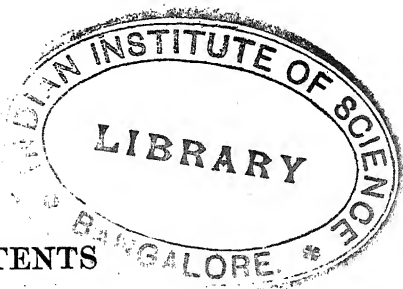
Valuable suggestions in regard to the material to be included were received from Mr. Edward P. Warner, now editor of *Avia-*

gan, and Prof. E. G. Reid of Stanford University. Acknowledgment is also due to Dr. Clark B. Millikan and Dr. A. L. Klein of California Institute of Technology and to Mr. Donald H. Wood and Mr. John Stack, the author's associates at the Langley Memorial Aeronautical Laboratory, all of whom checked and made helpful criticisms of portions of the material. The author is also indebted to his wife for revision of the manuscript.

FRED E. WEICK.

LANGLEY FIELD, VA.,  
*September, 1930.*





## CONTENTS

	PAGE
PREFACE. . . . .	v
CHAPTER I	
INTRODUCTION . . . . .	1
Propeller terminology.	
CHAPTER II	
THE MOMENTUM THEORY. . . . .	5
The simple momentum or Froude theory—Ideal efficiency.	
CHAPTER III	
THE AIRFOIL. . . . .	11
Fluid resistance and dynamical similarity—The aerodynamic forces on airfoils—Coefficients and methods of plotting—Effect of variations in the shape of airfoils—Elementary airfoil theory—Airfoil sections suitable for propellers.	
CHAPTER IV	
THE SIMPLE BLADE-ELEMENT THEORY . . . . .	37
The air forces on a blade element—The efficiency of an element—Limitations of the simple theory—Example of analysis with blade-element theory.	
CHAPTER V	
MODIFICATIONS OF THE BLADE-ELEMENT THEORY . . . . .	51
The combined or inflow theory—The blade-element theory with multiplane interference corrections—Example with multiplane interference corrections—The induction or vortex theory—Example with vortex theory—Résumé, and comparison of various theories.	
CHAPTER VI	
AERODYNAMIC TESTS ON PROPELLERS. . . . .	82
Flight tests—Wind tunnel tests—Coefficients and methods of plotting results—The flow of air through a propeller.	

## CHAPTER VII

THE EFFECT OF TIP SPEED ON PROPELLER PERFORMANCE . . . . .	119
Tests on model airfoils at high speed—Tests on model propellers at high tip speeds—Tests on full-scale propellers at high tip speeds—Practical data for finding efficiency at high tip speeds.	

## CHAPTER IX

BODY AND PROPELLER INTERFERENCE . . . . .	136
Expressions for efficiency with a body—Effect of body size, shape, and drag—Comparison of tractor and pusher arrangements—Practical use of body interference data.	

## CHAPTER X

THE EFFECT OF PROPELLER CHARACTERISTICS ON AIRPLANE PERFORMANCE . . . . .	159
Effect of propeller characteristics on speed, climb, take-off, cruising performance, range, and endurance—Effect on performance at high altitudes, with ordinary and with supercharged engines.	

## CHAPTER XI

THE VARIABLE-PITCH PROPELLER. . . . .	180
Effect on speed, climb, take-off, and cruising performance of airplanes with unsupercharged engines—Performance with variable-pitch propellers and supercharged engines.	

## CHAPTER XII

THE GEARING OF PROPELLERS . . . . .	190
Example in which gearing greatly improves the performance—Example in which the performance is poorer with gearing than with direct drive—Method of determining whether or not gearing is desirable.	

## CHAPTER XIII

TANDEM PROPELLERS. . . . .	201
Calculation of operating conditions and air forces on rear propeller—Model tests with tandem propellers—Method of dealing with tandem propellers in which each propeller is treated as a complete unit, with examples.	

## CHAPTER XIV

MATERIALS AND FORMS OF CONSTRUCTION . . . . .	213
Propellers constructed of wood, micarta, steel, and aluminum alloy—The construction of variable-pitch propellers.	

## CHAPTER XV

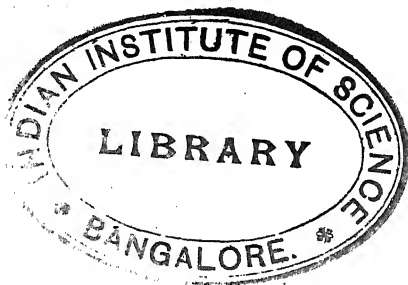
THE STRENGTH OF PROPELLERS . . . . .	229
Calculation of stresses—Approximate method of stress analysis—	
Example showing approximate stress analysis—Effect of deflection	
on the stresses—Destructive whirling test.	

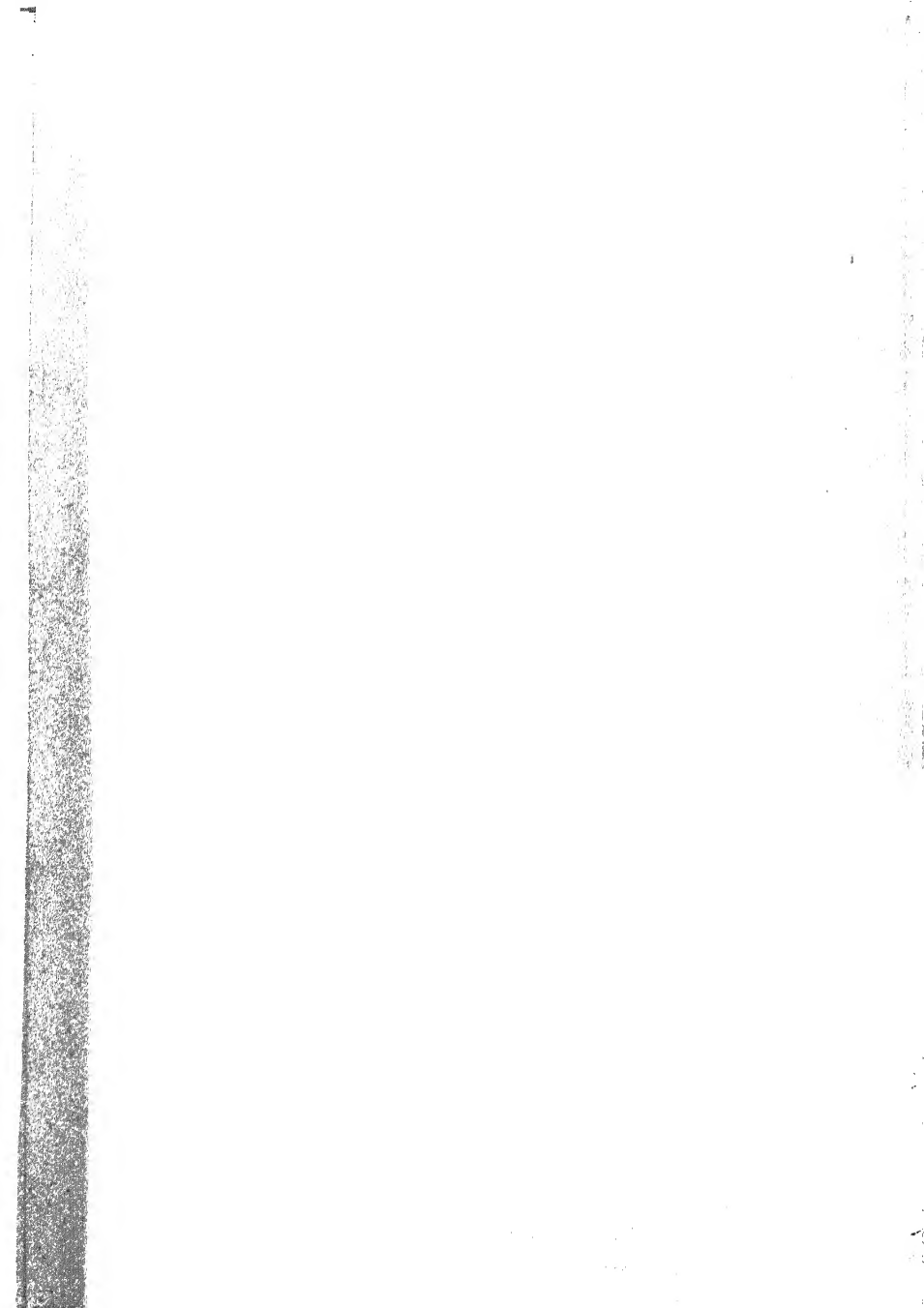
## CHAPTER XVI

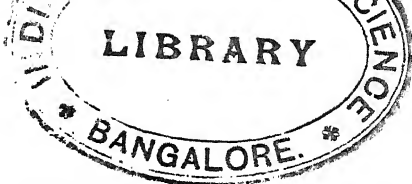
SUMMARY OF FACTORS TO BE CONSIDERED IN THE DESIGN OF A PROPELLER . . . . .	249
The selection of propellers to give the best high speed, climb, take-off, angle of climb, cruising, or all-around performance—Limitations imposed by airplane and engine—Choice of the number of blades—Résumé of factors affecting propulsive efficiency.	

## CHAPTER XVII

DESIGN PROCEDURE, WITH CHARTS AND EXAMPLES . . . . .	257
Information furnished propeller designer—A simple system for selecting propellers of standard form, with examples—Approximate method for propellers of any form, with examples—Design by means of the blade-element theory.	
SYMBOLS. . . . .	285
INDEX. . . . .	289







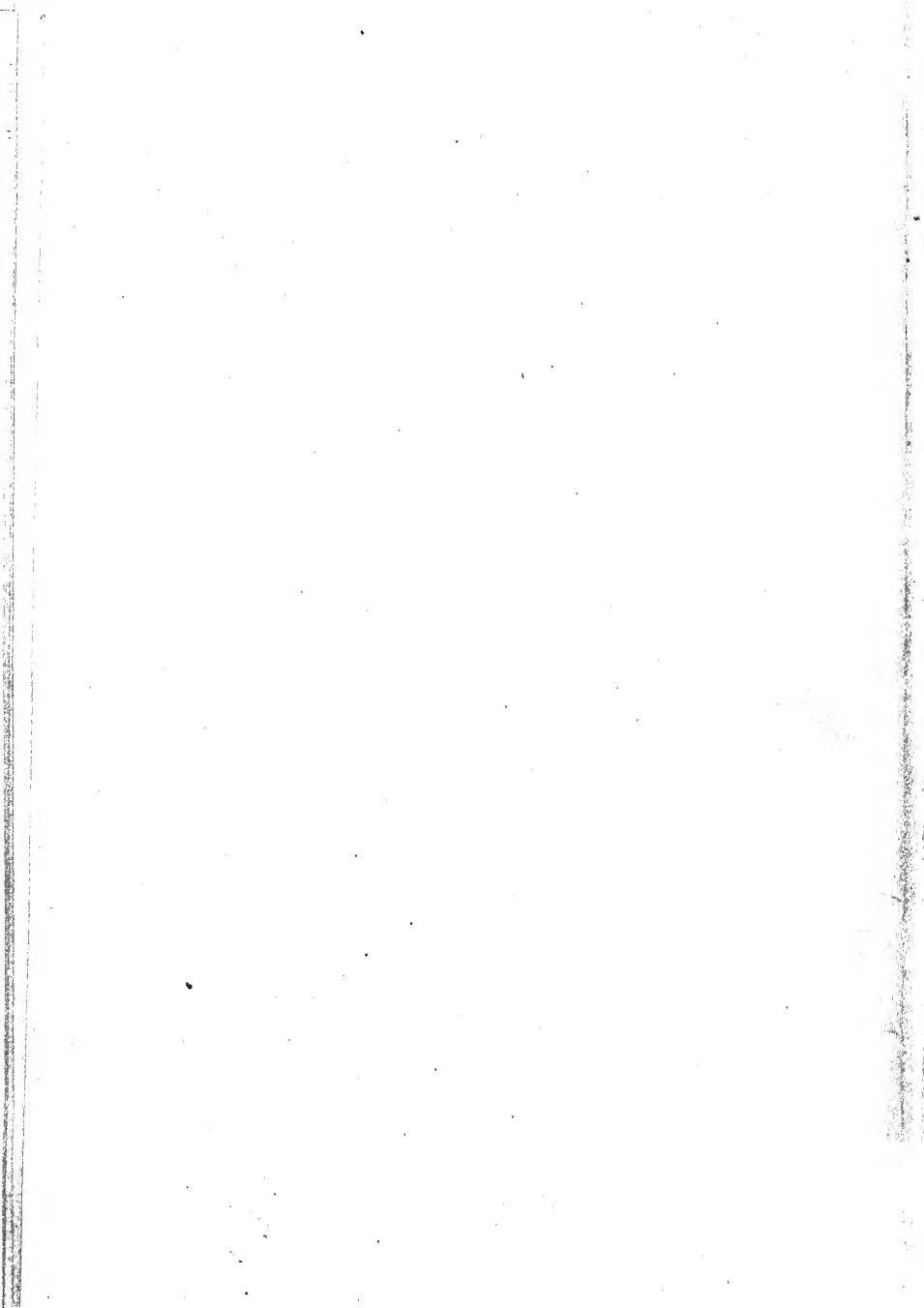
## LIST OF SYMBOLS

- A* Propeller disc area.
- A* Area of section.
- A* Cross-sectional area of wind tunnel air stream.
- a* Slope of lift curve =  $dC_L/d\alpha$ ,  $\alpha$  being in radians.
- a* Inflow velocity factor.
- a'* Rotational interference velocity factor.
- B* Number of blades in a propeller.
- b* Blade width.
- b* Final slipstream or wake-velocity factor.
- c* Chord length of airfoil.
- c* Velocity of sound in air.
- CF* Centrifugal force.
- C.P.* Center of pressure.
- C<sub>a</sub>* German lift coefficient =  $100C_L$ .
- C<sub>w</sub>* German drag coefficient =  $100C_D$ .
- C<sub>L</sub>* Absolute lift coefficient =  $L/qS$ .
- C<sub>D</sub>* Absolute drag coefficient =  $D/qS$ .
- C<sub>D<sub>i</sub></sub>* Induced drag coefficient.
- C<sub>D<sub>0</sub></sub>* Profile drag coefficient =  $C_D - C_{D_i}$ .
- C<sub>M</sub>* Pitching-moment coefficient =  $M/qcS$ .
- C<sub>P</sub>* Power coefficient =  $P/\rho n^3 D^5$ .
- C<sub>Q</sub>* Torque coefficient =  $Q/\rho n^2 D^5$ .
- C<sub>R</sub>* Coefficient of resultant force =  $R/qS$ .
- C<sub>S</sub>* Speed-power coefficient =  $\sqrt[5]{\frac{\rho V^5}{P n^2}}$ .
- C<sub>T</sub>* Thrust coefficient =  $T/\rho n^2 D^4$ .
- C<sub>T'</sub>* Thrust coefficient =  $T/qA$ .
- D* Propeller diameter.
- d* Body diameter.
- D* Drag or air resistance.
- D<sub>c</sub>* Drag coefficient =  $k_D = D/\rho S V^2$ .
- D<sub>i</sub>* Induced drag.
- D<sub>0</sub>* Profile drag.
- EHP* Excess horsepower available over that required for horizontal flight.
- g* Standard acceleration due to gravity = 32.17 ft./sec.<sup>2</sup>
- H* Total pressure head.
- h* Maximum thickness of an airfoil section.
- HP* Power, in horsepower units.
- HP<sub>r</sub>* Horsepower required.
- hp* Horsepower.

- $I$  Moment of inertia.  
 $J$  Slip function  $= V/nD$ .  
 $k_L$  British lift coefficient  $= L/\rho SV^2$ .  
 $k_D$  British drag coefficient  $= D/\rho SV^2$ .  
 $k_T$  British thrust coefficient  $= T/\rho n^2 D^4$ .  
 $k_Q$  British torque coefficient  $= Q/\rho n^2 D^5$ .  
 $K_L$  Engineering lift coefficient  $= L/SV^2$ .  
 $K_D$  Engineering drag coefficient  $= D/SV^2$ .  
 $L$  Representative linear dimension.  
 $L$  Lift.  
 $L$  Lift coefficient  $= k_L = L/\rho SV^2$ .  
 $M$  Pitching moment.  
 $M$  Resultant bending moment.  
 $M_T$  Twisting moment due to air loading.  
 $M_C$  Twisting moment due to centrifugal loading.  
 $M_Q$  Component of air bending moment due to torque.  
 $M_Q'$  Component of centrifugal bending moment in direction of torque.  
 $M_T$  Component of air bending moment due to thrust.  
 $M_T'$  Component of centrifugal bending moment in direction of thrust.  
 $MPH$  Velocity, in miles per hour.  
 $m.p.h.$  Miles per hour.  
 $N$  Revolution speed, in revolutions per minute.  
 $N'$  Equivalent revolution speed of rear propeller of tandem series.  
 $n$  Revolutions per second.  
 $P$  Power.  
 $p$  Pressure.  
 $p$  Pitch, geometrical.  
 $p'$  Pitch at  $0.75R$ .  
 $Q$  Torque.  
 $Q$  Torque coefficient  $= Q/\rho V^2 D^3$ .  
 $QHP$  Torque or brake horsepower.  
 $q$  Dynamic (or impact) pressure  $= \frac{1}{2}\rho V^2$ .  
 $R$  Resistance.  
 $R$  Resultant force.  
 $R$  Aspect ratio  $= \text{span squared divided by area}$ .  
 $R$  Tip radius of propeller blade.  
 $r$  Radius.  
 $RPM$  Revolution speed in revolutions per minute.  
 $r.p.m.$  Revolutions per minute.  
 $S$  Area, wing area.  
 $S$  Nominal slip, where  $1 - S = V/np$ .  
 $S$  Solidity factor  $= 2\pi r/Bb$ .  
 $S$  Stress.  
 $S_c$  Compressive stress.  
 $S_t$  Tensile stress.  
 $T$  Thrust.  
 $T$  Thrust coefficient  $= T/\rho V^2 D^3$ .  
 $THP$  Thrust horsepower.

- TR* Thickness ratio of whole propeller = the thickness ratio of the section at  $0.75R$ .
- TWR* Total width ratio =  $WR \times B$ .
- V* Velocity, usually considered velocity of advance or forward velocity.
- V<sub>r</sub>* Resultant velocity of advance of a blade section.
- V<sub>1</sub>* Axial component of full slipstream velocity =  $V(1 + 2a)$ .
- W* Weight.
- w* Specific weight, lb./cu. in.
- w* Tangential velocity.
- WR* Width ratio of a propeller blade = blade width at  $0.75R$  divided by  $D$ .
- 
- $\alpha$  Angle of attack.
- $\alpha_0$  Angle of attack for infinite aspect ratio.
- $\alpha_i$  Induced angle =  $\epsilon/2$ .
- $\beta$  Blade angle.
- $\beta'$  Blade angle at  $0.75R$ .
- $\gamma$  Angle between lift and resultant force vectors of an airfoil, where  $\tan \gamma = D/L$ .
- $\epsilon$  Angle of downwash.
- $\eta$  Efficiency.
- $\theta$  Interference angle.
- $\nu$  Kinematic viscosity.
- $\rho$  Air density, mass per unit volume.
- $\rho_0$  Mass density of standard air at sea level = 0.002378 slugs per cu. ft.
- $\phi$  Angle between direction of motion of a blade element and the plane of rotation, where  $\tan \phi = V/2\pi r n$ .
- $\omega$  Angular velocity.









# AIRCRAFT PROPELLER DESIGN

## CHAPTER I

### INTRODUCTION

A propeller is a device for providing a force or thrust, at the expense of power generated by a motor, for driving a craft of some type through a fluid medium, such as air or water. In order to provide this thrust, the propeller must set a mass of the fluid in motion in a direction opposite to that of the craft being propelled.

While many types of propellers, including paddle wheels and various feathering blade devices, have been proposed and in some cases used, the screw propeller has been universally adopted for aircraft propulsion. The air screw propeller, as its name implies, screws or twists its way through the air, advancing as it turns, and moving the aircraft with it. The force which drives the aircraft is the reaction obtained because the propeller has pushed a certain mass of air backward. The backward-moving air, called the slipstream, has kinetic energy due to its motion, and this energy represents a loss. There are also other losses, one being that due to the friction of the air on the blades. The useful or thrust power developed by the propeller is therefore less than the power delivered by the engine to the propeller, and one of the most important aims of the propeller designer is to obtain a high ratio of useful power to engine power or, in other words, a high propulsive efficiency.

Aircraft propellers are nearly always driven by internal-combustion engines, and each design of engine develops its power most satisfactorily at some definite speed of revolution. A propeller, therefore, should not only be efficient but should also be designed to absorb the power of the engine at the correct revolution speed.

In addition to its aerodynamic qualities, a propeller must have sufficient strength to be safe and reliable. The attainment of sufficient strength and resistance to fatigue for safety is a stumbling block in the designing of propellers having radical or unusual shapes or constructions but is relatively simple if standard proved forms are adhered to.

**Propeller Terminology.**<sup>1</sup>—The term **propeller** is used almost universally in this country, whereas the word *airscrew* (or its equivalent in French or German) is used in Great Britain,

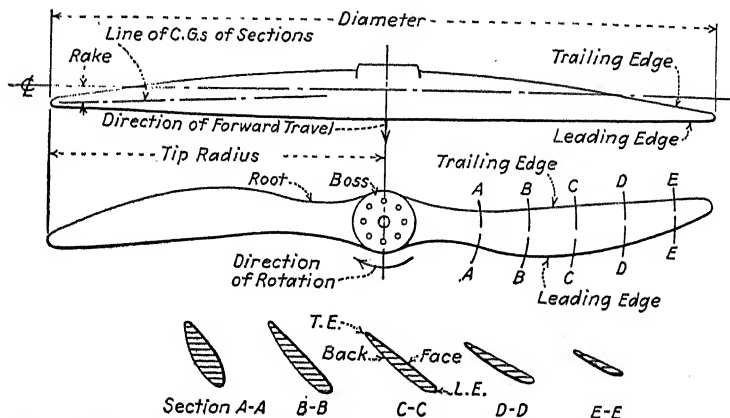


FIG. 1.—Typical wood propeller and some terms which apply to propellers.

Germany, and France. From the propulsion point of view, propeller seems the more fundamental term, but on the other hand it may be said that the propeller operating in air is just one form of airscrew, other types being the fan, the windmill, and the anemometer. Either term is satisfactory, but the American practice of using the term propeller is adhered to in this book.

The **diameter**  $D$  of a propeller is the diameter of the circle swept by the blade tips, or the distance between the tips (Fig. 1).

The **pitch** of any screw is the advance per revolution. A propeller of fixed geometrical form, since it operates in a fluid,

<sup>1</sup> A complete nomenclature for aeronautics including propellers is given in *Technical Report 240* of the National Advisory Committee for Aeronautics (hereafter abbreviated to N.A.C.A.T.R., also the Reports and Memoranda of the British Advisory Committee for Aeronautics and its successor, the Aeronautical Research Committee, are abbreviated to British *R. and M.*), 1927, and many of the definitions in this chapter are taken directly therefrom.

may have a variety of forward speeds at the same revolution speed, so that the pitch, in the usual sense, is not fixed. The **advance per revolution**, however, is of fundamental importance in propeller operation and is called the **effective pitch** (Fig. 2).

There are two other kinds of pitch which are generally used in connection with propellers: the geometrical pitch, and the experimental pitch. These forms of pitch are not necessarily constant along the radius of a propeller but may vary from section to section. The **geometrical pitch**  $p$  of an element of a propeller is the distance which the element would advance along the axis of rotation in one revolution, if it were moving along a helix having an angle equal to its blade angle (Fig. 2.). The **nominal or standard geometrical pitch** of a whole propeller is the

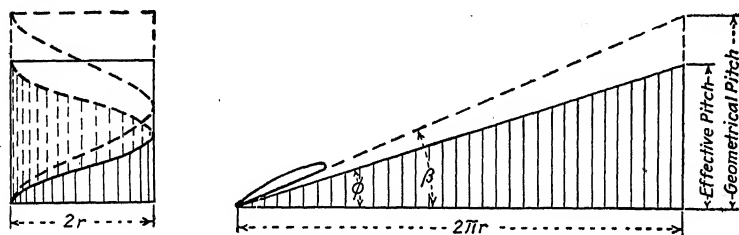


FIG. 2.—Illustration of effective and geometrical pitch.

pitch of the section at two-thirds of the radius. If all of the elements of a propeller have the same geometrical pitch, the propeller is said to have **uniform geometrical pitch**.

The **experimental pitch** of an element of a propeller is the distance the element would have to advance in one revolution in order that there might be no thrust. The **mean experimental pitch**, sometimes called the **zero thrust pitch**, of a whole propeller is the distance the propeller would have to advance in one revolution in order that there might be no thrust.

The **boss** of a propeller is the central portion in which the hub is formed or mounted (Fig. 1).

The **hub** is the metal fitting inserted or incorporated in or with the propeller for the purpose of mounting it on the propeller or engine shaft.

The **root** of the blade is the portion near the boss or hub (Fig. 1).

The **aspect ratio** of a propeller blade is the tip radius  $R$  which is half the diameter, divided by the maximum blade width.

The **width ratio**  $WR$  of a propeller blade is the blade width at radius  $0.75R$  divided by the diameter.

The **total width ratio**  $TWR$  of a whole propeller is the width ratio of one blade multiplied by the number of blades.

The **thickness ratio** of a section of a propeller blade is the ratio of the thickness at that section to the blade width.

The **thickness ratio**  $TR$  of a whole propeller is taken as the thickness ratio of the section at  $0.75R$ .

The **blade angle** is the acute angle between the chord of a propeller section and a plane perpendicular to the axis of rotation of the propeller.

The **rake** or **tilt** of a propeller blade is defined as the mean angle which the line joining the centers of area of the sections makes with a plane perpendicular to the axis of rotation (Fig. 1).

A **tractor propeller** is one which works in front of the body or engine, relative to the direction of flight, while a **pusher** is one which is placed behind the body or engine.

A propeller is termed **right-hand**, if, when viewed from a position to the rear (in the slipstream), it rotates in a clockwise direction. Conversely, if from the same position the rotation is counterclockwise, the propeller is **left-hand**.

An **engine** is called right- or left-hand according to its rotation when fitted with a tractor propeller. A left-hand engine is therefore required by a right-hand pusher propeller.



## CHAPTER II

### THE MOMENTUM THEORY

As stated in the introduction, the propeller, in order to provide a thrust, must give motion to a mass of air in a direction opposite to the thrust. The simple momentum theory, developed by Rankine and R. E. Froude, is based on a consideration of the momentum and kinetic energy imparted to this mass of air. The Froude and Rankine theories are essentially the same, the main difference being that the Froude theory considers the propeller disc as a whole, while the Rankine divides it into elementary annular rings and deals with one ring at a time, afterward summing up the effects of each to obtain the effect of the whole.

In the Froude theory the propeller is assumed to be an advancing disc producing a uniform thrust  $T$ , the air pressure being therefore different in front of and in back of the disc by a constant amount over its area. This hypothetical disc, sometimes called an actuator disc, can be imagined as a propeller having an infinite number of blades. It is also assumed that the flow of air is streamline in character on either side of the disc and continuous through the propeller, so that the axial velocity is the same immediately in front of and immediately in back of the disc. There is no torque on the disc, and no rotation or twist is imparted to the air going through it.<sup>1</sup> It is further assumed that the air is a perfect fluid, being incompressible and having no viscosity.

In practice the propeller actually advances through the air but it is more convenient for the purpose of analysis, and is relatively the same, to consider the propeller disc as stationary in a uniformly moving stream of air. The general conception of the flow is then as shown in Fig. 3. The air stream, where it is not influenced by the propeller, has the velocity  $V$  and pressure  $p$ . The pressure is reduced to  $p'$  at the front of the

<sup>1</sup> A. Betz has developed an extension of the momentum theory including rotation, entitled *Eine Erweiterung der Schraubenstrahl-Theorie*, published in *Z.F.M.*, p. 105, 1920.

disc and receives an increment  $\Delta p$  in passing through it. The velocity is given an increment  $aV$  on approaching the disc and has the constant value  $V + aV$  in passing through it (the disc is assumed to have no thickness). In the final slipstream or wake the velocity has been given a further increase to  $V + bV$ , where  $bV$  is the added velocity of the slipstream, and the pressure has fallen to its original value  $p$ .

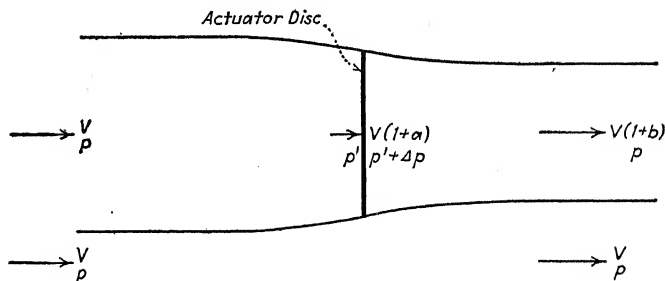


FIG. 3.

The flow being regarded as potential except in passing through the actuator disc, Bernoulli's equation<sup>1</sup> may be applied separately to the air in front of the disc and the air in back of the disc. The total head in front of the disc is

$$H = p + \frac{1}{2}\rho V^2 = p' + \frac{1}{2}\rho V^2(1 + a)^2$$

where  $\rho$  is the mass of air per unit volume; and the total head in back of the disc is

$$H_1 = p' + \Delta p + \frac{1}{2}\rho V^2(1 + a)^2 = p + \frac{1}{2}\rho V^2(1 + b)^2.$$

The difference in pressure in front of and behind the disc is therefore

$$\begin{aligned} \Delta p &= H_1 - H \\ &= [p + \frac{1}{2}\rho V^2(1 + b)^2] - [p + \frac{1}{2}\rho V^2] \\ &= \rho V^2 b \left(1 + \frac{b}{2}\right). \end{aligned}$$

and if  $A$  is the area of the disc the thrust is

$$\begin{aligned} T &= A\Delta p \\ &= A\rho V^2 b \left(1 + \frac{b}{2}\right). \end{aligned}$$

<sup>1</sup> Bernoulli's equation states that along a stream tube the total head of the fluid  $H = p + \frac{1}{2}\rho V^2 = \text{constant}$ . Its proof can be found in any good textbook on hydrodynamics.

Also, since the thrust is equal to the change of axial momentum in unit time,

$$\begin{aligned} T &= \text{mass per unit time} \times \text{velocity imparted} \\ &= AV(1+a)\rho bV \\ &= A\rho V^2b(1+a). \end{aligned}$$

Equating the two expressions for thrust,

$$A\rho V^2b(1+a) = A\rho V^2b\left(1 + \frac{b}{2}\right)$$

and

$$a = \frac{1}{2}b.$$

Thus, according to the momentum theory, half of the velocity imparted to the slipstream occurs in front of the propeller disc, and half behind.

**Ideal Efficiency.**—The work done on the fluid per unit time, which is the same as the rate of increase of kinetic energy of the fluid, is

$$\begin{aligned} \text{Energy} &= \frac{1}{2}\rho AV(1+a)[V^2(1+b)^2 - V^2] \\ &= \rho AbV^3(1+a)^2. \end{aligned}$$

In order to find the useful work done by the thrust, it is convenient to go back to the state in which the propeller is advancing with velocity  $V$  through fluid at rest, the thrust and velocity still being in the same relation to each other as before. The work done by the thrust on the propeller and aircraft in unit time is now  $TV$ .

The efficiency, which is the ratio of the useful work to the total work done on the air, is therefore

$$\begin{aligned} \eta &= \frac{TV}{\rho AbV^3(1+a)^2} \\ &= \frac{\rho AbV^3(1+a)}{\rho AbV^3(1+a)^2} \\ &= \frac{1}{1+a}. \end{aligned}$$

The efficiency can also be obtained by considering the useful work and the energy lost in the slipstream. When the propeller is moving through a fluid which is at rest, the work done by the thrust on the fluid is equal to the increase of kinetic energy of the fluid in unit time, or

$$\begin{aligned} \text{Energy} &= \frac{1}{2} (\text{mass per unit time}) (\text{velocity imparted})^2 \\ &= \frac{1}{2}\rho AV(1+a)(bV)^2 \end{aligned}$$

$$\begin{aligned}
 &= \frac{1}{2}\rho AV^2b(1+a)bV \\
 &= \frac{1}{2}TbV \\
 &= TVa.
 \end{aligned}$$

This energy is not regained from the air, and it represents a loss. The efficiency is then

$$\begin{aligned}
 \eta &= \frac{\text{useful work}}{\text{useful work} + \text{energy lost in slipstream}} \\
 &= \frac{TV}{TV + TVa} \\
 &= \frac{1}{1+a}.
 \end{aligned}$$

This expression represents the ideal or limiting value of the efficiency of a perfect propeller. It is never reached with actual propellers because of the following additional losses:

1. The energy of rotation of the slipstream due to the torque.
2. The profile drag or friction of the propeller blades moving through the air.
3. The loss due to the fact that the thrust is not actually uniform over the disc area, but at best falls off near the perimeter due to tip losses and at the center due to hub losses.
4. The loss due to the finite number of blades and the consequent variation of thrust at any one point with time.

**Usefulness of the Ideal Efficiency.**—While the ideal efficiency is never attained in practice, it represents a mark at which the propeller designer can aim. The actual propeller efficiencies obtained throughout the working range are usually from 80 to 88 per cent of the ideal efficiency, and so the ideal is useful in determining approximately the actual efficiency which can be obtained with a propeller under given conditions. The ideal efficiency can be taken as a measure of how favorable the conditions for the operation of the propeller are, and the ratio of the actual to the ideal can be taken as a measure of how well the propeller works under the given conditions.

In examining the expression for the ideal efficiency it is interesting to note that the efficiency depends only on the ratio of the velocity imparted to the air by the propeller to the forward velocity of the propeller itself. It is instructive to examine this expression to see how it is affected by variations in the forward speed, the thrust, and the diameter of the propeller. Consider the equation already obtained for the thrust,

$$T = A\rho V^2b(1+a).$$



Since  $\eta = \frac{1}{1+a}$  and  $a = \frac{1}{2}b$ , the equation can be written

$$T = \frac{2\rho AV^2(1-\eta)}{\eta^2},$$

or

$$\frac{\eta^2}{1-\eta} = \frac{2\rho AV^2}{T}.$$

It is convenient here to introduce a thrust coefficient

$$C'_T = \frac{T}{qA},$$

where  $q$  is the dynamic pressure of the fluid and is equal to  $\frac{1}{2}\rho V^2$ . The above expression involving efficiency then becomes

$$\frac{\eta^2}{1-\eta} = \frac{4}{C'_T}$$

and the variation of efficiency with  $C'_T$  is shown in Fig. 4. It will be observed that as the thrust coefficient, which represents the thrust per unit area per unit dynamic pressure, increases,

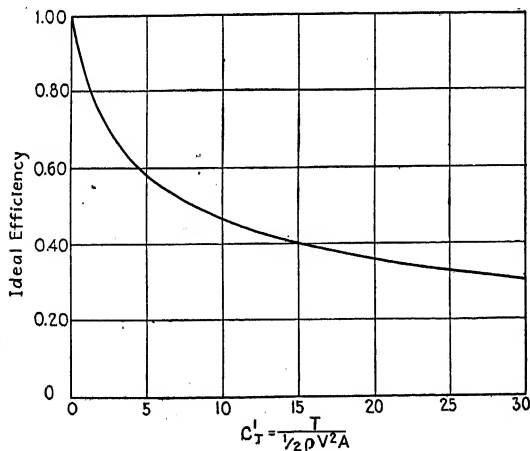


FIG. 4.—Ideal efficiency vs. thrust coefficient

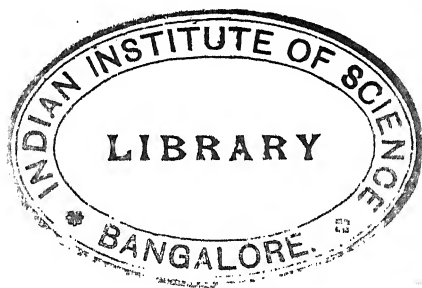
the efficiency drops rapidly at first and then more gradually. By varying only one factor of  $C'_T$  at a time, Fig. 4 illustrates the following points:

1. The ideal efficiency decreases with increase of thrust.
2. The ideal efficiency increases with increase of forward velocity.

3. The ideal efficiency increases with increase of density of the fluid.

4. The ideal efficiency increases with increase of disc area or propeller diameter.

While considerations of the ideal efficiency indicate that the diameter should be as large as possible, the loss due to the friction of the blades increases as the diameter becomes greater, so that it does not increase the efficiency of actual propellers to increase the diameter beyond a certain limit.



## CHAPTER III

### THE AIRFOIL

In the blade-element theory of the propeller, the propeller blade is considered an airfoil varying in cross-section and angle from hub to tip. It is necessary, therefore, to have a general understanding of airfoils and the aerodynamic reactions on them before taking up the blade-element theory. The aim of this chapter is merely to cover briefly the characteristics of airfoils which are of importance in propeller design. More comprehensive treatments can be found in some of the modern books on aerodynamics.<sup>1</sup>

**Fluid Resistance.**—If an object such as a flat plate is held in a wind or air current, it is at once apparent that a force is acting upon it. If the plate is held perpendicular to the direction of the air flow, the only force will be resistance or drag in the direction of the flow. If, however, the plate is inclined at some angle, the force will also be inclined and its lateral or cross-wind component may become much greater than the drag in the direction of flow. An airfoil is a body so shaped that the cross-force, called the lift, is high compared with the drag.

The forces acting on a solid body moving in a perfect fluid, that is, a fluid which has no viscosity and is incompressible, would vary as the square of the velocity  $V$  and would be proportional to the area on which the fluid particles acted. If  $S$  is an area denoting the size of the object, the resistance  $R$  would be expressed by the equation,

$$R = KSV^2,$$

where  $K$  is a constant or resistance coefficient determined by experiment. Air, however, is not a perfect fluid and it has been found by experiment that the resistance does not always vary exactly as the square of the velocity and that the coefficient  $K$  is not a true constant.

<sup>1</sup>"Airplane Design—Aerodynamics," by Edward P. Warner, McGraw-Hill Book Company, Inc., 1927, is recommended.

**Dynamical Similarity.** If  $K$  of the above formula were always a true constant, it would be possible to make aerodynamic tests on models of any size at any speed and apply the results with perfect accuracy to geometrically similar bodies having any other size and speed. The principle of dynamic similarity,<sup>1</sup> as developed by Riabouchinski and Buckingham, states that in the case of the motion of objects in a real fluid medium such as air, having viscosity and being compressible, the resistance varies according to the following equation:

$$R = \rho S V^2 f\left(\frac{VL}{\nu}\right) f_1\left(\frac{V}{c}\right) f_2\left(\frac{Lg}{V^2}\right),$$

where  $L$  is a convenient representative linear dimension of the object,  $\nu$  is the kinematic viscosity of the fluid, and  $c$  is the velocity of sound or the rate of travel of any compressive wave in the fluid. From an examination of the above equation it is at once apparent that if all factors materially affected the results, aerodynamic tests would be representative only of the actual conditions of speed and size at which they were made, and model tests would be of no value for predicting full-size performance.

Fortunately, however, all of the factors are not of great importance, and the expression,

$$R = \rho S V^2 \times \text{a constant},$$

is a fairly good first approximation. The factor  $f_2 (Lg/V^2)$ , while important in marine work, can be considered a constant for air and eliminated from the expression. The factor  $f_1 (V/c)$ , representing the effect of compressibility, is usually eliminated as unimportant for general airfoil work, since the velocities ordinarily dealt with are far below the velocity of sound, but it is of great importance in connection with propellers, for the tips of the blades often travel at speeds higher than that of sound in air, and the variation of  $R$  with  $V/c$  is great at these high speeds. The expression  $LV/\nu$  is called Reynolds number and is of considerable importance in airplane work, for there is usually a great difference in size between the model and the actual airplane.

<sup>1</sup> A clear statement of the principles of dynamic similarity and dimensional homogeneity is given in *Some Aspects of the Comparison of Model and*

The exact variation of the aerodynamic characteristics with Reynolds number and  $V/c$  is not known, and the results of tests are usually assumed to vary in accordance with the first approximation

$$R = \rho S V^2 \times \text{a constant,}$$

and attempts are made to correct for differences in Reynolds number or "scale effect."

**The Aerodynamic Forces on Airfoils.**—As stated at the beginning of this chapter, if a flat plate is placed in a smooth stream of air, either parallel or perpendicular to the flow, there is a resistance in the direction of flow, but obviously no resultant cross-force on the plate, since the air flow and pressures are equal but opposite on opposite sides and therefore balance each other. If, however, the plate is inclined at an angle between

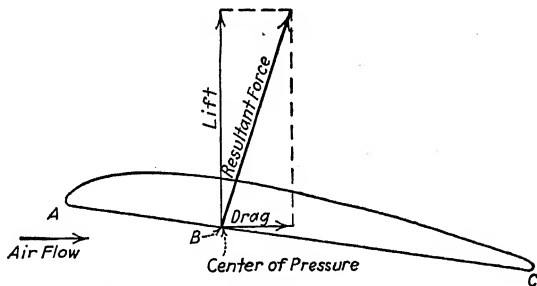


FIG. 5.

0 and 90 deg., there will be both a resistance and a lateral force on the plate, and the respective proportion of these will vary with every different angle. In many aeronautical problems it is desirable to obtain a large cross-force or lift with a small resistance or drag, and bodies called airfoils have been developed which are much more effective in this respect than the flat plate. Figure 5 shows a cross-section of an airfoil and the resultant force acting upon it when it is inclined at a small angle in a stream of air. The resultant force is usually resolved into components perpendicular to and parallel to the relative airflow, and these components represent the lift and drag of the airfoil. The point where the resultant force vector intersects the chord or base line of the airfoil section is called the center of pressure.

**Force Coefficients.**—The aerodynamic forces on airfoils are usually given for convenience in terms of dimensionless coeffi-

cients of lift and drag. The coefficients used by the N.A.C.A. are adhered to throughout this book, since they are considered the most fundamental, having a physical significance, and are also quite satisfactory for purposes of propeller design. These are

$$\text{Lift coefficient} = C_L = \frac{L}{qS} = \frac{L}{\frac{1}{2}\rho V^2 S}$$

and

$$\text{Drag coefficient} = C_D = \frac{D}{qS} = \frac{D}{\frac{1}{2}\rho V^2 S}$$

where  $L$  is the lift,  $D$  is the drag,  $q = \frac{1}{2}\rho V^2$  is the dynamic pressure due to the velocity of the air, and  $S$  is the projected area of the airfoil in plan. The symbols  $C_L$  and  $C_D$  are used to represent these particular coefficients only.

The Germans were the first to use the dynamic or impact pressure in their lift and drag coefficients  $C_a$  and  $C_w$ . These coefficients are the same as those used by the N.A.C.A. excepting that they are made one hundred times as large in order that whole numbers rather than small decimals may be dealt with.

The British do not use the dynamic pressure in their coefficients but use the density and velocity as such. Their coefficients are therefore just one-half as large as the American N.A.C.A. coefficients and are given by the expressions

$$k_L = \frac{L}{\rho S V^2}$$

and

$$k_D = \frac{D}{\rho S V^2}$$

The symbols  $L_c$  and  $D_c$  are often used in place of  $k_L$  and  $k_D$  in these expressions.

All of the above coefficients are dimensionless (that is, they are pure or abstract numbers) and may be used with any consistent system of units such as the foot-pound-second or the kilogram-meter-second systems. The English, or foot-pound-second, system is used throughout this book.

Airplane designers have another set of coefficients called engineering coefficients in which the velocity is in terms of miles per hour, the area in square feet, and the mass density  $\rho$  is included in the constant. The coefficients are therefore always

corrected to standard air for which  $\rho = 0.002378 \text{ lb.-ft.}^{-4}\text{-sec.}^2$ . They are

$$\text{Lift coefficient, } K_y = \frac{L}{SV^2}$$

and

$$\text{Drag coefficient, } K_x = \frac{D}{SV^2}.$$

It is unfortunate that so many different coefficients exist for practically the same purpose. Each one is related to any other by a simple constant, however, and coefficients may be converted from one type to another by the use of the following relations:

$$\begin{aligned} C_L &= 2(L_c \text{ or } k_L), \\ C_L &= 392K_y, \\ C_L &= 0.01C_a, \\ L_c \text{ or } k_L &= 0.5C_L, \\ L_c \text{ or } k_L &= 196K_y, \\ L_c \text{ or } k_L &= 0.005C_a, \\ K_y &= 0.00255C_L, \\ K_y &= 0.0051(L_c \text{ or } k_L), \\ K_y &= 0.0000255C_a. \end{aligned}$$

The various drag coefficients have the same relations with each other as the corresponding lift coefficients.

The ratio of lift to drag,  $L/D$ , which is the same as the ratio of the lift coefficient to the drag coefficient, is used as a measure of the effectiveness of an airfoil in producing lift at the cost of drag. The  $L/D$  is especially important in connection with propeller sections, for it affects the efficiency of the propeller.

The center of pressure C.P. is usually given in the form of the ratio  $AB/AC$ , shown in Fig. 5, which is the ratio of the distance of the resultant force from the leading edge, on the chord line, to the chord of the airfoil. Sometimes the moment about the leading edge or that about the quarter chord point is used instead of the C.P. The moment coefficient used by N.A.C.A. is

$$C_M = \frac{M}{qcS}$$

where  $c$  is the chord of the airfoil.

**Methods of Plotting Coefficients.**—The lift and drag forces on an airfoil are different for each different angle of attack. The variations of lift, drag, and angle of attack are most con-

veniently presented in graphical form, and many systems have been devised for this purpose. In the one which until recently has been in most common use, the coefficients of lift and drag, and the ratio of lift to drag, are plotted as three separate curves against the angle of attack. This method of plotting airfoil characteristics is shown in Fig. 6. It is useful in connection with the designing of propellers, because the angle of attack has an important bearing on the pitch of a propeller.

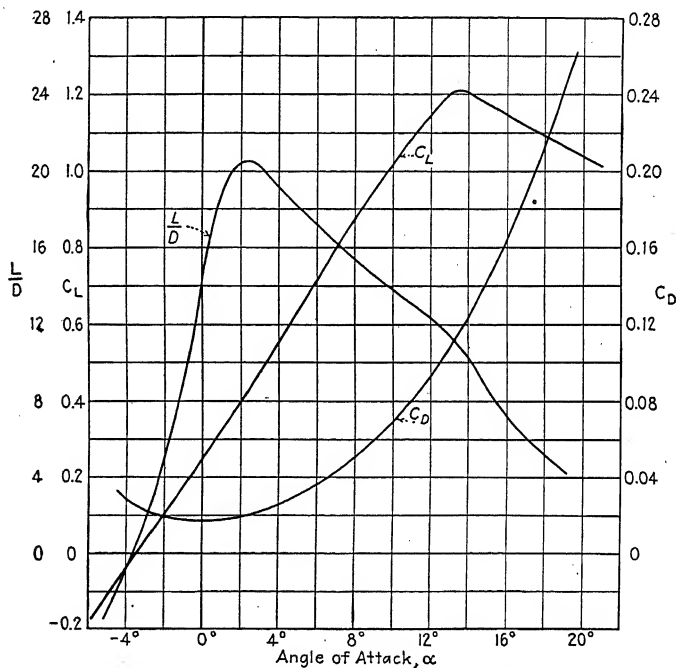


FIG. 6.—Airfoil characteristics plotted against angle of attack.

The curves in Fig. 6 are for a typical propeller section. It will be noticed that the lift coefficient increases with increased angle of attack up to a certain maximum value, after which it falls off as the angle becomes still greater. The drag coefficient has a minimum value near zero degrees and increases with change of angle of attack in either direction, becoming very great for the high angles beyond maximum lift. It will also be noticed that the lift coefficient is not zero at zero angle of attack but at an angle of attack considerably less than zero. The attitude of a typical airfoil when the lift is zero is shown in Fig. 7.



In comparing the aerodynamic qualities of various airfoils, the angle of attack is not of great importance, and a simpler arrangement in which only one curve is used in place of the above three is now in wide use. In this device, called a polar

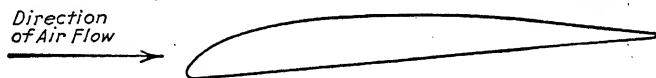


FIG. 7.

diagram, the lift coefficients as ordinates are plotted directly against the drag coefficients as abscissas, and the angles of attack are indicated on the curve, as shown in Fig. 8. Since the drag coefficients are relatively small, the scale for the drag coefficients

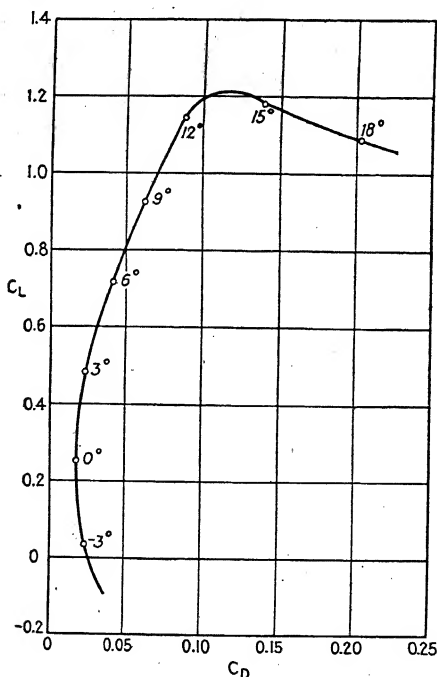


FIG. 8.—Polar curve for an airfoil.

is usually made four or five times as large as that for the lift coefficients. If the lift and drag coefficient scales are made equal, the length of a vector from zero to any point on the curve represents the coefficient of resultant force (hence the name polar

The C.P. is not of the same interest in connection with propellers as with airplanes. It is of importance in propeller design only because it affects the twisting of the blades which in turn affects the pitch of the propeller. The C.P. coefficient is usually plotted against angle of attack and is shown for a typical propeller section in Fig. 9. It will be noted that as the angle of attack is increased the C.P. moves forward, tending to increase the angle still further.

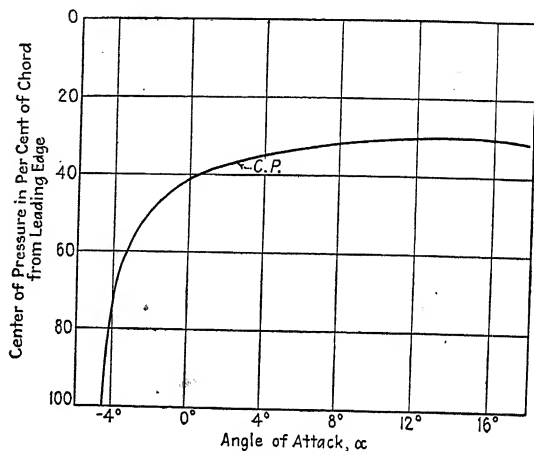


FIG. 9.

**Pressure Distribution over Airfoils.**—The coefficients dealt with up to this point apply to the position and the components of the resultant force on an airfoil. This force is due to differences in pressure over the upper and lower surfaces of the airfoil, and it is sometimes of interest to know how the intensity of pressure varies from point to point. Figure 10 shows the pressure distribution over the midspan section of an airfoil at low and high angles of attack.<sup>1</sup> At the low angle, which is very nearly that for zero lift, there is a positive pressure on the nose and there are negative pressures on both the upper and lower surfaces. (Positive and negative are relative to the static atmospheric pressure. There is of course no absolute negative value of pressure.) At the high angle, on the other hand, there is a positive pressure on the lower surface and a negative pressure

<sup>1</sup> The data for Fig. 10 were obtained from Pressure Distribution over Thick Airfoils—Model Tests, by F. H. Norton and D. L. Bacon, N.A.C.A.T.R. 150, 1922.

on the upper, both contributing to the lift. It is interesting to note that at the high angle, the negative pressures on the upper surface attain values much greater than the positive pressures on the lower side, and the maximum pressures occur near the nose, which explains the forward position of the C.P. at high angles. The total lift and drag forces can be obtained by an integration of the pressures, but the drag obtained in this manner is less than that obtained from force tests by the amount of skin friction.

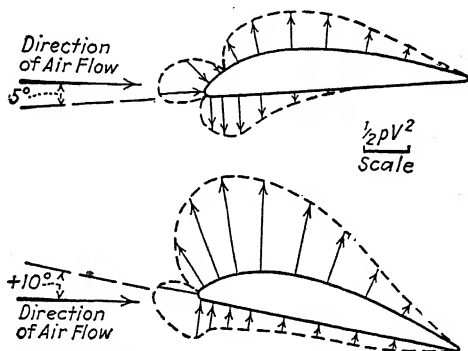


FIG. 10.—Pressure distribution at low and high angles of attack.

**Effect of Variations in the Shape of Airfoils.**—From the pressure-distribution diagrams in Fig. 10 it is evident that the characteristics of an airfoil are mainly dependent on the upper surface, so it is natural that changes in the upper surface have considerably greater effect on the airfoil characteristics than changes in the lower. Of the changes which have been made in the upper surface, the variation of the amount of upper camber is one of the most important, and many researches have been made on series of airfoils having the same lower surfaces and varying amounts of upper camber.<sup>1</sup> The results of one of these researches (N.A.C.A.T.R. 259) made on a series of flat-bottomed propeller sections are shown in Fig. 11. In general,

<sup>1</sup> Characteristics of Propeller Sections Tested in the Variable Density Wind Tunnel, by Eastman N. Jacobs, N.A.C.A.T.R. 259, 1927. The Aerodynamic Properties of Thick Airfoils, II, by F. H. Norton and D. L. Bacon, N.A.C.A.T.R. 152, 1922. Airfoils for Airscrew Design, by W. L. Cowley and H. Levy, British A.C.A.R. and M. 362, 1917-1918. Determination of the Lift and Drift of Airfoils having a Plain Lower Surface and Variable Camber, the Upper Surfaces Being Obtained by Varying the Ordinates in a Constant Ratio. British R. and M. 60, 1911-1912.

the lift coefficients are higher for the thicker sections at any particular angle of attack, although the slopes of the lift curves are lower for the thickest sections and the maximum lift coefficients are lower than those for the sections of medium thickness. The angle of attack for zero lift becomes lower as the upper

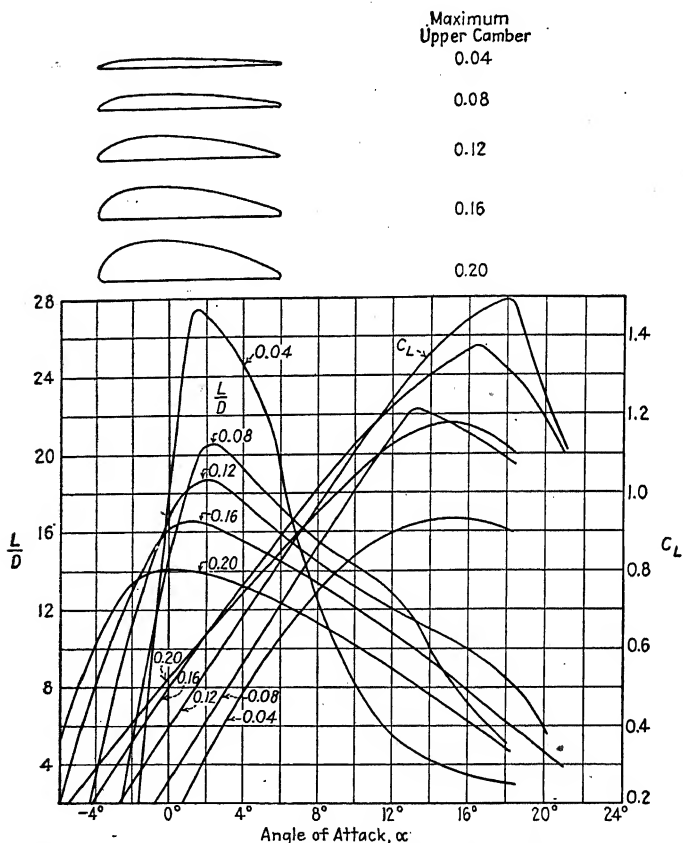


FIG. 11.—Variation of airfoil characteristics with upper camber.

camber is increased, reaching comparatively large negative values for the thickest sections. Most important of all from the point of view of propeller efficiency, the maximum effectiveness or  $L/D$  of the sections becomes lower as the upper camber is increased.

A few tests have been made to determine the effect of varying the position of the maximum ordinate of the upper surface of an

airfoil.<sup>1</sup> The general conclusion from these tests is that for most airfoils the best position of the maximum ordinate is about one-third of the chord back from the leading edge. Moving it forward slightly helps the maximum lift, while moving it backward slightly helps the maximum  $L/D$ . Thick sections seem to be best when the maximum ordinate is a little back, and thin sections when it is somewhat forward of the one-third position.

Variations in the amount of lower camber have less effect on the characteristics of airfoils than variations in the upper camber, but they are nevertheless of some importance. Many tests have also been made to determine the effect of varying the amount of lower camber, and Fig. 12 shows the results found from one investigation<sup>2</sup> in which the models were tested at the relatively high speed of 164 ft. per sec. Five airfoils were tested in which the maximum lower camber varied from  $+0.05$  (concave lower surface) to  $-0.07$  (convex lower surface), although the variations were not made in uniform steps. The upper surfaces of all the sections were the same, having a maximum ordinate of approximately 0.16. As can be seen from Fig. 12, concave lower camber increases the lift and convex lower camber decreases it. Convex lower camber seems to have very little effect on the  $L/D$ , but judging from these tests the  $L/D$  is reduced by concave lower camber. Other tests (*R. and M.* 60)<sup>2</sup> indicate that concave lower camber also has very little effect on  $L/D$ .

The effects of a multitude of other changes in the shapes of airfoil sections have been tested, but a discussion of them all does not lie within the scope of this chapter. The effect of plan form is, however, of considerable importance. A series of five airfoils having tips, as shown in Fig. 13, ranging from a

<sup>1</sup> One of the best is The Determination of the Lift and Drift of Aerofoils Having a Plain Lower Surface and Camber 0.10 of the Upper Surface, the Position of the Maximum Ordinate Being Varied, British *R. and M.* 72, 1912-1913.

<sup>2</sup> The Aerodynamic Properties of Thick Airfoils, II, by F. H. Norton and D. L. Bacon, N.A.C.A.T.R. 152, 1922. Other tests on the effect of lower camber are: Experiments on Thick Wing Sections, Expt. Dept., Airplane Eng. Div., U. S. Army Air Service *Bull.* for December, 1918. Experiments on a Series of Airfoils Having the Same Upper Surface and Lower Surfaces of Different Camber, by L. Bairstow and B. M. Jones, British *R. and M.* 60. 1911-1912.

rectangle to a very slender ellipse, have been tested and the results indicate that there is a minor improvement in  $L/D$  due to rounding the tips but that there is no improvement to be had

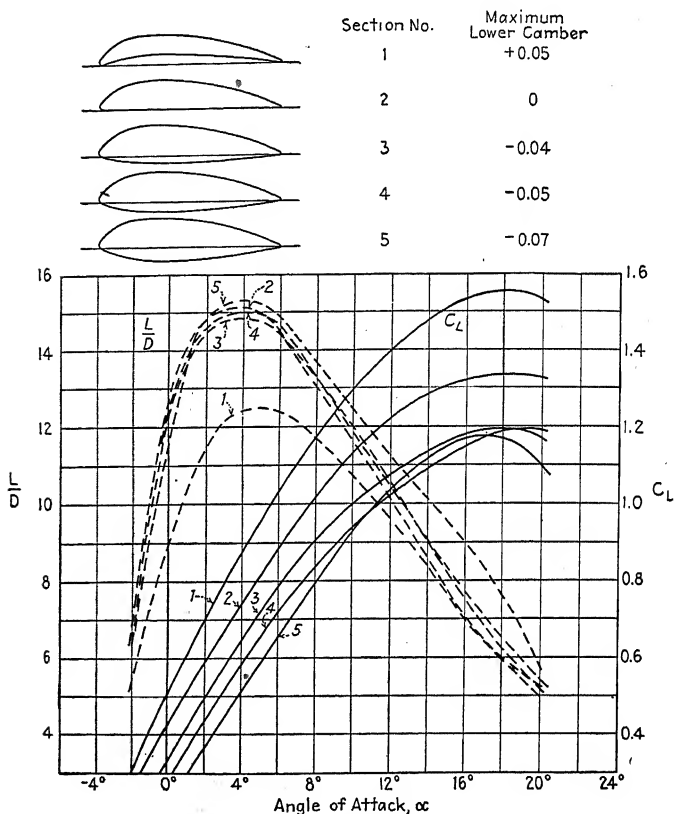


FIG. 12.—Variation of airfoil characteristics with lower camber.

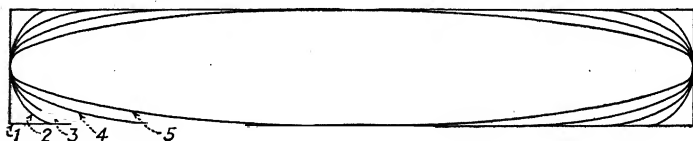


FIG. 13.

by making them narrower than the medium one, No. 3.<sup>1</sup> Another series of tests was made on the characteristics of four airfoils

<sup>1</sup> British A. C. A. Rept. T-477, February, 1915.

with various amounts of taper in plan, as shown in Fig. 14.<sup>1</sup> Those having a medium amount of taper had higher values of  $L/D$  than either the one with no taper or the one tapered to a point, and No. 3 was very slightly superior to No. 2. These two sets of tests seem to indicate that in order to obtain the highest possible efficiency, a wing or propeller blade should be somewhat tapered and rounded at the tip, although of course it is not certain that airfoil data of this kind can be applied directly to propeller blades.

The change in plan form having the greatest effect on airfoil characteristics is change of aspect ratio, which is defined as the span divided by the mean chord, or the square of the span divided by the wing area. The effect of aspect ratio on the characteristics of an airfoil can be

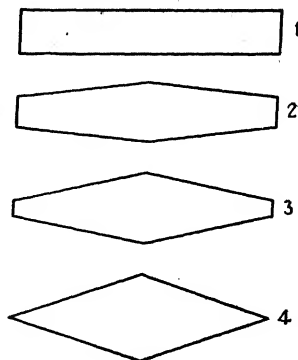


FIG. 14.

satisfactorily explained and calculated theoretically and will be considered in the next section.

**Elementary Airfoil Theory.**—A theory of the airfoil, called the induced-drag theory or the Lanchester-Prandtl wing theory, was suggested by Lanchester in Great Britain in 1907 and worked out separately by Prandtl and some of his associates in Germany.<sup>2</sup> A brief physical concept and the results of the theory in the form of final simple equations are all that will be given here.

Just as a propeller must give a backward motion to a mass of air in order to develop a forward thrust (as was brought out in the momentum theory), a wing must give a mass of air a downward motion in order to obtain an upward lift. If, then, a horizontal stream of air is flowing past an airfoil which is giving lift, the direction of some of the air is changed downward from the horizontal by a certain angle called the downwash angle

<sup>1</sup> The Aerodynamic Properties of Thick Aerofoils, II, by F. H. Norton and D. L. Bacon, N.A.C.A.T.R. 152, 1922.

<sup>2</sup> Prandtl has made a brief statement of his theory in English in Applications of Modern Hydrodynamics to Aeronautics, by L. Prandtl, N.A.C.A.T.R. 116, 1925. See also Aerofoil Theory, by H. Glauert, British R. and M. 723, 1920-1921, which is a survey of the work of Prandtl, Betz, and others; and "Aerofoil and Airscrew Theory," by H. Glauert, Cambridge University Press, 1926.

(see Fig. 15). The mean direction of airflow past the wing is indicated by the dotted arrow in Fig. 15 and has an angle equal to half the downwash angle, or  $\frac{\epsilon}{2}$ ; and according to the induced-drag theory, the angle of attack of the airfoil with respect to this line of mean flow direction is the angle of attack which the airfoil would have if its span were infinite. The flow would then be two dimensional and there would be no downwash, for the wing would be acting upon an infinite mass of air. The flow about a finite airfoil relative to the mean direction is assumed to be the same as that for infinite span, and the components of the resultant

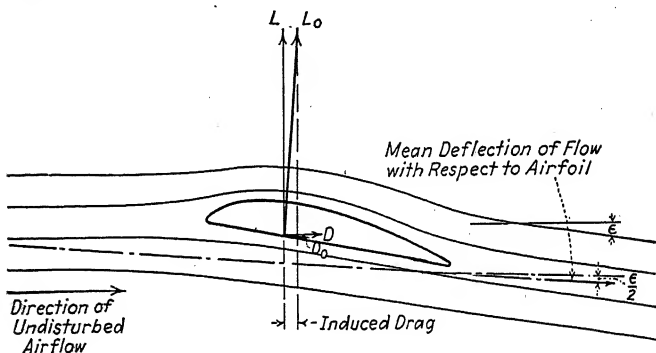


FIG. 15.

force referred to the mean direction of flow are called profile lift and profile drag because they depend only on the cross-sectional shape or profile of the airfoil.

The profile lift  $L_0$  and profile drag  $D_0$  are shown in Fig. 15 along with the ordinary lift  $L$  and drag  $D$ , which are referred to the direction of the airflow before it is disturbed by the airfoil. The two lifts  $L$  and  $L_0$  may be considered as having the same magnitude, for they differ only by an insignificant component of the small profile drag. The component of the profile lift, however, has considerable magnitude in the direction of the ordinary drag, and this component is called the induced drag, for it is the drag which occurs because lift is obtained with a wing of finite span.

The induced drag has the minimum value for an airfoil having what is known as elliptical lift distribution, which means that the lift grading across the span has the form of a semiellipse.



For this type of span loading the induced-drag coefficient is given by the following expression:

$$C_{D_i} = \frac{C_L^2}{\pi R}, \quad = \frac{C_L^2}{\pi AR}$$

where  $R$  is the aspect ratio, or the span squared divided by the area. According to this equation the induced drag depends only on the square of the lift coefficient and the aspect ratio and is entirely independent of the airfoil section. The induced angle, which is half the downwash angle is,

$$\alpha_i = \frac{\epsilon}{2} = \frac{C_L}{\pi R},$$

where  $\alpha_i$  is in radians.

The lift coefficient for infinite aspect ratio is then considered the same as that for a finite airfoil, and the drag (profile) and angle of attack for infinite aspect ratio are

$$C_{D_0} = C_D - \frac{C_L^2}{\pi R}$$

and

$$\alpha_0 = \alpha - \frac{C_L}{\pi R},$$

all of the angles being in radians.

Most model airfoil tests are made with airfoils having a rectangular plan form, for which the lift distribution across the span is not elliptical. The above equations give values of the induced drag which are as much as 5 per cent too low and values of the induced angle as much as 25 per cent too low for wings of rectangular plan form and aspect ratio 6, and since the angles are important in dealing with propeller sections, the equations are not satisfactory. More accurate expressions are used which were developed by Betz for wings of rectangular plan form and simplified to the following form by Glauert:<sup>1</sup>

$$C_{D_0} = C_D - \frac{C_L^2 \delta}{a},$$

$$\alpha_0 = \alpha - \frac{C_L \xi}{a},$$

<sup>1</sup> The Calculation of the Characteristics of Tapered Wings, by H. Glauert, British R. and M. 767, 1921-1922.

where  $a$  is the slope of the straight portion of the lift curve, or  $dC_L/d\alpha$ , and the angles are measured in radians. The values of  $\delta$  and  $\xi$  are functions of  $R/a$ , where  $R$  is the aspect ratio, and these functions are given in Fig. 16. If the angles are expressed in degrees, the slope becomes

$$a = \frac{180}{\pi} \frac{dC_L}{d\alpha},$$

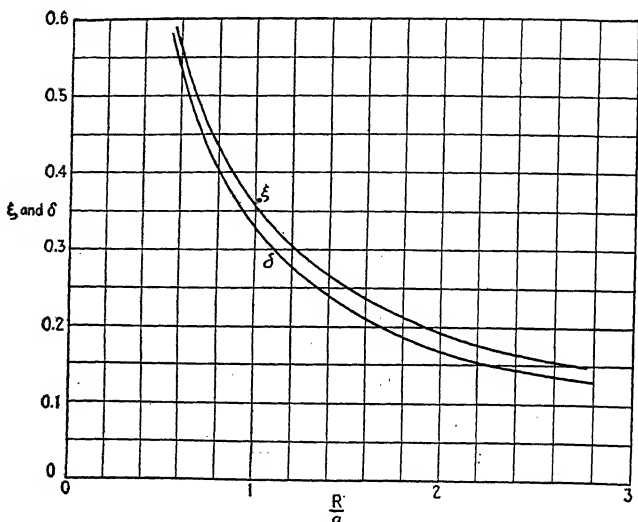


Fig. 16.

and the angle of attack for infinite aspect ratio becomes

$$\alpha_0 = \alpha - \frac{180}{\pi} \frac{C_L \xi}{a}.$$

The use of these transformation formulas can be made clear by means of an example. Consider the airfoil of aspect ratio 6 and camber 0.10 (Fig. 20). At an angle of attack of  $3.2^\circ$ ,  $C_L = 0.543$  and  $C_D = 0.0300$ . The slope of the lift curve is  $a = 4.08$ , and  $R/a = 6/4.08 = 1.47$ . Then, from Fig. 16,  $\xi = 0.256$  and  $\delta = 0.228$ , and the induced drag is

$$C_{D_i} = \frac{C_L^2 \delta}{a} = 0.0559 C_L^2 = 0.0164,$$

and the profile drag is

$$C_{D_p} = C_D - C_{D_i} = 0.0136.$$

In like manner the induced angle is

$$\alpha_i = \frac{180C_L\xi}{\pi a} = 3.60C_L = 2.0^\circ,$$

and the angle for infinite aspect ratio is

$$\alpha_0 = \alpha - \alpha_i = 1.2^\circ.$$

In recent years there has been a tendency in wind tunnel airfoil tests to use larger models with respect to the size of the tunnel than formerly, the span now often being half the diameter of the air stream or greater. In this way a larger scale or Reynolds number is obtained but the effect of the tunnel wall interference on the airfoil characteristics is important, and the airfoil characteristics should be corrected to free air conditions before being applied to propellers. Prandtl has developed theoretical expressions for calculating the tunnel wall effect,<sup>1</sup> and as in the case of the Betz rectangular wing formulas, Glauert has put them in slightly more usable form.<sup>2</sup> As in the transformation to infinite aspect ratio, corrections are made for the drag and the angle of attack at a constant lift. The correction factors for wind tunnels of circular cross-section are

$$\Delta C_D = \frac{SC_L^2}{8A},$$

$$\Delta \alpha = \frac{SC_L}{8A},$$

where  $A$  is the cross-sectional area of the air stream and  $S$  is the area of the airfoil. The corrections are to be added to the drag coefficient and angle of attack as measured in a closed tunnel and subtracted from the values measured in an open jet tunnel. Since the corrections depend on the lift and area of the airfoil and are independent of the aspect ratio or plan form, they apply to any wing system whether of one or more planes.

The theoretical corrections for tunnel wall interference and the transformation equations to infinite aspect ratio have been well checked experimentally and are sufficiently accurate for practical use.

<sup>1</sup> Applications of Modern Hydrodynamics to Aeronautics, by L. Prandtl, N.A.C.A.T.R. 116, p. 49, 1925.

<sup>2</sup> Aerofoil and Airscrew Theory," by H. Glauert, Cambridge University Press, 1926.

**Effects of Scale and Compressibility.**—The principle of dynamic similarity indicates that the lift and drag coefficients of airfoils are not constants but vary with Reynolds number and the compressibility factor  $V/c$ . A number of tests have been made at values of Reynolds number ranging from those commonly used in model tests to full scale for airplane wings and propeller blades. These tests have been made in the variable-density wind tunnel of the N.A.C.A., in which the Reynolds number is varied by compressing the air and thereby changing the kinematic viscosity  $\nu$ . The variation of maximum  $L/D$  with Reynolds number is shown for the U. S. A. 35-B airfoil in Fig. 17.<sup>1</sup> The lift and drag of different airfoils vary in different

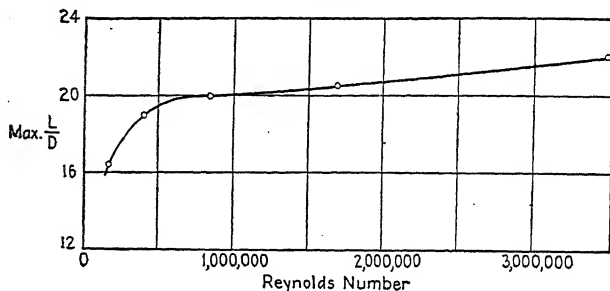


Fig. 17.

ways with Reynolds number, and no general rule can be given at this stage. The greatest variation, however, occurs at the low values of Reynolds number, and the high-scale tests are more consistent and reliable.

No tests of real quantitative value have been made to date on airfoils at velocities approaching that of sound in air, but two series of tests have been made by Briggs and Dryden<sup>2</sup> which are of interest in showing the general trend of the variation of airfoil characteristics with  $V/c$ . The variation of the maximum value of  $L/D$  for a propeller section of thickness ratio

<sup>1</sup> The data for Fig. 17 were obtained from *The Comparison of Well Known and New Wing Sections Tested in the Variable Density Tunnel*, by George J. Higgins, N.A.C.A.T.N. 219, May, 1925.

<sup>2</sup> *Aerodynamic Characteristics of Airfoils at High Speeds*, by L. J. Briggs, G. F. Hull, and H. L. Dryden, N.A.C.A.T.R. 207, 1925. *Pressure Distribution over Airfoils at High Speeds*, by L. J. Briggs, and H. L. Dryden, N.A.C.A.T.R. 255, 1927. *Aerodynamic Characteristics of Twenty-four Airfoils at High Speeds*, by L. J. Briggs, and H. L. Dryden, N.A.C.A.T.R. 222, 1926.

LIBRARY

0.12 is shown in Fig. 18. It may be said that in general there is a decrease in lift and an increase in drag with increasing  $V/c$  and a consequent reduction in effectiveness or  $L/D$  as the speed approaches that of sound. Also, the variation of the characteristics of thin sections is considerably less than for thick sections, with both  $V/c$  and Reynolds number.

**Airfoil Sections Suitable for Propellers.**—Because of strength considerations, aircraft propeller blades are usually tapered in thickness and plan form, so that the chord and camber of the

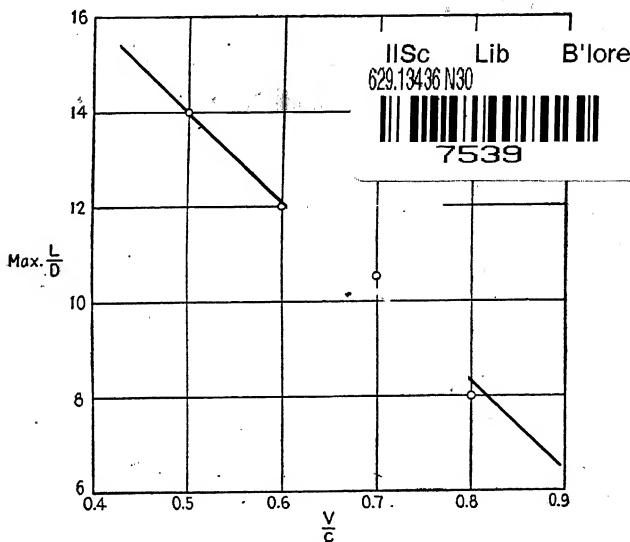
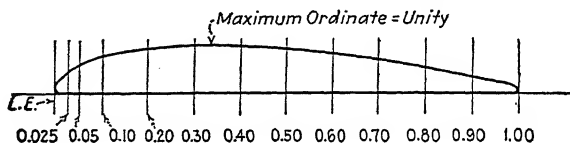


FIG. 18.

airfoil sections are different at different radii along the blade. It is necessary, of course, in order to analyze the aerodynamic performance of a propeller, section by section, to have some knowledge of the airfoil characteristics of the sections along the blade. Since it is not feasible to test a series of airfoils for every propeller designed, it is customary either to adhere to a standard form of blade, representative airfoils of which have been tested, or to use data from a series of airfoils of varying thickness ratio and interpolate for the actual thickness ratio at each section of the propeller if necessary. The latter method allows the propeller designer greater freedom, for it can be used with any plan form and variation of thickness along the radius, and it is at present in general use in the United States.

The series of propeller sections which has been most widely employed and tested is based upon the R.A.F.-6 airfoil modified so as to have a flat lower surface. (The practice of making the lower surface or face of propeller sections flat over the working or outer portion of the blades is almost universal because it facilitates construction, and it is entirely justified, since the best flat-bottomed airfoils are quite as effective aerodynamically as any others.) In the series based on the modified R.A.F.-6 section, the upper camber is varied by scaling all of the ordinates up or down in the same proportion as the maximum ordinate. The ordinates for these sections are given in terms of the maximum ordinate in Fig. 19. If the blade width or chord and the thickness of a section are known, all of the ordinates of the section



Fraction of Chord	L. E. Rad.	0.025	0.05	0.10	0.20	0.30	0.40	0.50	0.60	0.70	0.80	0.90	T. E. Rad.
Ordinate	0.10	0.41	0.59	0.79	0.95	0.998	0.99	0.95	0.87	0.74	0.56	0.35	0.08

FIG. 19.—Ordinates of standard propeller section based on R.A.F.-6.

can be calculated by means of the relations given in Fig. 19. The aerodynamic characteristics are given for this series of sections in Figs. 20 and 21 for aspect ratio 6. The values have been corrected for tunnel wall interference to free air conditions and have been faired and cross-faired to eliminate minor irregularities due to experimental error. The airfoils were tested in the variable-density wind tunnel of the N.A.C.A., both at 1 atmosphere and at 20 atmospheres pressure, corresponding to ordinary model test-scale and full-scale Reynolds numbers, respectively.<sup>1</sup> The sections, excepting for the very thickest ones, have very little scale effect with Reynolds number, and the characteristics given in Figs. 20 and 21, which are taken from the high-scale tests, are considered satisfactory as far as scale is concerned for propeller sections moving at velocities up to 300 or 400 ft. per sec. Model propeller tests usually fall within this

<sup>1</sup> Characteristics of Propeller Sections Tested in the Variable Density Wind Tunnel of the National Aeronautics Administration, NACA Report 250, 1927.

range of tip speed but full-scale propellers do not, so that for full-scale propellers a scale correction of some kind is ordinarily applied.

It will be noticed that in Fig. 21 the effectiveness of the airfoils is plotted in terms of  $D/L$  and that a scale for  $\gamma$ , which is the angle between the lift and the resultant force vectors, is

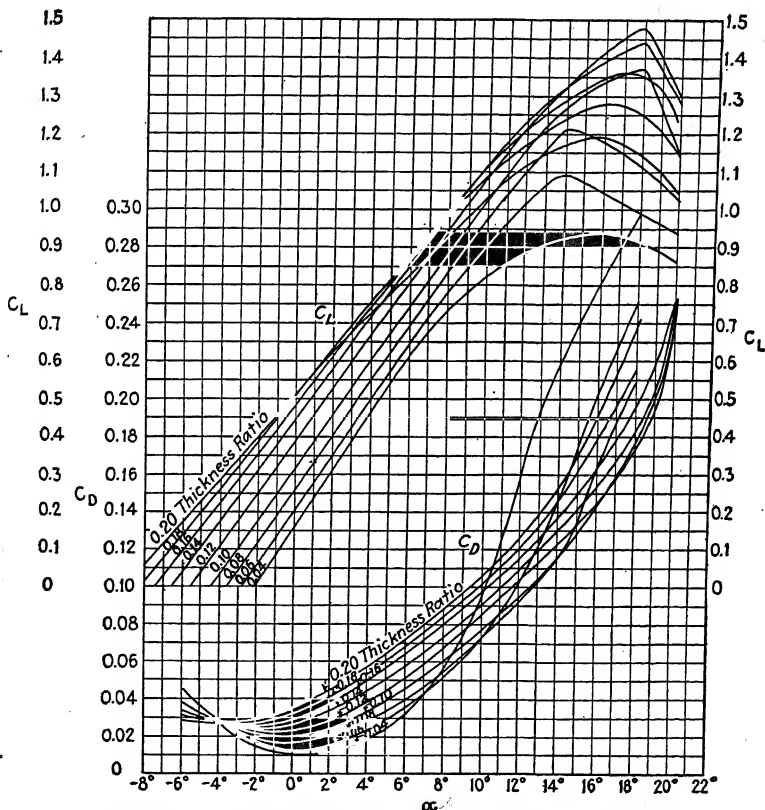


FIG. 20.—Standard propeller sections based on R.A.F.-6. Aspect ratio = 6.

also given. This is for convenience in working with the blade-element theory, in which  $\gamma$  or its tangent  $D/L$  is used directly.

The sections near the hub of a propeller are usually given a convex shape or negative lower camber. If the series of propeller sections based on the modified R.A.F.-6 is used, the convex sections are obtained by putting two regular flat-faced

as shown in Fig. 22. There are no entirely satisfactory data regarding the effect on the aerodynamic characteristics of adding

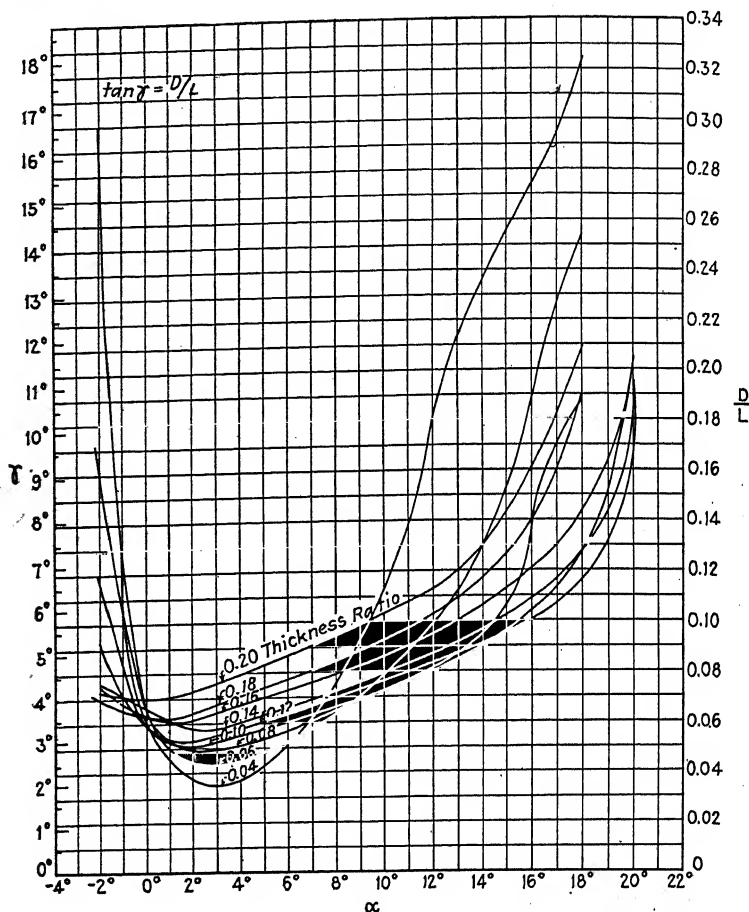


FIG. 21.—Standard propeller sections based on R.A.F.-6. Aspect ratio = 6.

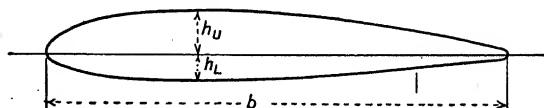


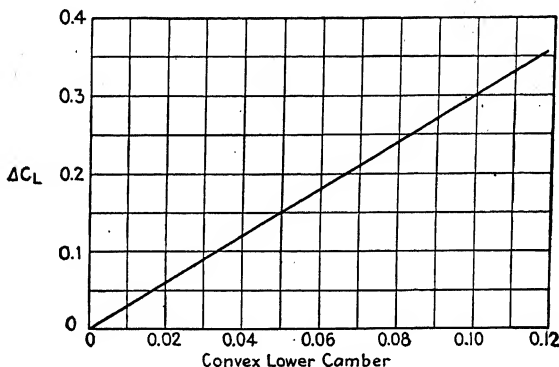
FIG. 22.

various amounts of lower camber in this manner to airfoil sections of various thickness. The sections having convex lower camber,



is sufficiently accurate for ordinary purposes to reduce the lift of the upper flat-faced section alone by an amount depending on the added lower camber as given in Fig. 23. The  $L/D$  is but very slightly affected by a moderate addition of lower camber and may be taken as being the same as that for the flat-faced upper section alone.

The characteristics for the standard series of flat-faced propeller sections based on the modified R.A.F.-6 are also given for infinite aspect ratio, or two-dimensional flow, in Figs. 24 and 25.



NOTE: For a Section with Lower Camber,  $C_L = C_{L(\text{flat face})} - \Delta C_L$

FIG. 23.—Correction to lift coefficient for convex lower camber.

These propeller sections have become more or less standard, mainly because of the considerable amount of test data available regarding them,<sup>1</sup> although lately other sections have been developed similar to the Clark-Y and the U. S. A. 35-B which are somewhat better aerodynamically and are being used in propellers where very high efficiency is desired. The Clark-Y and U. S. A. 35-B sections have approximately the same thickness as the standard propeller section of thickness ratio 0.12, and the

<sup>1</sup> In addition to the reference in the previous footnote, test data on these propeller sections may be obtained from the following sources: "The Airplane Propeller," prepared by the Propeller Section, Eng. Div., U. S. Army Air Service, 1920, and published by the Government Printing Office. Wind Tunnel Studies in Aerodynamic Phenomena at High Speed, by F. W. Caldwell, and E. N. Fales, N.A.C.A.T.R. 83, 1920. Aerodynamic Characteristics of Airfoils at High Speeds, by L. J. Briggs, G. F. Hull, and H. L. Dryden, N.A.C.A.T.R. 207, 1925. Pressure Distribution over Airfoils at High Speeds, by L. J. Briggs, and H. L. Dryden, N.A.C.A.T.R. 207, 1925.

$C_L$  and  $L/D$  curves obtained from high-scale tests in the variable-density tunnel are plotted for these three sections in Fig. 26. The lift curves for all three airfoils are practically the same

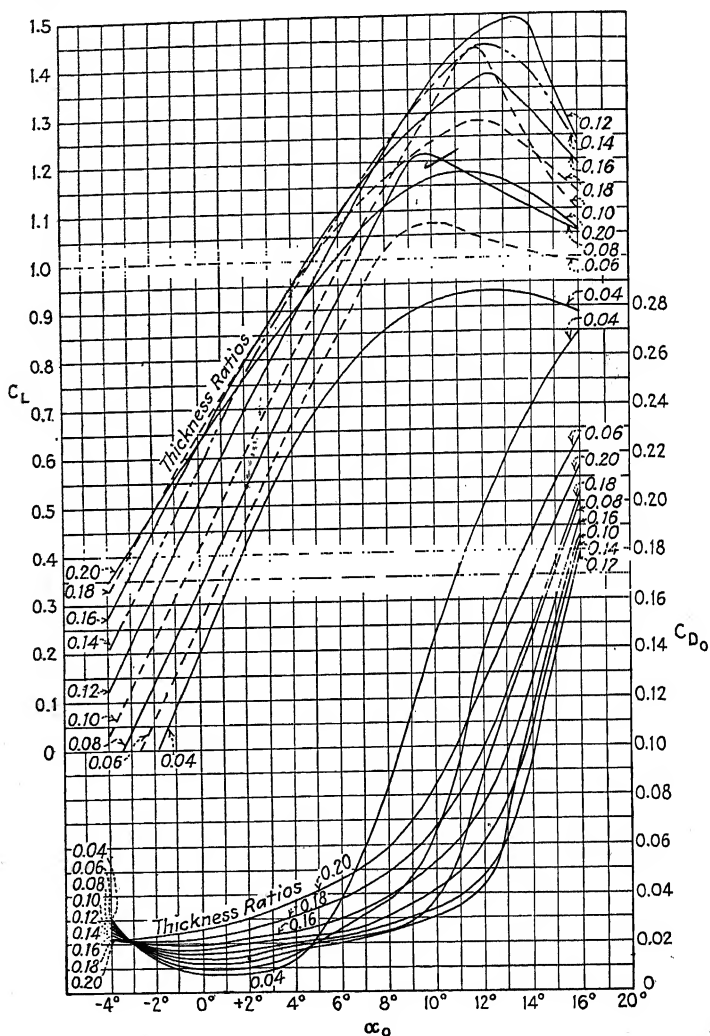


FIG. 24.—Standard propeller sections based on R.A.F.-6. Infinite aspect ratio.

for ordinary angles of attack, so that in the absence of test data on a series of propeller sections based on the Clark-Y or

be used directly for the new-type sections. The values of  $L/D$  for the newer sections range from 10 to 30 per cent higher than those for the standard propeller sections.

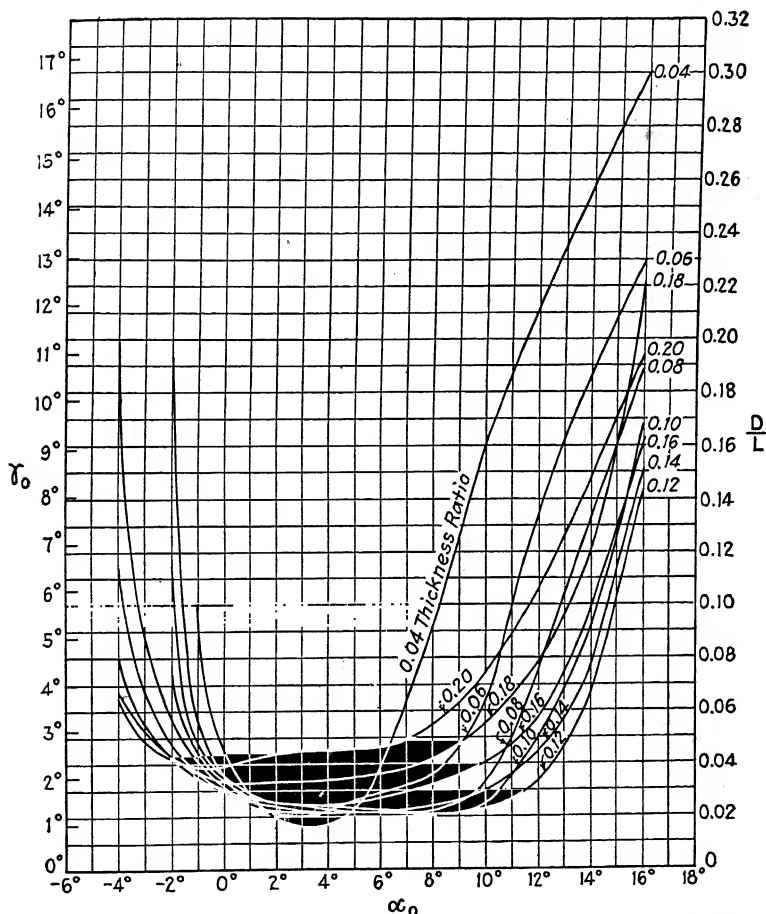


FIG. 25.—Standard propeller sections based on R.A.F.-6. Infinite aspect ratio.

Several other series of sections suitable for propellers have been tested,<sup>1</sup> mainly for the purpose of checking various forms

<sup>1</sup> Airfoils for Airscrew Design, by W. L. Cowley and H. Levy, British R. and M. 362, 1917–1918. Aerodynamic Characteristics of Aerofoils, II, N.A.-C.A.T.R. 124, 1921, Fage and Collins airfoils 1 to 6. Comparison of Model Propeller Tests with Airfoil Theory, by W. F. Durand, and E. P. Lesley, N.A.C.A. T.R. 122, 1921. The Airfoil Section, by W. F. Durand, The

of blade-element analysis against model propeller tests. In some of these, the airfoils were tested at the same values of Reynolds number as the corresponding sections in the model

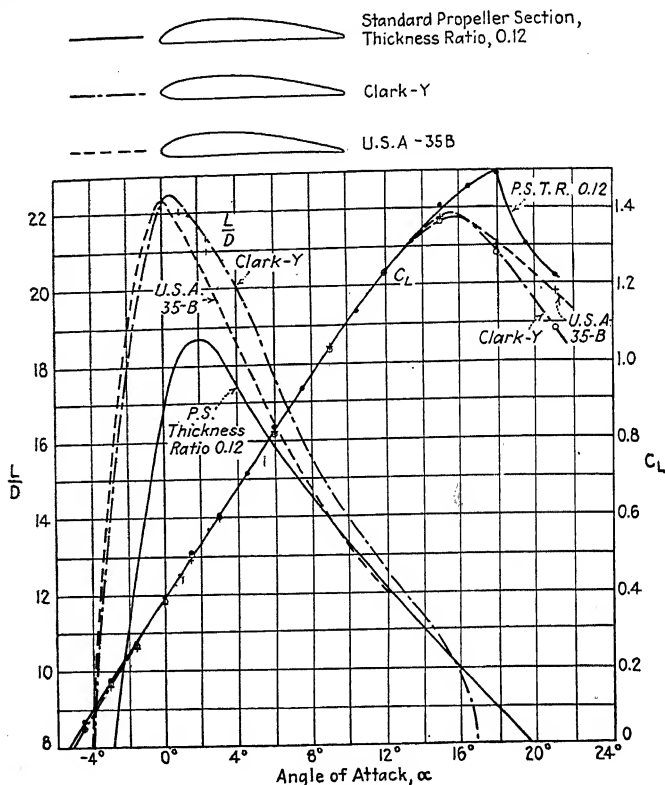


FIG. 26.

propellers, and since the tip speeds were very low compared with the speed of sound in air, this practically eliminated errors due to scale.

Light of Data Derived from an Experimental Investigation of the Distribution of Pressure over the Entire Surface of an Airscrew Blade, and also over Aerofoils of Appropriate Shapes, by A. Fage, and R. G. Howard, British *R. and M.* 681, 1921-1922. Experiments with a Family of Airscrews, Part III. Analysis of the Family of Airscrews by Means of the Vortex Theory and Measurements of Total Head, by C. N. H. Lock, and H. Bateman, British *R. and M.* 892, 1923-1924.



## CHAPTER IV

### THE SIMPLE BLADE-ELEMENT THEORY

While the momentum theory is useful for determining ideal efficiency, it gives a very incomplete account of the action of screw propellers, neglecting among other things the torque. In order to investigate propeller action in greater detail, the blades are considered as made up of a number of small elements, and the air forces on each element are calculated. Thus, while the momentum theory deals with the flow of the air, the blade-element theory deals primarily with the forces on the propeller blades. The idea of analyzing the forces on elementary strips of propeller blades was first published by William Froude in 1878.<sup>1</sup> It was also worked out independently by Drzewiecki and given in a book on mechanical flight published in Russia seven years later, in 1885.<sup>2</sup> Again, in 1907, Lanchester published a somewhat more advanced form of the blade-element theory without knowledge of previous work on the subject. The simple blade-element theory is usually referred to, however, as the Drzewiecki theory, for it was Drzewiecki who put it into practical form and brought it into general use. Also, he was the first to sum up the forces on the blade elements to obtain the thrust and torque for a whole propeller and the first to introduce the idea of using airfoil data to find the forces on the blade elements.

In the Drzewiecki blade-element theory the propeller is considered a warped or twisted airfoil, each segment of which

<sup>1</sup> The Elementary Relation between Pitch, Slip, and Propulsive Efficiency, by William Froude, *Trans. Inst. Naval Architects*, 1878.

<sup>2</sup> This fact, which is not generally known in English-speaking countries, was called to the author's attention by Prof. F. W. Pawlowski of the University of Michigan. Drzewiecki's first French paper on his theory was published in 1892. He wrote in all seven papers on aircraft propulsion which were presented to l'Académie des Sciences, l'Association Technique Maritime, and Le Congrès International d'Architecture et de Construction Navale, held on July 15, 1900. He finally wrote a book summing up all of his work called "Théorie Générale de l'Hélice Propulsive." published

follows a helical path and is treated as a segment of an ordinary wing. It is usually assumed in the simple theory that airfoil coefficients obtained from wind tunnel tests of model wings (ordinarily tested with an aspect ratio of 6) apply directly to

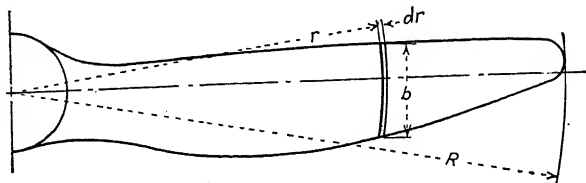


FIG. 27.

propeller blade elements of the same cross-sectional shape.<sup>1</sup> The air flow around each element is considered two-dimensional and therefore unaffected by the adjacent parts of the blade. The independence of the blade elements at any given radius

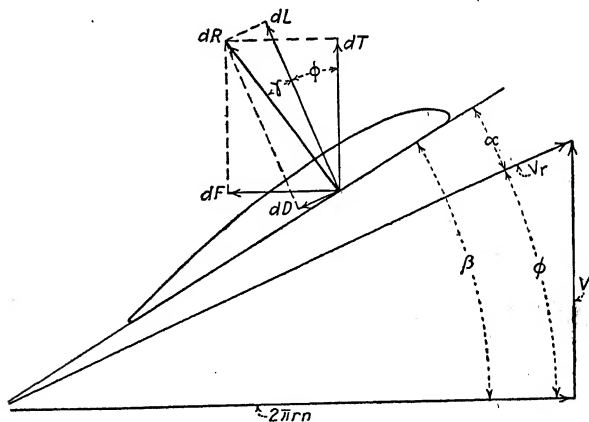


FIG. 28.

with respect to the neighboring elements has been established theoretically<sup>2</sup> and has also been shown to be substantially true for the working sections of the blade by special experiments<sup>3</sup>

<sup>1</sup> In his book, Drzewiecki suggested that the airfoil characteristics could be obtained from tests on special model propellers.

\*"Aerofoil and Airscrew Theory," by H. Glauert, Cambridge University Press, 1926.

<sup>3</sup>Experiments to Verify the Independence of the Elements of an Airscrew Blade, by C. N. H. Lock, H. Bateman, and H. C. H. Townend,

made for the purpose. It is also assumed that the air passes through the propeller with no radial flow (*i.e.*, there is no contraction of the slipstream in passing through the propeller disc) and that there is no blade interference.

**The Aerodynamic Forces on a Blade Element.**—Consider the element at radius  $r$ , shown in Fig. 27, which has the infinitesimal length  $dr$  and the width  $b$ . The motion of the element in an aircraft propeller in flight is along a helical path determined by the forward velocity  $V$  of the aircraft and the tangential velocity  $2\pi rn$  of the element in the plane of the propeller disc, where  $n$  represents the revolutions per unit time. The velocity of the element with respect to the air  $V_r$  is then the resultant of the forward and tangential velocities, as shown in Fig. 28. Call the angle between the direction of motion of the element and the plane of rotation  $\phi$ , and the blade angle  $\beta$ . The angle of attack  $\alpha$  of the element relative to the air is then  $\alpha = \beta - \phi$ .

Applying ordinary airfoil coefficients, the lift force on the element is

$$dL = \frac{1}{2}\rho V_r^2 C_L b dr.$$

Let  $\gamma$  be the angle between the lift component and the resultant force, or  $\gamma = \arctan D/L$ . Then the total resultant air force on the element is

$$dR = \frac{\frac{1}{2}\rho V_r^2 C_L b dr}{\cos \gamma}.$$

The thrust of the element is the component of the resultant force in the direction of the propeller axis (Fig. 28), or

$$\begin{aligned} dT &= dR \cos(\phi + \gamma) \\ &= \frac{\frac{1}{2}\rho V_r^2 C_L b dr \cos(\phi + \gamma)}{\cos \gamma}, \end{aligned}$$

and since  $V_r = \frac{V}{\sin \phi}$ .

$$dT = \frac{\frac{1}{2}\rho V^2 C_L b dr \cos(\phi + \gamma)}{\sin^2 \phi \cos \gamma}.$$

For convenience let

$$K = \frac{C_L b}{\sin^2 \phi \cos \gamma}$$

and

$$T_c = K \cos(\phi + \gamma).$$

Then

$$dT = \frac{1}{2}\rho V^2 T_c dr,$$

and the total thrust for the propeller (of  $B$  blades) is

$$T = \frac{1}{2}\rho V^2 B \int_0^R T_c dr.$$

Referring again to Fig. 28, the tangential or torque force is

$$dF = dR \sin(\phi + \gamma),$$

and the torque on the element is

$$dQ = r dR \sin(\phi + \gamma),$$

which, if  $Q_c = Kr \sin(\phi + \gamma)$ , can be written

$$dQ = \frac{1}{2}\rho V^2 Q_c dr.$$

The expression for the torque of the whole propeller is therefore

$$Q = \frac{1}{2}\rho V^2 B \int_0^R Q_c dr.$$

The horsepower absorbed by the propeller, or the torque horsepower, is

$$QHP = \frac{2\pi n Q}{550},$$

and the efficiency is

$$\eta = \frac{THP}{QHP} = \frac{TV}{2\pi n Q}.$$

**The Efficiency of an Element.**—Because of the variation of the blade width, angle, and airfoil section along the blade, it is not possible to obtain a simple expression for the thrust, torque, and efficiency of propellers in general. A single element at about two-thirds or three-fourths of the tip radius is, however, fairly representative of the whole propeller, and it is therefore interesting to examine the expression for the efficiency of a single element. The efficiency of an element is the ratio of the useful power to the power absorbed, or

$$\begin{aligned} \eta &= \frac{dTV}{dQ2\pi n} \\ &= \frac{dR \cos(\phi + \gamma)V}{dR \sin(\phi + \gamma)2\pi nr} \\ &= \frac{\tan \phi}{\tan(\phi + \gamma)}. \end{aligned}$$

Now  $\tan \phi$  is the ratio of the forward to the tangential velocity, and  $\tan \gamma = D/L$ . According to the simple blade-element theory, the efficiency of an element of a propeller



depends only on the ratio of the forward to the tangential velocity and on the  $L/D$  of the airfoil section.

The value of  $\phi$  which gives the maximum efficiency for an element, as found by differentiating the efficiency with respect to  $\phi$  and equating the result to zero, is

$$\phi = 45^\circ - \frac{\gamma}{2}$$

The variation of efficiency with  $\phi$  is shown in Fig. 29 for two extreme values of  $\gamma$ . The efficiency rises to a maximum at  $45^\circ - \gamma/2$  and then falls to zero again at  $90^\circ - \gamma$ . With an  $L/D$  of 28.6 the maximum possible efficiency of an element according to the simple theory is 0.932, while with an  $L/D$  of

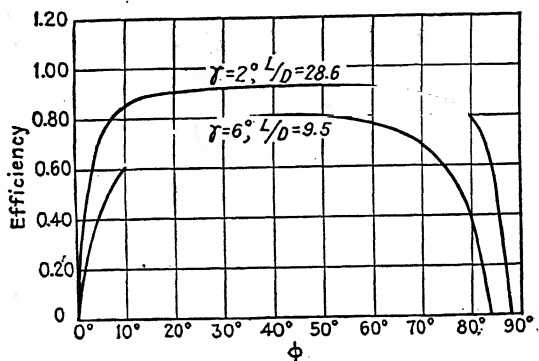


FIG. 29.

9.5 it is only 0.812. At the values of  $\phi$  at which the most important elements of the majority of propellers work ( $10^\circ$  to  $15^\circ$ ), the effect of  $L/D$  on efficiency is still greater. Within the range of  $10^\circ$  to  $15^\circ$ , the curves in Fig. 29 indicate that it is advantageous to have both the  $L/D$  of the airfoil sections and the angle  $\phi$  (or the advance per revolution, and consequently the pitch) as high as possible.

#### The Limitations of the Simple Blade-element Theory.—

According to the momentum theory a velocity is imparted to the air passing through the propeller, and half of this velocity is given the air by the time it reaches the propeller plane. This increase of velocity of the air as it passes into the propeller disc is called the inflow velocity. It is always found where there is pressure discontinuity in a fluid. In the case of a wing moving horizontally, the air is given a downward velocity,

as shown in Fig. 15 of Chap. III, and theoretically half of this velocity is imparted in front of and above the wing, and the other half below and behind. This induced downflow is present in the model wing tests from which the airfoil coefficients used in the blade-element theory are obtained; the inflow indicated by the momentum theory is therefore automatically taken into account in the simple blade-element theory. As shown in Chap. III, however, the induced downflow is widely different for different aspect ratios, being zero for infinite aspect ratio. Most model airfoil tests are made with rectangular wings having an arbitrarily chosen aspect ratio of 6, and there is no reason to

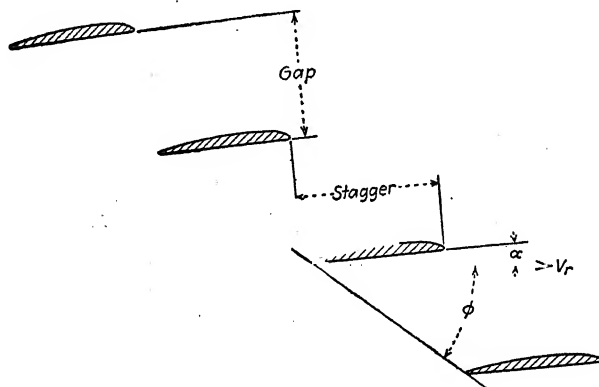


Fig. 30.

suppose that the downflow in such a test corresponds to the inflow for each element of a propeller blade. In fact, the general conclusion drawn from an exhaustive series of tests,<sup>1</sup> in which the pressure distribution was measured over 12 sections of a model propeller running in a wind tunnel, is that the lift coefficient of the propeller blade element differs considerably from that measured at the same angle of attack on an airfoil of aspect ratio 6. This is one of the greatest weaknesses of the simple blade-element theory.

Another weakness is that the interference between the propeller blades is not considered. The elements of the blades at any

<sup>1</sup> A Consideration of Airscrew Theory in the Light of Data Derived from an Experimental Investigation of the Distribution of Pressure over the Entire Surface of an Airscrew Blade, and also over Airfoils of Appropriate Shapes, by A. Fage, and R. G. Howard, British R. and M. 681, 1921.

particular radius form a cascade similar to a multiplane with negative stagger, as shown in Fig. 30. Near the tips where the gap is large the interference is very small, but in toward the blade roots it is quite large.

In actual propellers there is a tip loss which the blade-element theory does not take into consideration. The thrust and torque forces as computed by means of the theory are therefore greater for the elements near the tip than those found by experiment.<sup>1</sup>

In order to eliminate scale effect, the wind tunnel tests on model wings should be run at the same value of Reynolds number (scale) as the corresponding elements in the propeller blades. Airfoil characteristics measured at such a low scale as, for example, an air velocity of 30 m.p.h. with a 3-in. chord airfoil, show peculiarities not found when the tests are run at a scale comparable with that of propeller elements. The standard propeller section characteristics given in Figs. 20, 21, 24, and 25 (Chap. III) were obtained from high Reynolds-number tests in the Variable Density Tunnel of the N.A.C.A., and, fortunately, for all excepting the thickest of these sections there is very little difference in characteristics at high and low Reynolds numbers. These values may be used with reasonable accuracy as to scale for propellers operating at tip speeds well below the speed of sound in air, and therefore relatively free from any effects of compressibility.

The poor accuracy of the simple blade-element theory is very well shown in a report by Durand and Lesley,<sup>2</sup> in which they have computed the performance of a large number of model propellers (80) and compared the computed values with the actual performances obtained from tests on the model propellers themselves. In the words of the authors:

The divergencies between the two sets of results, while showing certain elements of consistency, are on the whole too large and too capriciously distributed to justify the use of the theory in this simplest form for other than approximate estimates or for comparative purposes.

The airfoils were tested in two different wind tunnels and in one of the tunnels at two different air velocities, and the propeller characteristics computed from the three sets of airfoil data

<sup>1</sup> An Analysis of the Family of Airscrews by Means of the Vortex Theory and Measurements of Total Head, by C. N. H. Lock, and H. Bateman, British R. and M. 892, 1923.

<sup>2</sup> Comparison of Model Propeller Tests with Airfoil Theory, by William

differ by as much as 28 per cent, illustrating quite forcibly the necessity for having the airfoil tests made at the correct scale.

In spite of all its inaccuracies the simple blade-element theory has been a useful tool in the hands of experienced propeller designers. With it a skilful designer having a knowledge of suitable empirical factors can design propellers which usually fit the main conditions imposed upon them fairly well in that they absorb the engine power at very nearly the proper revolution speed. They are not, however, necessarily the most efficient propellers for their purpose, for the simple theory is not sufficiently accurate to show slight differences in efficiency due to changes in pitch distribution, plan forms, etc.

**Example of Analysis with the Simple Blade-element Theory.**—In choosing a propeller to analyze, it is desirable that its aerodynamic characteristics be known so that the accuracy of the calculated results can be checked. It is also desirable that the analysis be made of a propeller operating at a relatively low tip speed in order to be free from any effects of compressibility and that it be running free from body interference. The only propeller tests which satisfy all of these conditions are tests of model propellers in a wind tunnel. We shall therefore take for our example the central or master propeller of a series of model wood propellers of standard Navy form, tested by Dr. W. F. Durand at Stanford University.<sup>1</sup> This is a two-bladed propeller 3 ft. in diameter, with a uniform geometrical pitch of 2.1 ft. (or a pitch-diameter ratio of 0.7). The blades have standard propeller sections based on the R.A.F.-6 airfoil (Fig. 19), and the blade widths, thicknesses, and angles are as given in the first part of Table I. In our analysis we shall consider the propeller as advancing with a velocity of 40 m.p.h. and turning at the rate of 1,800 r.p.m.

For the section at 75 per cent of the tip radius, the radius is 1.125 ft., the blade width is 0.198 ft., the thickness ratio is 0.107, the lower camber is zero, and the blade angle  $\beta$  is 16.6°.

The forward velocity  $V = 40$  m.p.h.

$$\begin{aligned} &= \frac{40 \times 88}{60} \\ &= 58.65 \text{ ft. per sec.,} \end{aligned}$$

<sup>1</sup>Tests on Thirteen Navy Type Model Propellers, by W. F. Durand,

and

$$\begin{aligned} n &= \frac{1,800}{60} \\ &= 30 \text{ r.p.s.} \end{aligned}$$

$$\begin{aligned} \text{The path angle } \phi &= \arctan \frac{V}{2\pi r n} \\ &= \arctan \frac{58.65}{2\pi \times 1.125 \times 30} \\ &= 15.5^\circ. \end{aligned}$$

The angle of attack is therefore

$$\begin{aligned} \alpha &= \beta - \phi \\ &= 16.6^\circ - 15.5^\circ \\ &= 1.1^\circ. \end{aligned}$$

From Fig. 21, for a flat-faced section of thickness ratio 0.107 at an angle of attack of  $1.1^\circ$ ,  $\gamma = 3.0^\circ$ , and, from Fig. 20,  $C_L = 0.425$ . (For sections having lower camber,  $C_L$  should be corrected in accordance with the relation given in Fig. 23, and  $\gamma$  is given the same value as that for a flat-faced section having the upper camber only.)

Then

$$\begin{aligned} K &= \frac{C_L b}{\sin^2 \phi \cos \gamma} \\ &= \frac{0.425 \times 0.198}{0.2672^2 \times 0.999} \\ &= 1.180, \end{aligned}$$

and

$$\begin{aligned} T_c &= K \cos (\phi + \gamma) \\ &= 1.180 \times \cos 18.5^\circ \\ &= 1.119. \end{aligned}$$

Also,

$$\begin{aligned} Q_c &= K r \sin (\phi + \gamma) \\ &= 1.180 \times 1.125 \times \sin 18.5^\circ \\ &= 0.421. \end{aligned}$$

The computations of  $T_c$  and  $Q_c$  for six representative elements of the propeller are given in convenient tabular form in Table I, and the values of  $T_c$  and  $Q_c$  are plotted against radius in Fig. 31. The curves drawn through these points are sometimes referred

to as the thrust and torque grading curves. The areas under the curves represent

$$\int_0^R T_c dr$$

and

$$\int_0^R Q_c dr,$$

these being the expressions for the total thrust and torque per blade per unit of dynamic pressure due to the velocity of advance. The areas may be found by means of a planimeter,

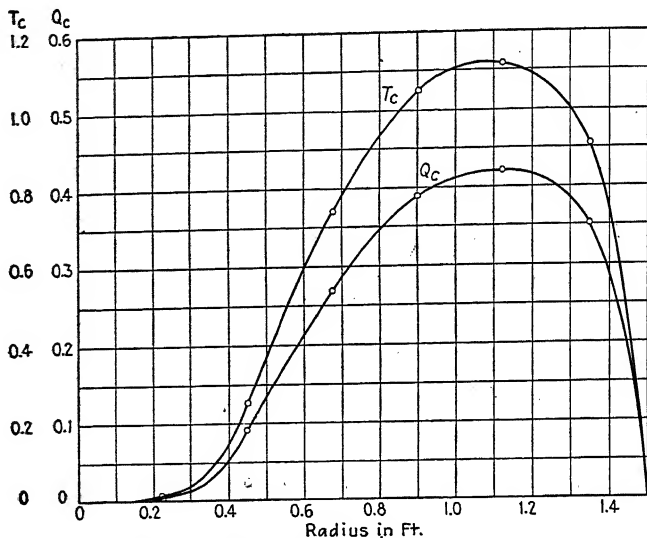


FIG. 31.—Thrust and torque grading curves.

proper consideration, of course, being given to the scales of values, or the integration may be performed approximately (but with satisfactory accuracy) by means of Simpson's rule. In using Simpson's rule the radius is divided into an even number of equal parts, such as ten. The ordinate at each division can then be found from the grading curve. If the original blade elements divide the blade into an even number of equal parts it is not necessary to plot the grading curves, but the curves are advantageous in that they show graphically the distribution of thrust and torque along the blade. They also provide a check upon the computations, for incorrect points will not usually form

TABLE I.—COMPUTATIONS FOR PROPELLER ANALYSIS WITH SIMPLE BLADE-ELEMENT THEORY

$D = 3.0$ ft.	Forward velocity = 40 m.p.h. = 58.65 ft./sec.					
$p = 2.1$ ft.	Rotational velocity = 1,800 r.p.m. = 30 r.p.s.					
$r/R$ .....	0.15	0.30	0.45	0.60	0.75	0.90
$r$ (ft.).....	0.225	0.450	0.675	0.900	1.125	1.350
$b$ (ft.).....	0.225	0.236	0.250	0.236	0.198	0.135
$h_U/b$ .....	0.190	0.200	0.167	0.133	0.107	0.090
$h_L/b$ .....	0.180	0.058	0.007	0.000	0.000	0.000
$\beta$ (deg.).....	56.1	36.6	26.4	20.4	16.6	13.9
$2\pi rn$ .....	42.3	84.7	127.1	169.6	212.0	254.0
$\tan \phi = V/2\pi rn$ .....	1.389	0.693	0.461	0.346	0.277	0.231
$\phi$ (deg.).....	54.2	34.7	24.7	19.1	15.5	13.0
$\alpha = \beta - \phi$ (deg.).....	1.9	1.9	1.7	1.3	1.1	0.9
$\gamma$ (deg.).....	3.9	4.1	3.6	3.3	3.0	3.0
$\cos \gamma$ .....	0.998	0.997	0.998	0.998	0.999	0.999
$C_L$ .....	0.084	0.445	0.588	0.514	0.425	0.356
$\sin \phi$ .....	0.8111	0.5693	0.4179	0.3272	0.2672	0.2250
$K = \frac{C_L b}{\cos \gamma \sin^2 \phi}$ .....	0.0288	0.325	0.843	1.135	1.180	0.949
$\phi + \gamma$ (deg.).....	58.1	38.8	28.3	22.4	18.5	16.0
$\cos (\phi + \gamma)$ .....	0.5280	0.7793	0.8805	0.9245	0.9483	0.9613
$T_c = K \cos (\phi + \gamma)$ .....	0.0152	0.253	0.742	1.050	1.119	0.912
$\sin (\phi + \gamma)$ .....	0.8490	0.6266	0.4741	0.3811	0.3173	0.2756
$Q_c = Kr \sin (\phi + \gamma)$ ...	0.0055	0.0916	0.270	0.389	0.421	0.353

If the abscissas are denoted by  $r$  and the ordinates at the various divisions by  $y_1, y_2, \dots, y_{11}$ , according to Simpson's rule the area with ten equal divisions will be

$$\int_0^R F(r)dr = \frac{\Delta r}{3}[y_1 + 2(y_3 + y_5 + y_7 + y_9) + 4(y_2 + y_4 + y_6 + y_8 + y_{10}) + y_{11}].$$

The area under the thrust-grading curve of our example is therefore

$$\begin{aligned} \int_0^R T_c dr &= \frac{0.15}{3}[0 + 2(0.038 + 0.600 + 1.050 + 1.091) + \\ &\quad 4(0 + 0.253 + 0.863 + 1.120 + 0.912) + 0] \\ &= 0.9075, \end{aligned}$$

and in like manner

$$\int_0^R Q_c dr = 0.340$$

The above integrations have also been made by means of a planimeter, and the average results from five trials agree with those obtained by means of Simpson's rule within one-fourth of one per cent.

The thrust of the propeller in standard air is

$$\begin{aligned} T &= \frac{1}{2} \rho V^2 B \int_0^R T_c dr \\ &= \frac{1}{2} \times 0.002378 \times 58.65^2 \times 2 \times 0.9075 \\ &= 7.42 \text{ lb.}, \end{aligned}$$

and the torque is

$$\begin{aligned} Q &= \frac{1}{2} \rho V^2 B \int_0^R Q_c dr \\ &= \frac{1}{2} \times 0.002378 \times 58.65^2 \times 2 \times 0.340 \\ &= 2.78 \text{ lb.-ft.} \end{aligned}$$

The power absorbed by the propeller is

$$\begin{aligned} P &= 2\pi nQ \\ &= 2 \times \pi \times 30 \times 2.78 \\ &= 524 \text{ ft.-lb. per sec.} \end{aligned}$$

or

$$\begin{aligned} HP &= \frac{524}{550} \\ &= 0.953, \end{aligned}$$

and the efficiency is

$$\begin{aligned} \eta &= \frac{TV}{2\pi nQ} \\ &= \frac{7.42 \times 58.65}{524} \\ &= 0.830. \end{aligned}$$

The above-calculated performance compares with that measured in the wind tunnel as follows:

	Calculated	Model test
Power absorbed, horsepower.....	0.953	1.073
Thrust, pounds.....	7.42	7.77
Efficiency.....	0.830	0.771

The power as calculated by the simple blade-element theory



per cent low, and the efficiency is about 8 per cent high. Of course, a differently calculated performance would have been obtained if propeller-section characteristics from tests on the same series of airfoils in a different wind tunnel had been used; but the variable-density tunnel tests are probably the most reliable of all.

Some light may be thrown upon the discrepancy between the calculated and observed performance by referring again to the pressure distribution tests on a model propeller.<sup>1</sup> In these

#### AERODYNAMIC DATA OF AEROFOIL SECTION C.

- Direct measurement of forces on an aerofoil of aspect ratio 6 with square ends
- Calculated from the pressure distribution over the median section of the aerofoil of aspect ratio 6
- × Calculated from the pressure distribution over the section C of an aerofoil shaped as an airscrew blade but without twist

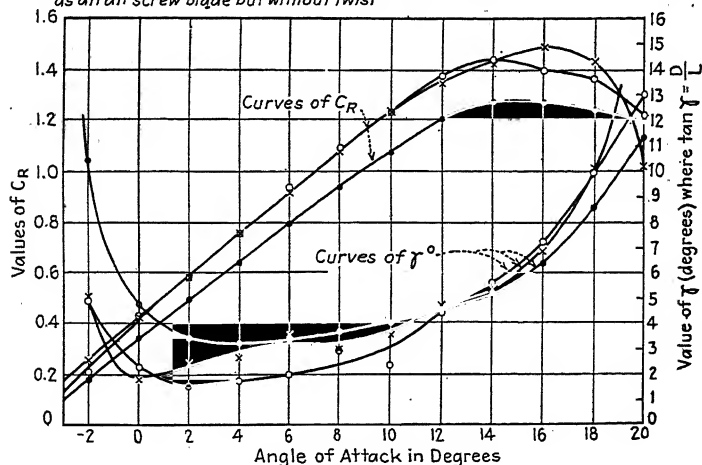


FIG. 32.—(From R. and M. 681.)

tests the pressure distribution over several sections of a propeller blade was measured while the propeller was running in a wind tunnel, and the three following sets of tests were made on corresponding airfoils:

- a. Standard force tests on airfoils of aspect ratio 6.
- b. Tests of the pressure distribution on the median section of the above airfoils of aspect ratio 6.

<sup>1</sup> A Consideration of Airscrew Theory in the Light of Data Derived from an Experimental Investigation of the Distribution of Pressure over the Entire Surface of an Airscrew Blade, and also over Airfoils of Appropriate Shapes, by A. Fage and R. G. Howard, British R. and M. 681, 1921.

c. Tests of the pressure distribution over a special airfoil made in the form of one blade of the propeller, but without twist, the pressure being measured at the same sections as in the propeller blade.

The results of these three sets of airfoil tests are shown for the section at three-fourths of the tip radius in Fig. 32, which has been taken from the report. It will be noticed that the coefficients of resultant force  $C_R$  agree quite well for the median section of the airfoil of aspect ratio 6 and the corresponding section of the special propeller-blade airfoil but that the resultant force coefficient for the entire airfoil of aspect ratio 6 is considerably lower. It is natural, then, that the calculated thrust and power of a propeller should be too low when based on airfoil characteristics for aspect ratio 6.

## CHAPTER V

### MODIFICATIONS OF THE BLADE-ELEMENT THEORY

Many modifications to the simple blade-element theory have been suggested in order to make it more complete and to improve its accuracy. Most of these modified theories attempt to take into account the blade interference, and, in some of them, attempts are also made to eliminate the inaccuracy due to the use of airfoil data from tests on wings having a finite aspect ratio, such as 6. The first modification to be made was in the nature of a combination of the simple Drzewiecki theory with the Froude momentum theory.

**The Combined Momentum and Blade-element Theory.**—According to the momentum theory, half of the increase in velocity in the slipstream occurs in front of the propeller. The forward velocity of the propeller with respect to the air passing through the propeller disc is therefore greater than the aircraft velocity  $V$ . In the combined theory the inflow is calculated by means of the momentum theory, and the sum of the inflow velocity and the aircraft velocity  $V$  is used in place of  $V$  in calculating the angles of attack and the forces on the blade elements.

When an airfoil of aspect ratio 6 (or any other finite aspect ratio) is tested in an airstream, there is a certain downwash, and the portion of the downwash which occurs in front of the airfoil corresponds to the inflow to a propeller blade. Thus, part of the inflow, and usually the larger part of it, is inherently accounted for in the airfoil tests, although not correctly, for the conditions in the propeller do not necessarily correspond to those for aspect ratio 6. Now since a certain portion of the inflow is present in the model wing tests as downwash, the value of one-half the wake velocity does not apply, and the portion of the wake velocity representing the inflow correction is, in practice, nothing more than an empirical factor, ranging in value from one-third to two-thirds, to make the calculated performance fit the actual. Obviously any value greater than

*Calculation of Inflow.*—The inflow is calculated by equating the thrust to the momentum imparted to the air per unit time. For an elemental annulus of a propeller the relation for axial inflow is

$$\begin{aligned}dT &= \text{mass per unit time} \times \text{velocity imparted} \\&= 2\pi r dr V(1 + xb)\rho bV \\&= 2\pi\rho V^2 b(1 + xb)r dr,\end{aligned}$$

where  $x$  is an empirical factor representing the ratio of the inflow to the total increase of velocity in the wake  $bV$ .

The air in passing through a screw propeller having both thrust and torque receives not only an increase in axial velocity but a rotational velocity or twist as well. This rotational velocity in the wake may be calculated by equating the torque to the rate of change of angular momentum. For an elemental annulus the relation is

$$\begin{aligned}dQ &= \text{mass per unit time} \times \text{tangential velocity} \times \text{radius} \\&= 2\pi r dr V(1 + xb)\rho wr \\&= 2\pi\rho Vw(1 + xb)r^2 dr,\end{aligned}$$

where  $w$  is the tangential velocity in the wake and is in the direction of the torque.

According to the Prandtl airfoil theory,<sup>1</sup> there can be no rotational inflow in front of the propeller, and this has been shown by experiment to be substantially true.<sup>2</sup> There is, however, an interference flow in the plane of the blades themselves, the air being carried around a certain amount in the direction of the torque before it has passed entirely through the propeller. This rotational interference flow is ordinarily very small and is usually neglected in the application of the combined theory. As in the case of the axial inflow, the greater portion of it is taken into account in the use of airfoil data for aspect ratio 6, although not, of course, accurately.

In the routine application of the combined theory it is customary not only to neglect rotation but also to calculate only the average axial inflow for the entire propeller instead of that for each element. Sometimes the central portion of the propeller

<sup>1</sup> "Aerofoil and Airscrew Theory," by H. Glauert, Cambridge University Press, p. 209, 1926.

<sup>2</sup> The Measurement of Airflow round an Airscrew, by C. N. H. Lock and H. Bateman, British R. and M. 955, 1924. An Investigation into the Nature of the Flow in the Neighborhood of an Airscrew by J. R. Pannell



These can be written

$$\begin{aligned}dT &= \frac{1}{2}\rho u^2 T_c' dr, \\dQ &= \frac{1}{2}\rho u^2 Q_c' dr,\end{aligned}$$

where

$$\begin{aligned}T_c' &= K' \cos(\phi' + \gamma), \\Q_c' &= K' r \sin(\phi' + \gamma),\end{aligned}$$

and

$$K' = \frac{C_{Lb}}{\sin^2 \phi' \cos \gamma}.$$

The efficiency of an element according to the combined theory is then

$$\begin{aligned}\eta &= \frac{dT V}{dQ 2\pi n} \\&= \frac{\tan \phi'}{(1 + xb) \tan(\phi' + \gamma)}.\end{aligned}$$

The total thrust and torque for the whole propeller are found in the same manner as with the simple blade-element theory. In fact, the entire procedure is the same except that  $u$ ,  $\phi'$ , and  $\alpha'$  are substituted respectively for  $V$ ,  $\phi$ , and  $\alpha$ .

*Limitations of the Combined Theory.*—The combined momentum and blade-element theory is subject to the same limitations as the simple blade-element theory regarding the use of airfoil data from tests of model wings having a finite aspect ratio and with regard to tip losses and scale effect. Theoretically the only possible point of improvement over the simple theory is that it may be said that the empirical inflow factor takes into account, in a rough manner, the blade interference. It does this very inaccurately, however, for the factor  $x$ , representing the portion of the added velocity of the slipstream which occurs in front of the propeller, should not actually be a constant for all propellers but should vary considerably even when only one set of airfoil data is used. From the practical point of view, it seems to be a fact that, in general, analyses made by means of the simple theory come closer to the measured propeller performance than those made with the combined or inflow theory.<sup>1</sup> This is the case with our example in the last chapter, where the power and thrust calculated by means

<sup>1</sup> See "The Design of Screw Propellers for Aircraft," by H. C. Watts, Appendix to Chap. VII, *Lanchester's Aeroplanes and the Propeller*.

of the simple theory were low. Since any amount of inflow would reduce the effective angle of attack of the blade elements, the power and thrust calculated by means of the combined theory would be even lower.

It seems that the combined Froude-Drzewiecki theory, although it has been widely used in the past, is gradually being abandoned for more accurate methods of analysis and will probably soon pass out of use entirely.

**The Blade-element Theory with Multiplane Interference Corrections.**—As stated in Chap. IV and illustrated in Fig. 30, the elements of the blades of a propeller at any given radius may be considered as forming an infinite multiplane having negative stagger. The interference effect on an element caused by the corresponding elements of the other blades, and also by the position of the original element itself on previous and following revolutions, is analogous to the downwash and other interference effects on one plane of an infinite multiplane system.

A series of wind tunnel tests has been made by R. McKinnon Wood and associates, in which the changes in lift and drag on an airfoil, due to the interference of a cascade or multiplane series of airfoils, were measured.<sup>1</sup> From the multiplane interference data obtained from these tests, factors have been derived with which propeller elements may be corrected for blade interference. The experiments show that the interference depends on the lift of the airfoils but is practically independent of the drag and therefore of the airfoil section. The interference also depends on the spacing of the airfoils and the angle  $\phi$  between the airflow and the line joining the cascade (Fig. 30). The results of the experiments are given as a correction  $\delta C_L$  to the lift coefficient and another correction  $\epsilon$  to the angle of attack. The angle  $\epsilon$  is in the nature of a downwash angle and is defined by the relation

$$\frac{C_D'}{C_L'} = \left( \frac{C_D - \delta C_D}{C_L - \delta C_L} \right)_a = \left( \frac{C_D}{C_L} \right)_{\alpha - \epsilon} + \tan \epsilon,$$

$C_D'$  and  $C_L'$  being values with interference.

<sup>1</sup> Multiplane Interference Applied to Aircscrew Theory, by R. McK. Wood, F. B. Bradfield, and M. Barker, British *R. and M.* 639, 1919. Also Preliminary Investigation of Multiplane Interference Applied to Propeller Theory, by R. McK. Wood and H. Glauert, British *R. and M.* 620, 1918. Also, Experimental Investigation of a Wing Profile in a Lattice Arrange-

Since  $\epsilon$  was found in the experiments to be practically independent of the drag, it has been assumed that the interference corrections can be expressed as functions of  $C_L$ ,  $\phi$ , and  $S$ , where

$$S = \frac{2\pi r}{Bb},$$

which is the circumference at any radius divided by the total blade width at that radius and represents, in a way, the solidity. The interference corrections  $\delta C_L$  and  $\epsilon$  are plotted in terms of  $C_L$ ,  $\phi$ , and  $S$ , in Figs. 35 and 36.

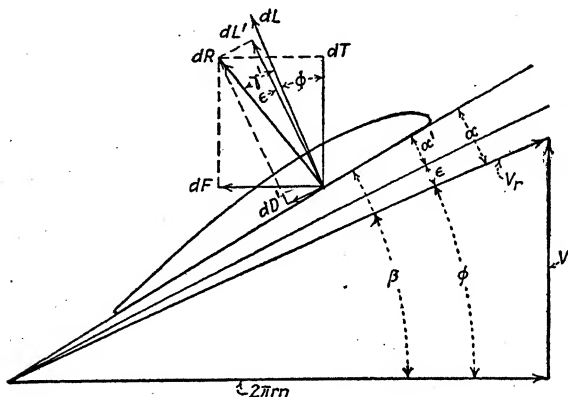


FIG. 34.

*Calculation of the Forces on a Blade Element.*—The forces on a blade element are calculated in the same manner as with the simple blade-element theory, excepting that the airfoil coefficients are corrected for blade (or multiplane) interference. Referring to Fig. 34, the lift component on an element is now

$$dL' = \frac{1}{2}\rho V_r^2 C_L' b dr,$$

where

$$C_L' = C_L - \delta C_L,$$

and the resultant air force on the element is

$$dR = \frac{\frac{1}{2}\rho V_r^2 C_L' b dr}{\cos(\gamma' - \epsilon)}.$$

The thrust component is then

$$\begin{aligned} dT &= dR \cos(\phi + \gamma') \\ &= \frac{\frac{1}{2}\rho V_r^2 C_L' b dr \cos(\phi + \gamma')}{\cos(\gamma' - \epsilon)}, \end{aligned}$$



and since the corrected forces still refer to the original velocity and angle of attack,

$$V_r = \frac{V}{\sin \phi},$$

and

$$dT = \frac{\frac{1}{2}\rho V^2 C_L' b dr \cos(\phi + \gamma')}{\sin^2 \phi \cos(\gamma' - \epsilon)}.$$

Let

$$K = \frac{C_L' b}{\sin^2 \phi \cos(\gamma' - \epsilon)}$$

and

$$T_c = K \cos(\phi + \gamma').$$

Then

$$dT = \frac{1}{2}\rho V^2 T_c dr,$$

and the total thrust for the propeller (of  $B$  blades) is

$$T = \frac{1}{2}\rho V^2 B \int_0^R T_c dr.$$

The component of the resultant force on the element contributing to the torque (Fig. 34) is

$$dF = dR \sin(\phi + \gamma'),$$

the torque on the element is

$$dQ = r dR \sin(\phi + \gamma'),$$

and if

$$Q_c = Kr \sin(\phi + \gamma'),$$

$$dQ = \frac{1}{2}\rho V^2 Q_c dr.$$

Then the torque for the whole propeller is

$$Q = \frac{1}{2}\rho V^2 B \int_0^R Q_c dr.$$

The efficiency of an element with interference corrections is

$$\begin{aligned} \eta &= \frac{dT V}{dQ 2\pi n} \\ &= \frac{dR \cos(\phi + \gamma') V}{dR \sin(\phi + \gamma') 2\pi r n} \\ &= \frac{\tan \phi}{\tan(\phi + \gamma')}. \end{aligned}$$

*The Limitations of the Blade-element Theory with Multiplane Interference Corrections.*—This modification is subject to the same limitations as the simple blade-element theory in regard to the unsuitability of airfoil data obtained with aspect ratio 6, but it is subject to the same limitations in regard to the effect in the

multiplane tests, in which airfoils of aspect ratio 6 were mounted with one end against a large plate. Check tests were run on a series of airfoils of aspect ratio 12 without a plate, however, and although the lift and drag coefficients were different, the correction factors  $\delta C_L$  and  $\epsilon$  agreed quite well with those found with the plate.

The theory with interference corrections necessitates the same apparently justifiable assumption as the simple theory regarding the independence of the neighboring blade elements and has the same limitations concerning tip losses and scale and compressibility effects.

In practice, it has been found that the blade interference is apparently well represented by the multiplane corrections but that with airfoil characteristics obtained from tests in any one particular wind tunnel on model wings of aspect ratio 6, the calculations have a consistent error when compared with model propeller tests. This fact led to the idea of calculating the airfoil characteristics backward from model propeller tests, so that when these calculated airfoil characteristics were used in the blade-element analysis along with multiplane interference corrections, the propeller characteristics could be computed more accurately. This was done, using data from tests on a series of 13 Navy-type model propellers as a basis.<sup>1</sup> The method used would require too much space to describe here, but the details may be found in three *Technical Notes* published by the N.A.C.A.<sup>2</sup> The propeller-section characteristics as calculated from the model propeller test data are given in Fig. 37.

Analyses by means of the blade-element theory with multiplane interference corrections, when made using the calculated airfoil characteristics of Fig. 37, agree with the measured performance of the 13 model propellers throughout the range of the tests within two or three per cent, or within approximately the limits of experimental error of the model propeller tests. Since the family of 13 propellers covers the ordinary range of

<sup>1</sup> Tests on Thirteen Navy Type Model Propellers, by W. F. Durand, N.A.C.A.T.R. 237, 1926.

<sup>2</sup> Propeller Design—Practical Application of the Blade-element Theory, by Fred E. Weick, N.A.C.A.T.N. 235, 1926. Propeller Design—Extension of Test Data on a Family of Model Propellers by Means of the Modified Blade-element Theory, by Fred E. Weick, N.A.C.A.T.N. 236, 1926. Navy Propeller Section Characteristics as Used in Propeller Design, by Fred E.

pitch ratios, blade widths, and blade thicknesses likely to be found in practice, apparently the blade interference is sufficiently well represented by the multiplane interference corrections for ordinary design purposes. In fact, this method with the calculated propeller-section characteristics is used by the writer

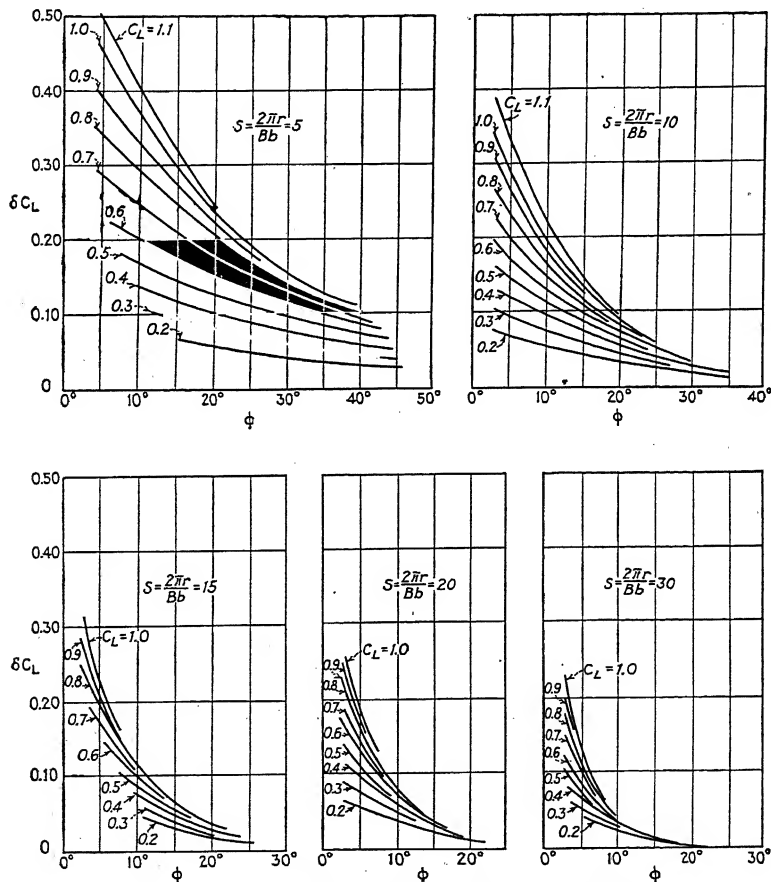


FIG. 35.—Lift correction  $\delta C_L$  for multiplane interference.

in preference to all other forms of the blade-element theory because in his experience it has proved to be the most accurate.

*Example of Analysis by Means of the Blade-element Theory with Multiplane Interference Corrections, Using Calculated Airfoil Characteristics.*—For purposes of comparison, we shall calculate the performance of the same propeller which was

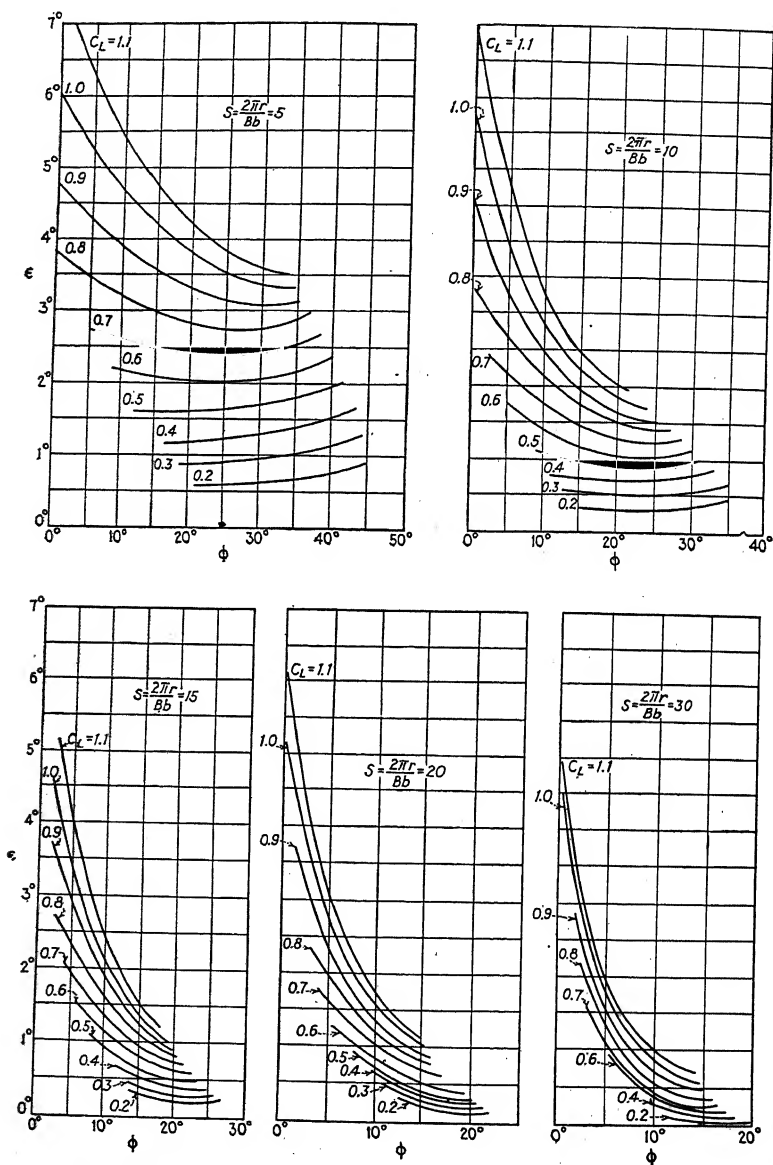


FIG. 36.—Downwash correction  $\epsilon$  for multiplane interference.

analyzed by means of the simple blade-element theory in Chap. IV. The dimensions of the propeller are given again in the first part of Table II. The propeller is advancing with a velocity

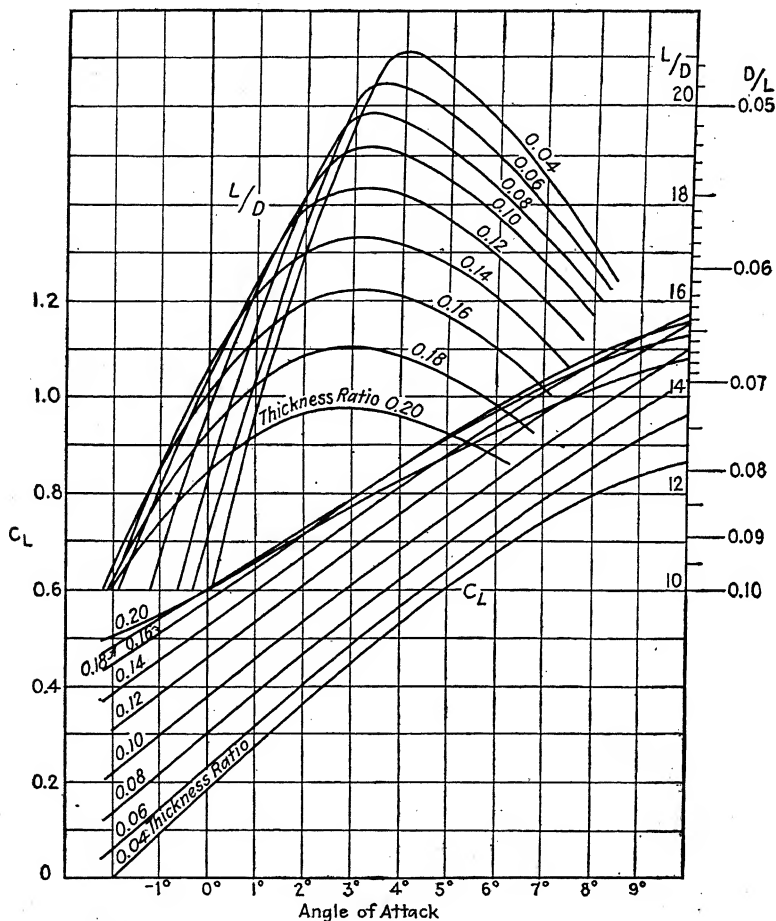


FIG. 37.—Propeller airfoil characteristics calculated from model propeller tests. Standard propeller sections based on R.A.F.-6.

of 40 m.p.h. and turning at the rate of 1,800 r.p.m. We shall run through the analysis, as before, for the section at 75 per cent of the tip radius. For this section, as before,

$$\phi = \arctan \frac{V}{2\pi rn}$$

and the angle of attack is

$$\begin{aligned}\alpha &= \beta - \phi \\ &= 1.1^\circ.\end{aligned}$$

From Fig. 37, for a flat-faced section of thickness ratio 0.107 at an angle of attack of  $1.1^\circ$ ,  $C_L = 0.490$ . (For sections having a convex face,  $C_L$  is corrected in accordance with the relation given in Fig. 23.)

Now, in order to find the multiplane interference corrections it is necessary to calculate the value of  $S$ :

$$\begin{aligned}S &= \frac{2\pi r}{Bb} \\ &= \frac{2 \times \pi \times 1.125}{2 \times .198} \\ &= 17.84.\end{aligned}$$

From Fig. 35, for  $C_L = 0.490$  and  $\phi = 15.5^\circ$ ,  $\delta C_L = 0.050$  for  $S = 15$  and  $\delta C_L = 0.030$  for  $S = 20$ . Interpolating, for  $S = 17.84$ ,  $\delta C_L = 0.035$ . (This interpolation can be made quite accurately, if desired, by finding  $\delta C_L$  for three or four values of  $S$ , plotting a curve of  $\delta C_L$  against  $S$ , and finding  $\delta C_L$  for the desired value of  $S$  from the curve.)

Then

$$\begin{aligned}C_L' &= C_L - \delta C_L \\ &= 0.490 - 0.035 \\ &= 0.455.\end{aligned}$$

From Fig. 36, with proper interpolation, the downwash correction  $\epsilon$  is found to be  $0.5^\circ$ .

Then

$$\begin{aligned}\alpha' &= \alpha - \epsilon \\ &= 0.6^\circ,\end{aligned}$$

and from Fig. 37, the value of  $D/L$  for an angle of attack of  $0.6^\circ$  is 0.0650 for this section.

Since by definition,

$$\tan \gamma' = \left( \frac{C_D'}{C_L'} \right)_\alpha = \left( \frac{D}{L} \right)_{\alpha'} + \tan \epsilon,$$

it follows that

$$\gamma' = \arctan (0.0650 + \tan 0.5^\circ)$$

Then

$$\begin{aligned}
 K &= \frac{C_L' b}{\sin^2 \phi \cos (\gamma' - \epsilon)} \\
 &= \frac{0.455 \times 0.198}{0.2672^2 \times 0.998} \\
 &= 1.264,
 \end{aligned}$$

and

$$\begin{aligned}
 T_c &= K \cos (\phi + \gamma') \\
 &= 1.264 \times \cos 19.7^\circ \\
 &= 1.190,
 \end{aligned}$$

TABLE II.—COMPUTATIONS FOR PROPELLER ANALYSIS WITH MULTIPLANE INTERFERENCE CORRECTIONS AND CALCULATED AIRFOIL DATA

$D = 3.0$ ft.	Forward velocity = 40 m.p.h. = 58.65 ft./sec.					
$p = 2.1$ ft.	Rotational velocity = 1,800 r.p.m. = 30 r.p.s.					
$r/R$ .....	0.15	0.30	0.45	0.60	0.75	0.90
$r$ (ft.).....	0.225	0.450	0.675	0.900	1.125	1.350
$b$ (ft.).....	0.225	0.236	0.250	0.236	0.198	0.135
$h_U/b$ .....	0.190	0.200	0.167	0.133	0.107	0.090
$h_L/b$ .....	0.180	0.058	0.007	0.000	0.000	0.000
$\beta$ (deg.).....	56.1	36.6	26.4	20.4	16.6	13.9
$2\pi r n$ .....	42.3	84.7	127.1	169.6	212.0	254.0
$\tan \phi = V/2\pi r n$ .....	1.389	0.693	0.461	0.346	0.277	0.231
$\phi$ (deg.).....	54.2	34.7	24.7	19.1	15.5	13.0
$\alpha = \beta - \phi$ (deg.).....	1.9	1.9	1.7	1.3	1.1	0.9
$C_L$ .....	0.175	0.535	0.680	0.600	0.490	0.410
$S = 2\pi r/Bb$ .....	3.140	5.99	8.49	11.99	17.84	31.42
$\delta C_L$ .....	0.030	0.070	0.075	0.055	0.035	0.020
$C_L' = C_L - \delta C_L$ .....	0.145	0.465	0.605	0.545	0.455	0.390
$\epsilon$ (deg.).....	0.9	1.7	1.4	0.9	0.5	0.2
$\alpha' = \alpha - \epsilon$ (deg.).....	1.0	0.2	0.3	0.4	0.6	0.7
$(D/L)\alpha'$ .....	0.0730	0.0792	0.7060	0.0652	0.0650	0.0662
$\tan \epsilon$ .....	0.0157	0.0297	0.0244	0.0157	0.0087	0.0035
$\tan \gamma' = (D/L)\alpha' + \tan \epsilon$ .....	0.0887	0.1089	0.0950	0.0809	0.0737	0.0697
$\gamma'$ (deg.).....	5.1	6.2	5.4	4.6	4.2	4.0
$\phi + \gamma'$ (deg.).....	59.3	40.9	30.1	23.7	19.7	17.0
$\sin \phi$ .....	0.8111	0.5693	0.4179	0.3272	0.2672	0.2250
$K = \frac{C_L' b}{\sin^2 \phi \cos (\gamma' - \epsilon)}$ .....	0.0496	0.339	0.868	1.203	1.264	1.041
$\cos (\phi + \gamma')$ .....	0.5105	0.7558	0.8652	0.9157	0.9415	0.9563
$T_c = K \cos (\phi + \gamma')$ .....	0.0253	0.256	0.751	1.101	1.190	0.996
$\sin (\phi + \gamma')$ .....	0.8598	0.6547	0.5015	0.4020	0.3371	0.2924
$Q_c = K r \sin (\phi + \gamma')$ .....	0.0096	0.0998	0.294	0.436	0.479	0.411

and

$$\begin{aligned} Q_c &= Kr \sin (\phi + \gamma') \\ &= 1.264 \times 1.125 \times \sin 19.7^\circ \\ &= 0.479. \end{aligned}$$

The computations of  $T_c$  and  $Q_c$  for the six elements of the propeller are given in Table II.

The procedure of plotting  $T_c$  and  $Q_c$  against the radius, and integrating for the total thrust and torque, is exactly the same as with the simple blade-element theory and gives the following values for thrust, power, and efficiency:

	Calculated	Model test
Power absorbed, horsepower.....	1.077	1.073
Thrust, pounds.....	7.84	7.77
Efficiency.....	0.776	0.771

For this analysis it will be noted that the calculated values are within one per cent of the model test results, but the fact that they are closer than two or three per cent is merely fortuitous.

**Modern Wing Theory Applied to the Blade-element Analysis; the Induction or Vortex Theory of the Propeller.**—The Lanchester-Prandtl wing theory has been applied to propeller analysis by Betz and Prandtl<sup>1</sup> but not in a practical form suitable for the designing of propellers. Glauert, with the aid of a simplifying assumption, was the first to combine the wing theory with the blade-element analysis in a form similar to that of the older blade-element theories familiar to propeller designers,<sup>2</sup> and his method is followed in all essentials here. The method of procedure is changed, however, to facilitate its use.

It will be recalled that, according to the wing theory, a finite wing giving lift is accompanied by a change of direction or down-

<sup>1</sup> *Schraubenpropeller mit geringstem Energieverlust* (The Screw Propeller Having the Least Energy Loss), by A. Betz, with an addendum by L. Prandtl. Math.-phys. class paper, Göttingen, 1919. Also published in "Vier Abhandlungen zur Hydrodynamik und Aerodynamik," pp. 68–92, Göttingen, 1927. Applications of Modern Hydrodynamics to Aeronautics, by L. Prandtl, N.A.C.A.T.R. 116, pp. 53–59, 1925.

<sup>2</sup> "Aerofoil and Airscrew Theory," by H. Glauert, Cambridge University Press, 1926. An Aerodynamic Theory of the Airscrew, by H. Glauert, British R. and M. 786, 1922. Notes on the Vortex Theory of Airscrews, by H. Glauert, British R. and M. 869, 1922.



wash of the airflow. The amount of downwash depends on the lift of the wing and the span, and it becomes zero for a wing having infinite span. In the case of infinite span, the flow past the wing depends only on the shape or profile of the airfoil section.

Now the flow about a finite wing may be divided into two parts: that due to the profile and that due to the downwash. The part due to the profile, which is the local flow at the airfoil, is the same as that for the infinite span wing. This profile or two-dimensional flow is influenced by the downwash only in that the angle of attack is affected to the extent of half the downwash angle. Thus the downwash, or induced downflow, represents an interference flow within which the two-dimensional profile flow takes place.

In the application of the airfoil theory to propeller blade-element analysis, the two-dimensional or profile characteristics are used for the airfoil elements, and the interference flow is calculated from the momentum generated, after the manner of Froude and Rankine. Thus, since only the profile lift and profile drag are used, the questionable aspect ratio effect is eliminated. Also, since the interference flow is determined by the number of blades, their spacing, and the forces on each, the blade interference is accounted for.

In this form of the blade-element theory, as in the others, it is assumed that there is no radial flow through the propeller.

The interference flow is distinguished from the inflow and outflow as follows:

The inflow is the flow immediately in front of the propeller.

The outflow is the flow immediately in back of the propeller.

The interference flow is the average flow through the propeller (described by Glauert as the velocity field of the system of trailing vortices which acts as an interference on the blade elements).

The wake is the final flow in the slipstream far behind the propeller.

*Calculation of the Interference Flow.*—The interference flow at any one point in the propeller plane is periodic, varying as each blade passes. The exact calculation of this periodic flow is difficult and complicated, so that Glauert replaces the actual flow by its average value. This is the simplification previously referred to and is the same as assuming that, for the calculation of the interference flow, the propeller has an

infinite number of blades and therefore constant thrust and torque throughout each annulus.

Considering only the axial component of the airflow through the propeller, the interference flow, inflow, and outflow velocities all have the same value, which, according to the momentum theory, is half the wake velocity. Calling the axial interference velocity  $aV$  and neglecting the rotation in the outflow, the momentum theory yields the following value for the thrust on an elemental ring or annulus:

$$\begin{aligned} dT &= \text{mass per unit time} \times \text{velocity imparted} \\ &= 2\pi r dr V(1 + a)\rho \times 2aV \\ &= 4\pi\rho V^2(1 + a)ardr. \end{aligned}$$

The rotational velocity or twist given to the air flowing through the propeller may be calculated by equating the torque to the rate of change of angular momentum. The rotational interference velocity is equal to half the rotational velocity in the wake, although there can be no rotational inflow.<sup>1</sup> The flow may be visualized by considering the propeller disc as having a certain finite thickness. There is no rotation in front of the disc and full rotation immediately back of it. The rotational interference velocity, or the average value of the rotational velocity passing through the disc, is half the rotational outflow, and the rotation in the outflow is the same as that in the wake. (The rotational velocity can be imparted suddenly because it does not involve a large change in diameter of the slipstream. The increase of axial velocity does involve a considerable change in diameter, which, since the static pressure outside the slipstream is constant all over it, requires a correspondingly large distance in which the change of diameter takes place.) If  $w$  is the tangential interference velocity, the torque for an annulus may be written

$$\begin{aligned} dQ &= \text{mass per unit time} \times \text{tangential velocity} \times \text{radius} \\ &= 2\pi r dr V(1 + a)\rho \times 2w \times r, \end{aligned}$$

and calling the rotational interference factor  $a'$ , where

$$w = a' \times 2\pi rn,$$

<sup>1</sup> The fact that there can be no rotation before the air reaches the propeller is clearly shown by Glauert in his book "Aerofoil and Airscrew Theory." He states in effect that the circulation around the blade and the trailing vortices, which have equal strength but opposite rotation, nullify each other in front of the propeller blades.

the expression for torque becomes

$$dQ = 4\pi\rho V(1+a)(2\pi rn)a'r^2dr.$$

Thus if the total thrust and torque for an elemental annulus are known, the axial and rotational interference factors can be calculated by means of the above equations.

*The Aerodynamic Forces on a Blade Element.*—The forces on a blade element are calculated in much the same manner as with the other types of the blade-element theory, excepting that airfoil characteristics for two-dimensional flow are used (the

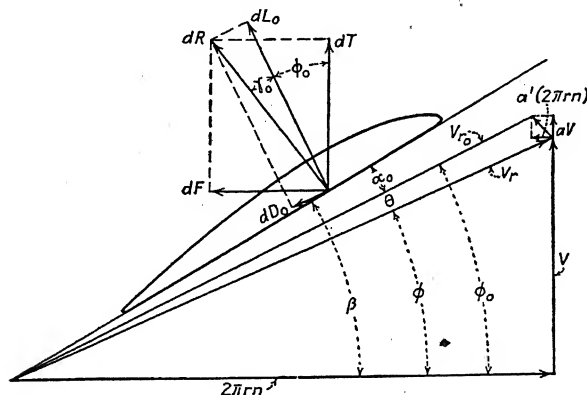


FIG. 38.

subscript zero denoting two-dimensional flow or infinite aspect ratio characteristics), and the angle of attack is based on the interference flow. Referring to Fig. 38, the lift on an element is

$$dL_0 = \frac{1}{2}\rho V_{r0}^2 C_L b dr,$$

and the resultant air force on the element is

$$dR = \frac{\frac{1}{2}\rho V_{r0}^2 C_L b dr}{\cos \gamma_0}.$$

The thrust component is then

$$\begin{aligned} dT &= dR \cos (\phi_0 + \gamma_0) \\ &= \frac{\frac{1}{2}\rho V_{r0}^2 C_L b dr \cos (\phi_0 + \gamma_0)}{\cos \gamma_0}, \end{aligned}$$

and since

$$V_{r0} = \frac{V(1+a)}{\sin \phi_0},$$

$$dT = \frac{\frac{1}{2}\rho V^2(1+a)^2 C_L b dr \cos (\phi_0 + \gamma_0)}{\sin^2 \phi_0 \cos \gamma_0}.$$

Let

$$K = \frac{C_L b (1 + a)^2}{\sin^2 \phi_0 \cos \gamma_0}$$

and

$$T_c = K \cos (\phi_0 + \gamma_0).$$

Then

$$dT = \frac{1}{2} \rho V^2 T_c dr,$$

and the total thrust for the propeller is

$$T = \frac{1}{2} \rho V^2 B \int_0^R T_c dr.$$

The component of the resultant force on the element contributing to the torque (Fig. 38) is

$$dF = dR \sin (\phi_0 + \gamma_0).$$

The torque on the element is

$$dQ = r dR \sin (\phi_0 + \gamma_0),$$

and if

$$Q_c = Kr \sin (\phi_0 + \gamma_0),$$

then

$$dQ = \frac{1}{2} \rho V^2 Q_c dr,$$

and the torque for the whole propeller is

$$Q = \frac{1}{2} \rho V^2 B \int_0^R Q_c dr.$$

The efficiency of an element is now

$$\begin{aligned} \eta &= \frac{dT V}{dQ 2\pi n} \\ &= \frac{dR \cos (\phi_0 + \gamma_0) V}{dR \sin (\phi_0 + \gamma_0) 2\pi r n} \\ &= \frac{\tan \phi}{\tan (\phi_0 + \gamma_0)}, \end{aligned}$$

and since from Fig. 38,

$$\tan \phi = \frac{1 - a'}{1 + a} \tan \phi_0,$$

the expression for efficiency may be written

$$\eta = \frac{(1 - a') \tan \phi_0}{(1 + a) \tan (\phi_0 + \gamma_0)}.$$

This shows that the efficiency is reduced by both the rotational and axial interference factors and also by the profile drag of the

*Procedure in Computing the Performance of a Propeller.*—Glauert suggests calculating the characteristics of a propeller by first assuming a number of angles of attack for each of several blade elements for which  $r$ ,  $b$ ,  $B$ , and  $\beta$  are known.  $C_L$  and  $C_D$  are then found from two-dimensional airfoil data for each angle of attack, and calculations are made for  $a$ ,  $a'$ , the rate of advance, and the thrust and torque per blade element. Curves of thrust and torque are then plotted against rate of advance, and from these curves the thrust and torque for each element at any one desired rate of advance are found, plotted against radius to form grading curves, and integrated to give the thrust and torque for the whole propeller. This is an indirect method of solution which is very cumbersome for analyzing or designing a propeller for a given rate of advance.

A form of procedure suggested by Miller and Harpoothian,<sup>1</sup> in which the interference angle ( $\theta$ , Fig. 38) is calculated and the succeeding steps taken in the same manner as with other forms of the blade-element theory, has been found more satisfactory by the writer.

In order to obtain a solution for  $\theta$ , we may equate the two expressions for  $dT$ , one of which was obtained from the equation for momentum and the other from the forces on the blade elements (the elements of all the blades at a given radius). After simplifying, we get

$$\frac{a}{1+a} = \frac{C_L B b \cos(\phi_0 + \gamma_0)}{8\pi r \sin^2 \phi_0 \cos \gamma_0}.$$

It is convenient here to introduce the quantity

$$S = \frac{2\pi r}{Bb},$$

which is the ratio of the circumference of an annulus to the total blade width. This is the same quantity as is used in the multi-plane interference corrections. Then

$$\frac{a}{1+a} = \frac{C_L \cos(\phi_0 + \gamma_0)}{4S \sin^2 \phi_0 \cos \gamma_0}.$$

By equating the two expressions for  $dQ$ , we get in like manner

$$\frac{a'}{1+a} = \frac{C_L \tan \phi \sin(\phi_0 + \gamma_0)}{4S \sin^2 \phi_0 \cos \gamma_0},$$

<sup>1</sup> Applications of the Aerodynamic Theory of the Propeller, by William H. Miller and Edward Harpoothian, Curtiss Aeroplane and Motor Company, Rept. 3190, 1928.

and from the above two equations it follows that

$$a' = a \tan \phi \tan (\phi_0 + \gamma_0).$$

From Fig. 38 it is apparent that

$$\tan \phi = \frac{(1 - a')}{(1 + a)} \tan \phi_0,$$

from which

$$a' = 1 - (1 + a) \frac{\tan \phi}{\tan \phi_0}.$$

Now equating the two expressions for  $a'$ , we get, after simplification,

$$\frac{a}{1 + a} = \frac{\cot \phi_0 (\tan \phi_0 - \tan \phi)}{1 + \tan \phi \tan (\phi_0 + \gamma_0)},$$

and, in turn, equating the two expressions for  $\frac{a}{1 + a}$  we get

$$\frac{S}{C_L} = \frac{\cos (\phi_0 + \gamma_0) + \tan \phi \sin (\phi_0 + \gamma_0)}{4 \sin \phi_0 \cos \phi_0 (\tan \phi_0 - \tan \phi) \cos \gamma_0},$$

which simplifies to

$$\frac{S}{C_L} = \frac{1 - \tan \gamma_0 \tan (\phi_0 - \phi)}{4 \sin \phi_0 \tan (\phi_0 - \phi)},$$

and since  $\phi_0 - \phi = \theta$ , this may be written,

$$\frac{S}{C_L} = \frac{1 - \tan \gamma_0 \tan \theta}{4 \sin (\phi + \theta) \tan \theta}.$$

The interference angle  $\theta$  is in this equation an implicit function of  $S$ ,  $C_L$ ,  $\phi$ , and  $\gamma_0$ , which are, except for the almost negligible factor  $\gamma_0$ , the same quantities which govern the multiplane interference corrections.

It is interesting to note that the interference angle  $\theta$  is the same factor in the flow past a propeller element that half the downwash angle  $\epsilon/2$  is in the flow past an element of a wing.

Since  $\theta$  is an implicit function, it can not be solved directly from the above equation. It can be solved quite easily, however, by means of the chart in Fig. 39. In finding  $\theta$ , since  $\theta$  affects the angle of attack  $\alpha_0$  and therefore  $C_L$  and  $\gamma_0$ , the correct values of  $C_L$  and  $\gamma_0$  are obtained at the same time. The use of the chart is shown clearly in the example in the next section.

In order to solve the equations for the thrust and torque on a blade element, it is necessary to know only one more factor  $(1 + a)$ . We already have the equation

$$\frac{a}{1+a} = \frac{\cot \phi_0 (\tan \phi_0 - \tan \phi)}{1 + \tan \phi \tan (\phi_0 + \gamma_0)},$$

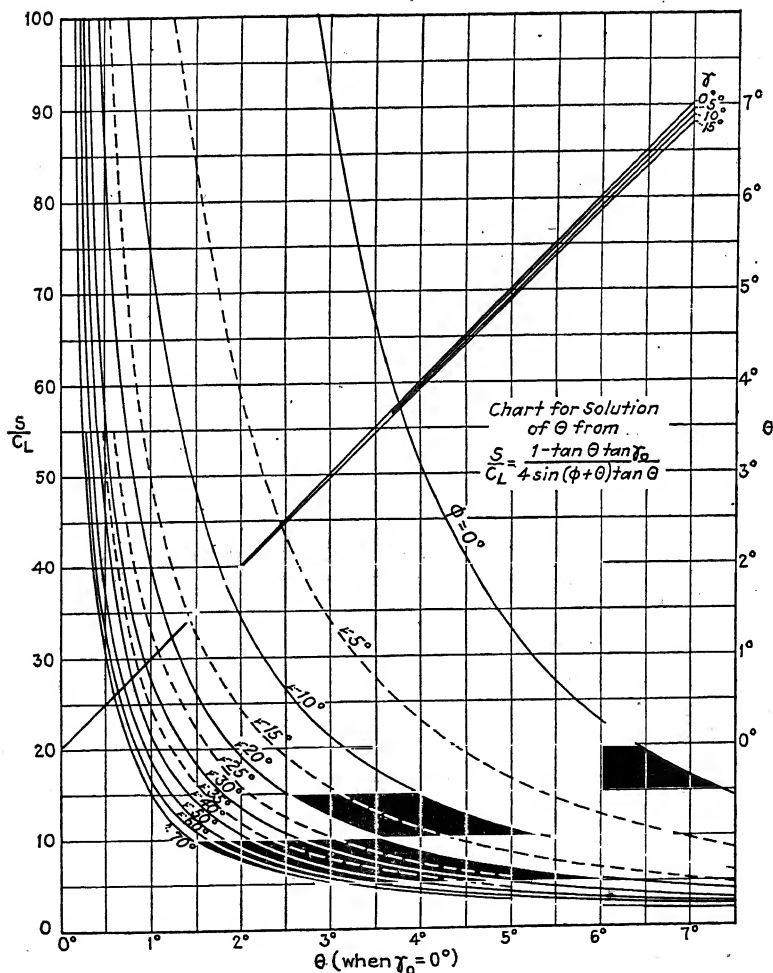


FIG. 39.

and solving for  $1 + a$  we get

$$1 + a = \frac{\tan \phi_0 [1 + \tan \phi \tan (\phi_0 + \gamma_0)]}{\tan \phi [1 + \tan \phi_0 \tan (\phi_0 + \gamma_0)]}$$

Since the solution of this equation is rather tedious, it is also accomplished by means of a chart (Fig. 40). The effect of the angle  $\gamma_0$  is not noticeable on the chart and so  $\gamma_0$  has been omitted.

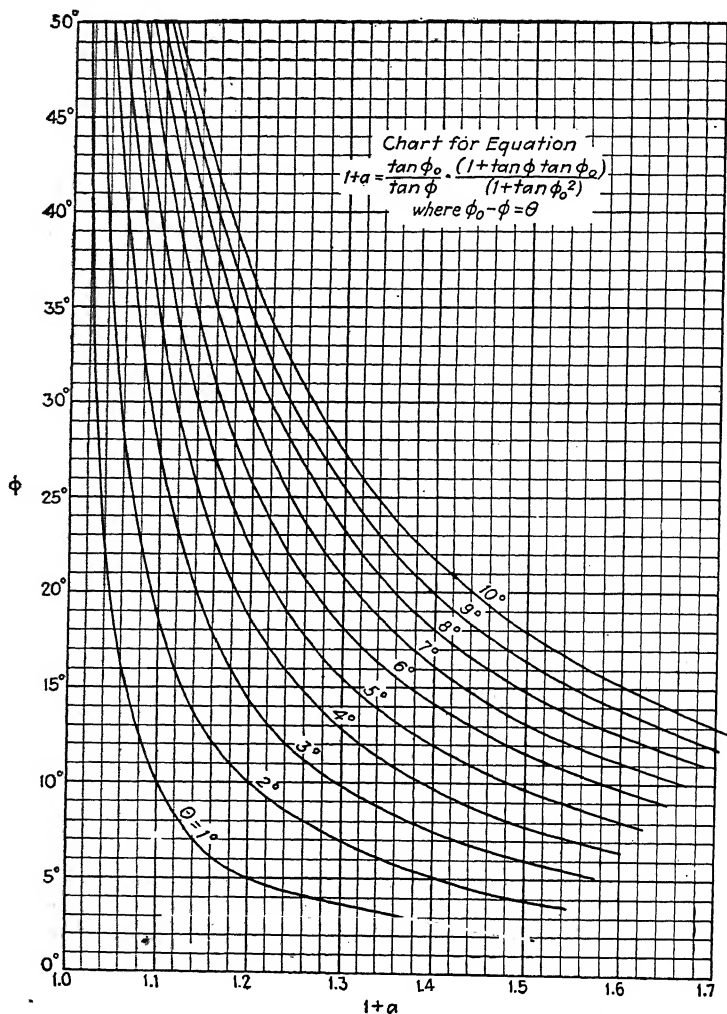


FIG. 40.

*Limitations of the Induction or Vortex Theory of Propeller.—*  
 With the application of airfoil theory to propeller blade-element.



analysis, the aspect ratio question is settled in a very satisfactory manner. The airfoil characteristics are still obtained from wind tunnel tests of model wings, however, and the calculated propeller performance is entirely dependent on the accuracy of the model wing tests, especially with regard to the angle of attack for zero lift and the profile drag. It also depends on the accuracy of the wing theory, which is based on many assumptions and is not entirely unquestionable, particularly where the angle of attack is of importance.

The blade interference is disposed of very neatly by the calculation of the interference flow, based upon the assumption that the thrust and torque are constant with time throughout any one annulus. It is known, however, that the air flow through a propeller is highly periodic in nature; and the assumption that, for the purpose of calculating the interference flow, it may be considered constant may lead to comparatively large errors for highly loaded propellers. In fact, from several comparisons between calculated and test performances made in England<sup>1</sup> it seems possible that the calculated interference flow may be noticeably in error, for in every case the calculated thrust is too high when the blades are working at high angles of attack and slightly low at very low angles of attack. Of course, this may be due to slight errors in the airfoil tests or the model propeller tests, either of which seems quite likely, for just the opposite has been found in some check calculations made on a family of Navy-type model propellers by the propeller research section of the N.A.C.A. In these checks the calculated thrusts were too high at the low angles of attack of the sections and the agreement was better for the higher-pitch propellers (in the British tests it was better for the low). The calculated efficiency for the Navy-type propellers was in every case at least 5 per cent too high.

In general, however, the agreement between calculated and measured performance is fair, being very much better than

<sup>1</sup> Experiments with a Family of Airscrews, Part III. Analysis of the Family of Airscrews by Means of the Vortex Theory and Measurements of Total Head, by C. N. H. Lock and H. Bateman, *British R. and M.* 892, 1923. The Accuracy of the Vortex Theory of Airscrews in the Light of Recent Experimental Work, and Its Application to Airscrew Design, by H. Glauert and C. N. H. Lock, *British R. and M.* 1040, 1926. An Analysis of the Pressure Distribution on a Model Airscrew by Means of the Vortex Theory, by A. Fage, *British R. and M.* 940, 1924.

with either the simple blade-element theory or the combined momentum and blade-element (inflow) theory. It can be used to bring out small relative differences in performance, such as those due to slight changes in pitch distribution along the radius, for which the simple and inflow theories are entirely inadequate. Apparently, however, it is not superior to the multiplane interference method in this respect, and it is considerably less accurate for calculating the performance of a propeller than the multiplane method with computed airfoil characteristics. On the other hand, it is of course possible that with airfoil characteristics for two-dimensional flow computed from model propeller test results, the accuracy of the induction or vortex theory might be equal to or better than that of the multiplane theory.

*Example of Propeller Analysis.*—For our example of analysis by means of the induction or vortex theory we shall again compute the performance of the propeller which was used with the other forms of the blade-element theory, and, as before, we shall run through the analysis in detail for the section at 75 per cent of the tip radius. With a velocity of advance of 40 m.p.h. and a rotational speed of 1,800 r.p.m., we have, as before,

$$\begin{aligned}\phi &= \arctan \frac{V}{2\pi r n} \\ &= 15.5^\circ,\end{aligned}$$

and

$$\begin{aligned}S &= \frac{2\pi r}{Bb} \\ &= 17.84.\end{aligned}$$

The gross angle of attack

$$\begin{aligned}\alpha_0 + \theta &= \beta - \phi \\ &= 16.6^\circ - 15.5^\circ \\ &= 1.1^\circ.\end{aligned}$$

We shall now find  $\theta$  from Fig. 39, and also get  $C_L$  and  $\gamma_0$ . The solution is simple if the steps given here are followed, and after a little practice it can be made in a moment or two. The procedure is as follows:

Assuming a value for  $\theta$  of, say,  $1.0^\circ$ ,

$$\alpha_0 \text{ approx.} = 1.1^\circ - 1.0^\circ = 0.1^\circ.$$

Then for  $\alpha_0 = 0.1^\circ$  and  $h_V/b = 0.107$ ,  $C_L = 0.470$  (from Fig. 24), and  $S/C_L = 17.84/0.470 = 38$ .

From Fig. 39, for  $S/C_L = 38$  and  $\phi = 15.5^\circ$ ,  $\theta$  (when  $\gamma_0 = 0$ )  $= 1.3^\circ$ . (The value of  $\theta$  when  $\gamma_0 = 0$  is found at the bottom of the chart.) Now with our first approximation of  $\theta = 1.3^\circ$ , the above steps are repeated, giving for the second approximation,

$$\begin{aligned}\alpha_0 &= -0.2^\circ, \\ C_L &= 0.438, \\ \frac{S}{C_L} &= 40.8; \\ \theta, (\gamma_0 = 0) &= 1.2^\circ,\end{aligned}$$

and repeating again for the third approximation,

$$\begin{aligned}\alpha_0 &= -0.1^\circ, \\ C_L &= 0.445, \\ \frac{S}{C_L} &= 40.1, \\ \theta, (\gamma_0 = 0) &= 1.2^\circ.\end{aligned}$$

This is the same as our second approximation, and in general it may be said that the second approximation usually gives the final result within the limits of accuracy of our computations, *i.e.*, one-tenth of  $1^\circ$ . We have, however, still to consider  $\gamma_0$ , which affects  $\theta$  very slightly. From Fig. 25, for  $\alpha_0 = -0.1^\circ$  and  $h_w/b = 0.107$ ,  $\gamma_0 = 1.9^\circ$ . Referring again to Fig. 39, the value of  $\theta$  when  $\gamma_0 = 0$ , in our case  $1.2^\circ$ , is projected vertically upward to the sloping lines of  $\gamma_0$ , and then from the value of  $\gamma_0$ , in our case  $1.9^\circ$ , a horizontal line is projected to the right-hand vertical scale for the final value of  $\theta$ . In our case  $\theta$  is still  $1.2^\circ$ , and in fact for nearly all practical cases the effect of  $\gamma_0$  is negligible. Our final values of  $\theta$ ,  $\alpha_0$ ,  $C_L$ , and  $\gamma_0$  are therefore

$$\begin{aligned}\theta &= 1.2^\circ, \\ \alpha_0 &= -0.1^\circ, \\ C_L &= 0.445, \\ \gamma_0 &= 1.9^\circ.\end{aligned}$$

Then, from Fig. 40, for  $\phi = 15.5^\circ$  and  $\theta = 1.2^\circ$ ,  $1 + a = 1.076$ . Next,

$$\begin{aligned}K &= \frac{C_L b (1 + a)^2}{\sin^2 \phi_0 \cos \gamma_0} \\ &= \frac{0.445 \times 0.198 \times (1.076)^2}{\sin^2 16.7^\circ \cos 1.9^\circ} \\ &= 1.234,\end{aligned}$$

$$\begin{aligned}
 T_c &= K \cos (\phi_0 + \gamma_0) \\
 &= 1.234 \cos 18.6^\circ \\
 &= 1.170,
 \end{aligned}$$

and

$$\begin{aligned}
 Q_c &= Kr \sin (\phi_0 + \gamma_0) \\
 &= 1.234 \times 1.125 \sin 18.6^\circ \\
 &= 0.443.
 \end{aligned}$$

The computations for  $T_c$  and  $Q_c$  for the six elements of the propeller are given in Table III.

TABLE III.—COMPUTATIONS FOR PROPELLER ANALYSIS BY MEANS OF THE INDUCTION OR VORTEX THEORY

$D = 3.0$ ft. $p = 2.1$ ft.	Forward velocity = 40 m.p.h. = 58.65 ft./sec. Rotational velocity = 1,800 r.p.m. = 30 r.p.s.					
$r/R$ .....	0.15	0.30	0.45	0.60	0.75	0.90
$r$ (ft.).....	0.225	0.450	0.675	0.900	1.125	1.350
$b$ (ft.).....	0.225	0.236	0.250	0.236	0.198	0.135
$h_U/b$ .....	0.190	0.200	0.167	0.133	0.107	0.090
$h_L/b$ .....	0.180	0.058	0.007	0.000	0.000	0.000
$\beta$ (deg.).....	56.1	36.6	26.4	20.4	16.6	13.9
$2\pi r n$ .....	42.3	84.7	127.1	169.6	212.0	254.0
$\tan \phi = V/2\pi r n$ .....	1.389	0.693	0.461	0.346	0.277	0.231
$\phi$ (deg.).....	54.2	34.7	24.7	19.1	15.5	13.0
$S = 2\pi r/Bb$ .....	3.14	5.99	8.49	11.99	17.84	31.42
$(\alpha_0 + \theta) = \beta - \phi$ (deg.)	1.9	1.9	1.7	1.3	1.1	0.9
$\theta$ , from chart (deg.)....	0.9	1.9	2.2	1.7	1.2	0.7
$\alpha_0$ (deg.).....	1.0	0	-0.5	-0.4	-0.1	0.2
$C_L$ .....	0.172	0.465	0.580	0.520	0.445	0.396
$\gamma_0$ (deg.).....	2.0	2.2	1.9	2.0	1.9	2.0
$1 + a$ .....	1.01	1.043	1.080	1.083	1.076	1.053
$\phi_0 = \phi + \theta$ (deg.)....	55.1	36.6	26.9	20.8	16.7	13.7
$\sin \phi_0$ .....	0.8201	0.5962	0.4524	0.3551	0.2874	0.2368
$K = \frac{C_L b (1 + a)^2}{\sin^2 \phi_0 \cos \gamma_0}$ .....	0.0581	0.336	0.827	1.144	1.234	1.060
$\phi_0 + \gamma_0$ (deg.).....	57.1	38.8	28.8	22.8	18.6	15.7
$\cos (\phi_0 + \gamma_0)$ .....	0.5432	0.7793	0.8763	0.9219	0.9478	0.9627
$T_c = K \cos (\phi_0 + \gamma_0)$ ..	0.0315	0.262	0.725	1.055	1.170	1.020
$\sin (\phi_0 + \gamma_0)$ .....	0.8396	0.6266	0.4817	0.3875	0.3190	0.2706
$Q_c = Kr \sin (\phi_0 + \gamma_0)$ ..	0.0110	0.0947	0.269	0.400	0.443	0.387

The procedure of plotting  $T_c$  and  $Q_c$  against the radius and integrating for total thrust and torque is the same as with the other blade-element analyses and gives the following values for power, thrust, and efficiency:

	Calculated	Model test
Power absorbed, horsepower.....	0.993	1.073
Thrust, pounds.....	7.71	7.77
Efficiency.....	0.829	0.771

The calculated thrust, it will be noted, is within 1 per cent of the test value, but the calculated power absorbed is 7.5 per cent low, and the calculated efficiency is therefore 7.5 per cent too high.

**Résumé, and Comparison of the Various Theories in Their Representation of the Flow through a Propeller.**—All of the forms of the blade-element theory discussed neglect the con-

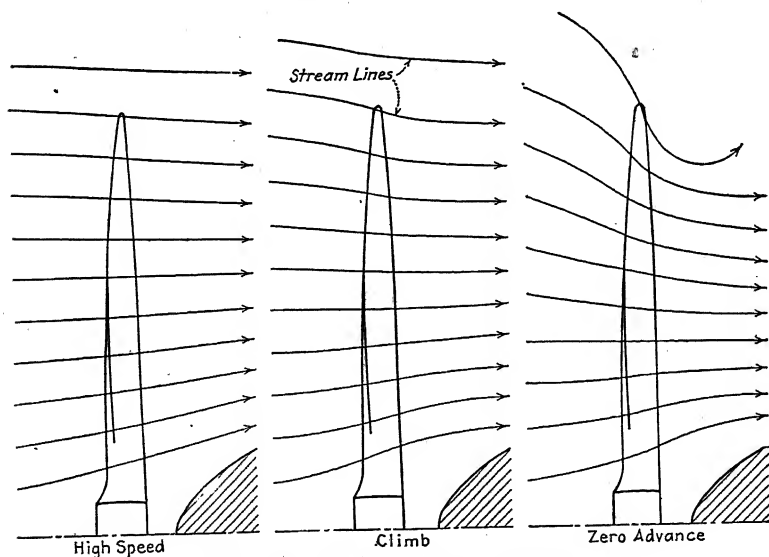


FIG. 41.—Airflow through a propeller.

traction of the slipstream and the radial component of the flow through the propeller. The flow of air through a conventional propeller has been accurately measured<sup>1</sup> for three different rates of advance corresponding to flying at high speed, climbing, and standing still on the ground. The streamlines in a longitudinal plane are shown in Fig. 41. In all three cases there is a

<sup>1</sup> The Measurement of Airflow round an Aircscrew, by C. N. H. Lock and H. Bateman, British R. and M. 955, 1924.

slight radial flow near the propeller axis due to the position of the small guard body, but since this is in the region of the hub it is unimportant. There is very little radial flow even through the tip sections for the high-speed condition and also very little contraction of the slipstream. For the high-speed condition, therefore, which is usually near the point of maximum efficiency of the propeller, it may be concluded that the neglect of radial flow and contraction of the slipstream will not cause appreciable errors in the computation of propeller performance. This is not quite so true for the climbing condition and apparently not true at all for the condition of zero advance, for which calculations with any of the theories may be expected to be seriously in error.

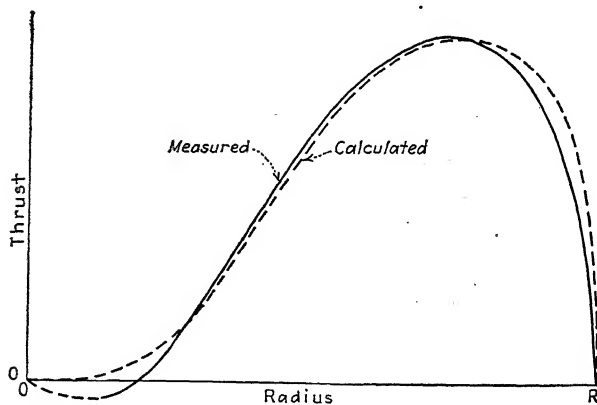


FIG. 42.—Typical calculated and measured thrust grading curves.

All forms of the blade-element theory also neglect tip losses. Figure 42 shows a typical comparison between the calculated thrust grading curve for a propeller and that measured from the difference in total head in front of and behind the propeller. It will be noticed that the calculated thrust is too high near the tip of the blade. This is true for torque, also.

Figure 42 brings out another point: that of the drag, or negative thrust at the center of the propeller. Although none of the forms of the blade-element theory shows a negative thrust at the center of the propeller, actually, due to the hub and a body, which, although it may be small, must be near the center of the propeller, the thrust grading curve usually passes through zero near the hub, and there is a region of negative

thrust at the center. The amount of this negative thrust is very difficult to determine accurately. Sometimes, especially in Great Britain, an amount equal to the drag of a disc the thickness and diameter of the hub boss is subtracted from total thrust. This is, however, a gross overestimate of the actual negative thrust, because the presence of even a very small guard body in back of the propeller tends to reduce the drag of the boss in two ways: It forms, in a sense, a continuation of the boss, relieving the region of low pressure behind the boss which is the cause of most of the drag; and, also, the body tends to slow the air ahead of it in which the hub is located, still further reducing the drag. It is probably more accurate to consider the hub a part of the body (as it actually becomes when a spinner or revolving nose fairing is used) and to neglect the small negative thrust in the propeller computations than to make any such correction as that mentioned above. It is of interest in this connection to note that for our examples the thrust is already low, and deducting a hub correction would make it still lower. The torque, of course, never becomes less than zero excepting at extremely high rates of advance entirely beyond the working range of the propeller.

The independence of the neighboring blade elements is another assumption common to all forms of the blade-element theory, and this seems well substantiated in theory and experiment excepting at the hub and tip, where radial flow and tip losses complicate the flow.

All forms of the blade-element theory are also limited by the accuracy of the airfoil tests upon which the forces are based (excepting when calculated airfoil characteristics are used) and by the effect of scale and the compressibility of the air.

As has been stated, the flow through a propeller is highly periodic in nature, and it is interesting to compare the various theories in regard to the manner in which this periodic flow is accounted for. The variation in velocity at one point behind a propeller has been measured by Drzewiecki by means of a strobometer. The strobometer is a stroboscopic pitot tube connected to a manometer by means of a valve which allows it to operate for only one particular instant during each revolution of the propeller. In his experiments Drzewiecki used a propeller having only one blade, the centrifugal force being balanced by a suitable counterweight, and the instantaneous velocity of the

air was measured at 20 points on a circle behind the blade. The variation in velocity found during one revolution is shown in Fig. 43.

The free air velocity with respect to the propeller was 16 meters per second, and it will be noticed that as the blade passed there was a rapid increase in velocity to over 21 meters per second, then a sudden decrease to about 18 meters per second,

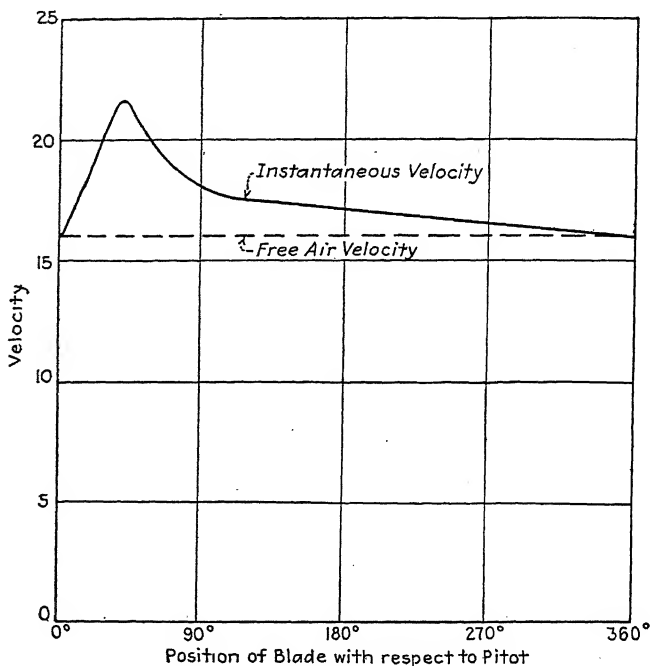


FIG. 43.

followed by a more gradual decrease to the original free air velocity. The interference inflow is evidently in this case zero, for the blade is always attacking air having the free air velocity.

It is also evident, however, that if the propeller had been equipped with two or more blades, the increase in velocity due to one blade would not have died out in 180 deg. or less, and the remaining increase over the free air velocity would have represented an interference velocity. There would also have been an interference velocity remaining after 360 deg. if Drzewiecki's single blade had been wider and consequently more powerful.

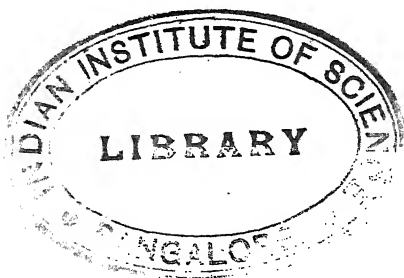


The accurate computation of this highly complicated periodic flow is not at the present time possible. The periodic flow is largely present, however, in the model wing tests. Thus in the simple blade-element theory the periodic nature of the flow is inherently accounted for empirically in the airfoil characteristics used, but incorrectly because of the aspect ratio factor, and also because interference is neglected.

The multiplane interference method takes account of both the periodic nature of the flow and the blade interference empirically, and does it more satisfactorily than any other system, but has the disadvantage of the questionable aspect ratio effect.

In the induction or vortex theory the periodic nature of the flow is neglected in so far as the interference calculations are concerned, but that portion of the local periodic velocity which is present in two-dimensional flow is represented empirically in the airfoil characteristics for infinite aspect ratio. In this theory, therefore, the periodic nature of the flow is not so well represented as in the multiplane interference theory, but the aspect ratio factor is satisfactorily cared for.<sup>1</sup>

<sup>1</sup> For an interesting comparison of various theories of the propeller, the reader is referred to a paper entitled *Review of Airscrew Theories* by Maj. A. R. Low, published in the *Journal of the Royal Aeronautical Society* for February, 1923. The discussion by McKinnon Wood, Fage, Bairstow, Glauert, Lanchester, and others is of particular interest.



## CHAPTER VI

### AERODYNAMIC TESTS ON PROPELLERS

In order to determine the performance characteristics of propellers, and also in order to provide a check for the theoretical computations, aerodynamic tests are made either in flight or in aerodynamic laboratories called wind tunnels. To determine the complete characteristics it is necessary to measure thrust, torque, revolutions, velocity of advance, and the temperature and pressure of the air. The density is calculated from the temperature and pressure. The results are usually given in terms of non-dimensional coefficients involving these quantities, in order to simplify the comparison of propellers with one another.

**Flight Tests.**—It is, of course, desirable that propellers be tested under the conditions in which they are used, and the only tests which fulfil these conditions perfectly are actual flight tests. In flight tests, however, the thrust and torque have not been successfully measured directly<sup>1</sup> but are obtained indirectly from the performance of the airplane and dynamometer tests on the engine.

The lift and drag characteristics of the airplane are first found from glide tests at various angles of attack, and then the airplane is flown full throttle at various air speeds and rates of climb. Measurements are taken of the flight-path angle, attitude of the airplane, air speed, revolutions, temperature, and atmospheric pressure. The thrust credited to the propeller is obtained partially from the drag of the airplane at the same speed and angle of attack, as found from the glide tests, and partially from the portion of the thrust power which produced the climb. This latter may be positive, zero, or negative, depending on the flight path.

<sup>1</sup> Hub dynamometers, or special propeller hubs, which measure the torque or thrust (or both) by means of springs or hydraulic pressure, have been built and tested but have either given inaccurate results or have been impractical to operate. A good, light hub dynamometer would be extremely valuable in determining propeller characteristics and engine power in flight.

The full-throttle power of the engine is usually measured for various revolution speeds on a dynamometer before and after the flight tests, and the engine is credited with the same power at the same revolutions in flight, corrections being applied for temperature and pressure. This procedure introduces an error, for the power of an engine varies considerably with changes in installation, cooling, carbureter altitude control setting, etc. It is also fairly well established that, in general, aircraft engines deliver somewhat less power in the air than under the more ideal conditions of a dynamometer test.

Since neither the thrust nor the power of the propeller can be determined accurately, flight tests are useful mainly as a rough check but will not bring out small differences in propeller characteristics such as those due to changes in pitch distribution, plan form, and blade section.

The flight tests require a great deal of time and labor and the use of several special instruments to measure the angle of flight path, angle of attack, air velocity, etc.

Rough information regarding the power absorbed at one rate of advance of a propeller can also be obtained from ordinary airplane performance tests, in which the high speed is obtained over a measured course in full-throttle level flight. In this type of test the power is usually obtained from a type test on another engine of the same design, providing an even greater chance for error.

**Wind Tunnel Tests on Model Propellers.**—A wind tunnel is an aerodynamic laboratory in which the object to be tested is placed in a moving stream of air. Thus while the relative motion of the body and the air is the same as in steady flight, actually the body does not advance. This makes it possible to support it on balances or scales with which the air forces on the body can be accurately measured. When the body is a propeller, suitable apparatus must be provided to rotate it and measure its torque and thrust. This apparatus is more complicated than that required for ordinary airfoil and drag tests, and probably for that reason nearly all tests on model propellers have been confined to a very few tunnels, notably the Stanford University tunnel in this country and one of the tunnels of the National Physical Laboratory in England.

The Stanford tunnel is of the open-jet, or Eiffel, type, having a large experiment chamber with a stream of air passing through

the center. Figure 44 is a diagram of the tunnel showing the cones used for the entrance and exit of the air. The model propeller being tested is mounted on a long spindle which amounts to little more than a shaft for over a diameter back of the propeller. The body interference may therefore be said to be nil for all practical purposes. Means are incorporated in the driving mechanism to measure the torque, thrust, and revolutions.

The British N.P.L. type of tunnel is similar to that at Stanford University except that the airstream is enclosed throughout the entire tunnel, including the portion passing through the experiment chamber, and the cross-section of the airstream is square instead of circular. This closed type has the disadvantage that it is necessary to apply a correction for wall interference, whereas none is required for the open-jet type for propeller tests.<sup>1</sup>

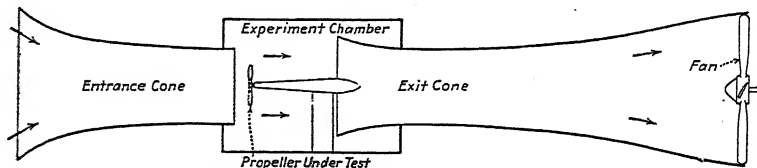


FIG. 44.—Diagram of wind tunnel at Stanford University.

In the British tests the model propellers are driven by an electric motor enclosed in a small guard body, the nose of which is shown in Fig. 41. The whole installation is supported by wires in such a manner that the thrust and torque can be measured.

The model propellers tested in wind tunnels usually have a diameter of 3 ft., although sometimes models as small as 2 ft. in diameter are used. The tests without a body or fuselage are useful for checking the theoretical computation of propeller performance and for finding the effect on propeller characteristics of variation of the number of blades, blade width, and other geometrical proportions. The model test results cannot be applied directly to full-scale aircraft propellers, however, on account of the effect of scale, compressibility, and distortion of the propeller blades in operation. Even when the model propellers are run at the same tip speed as the full-scale propellers, the results are not the same, due apparently to a difference in size and therefore Reynolds number. The body interference can

<sup>1</sup> See The Advantages of an Open-jet Type Wind Tunnel for Airscrew Tests, by H. Glauert and C. N. H. Lock, British *R. and M.* 1023, 1026.

be taken care of in the model propeller tests by providing a model body, and this has been done in a few cases.

**Full-scale Wind Tunnel Propeller Tests.**—In 1927, the N.A.C.A. completed a wind tunnel with a 20-ft. airstream capable of velocities up to 110 m.p.h. in which full-size propellers are tested under conditions that are, for all practical purposes, those of actual flight. The whole airplane, or the fuselage only if desired, is mounted in the experiment chamber and the propeller driven by an actual aircraft engine. This tunnel is of the open-jet, double-return passage type, as shown diagrammatically in Fig. 45. A view of the experiment chamber

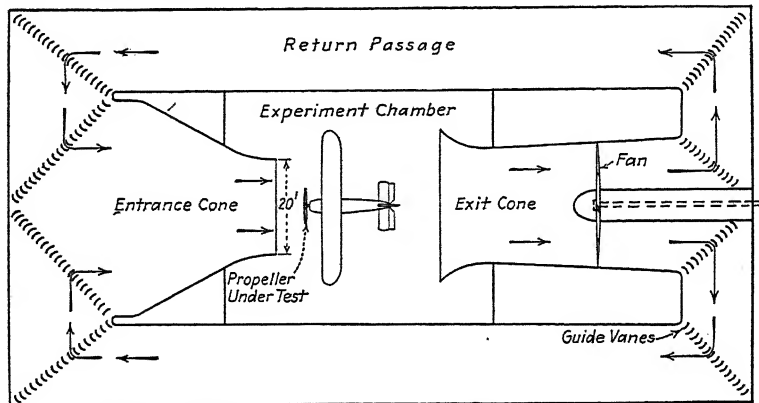


FIG. 45.—Diagram of N.A.C.A. 20-ft. Propeller Research Tunnel.

with a stub-winged cabin monoplane mounted on the balance is given in Fig. 46. The power of the engine is measured by means of a special dynamometer designed to fit inside the fuselage. The thrust, drag, lift, rolling moment, and pitching moment are measured on scales on the floor below. A special electric starter is used to start the aircraft engine and is then swung clear of the airstream during the tests. The deflection and twist of the propeller blades in operation are also measured, by means of a device in which a telescope is sighted on the leading and trailing edges.

Incidentally, the propeller fan shown in the exit cone in Fig. 46 afforded an interesting design problem. It is 28 ft. in diameter, weighs 7,000 lb., and is driven at 375 r.p.m. by a 2,000-hp. Diesel power plant. It was desired to make the blades adjustable in pitch because the exact requirements of

the tunnel could not be known in advance. Wooden blades could not be satisfactorily held in adjustable blade roots without a great deal of development work, and duralumin forgings could not be made in so large a size, and so finally the blades were made of heat-treated cast-aluminum alloy. They have been operating satisfactorily since May, 1927.

**Coefficients and Methods of Plotting Results of Propeller Tests.**—As with airfoils, non-dimensional coefficients are usually used for comparing the characteristics of propellers. In this

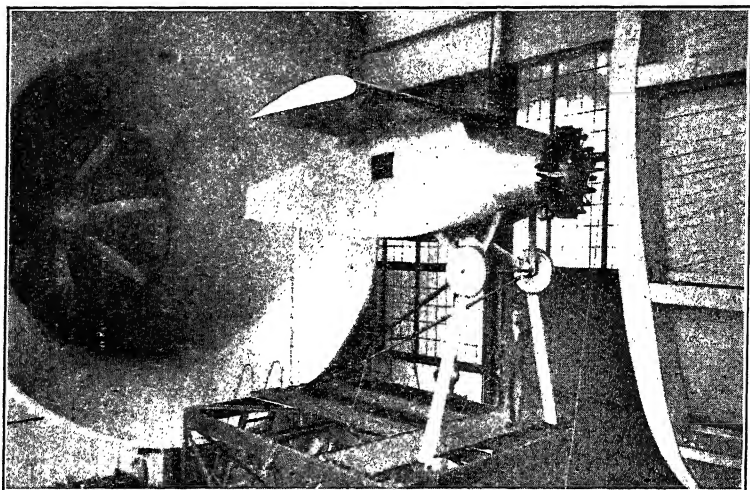


FIG. 46.—View of the 20-ft. Propeller Research Tunnel showing the experiment chamber, balances, exit cone, and propeller fan.

way the results of tests on a propeller can be applied directly to any geometrically similar propeller regardless of size or exact revolutions or velocity of advance, due consideration being given to scale and compressibility effects.

One of the most fundamental characteristic magnitudes affecting propeller performance is the advance per revolution  $V/n$ . This is made non-dimensional by giving it in terms of the diameter, in which case it is often called  $J$  and becomes

$$J = \frac{V}{nD},$$

where  $V$  is the velocity of advance,  $n$  the rate of rotation, and  $D$  the diameter, all in consistent units (such as foot-pound-second or kilogram-meter-second).

Plotting propeller characteristics on a basis of  $V/nD$  is similar to plotting airfoil characteristics on a basis of the angle of attack. The  $V/nD$  is closely related to the angle of advance  $\phi$  and therefore the angle of attack of each section of a given propeller. The relation is

$$\tan \phi = \frac{V}{2\pi rn} = \frac{V}{nD} \times \text{a constant.}$$

According to the blade-element theory, the efficiency of an element is given by the expression,

$$\eta = \frac{\tan \phi}{\tan (\phi + \gamma)}$$

The efficiency therefore depends on the angle  $\phi$ , and, consequently,  $V/nD$ .

The  $V/nD$  is sometimes termed the slip function, because it is intimately connected with the slip of a given propeller. The nominal slip  $S$  is defined by the relation,

$$1 - S = \frac{V/nD}{p/D} = \frac{V}{np}$$

This slip is merely nominal, because it is based on the pitch of the chord of the airfoil section, which has no particular aerodynamic significance when different airfoil sections are used. Its use is sometimes convenient, however.

Coefficients of propeller thrust and torque can be derived from the expressions for the thrust and torque on an element in the simple blade-element theory. The thrust for an element was found to be

$$dT = \frac{1}{2}\rho V^2 C_L b dr \frac{\cos (\phi + \gamma)}{\sin^2 \phi \cos \gamma}$$

Since  $b$  and  $r$  vary directly with the diameter, and since  $\phi$  is a function of  $V/nD$ , the expression for thrust may be written

$$dT \propto \rho V^2 D^2 f\left(\frac{V}{nD}\right),$$

and for the whole propeller,

$$T = T_c \rho V^2 D^2,$$

where the non-dimensional thrust coefficient  $T_c$  is a function of  $V/nD$ .

A similar but slightly different form of the coefficient is sometimes used (particularly in Germany) in which the dynamic

pressure  $q = \frac{1}{2}\rho V^2$  is used in place of  $\rho V^2$ , and the disc area  $A = \pi D^2/4$  in place of simply  $D^2$ . The expression then becomes

$$T = \text{thrust coefficient} \times qA.$$

The torque on an element of a propeller blade, according to the simple blade-element theory, is

$$dQ = \frac{1}{2}\rho V^2 C_L b dr \frac{\sin(\phi + \gamma)}{\sin^2 \phi \cos \gamma},$$

from which it follows that

$$dQ \propto \rho V^2 D^3 f\left(\frac{V}{nD}\right),$$

and for the whole propeller,

$$Q = Q_c \rho V^2 D^3.$$

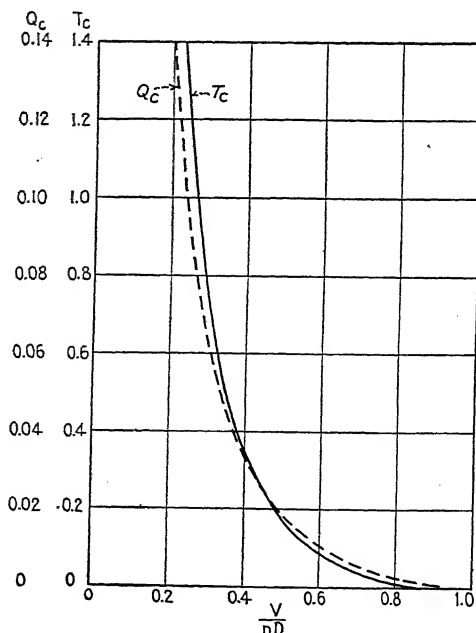


FIG. 47.

Both  $T_c$  and  $Q_c$  are usually plotted against  $V/nD$  as shown for a typical propeller in Fig. 47. The coefficients are applicable to propellers of any size as long as dimensional homogeneity is preserved as to both the propeller and the airflow. In other words, neglecting scale and compressibility effects, the coeffi-



cients apply to all geometrically similar propellers operating at the same value of  $V/nD$ .

The coefficients can be obtained by means of the principle of dimensional homogeneity as well as from the blade-element theory. The coefficients  $T_c$  and  $Q_c$  have more or less passed out of use and given way to more convenient ones with scales covering a smaller range of numbers so that more nearly uniform accuracy is maintained over all portions of the curves. Other non-dimensional coefficients can be obtained from  $T_c$  and  $Q_c$  by merely multiplying or dividing them by some power of the quantity  $V/nD$ . The power can be so chosen as to cancel out

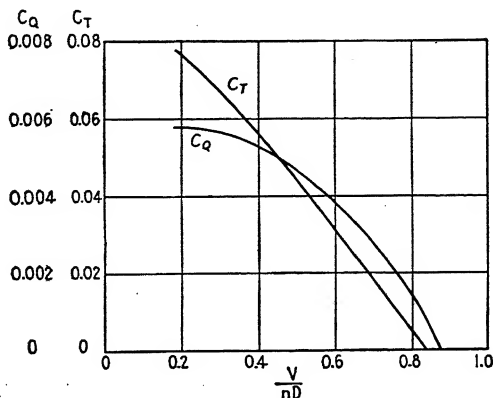


FIG. 48.

of the expression the terms for either the velocity or the diameter. The following coefficients are in terms of the revolution speed instead of the velocity:

$$\begin{aligned}
 C_T &= T_c \times \left( \frac{V}{nD} \right)^2 \\
 &= \frac{T}{\rho n^2 D^4} \\
 C_Q &= Q_c \times \left( \frac{V}{nD} \right)^2 \\
 &= \frac{Q}{\rho n^2 D^5}
 \end{aligned}$$

The coefficients are shown plotted against  $V/nD$  in Fig. 48. They are extensively used in England, where they are called  $k_t$  and  $k_q$ .

In practice it is usually desirable to use coefficients of power and efficiency instead of thrust and torque. If  $P$  represents the power absorbed by the propeller,

$$P = 2\pi nQ$$

and

$$Q \propto \frac{P}{n}$$

Substituting  $P/n$  for  $Q$  in the last equation for the torque coefficient, we get as a power coefficient,

$$C_P = \frac{P}{\rho n^3 D^5}, \quad \checkmark$$

where  $C_P = 2\pi C_Q$ , or, to relate the American power coefficient to the English torque coefficient,  $C_P = 2\pi k_Q$ .

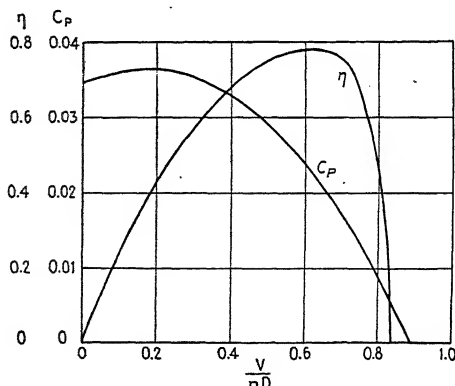


FIG. 49.

The efficiency may then be found from the thrust and power coefficients as follows:

$$\begin{aligned} \eta &= \frac{TV}{P} \\ &= \frac{C_T \rho n^2 D^4 V}{C_P \rho n^3 D^5} \\ &= \frac{C_T}{C_P} \times \frac{V}{nD} \end{aligned}$$

The curves of power coefficient and efficiency, when plotted against  $V/nD$  (Fig. 49), completely determine the aerodynamic characteristics of a propeller

**Speed-power Coefficient.**—All of the above coefficients are useful for comparing the thrust, torque, and power of different propellers. They are not particularly helpful, however, in selecting or designing propellers to fit certain specific requirements for driving some form of aircraft. Furthermore,  $V/nD$  is not a fair basis upon which to compare the efficiencies of various propellers which might fit the same aircraft at the same values of  $V$  and  $n$  but have different diameters and therefore different values of  $V/nD$ .

Frequently tests are made on series of propellers which are geometrically similar except that the pitch is varied in uniform steps. A propeller may be selected from such a series to fit any combination of conditions ( $P$ ,  $n$ ,  $V$ , and  $\eta$ ) required for a particular aircraft. In order to select conveniently the best possible propeller, it is desirable to have a coefficient involving the above required factors but not involving the diameter or any dimension of the propeller. Such a coefficient involving only the known or required factors ( $P$ ,  $n$ , and  $V$ ) is also a fair basis on which to compare the efficiency of different propellers which might be used to drive the same aircraft.

A coefficient involving  $P$ ,  $n$ , and  $V$  without  $D$  may be obtained from  $C_P$  and  $V/nD$  in the following manner:

$$\begin{aligned}\text{Coefficient} &= \frac{(V/nD)^5}{C_P} \\ &= \frac{V^5}{n^5 D^5} \times \frac{\rho n^3 D^5}{P} \\ &= \frac{\rho V^5}{P n^2}\end{aligned}$$

This is sometimes called a speed-power coefficient because it contains the rotational and forward speeds and the power absorbed. The reciprocal of the coefficient as given above was used by Drzewiecki. In this form, however, it covers a very wide range of values, making its use impractical. Admiral Taylor, in dealing with marine propellers,<sup>1</sup> has made use of the square root of the reciprocal of the above coefficient, but even in that case it is necessary to use logarithmic or semilogarithmic scales for plotting the data in order to obtain about the same degree of accuracy throughout the entire range of the curves. For aero-

<sup>1</sup> "The Speed and Power of Ships," by D. W. Taylor, John Wiley & Sons, Inc., 1916.

nautical propellers it has been found more convenient to use the square root of the above coefficient without inverting it, since it then gives curves of positive slope when the familiar term  $V/nD$  is used as the scale of ordinates. This form of speed-power coefficient is known as  $K_s$  and is defined by

$$K_s = \sqrt{\frac{\rho V^5}{P n^2}}$$

The writer has found it still more convenient to use the fifth root of the expression, where

$$\begin{aligned} C_s &= \sqrt[5]{\frac{\rho V^5}{P n^2}} \\ &= V \sqrt[5]{\frac{\rho}{P n^2}} \end{aligned}$$

This has the advantage that it can be plotted on ordinary squared paper giving curves with nearly a uniform slope, so that the accuracy is about the same at both ends. Also, all of the factors

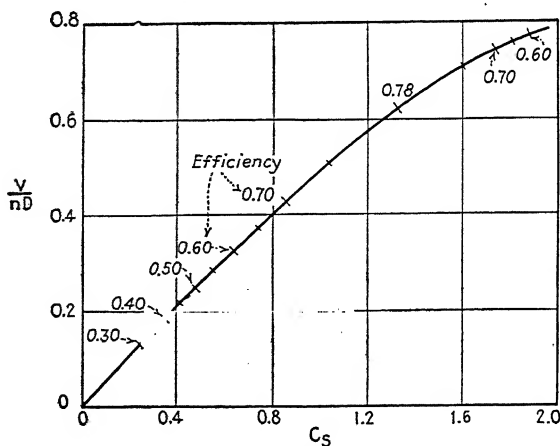


FIG. 50.

are in the coefficient in exactly, or nearly exactly, the power in which they affect the diameter, which is a very desirable feature when the diameter is being solved for. In plotting the results of propeller tests on a basis of  $C_s$  it is desirable to have another non-dimensional coefficient in which the diameter appears in the first power, to use for the scale of ordinates. The coefficient of effective pitch or advance per revolution  $V/nD$  is

quite satisfactory for this purpose. The efficiencies can then be spotted on the curve of  $V/nD$  vs.  $C_s$ , as shown in Fig. 50, or a separate curve can be drawn of efficiency vs.  $C_s$ .

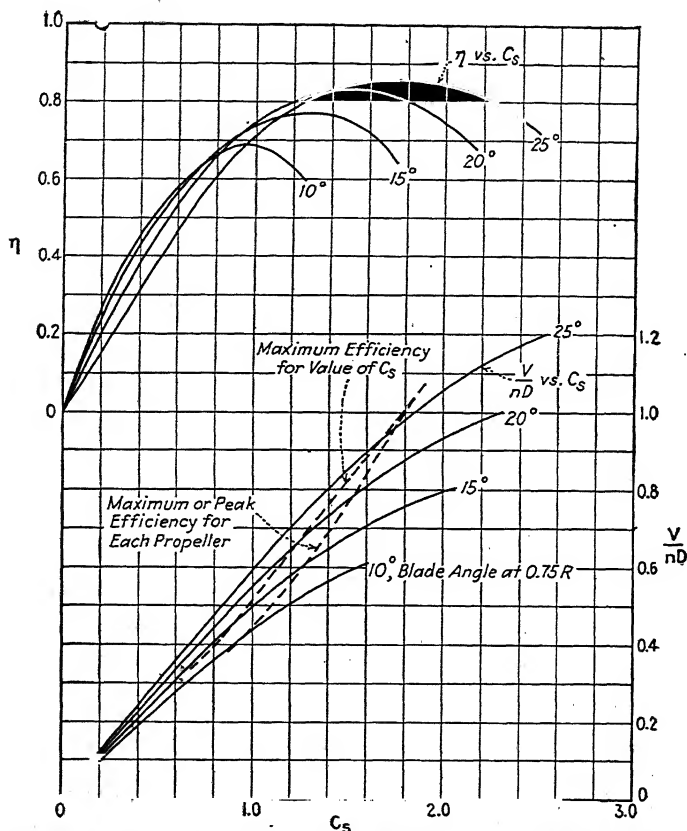


FIG. 51.—Efficiency and  $V/nD$  plotted against  $C_s$  for a series of metal propellers varying in pitch. The series was made by setting a standard adjustable pitch propeller at various blade angles. A two-bladed 9-ft. propeller (Navy Drawing 4412) having a wide tip plan form was tested on a Vought VE-7 airplane with a Wright E-2 engine in the 20-ft. Propeller Research Tunnel. A more accurate working chart made from the same test data is given in Fig. 167.

The curves of  $V/nD$  and efficiency vs.  $C_s$  are given for a series of propellers varying in pitch only, in Fig. 51. The pitch of these propellers is given in terms of the blade angle of the section at three-fourths of the tip radius. The pitch can also be designated by the ratio of the pitch at three-fourths of the tip radius to the

diameter. The relation between this ratio and the angle setting is

$$\begin{aligned}\frac{p'}{D} &= 0.75 \pi \tan \beta' \\ &= 2.36 \tan \beta'\end{aligned}$$

where  $p'$  and  $\beta'$  are the pitch and blade angle respectively of the section at  $0.75R$ . The values of  $p'/D$  for the four propellers in Fig. 51 are 0.42, 0.63, 0.86, and 1.10.

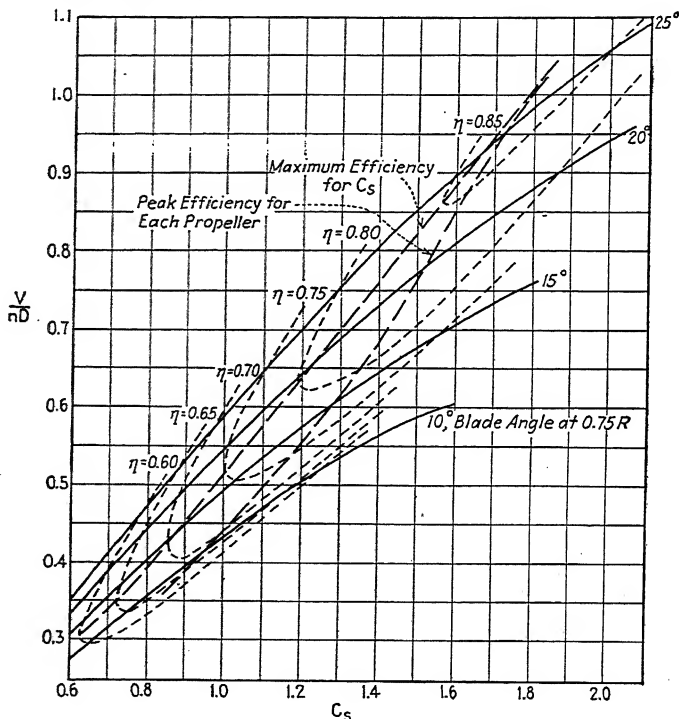


FIG. 52.—Curves of  $V/nD$  vs.  $C_s$  for the same series of propellers as in Fig. 51, with lines of constant efficiency cross-plotted.

It will be noticed that the maximum or peak efficiency for a propeller is not the highest efficiency which can be obtained at the same value of  $C_s$ , but that greater efficiency can be obtained with a propeller of somewhat higher pitch, operating at less than its peak efficiency. One of the dotted curves on Fig. 51 gives the value of  $V/nD$  at which the maximum possible efficiency is obtained for each value of  $C_s$ . The other gives the value of  $V/nD$

for the case of the propeller operating at the peak of its efficiency curve.

Another method of plotting the efficiencies is shown in Fig. 52, where lines of constant efficiency, similar to contour lines, are drawn through the curves of  $V/nD$  vs.  $C_s$ . This makes it possible, where  $C_s$  is known, to determine the efficiency,  $V/nD$ , and pitch, all from one point on the chart. The lines for maximum possible and peak efficiency are also included.

In order to use these charts to select from the series, or family, a propeller having the proper pitch and diameter to absorb a certain power at a given revolution speed and speed of advance, or in other words to fit a certain airplane, it is merely necessary to

1. Calculate  $C_s$  from the known values of  $P$ ,  $n$ ,  $V$ , and  $\rho$ .
2. Determine the pitch ratio (or angle setting for adjustable pitch propellers) from the efficiency curves.
3. From the  $V/nD$  curves, find the value of  $V/nD$  for the above  $C_s$  and pitch ratio.
4. Knowing  $V$ ,  $n$ , and  $V/nD$ , solve for  $D$ .

This method is very simple and can also be used to find the blade-angle setting which is required to make a propeller of known diameter absorb a given power at given values of the revolutions and air speed. In fact, it provides an easy and quick solution for any three of the factors  $P$ ,  $n$ ,  $V$ ,  $\rho$ ,  $D$ ,  $p$ , and  $\eta$ , if four of them are known or assumed. It is used in the method of propeller design, or, more properly, selection, described in detail in Chap. XVII, in which only the propeller as a whole is considered.

The calculation of  $C_s$  is made quite simply and directly from terms of m.p.h., r.p.m., and horsepower, by means of the scales of  $HP^{1/2}$  and  $RPM^{3/2}$  and the equation given in Fig. 53.

The use of the method is best shown by means of an example. Suppose that it is desired to select the propeller giving the highest possible speed on an airplane with an engine developing 200 hp. at 1,800 r.p.m., a speed of 125 m.p.h. at sea level being expected.

Using the scales of Fig. 53,

$$\begin{aligned} C_s &= \frac{0.638 \times 125}{200^{1/2} \times 1,800^{3/2}} \\ &= \frac{0.638 \times 125}{2.882 \times 20.08} \\ &= 1.38. \end{aligned}$$

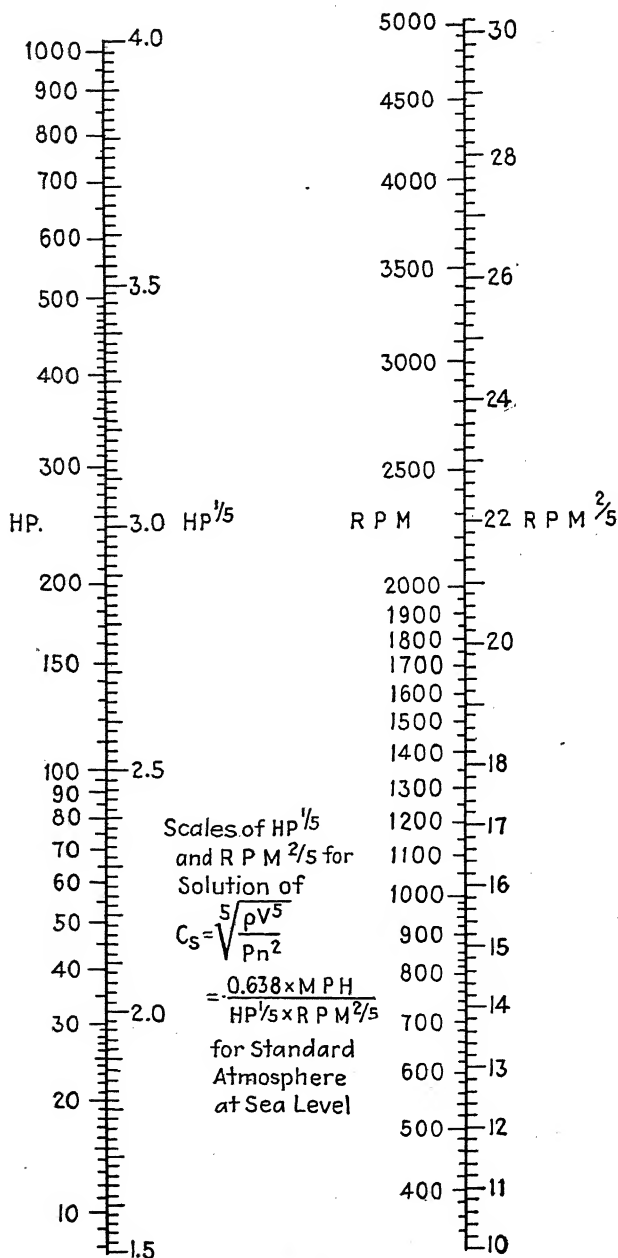


FIG. 53.



To obtain the highest possible speed, the highest possible propeller efficiency is desired at the high-speed condition of operation, *i.e.*, value of  $C_s$ . For the point at which the line of  $V/nD$  for maximum possible efficiency crosses  $C_s = 1.38$ , we find that  $V/nD = 0.75$  and the pitch is given by the blade angle 22 deg. at  $0.75R$  (Fig. 51 or Fig. 52).

The diameter is then

$$\begin{aligned} D &= \frac{88 \times \text{MPH}}{\text{RPM} (V/nD)} \\ &= \frac{88 \times 125}{1,800 \times 0.75} \\ &= 8.15 \text{ ft.} \end{aligned}$$

The efficiency of this propeller is 0.83. If with this efficiency the thrust horsepower is more or less than the amount required to drive the airplane at 125 m.p.h., the new speed may necessitate the selection of a slightly different propeller.

For a second example let us assume that a propeller of our series having a diameter of 9.0 ft. is on hand and that the blade-angle setting which will make it fit the above airplane is desired. In this case  $C_s$  remains the same at 1.38, but the  $V/nD$  becomes

$$\begin{aligned} \frac{V}{nD} &= \frac{88 \times 125}{1,800 \times 9} \\ &= 0.68. \end{aligned}$$

Now from either Fig. 51 or Fig. 52, for  $C_s = 1.38$  and  $V/nD = 0.68$ , the blade-angle setting is found to be 17.5 deg. at  $0.75R$ , and the efficiency is 0.81.<sup>1</sup>

**Eiffel Logarithmic Diagrams.**—Another method for choosing a propeller, which has had some use, is that of the logarithmic diagram devised by Eiffel.<sup>2</sup> In this type of chart,  $C_P$  is plotted against  $V/nD$  in a manner similar to that of Fig. 49, except that logarithmic scales are used, so that actually  $\log C_P$  is plotted against  $\log V/nD$ , (Fig. 54).

<sup>1</sup> Larger charts having more pitch settings represented than Figs. 51 or 52 are necessary for accurate use. Charts of this nature are given in Figs. 165 to 175.

<sup>2</sup> Only a brief description of one type of logarithmic diagram is given here. For a more complete treatment of the subject see "Les Recherches sur les Hélices Aériennes," by G. Eiffel (French text) 1919, "Nouvelles Recherches sur la Résistance de l'Air et l'Aviation," by G. Eiffel (French text), 1914, and Experimental Research on Air Propellers, by William F. Durand, N.A.C.A.T.R. 14, 1917.

The logarithmic scales enable us to deal directly with the quantities  $P$ ,  $V$ ,  $n$ , and  $D$ . Consider a point on the curve of  $\log C_P$ ; the abscissa is  $\log V/nD$  which is equal to  $\log V - \log n - \log D$ . This can be thought of as three individual segments placed end to end. In like manner, since  $C_P = P/\rho n^3 D^5$ , the ordinate can be formed of the three segments,  $\log P$ ,  $-3 \log n$ , and  $-5 \log D$ , placed end to end. Now the two segments involving  $n$ , one ordinate and one abscissa, can be combined to give an oblique segment the length of which is proportional

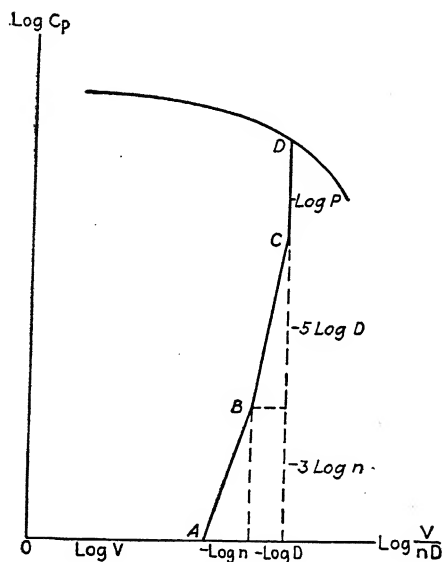


FIG. 54.

to  $n$ . In the same manner an oblique segment can be used instead of the two segments involving  $D$ . One can now pass from the origin to the point on the curve of  $\log C_P$  by the path  $OABCD$  (Fig. 54), and the segments measure respectively  $V$ ,  $n$ ,  $D$  and  $P$ .

The slope of the  $n$  segment will always be  $3/1$ , and that of the  $D$  segment  $5/1$ . For practical use the diagram is usually constructed with the scale for the abscissas twice that of the ordinates so that the slopes of the  $n$  and  $D$  segments become actually  $3/2$  and  $5/2$ , making possible more accurate plotting. Complete diagrams are given in Figs. 55 and 56. Scales of  $V$ ,  $n$ ,  $D$ , and  $P$

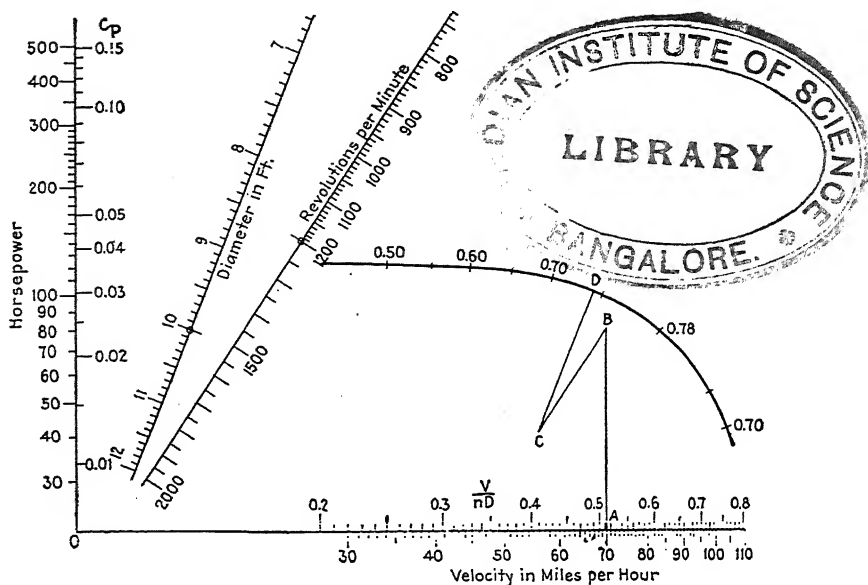


FIG. 55.—Logarithmic diagram for propeller 4412 set at  $15.0^\circ$  at  $0.75R$ , with efficiencies marked on curve of  $\log C_p$ .

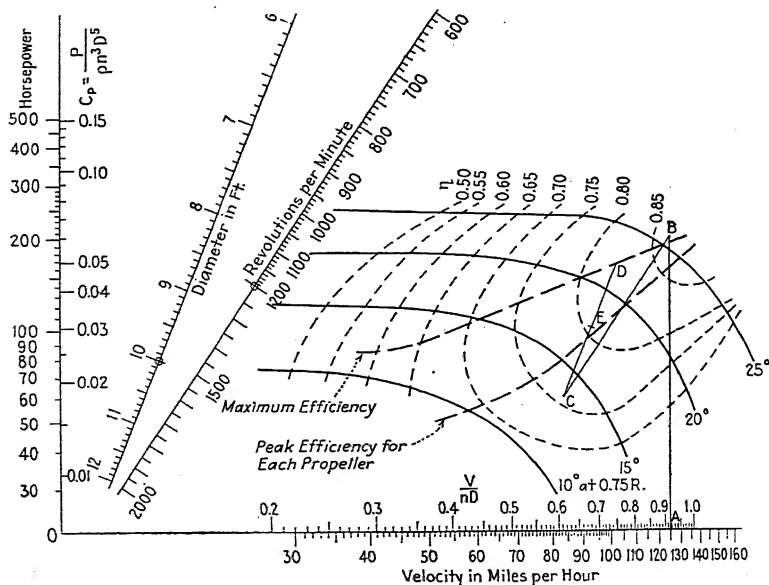


FIG. 56.—Logarithmic diagram with lines of constant efficiency, for the same

are added to the diagrams in units of m.p.h., r.p.m., feet, and horsepower, the scales for  $n$  and  $D$  being on lines of the proper slope placed at any convenient position on the diagram. Origins for the  $n$  and  $D$  scales are assumed at, say, 1,200 r.p.m. and 10 ft., respectively, and these determine the location of the scales of  $V$  with respect to  $V/nD$  and  $HP$  with respect to  $C_P$ . The scales are usually calculated for standard sea level atmosphere (15°C. and 760 mm. Hg). The efficiencies can be marked on the curves of  $\log C_P$ , as has been done in Fig. 55, or separate curves of thrust-power coefficient can be drawn, in which case the distance between the curves of input and thrust power is a measure of the efficiency.

In using the logarithmic diagram, the segments of  $V$ ,  $n$ ,  $D$ , and  $P$  are drawn in from the origin to a point on the curve of  $\log C_P$ , each segment being parallel to its respective scale. The lengths of the  $V$  and  $HP$  segments are measured from the origin, and the  $n$  and  $D$  segments from the circles (assumed origins) on the scales. In drawing the various segments, the direction of each should be in the sense that it is from the origin or assumed origin (up if above, down if below). The logarithmic diagram can be used for the graphical solution of the same problems as the charts of  $V/nD$  vs.  $C_s$ . If any three of the quantities  $P$ ,  $n$ ,  $V$ , and  $D$  are known or assumed, the fourth and also the pitch and efficiency can be determined. The method of procedure can be best shown by means of examples. Assume that we have a propeller geometrically similar to the one whose logarithmic diagram is given in Fig. 55 and that we wish to find the diameter required to absorb 80 hp. at 1,500 r.p.m. and 70 m.p.h. The velocity segment  $OA$  is the horizontal scale from the origin to 70 m.p.h. Obviously the segments can be drawn in any order as long as they are added vectorially, and so in order to keep within the diagram, the horsepower segment  $AB$  is put in next, parallel to the  $HP$  scale. Its length is equal to the distance from the origin to 80 hp. on the scale. Then the revolution segment  $BC$  is drawn parallel to the r.p.m. scale, its length being equal to the distance between the origin (1,200 r.p.m.) and 1,500 r.p.m. Finally the diameter segment is drawn parallel to the diameter scale from  $C$  to the propeller curve, and its length, when measured from the origin (10 ft.) on the diameter scale, gives a diameter of 8.35 ft. The efficiency is 0.74.

In Fig. 56 the same series of propellers is given as in Figs. 51 and 52, and curves of constant efficiency are drawn in the same manner as in Fig. 52, as well as the curves for maximum possible and peak efficiency. We shall take as an example the same problem as before; *i.e.*, we shall select the propeller giving the highest speed for an airplane with an engine developing 200 hp. at 1,800 r.p.m. and design for an airspeed of 125 m.p.h. at sea level. The velocity, power, and revolution segments *OA*, *AB*, and *BC* are drawn in as before, and the diameter segment is drawn from *C* to where it intersects the line for maximum possible efficiency, at *D*. The length *CD*, measured on the diameter scale, gives the diameter at 8.15 ft., the same as before. Also, the blade angle is again 22 deg. at 0.75*R*, and the efficiency is 0.83.

If we wish to find the blade angle of a 9-ft. diameter propeller to fulfil the above conditions, we go through the same process as before, but instead of drawing the diameter segment to intersect another line, it is terminated at the point *E*, corresponding to the 9-ft. diameter. For the point *E* we then see that the blade angle is 17.5 deg. at 0.75*R* and the efficiency is 0.81.

**Measuring the Flow of Air through Propellers.**—The momentum theory shows that in order to produce a thrust, a propeller must give the air through which it passes a backward motion. Similarly, due to the torque, the air is given a rotational motion. The result is a column of air, or slipstream, which follows a twisting or spiral path. The diameter of this column, according to Bernoulli's equation, will vary with the velocity, so that the greater the velocity the smaller is the cross-sectional area and consequently the diameter of the column. Figure 41 of Chap. V shows the lines of average flow in a longitudinal section of the slipstream of a propeller for three different rates of advance. It will be noted that the diameter of the slipstream changes more at the lower rates of advance where the thrust, and, therefore, the additional velocity, is greater.

The most complete measurements of the flow through a propeller have been made in England with a four-bladed 16-in. model propeller.<sup>1</sup> Using the data from these tests, Fig. 57 was drawn, showing the increase in velocity in a longitudinal section of the slipstream for a rate of advance corresponding

<sup>1</sup> An Investigation into the Nature of the Flow in the Neighborhood of an Airscrew, by J. R. Pannell and R. Jones, British R. and M. 371, 1917.

to climbing flight. The axial or fore-and-aft component of the added velocity in the slipstream is indicated by arrows whose ends are connected by dotted lines, in planes 2 and 4 in. ahead of the propeller plane and 1, 3, and 8 in. behind it. It will be seen that there is an appreciable increase of velocity, or inflow, 4 in. or one-fourth of a diameter ahead of the propeller. The contraction of the slipstream is evident from the radii at which the velocity becomes zero. Just behind the propeller the flow at the outer edge of the slipstream reverses slightly, and the edge

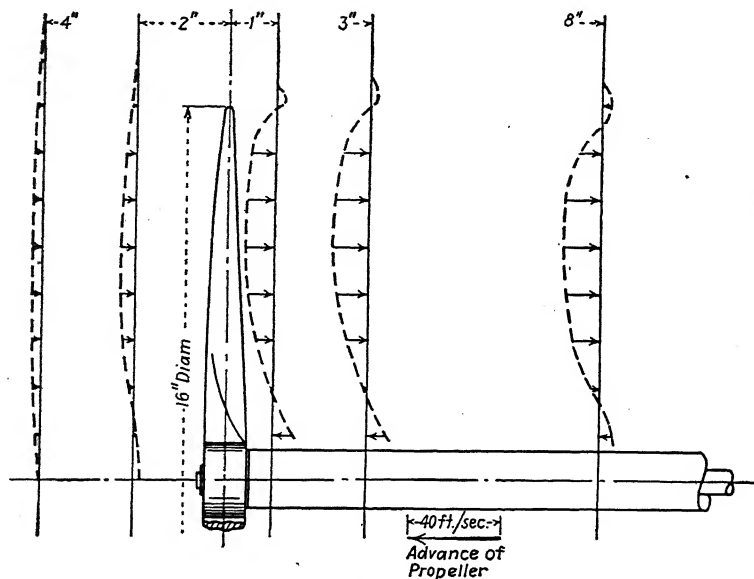


FIG. 57.—Longitudinal section of slipstream. Increase in axial velocity caused by propeller is shown by arrows. Four-blade propeller,  $p/D = 0.9$ ,  $V/nD = 0.63$ .

of the slipstream in this region is quite sharply defined. At the center the drag of the hub causes the velocity to become negative also.

In Fig. 58 the tangential or rotational component of the slipstream velocity is shown for each of the above positions in front of and in back of the propeller plane. While some rotational velocity was measured in front of the propeller, it was very small and in opposite directions at various radii, averaging about zero. It seems, therefore, that the assumption of no rotation in the inflow, as made in the vortex or induction theory of the propeller is true at any rate for practical purposes. The

rotational component of the velocity is seen to be greater near the center, and it also has the tendency to pass through zero and attain small negative values at the edge of the slipstream.

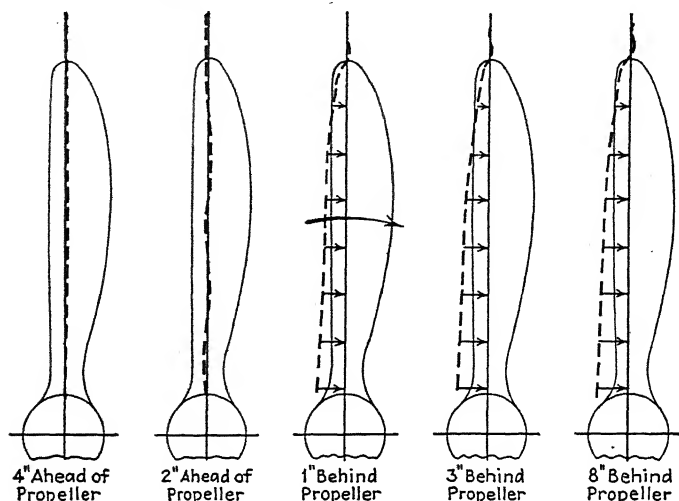


FIG. 58.—Tangential velocity of slipstream. Arrows indicate magnitude to same scale as in Fig. 57.

Figure 59 shows the change of both the axial and rotational components in passing through the propeller. Only the elemental annulus at three-fourths of the tip radius is considered,

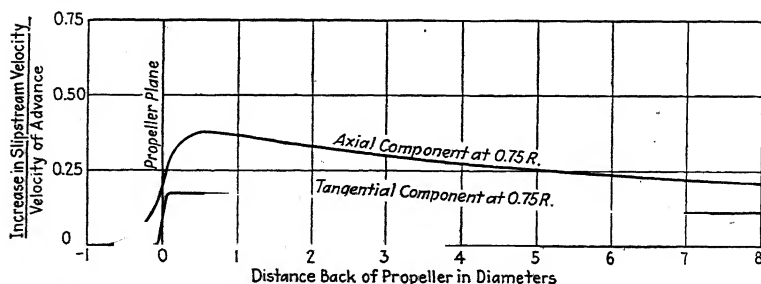


FIG. 59.—Variation of axial and tangential components of slipstream velocity with distance from propeller.

the values being obtained from the same data as Figs. 57 and 58. It is seen that for this propeller and rate of advance, the increase of axial velocity begins about three-fourths of a diameter forward of the propeller and reaches its maximum value at about

half of a diameter back of it, after which it gradually decreases, although it still has over half its maximum value at eight diameters back. The diameter of the slipstream is smallest at the point of maximum velocity. In a perfect frictionless fluid it would continue indefinitely with this diameter and velocity, but in air, which has considerable viscosity, the energy of the slipstream is gradually dissipated and the velocity becomes less and the diameter greater with increased distance. At the propeller plane, it will be noticed, the increase of axial velocity has reached just about half of its final maximum value, which is in agreement with the momentum and induction theories.

The rotational or tangential component is practically zero right up to the front of the propeller. It attains its full maximum value immediately on passing through the propeller and then gradually falls off, but less rapidly than the axial component. It appears reasonable also that the rotational interference velocity at the plane of rotation (halfway through the propeller) is half the final maximum value.

It should be remembered that all of these velocities and components of velocities represent average values. The velocity is not, of course, constant with time but is highly periodic in nature (see Fig. 43, Chap. V).

Also in these tests there was no body present. With a body of average size behind the propeller, the slipstream does not usually neck down but is spread so that its diameter is at no point smaller than that of the propeller.<sup>1</sup>

<sup>1</sup> See report on VE-7 flight test, Investigation of Slipstream Velocity, by J. W. Crowley, Jr., N.A.C.A.T.R. 194, 1924.



## CHAPTER VII

### THE EFFECT OF BLADE SHAPE ON PROPELLER CHARACTERISTICS

In this chapter the results of wind tunnel tests are used to show how variations of the blade shape effect the aerodynamic performance. Only propellers operating without body interference and at comparatively low tip speeds are considered, the effects of tip speed and body interference being taken up in separate chapters. Most of the effects could also be shown by means of an advanced form of the blade-element theory, but not that of tip shape or of pure size.

**The Effect of Pitch on Propeller Characteristics.**—In Fig. 49 are given curves of efficiency and power coefficient as a function of effective pitch  $V/nD$ . When  $V/nD$  is zero, the efficiency is also zero, which results from the definition of efficiency for a moving vehicle; for when the forward velocity is zero, no useful work is being done even though the thrust may be quite large. The efficiency for a given propeller increases with increase of  $V/nD$  up to a certain maximum point and then falls off with increasing rapidity as the  $V/nD$  is increased further, until it finally reaches zero again at the value of  $V/nD$  for zero thrust. The thrust and efficiency, of course, become zero at the same value of  $V/nD$ .

When the propeller is operating at a  $V/nD$  between zero and that for zero thrust, it is said to be in the *propeller state*. When it is between the values of  $V/nD$  for zero thrust and zero torque or power, it is in the *brake state*, for the thrust is negative but power is required to produce it. At values of  $V/nD$  above that for zero torque, the propeller is in the *windmill state*, for it then receives energy from the air and helps to turn the engine. This condition may have serious consequences in the case of an airplane in a steep dive where the speed of advance becomes very great and the engine is rotated more rapidly than is safe.

Curves of efficiency *vs.*  $V/nD$  for a series of model propellers varying in pitch are given in Fig. 60.<sup>1</sup>

<sup>1</sup> Tests on Thirteen Navy Type Model Propellers, by W. F. Durand,

The models were of the standard Navy wood form having uniform pitch; *i.e.*, the geometrical pitch based on the flat face of the sections was the same at all radii. The pitch-diameter ratios varied from 0.5 to 1.1. The maximum efficiency attained by the different propellers increases from 0.69 for  $p/D = 0.5$  to 0.83 for  $p/D = 1.1$ . If the pitches were carried higher, the maximum efficiencies would continue to increase at a lessening

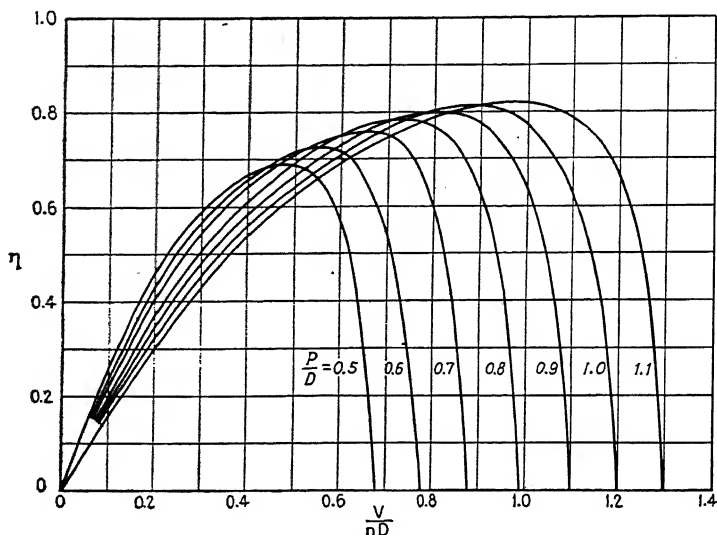


FIG. 60.—Efficiency curves for a series of model wood propellers.  $AR = 6$ , 2 blades,  $WR = 0.066$ ,  $TR = 0.107$ .

rate up to a  $p/D$  of about 1.6 or 1.7, after which they would decrease again. This is to be expected from the blade-element equation for efficiency,

$$\eta = \frac{\tan \phi}{\tan (\phi + \gamma)}$$

for  $V/nD$  is a function of  $\phi$  (Chap. IV, Fig. 29).

Most airplanes have propellers with pitch ratios of 0.6 to 0.8, and higher efficiencies could be obtained if the pitch could be increased. Since the propeller must fit particular values of  $P$ ,  $n$ , and  $V$ , however, it is usually possible to increase the  $V/nD$ , and thereby the  $p/D$ , only by gearing the propeller to operate at a lower revolution speed.

In order to compare the efficiencies of propellers having various pitch ratios on the basis of the performance required

on a given airplane, *i.e.*, at the same required values of  $P$ ,  $n$ , and  $V$ , the efficiencies can be plotted against the speed-power coefficient  $C_s$ , as has been done for a series of metal propellers in Fig. 51 (Chap. VI).

It is interesting to compare the efficiencies actually obtained with the ideal or limiting efficiency as determined by the momentum theory. In Chap. II it was shown that

$$\frac{\eta^2}{1 - \eta} = 2\rho \times \frac{\pi D^2}{4} \times \frac{V^2}{T}.$$

In order to express this in terms of power instead of thrust, we may substitute  $P\eta/V$  for  $T$ , which gives

$$\begin{aligned} \frac{\eta^3}{1 - \eta} &= 2\rho \times \frac{\pi D^2}{4} \times \frac{V^3}{P} \\ &= \frac{\pi}{2C_P} \left( \frac{V}{nD} \right)^3. \end{aligned}$$

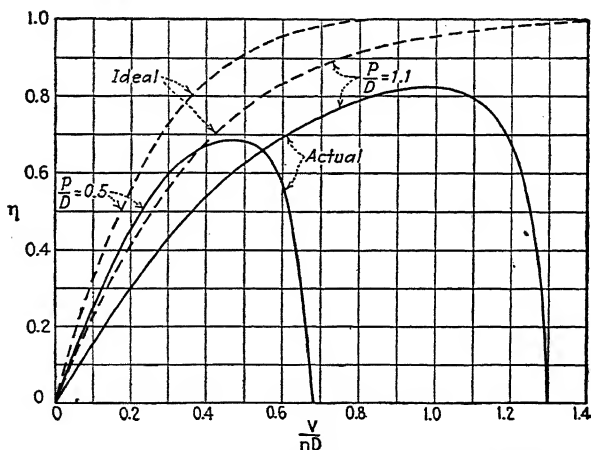


FIG. 61.—Comparison of actual and ideal efficiencies.

The ideal efficiencies as given by this expression are plotted in Fig. 61 along with the actual efficiencies for the two extreme propellers of the series of Navy wood models. The maximum efficiency of the high-pitch propeller is 88 per cent of the ideal, while that of the low-pitch propeller is only 78 per cent of the ideal. At the lower values of  $V/nD$ , however, the low-pitch propeller approaches the ideal more closely than the high-pitch propeller.

The variation of the thrust and power coefficients of this series of propellers is shown in Figs. 62 and 63, respectively.

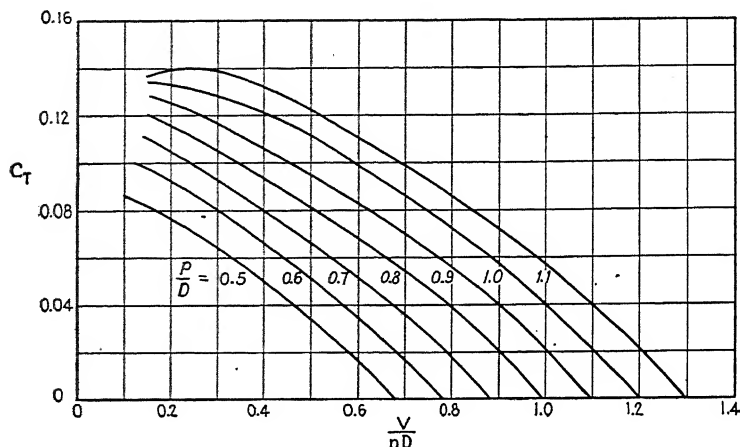


FIG. 62.—Thrust coefficient curves.

Both the thrust and power coefficients increase with the pitch ratio throughout the ordinary range.

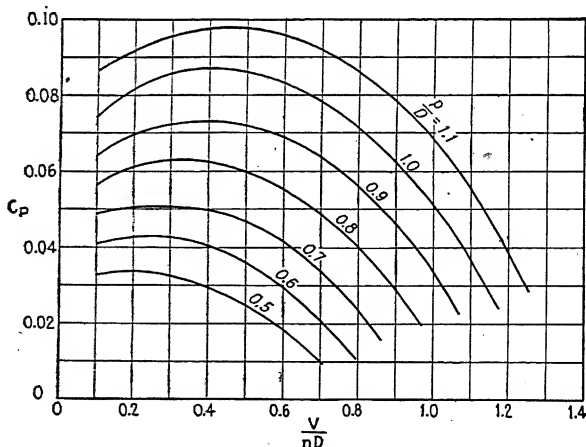


FIG. 63.—Power coefficient curves.

**Pitch Distribution.**—The effect of even wide variations of the distribution of the pitch along the radius is comparatively small, the average pitch for the whole propeller being the impor-

tant thing. The above Navy wood models were designed with uniform or constant pitch at all sections, for this has been found to give very nearly the best efficiency for all cases without body interference. A slightly greater efficiency can be obtained, however, by having the pitch increase with the radius so that it is somewhat higher than the average at the tip and lower at the hub.

This point is well illustrated by some British tests<sup>1</sup> on a family of model propellers. These propellers had detachable blades which could be turned in the hubs. The blades of one propeller

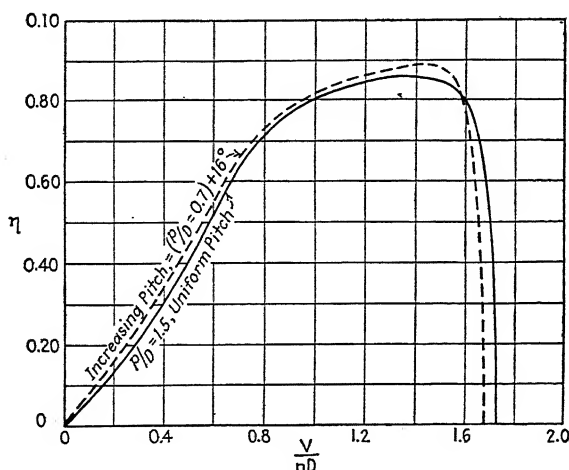


FIG. 64.—Effect of pitch distribution on efficiency.  $WR = 0.072$ .  $TR = 0.103$ .

which were designed to have a uniform pitch of 0.7 of the diameter were turned up 16 deg. so that the average pitch was about 1.5 times the diameter, and comparative tests were made with a uniform-pitch propeller of  $p/D = 1.5$ . The efficiency curves of the two propellers are given in Fig. 64, and it is seen that the efficiency of the reset propeller, which had a much greater pitch at the tip than at the hub, was slightly higher throughout the entire working range than that of the uniform-pitch propeller.

The effect of increasing the pitch with the radius is smaller on propellers of lower pitch. From an extensive series of tests on model metal propellers with various pitch distributions,

<sup>1</sup> Experiments with a Family of Airscrews, by A. Fage, C.N.H. Lock,

the curve in Fig. 65 is given as approximately the best pitch distribution for thin-bladed propellers of all pitches, without body interference. Fortunately the best conditions require a proportionately greater increase of pitch toward the tip for high-pitch than for low-pitch propellers, making it possible to design an adjustable-pitch propeller with a practically uniform pitch at a low pitch-diameter ratio, which can be set at any desired average pitch with the assurance that it will have very nearly the best pitch distribution at any setting. Thus one blade form does very well for propellers of any pitch within the ordinary limits of practice.

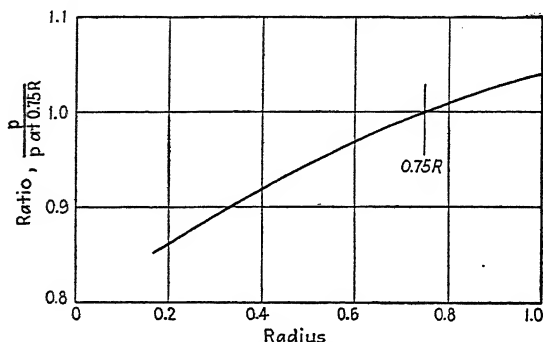


FIG. 65.—Approximately best pitch distribution for thin metal propellers without body interference.

With the propeller operating near a body such as a fuselage or nacelle, the above pitch distributions are no longer the best, for the body reduces the velocity of the air through the propeller, and this reduction is usually much more pronounced near the center than near the tips. Designers, therefore, sometimes reduce the pitch still more near the hub, and occasionally they reduce it or “wash it out” near the tip also, in the hope of reducing the tip losses.

**Blade Width.**—The blade width is sometimes expressed as the mean width of the working portion (the outer two-thirds or three-fourths) of the blade in terms of the diameter. Also, sometimes the aspect ratio, which is nominally considered the tip radius divided by the maximum blade width, is used as a measure of the blade width. Neither of these is satisfactory if propellers outside of a single family or series are to be compared, for neither is a criterion of the mean effective blade width.

The blade is more effective near the tip because of its greater speed there relative to the air. The radius which best represents the average of the thrust and torque grading curves is usually at from 70 to 75 per cent of the tip radius. We shall therefore take as a measure of the mean effective blade width the blade width at  $0.75R$ . This is expressed non-dimensionally in a ratio called the *width ratio*  $WR$ , which is defined by the relation

$$WR = \frac{b_{0.75R}}{D}.$$

In making changes in blade width alone, it is assumed that the blade sections remain of the same form, *i.e.*, that the thickness is varied in proportion to the width.

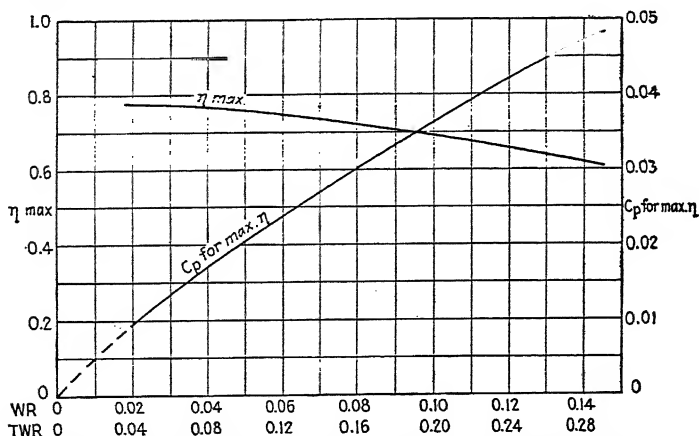


FIG. 66.—Variation of power and efficiency with blade width.

The variation of power and efficiency with blade width is shown in Fig. 66 for a series of propellers<sup>1</sup> all having a pitch-diameter ratio of 0.5 and operating at the value of  $V/nD$  for maximum efficiency ( $V/nD = 0.45$ ). The power coefficient increases with the blade width, but the increase in power is less than the increase in blade width. The efficiency drops off with increasing blade width. Both of these effects are due largely to the increased slipstream velocity with the wider blades and incidentally, could be found by means of the advanced forms of the blade-element theory, but not with the simple theory.

<sup>1</sup>Experiments with a Family of Airscrews, by A. Fage, C.N.H. Lock, R. G. Howard, and H. Bateman, British R. and M. 829, 1922.

Since high-pitch propellers act on more air per revolution, the effects are less pronounced than with propellers of low pitch.

**Number of Blades.**—According to the blade-element theory, the torque and thrust for all of the blade elements in an elementary annulus depend on a solidity factor  $S$ , where

$$S = \frac{2\pi r}{Bb}$$

This factor contains the product of the blade width and the number of blades, representing the total blade width for the annulus. As long as the product  $Bb$  is the same, the individual values of  $B$  and  $b$  are immaterial, and therefore according to the theory, a two-bladed propeller should have the same thrust, torque, and efficiency as a propeller having four blades, each being half as wide. The British model tests previously referred to<sup>1</sup> show that this is essentially true and that the curves of Fig. 66 also hold for propellers having any number of blades if the total width ratio is used, where

$$TWR = \frac{B \times b_{0.75R}}{D}$$

The model tests deviate slightly in the matter of efficiency, however, the efficiency of the multibladed models (three, four, and six blades) being on the average from one to two per cent lower than that of the two-bladed propeller having the same total blade width. It is possible that this is due to scale effect, for the tip speeds obtained in the tests were low and the maximum blade widths of some of the propellers were less than an inch and a half.

**Blade Thickness.**—Applying the same reasoning as in the case of the blade width, the most satisfactory measure of the thickness of a propeller blade is the thickness ratio of the section at  $0.75R$ , or

$$TR = \left( \frac{h}{b} \right)_{0.75R}$$

In Dr. Durand's tests on a family of Navy-type model wood propellers,<sup>2</sup> four propellers of  $p/D = 0.7$  formed a series varying

<sup>1</sup> Experiments with a Family of Airscrews, A. Fage, C. N. H. Lock, R. G. Howard, and H. Bateman, British *R. and M.* 829, 1922.

<sup>2</sup> Tests on Thirteen Navy Type Model Propellers, by W. F. Durand, N.A.C.A.T.R. 237, 1926.



only in thickness ratio. The power coefficient and efficiency curves for these four propellers are given in Fig. 67. It will be noticed that the  $V/nD$  for zero efficiency (or zero thrust) is greater for the thicker propellers. This is to be expected from the fact that the thicker airfoils reach zero lift at lower angles of attack (Chap. III). Also, just as the thicker airfoil sections have a greater lift and drag at the same angle of attack, the thicker propellers have greater power and thrust coefficients at

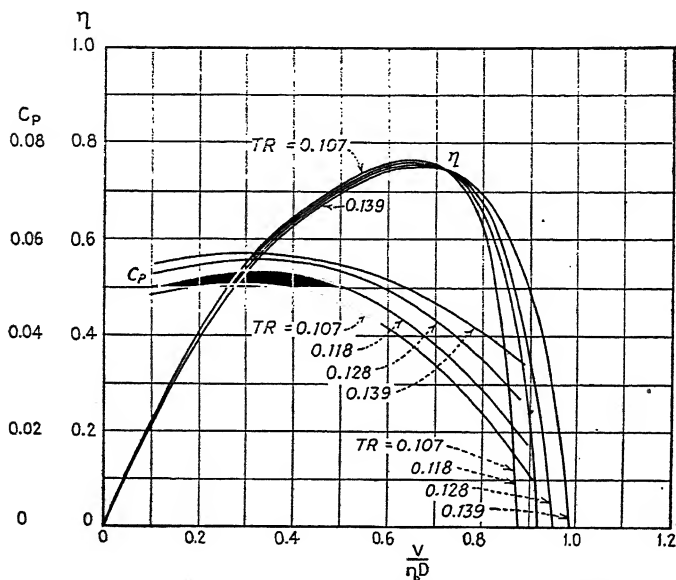


FIG. 67.—Efficiency curves for wood propellers of various thicknesses.  $WR = 0.066$ .

the same  $V/nD$ , and due to the higher drag the efficiency is slightly less. The range between the thinnest and thickest wood propellers is not great, and the thickest propeller of Fig. 67 is only a little over one per cent less efficient than the thinnest.

Aluminum-alloy propeller blades can be made much thinner, and the gain in efficiency over wood blades is appreciable but not great at ordinary tip speeds (up to about 900 ft. per sec.). In Fig. 68 a curve of the maximum efficiencies obtainable with a series of full-scale standard wood propellers is given along with a similar curve for a series of standard thin-bladed metal propellers, both being plotted against  $C_s$  so that they are on a fair

basis as regards similar operating conditions. Both series of propellers were tested on a Vought VE-7 airplane with a 180-hp. Wright E-2 engine in the N.A.C.A. 20-ft. Propeller Research Tunnel.<sup>1</sup> The thinner metal propellers are from 4 to 7 per cent more efficient than the wooden ones under the same operating conditions, *i.e.*, for the same values of  $P$ ,  $n$ , and  $V$ .

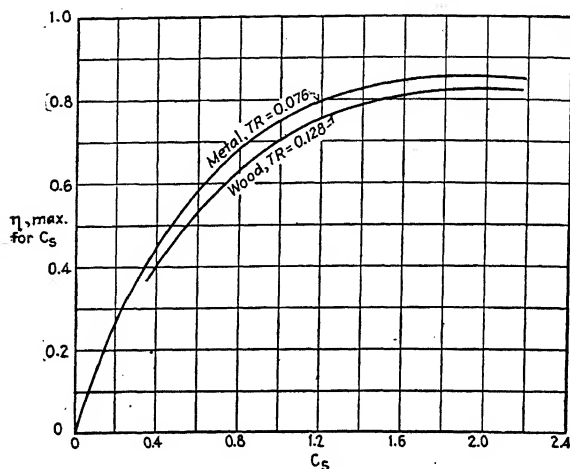


FIG. 68.—Maximum possible efficiencies of ordinary wood and metal propellers.

**Blade Section.**—If, as is nearly always the case, the airfoil sections of propellers are made with a flat lower surface, or face, the shape of the profile is fairly well limited by the thickness ratio. With these factors fixed, any reasonably good airfoil section will give very nearly the same propeller characteristics as the best possible section.

From the simple blade-element theory we have the relation

$$\eta = \frac{\tan \phi}{\tan (\phi + \gamma)},$$

where  $\phi$  is the helix angle of the path of the element and depends on the effective pitch and  $\gamma$  is the angle whose tangent is  $D/L$  and represents the effectiveness of the airfoil. Considering this relation, it would be expected that any particular change in airfoil

<sup>1</sup> Full-scale Tests of Wood Propellers on a VE-7 Airplane in the Propeller Research Tunnel, by Fred E. Weick, N.A.C.A.T.R. 301, 1928. Full-scale Wind Tunnel Tests of a Series of Metal Propellers on a VE-7 Airplane, by Fred E. Weick, N.A.C.A.T.R. 306, 1928.

effectiveness  $\gamma$  would have a greater importance at low than at high pitches.

This is verified by full-scale wind tunnel tests<sup>1</sup> on three pairs of metal propellers which were exactly the same except for the airfoil sections. In one pair the sections throughout the outer half of the blades all had a thickness ratio of 0.06, in one pair it was 0.08, and in the third, 0.10. One propeller of each pair had sections based on the R.A.F.-6 and the other, on the Clark-Y. The efficiency curves for the thinnest pair set at low, medium, and high pitches are given in Fig. 69. Wind tunnel tests on Clark-Y

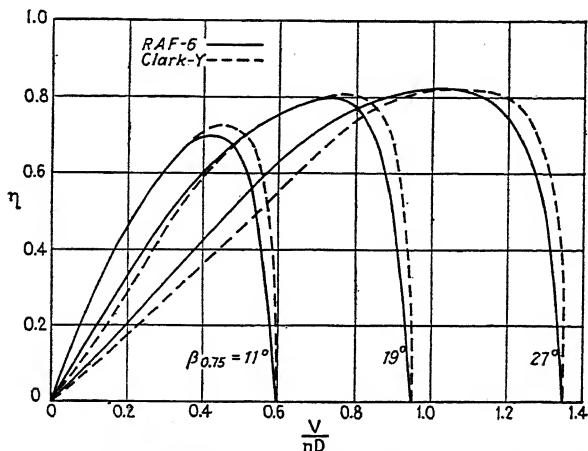


FIG. 69.—Comparative efficiency of propellers with R.A.F.-6 and Clark-Y type airfoil sections.

and R.A.F.-6 type airfoils of the same thickness have shown that the Clark-Y has lower drag at low lift coefficients, and a higher maximum  $L/D$ . In Fig. 69, the Clark-Y propellers have higher efficiencies at the high range of  $V/nD$  values near zero thrust and efficiency. Also, the peak efficiency of the low-pitch propellers is noticeably higher with the Clark-Y, but there is no appreciable difference at the high pitch. The differences are somewhat more pronounced with the thicker propellers.

It is of interest to note that the same envelope or "maximum efficiency for  $V/nD$ " curve is touched by all of the propellers regardless of airfoil section, indicating that if any pitch setting may be selected, the advantage of the Clark-Y is more apparent

<sup>1</sup> Comparison of Full-scale Propellers Having R.A.F.-6 and Clark-Y Airfoil Sections, by Jack R. F. and N. A. G. A. T. R. 275, 1929.

than real. It does have an advantage, however, for low-pitch propellers operating at or beyond their peak efficiency.

Although the Clark-Y has some advantage at the high values of  $V/nD$ , the curves show that with the higher-pitch propellers at the lower values of  $V/nD$  corresponding to the take-off and even the climbing range, the propellers with the R.A.F.-6 type sections are decidedly superior.

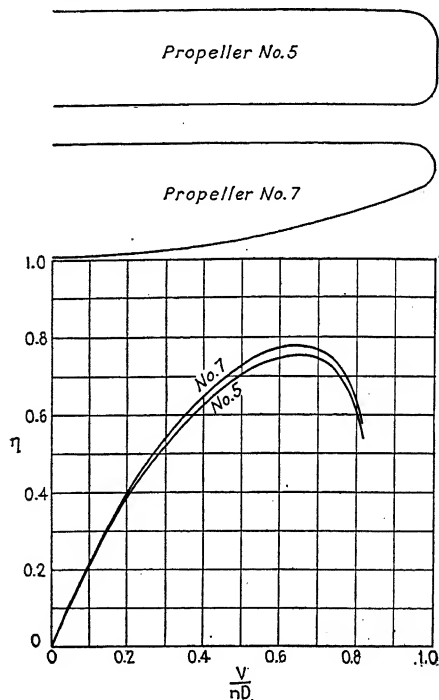


FIG. 70.—Effect of plan form on efficiency.

**Plan Form.**—The effect of plan form upon propeller performance is not great, although there is some aerodynamic advantage in a blade tapering toward and rounded at the tip. The tapering blade is also advantageous from the point of view of strength.

In Fig. 70 are plotted the efficiency curves for two Durand propellers<sup>1</sup> which are similar except for the plan form. One had a blade of constant width with slightly rounded corners at the tip,

<sup>1</sup> Experimental Research on Air Propellers V, by W. F. Durand and E. B. Loder, NACA Tech. Rep. 111, 1922, especially Figs. 1, 5.

and the other had a tapering blade with rounded tip. With this extreme difference in plan form the difference in maximum efficiency was only 3 per cent.

The two plan forms most commonly used with detachable-blade aluminum-alloy propellers are shown in Fig. 71. They are known as the wide-tip and narrow-tip plan forms. Tests on full-scale propellers in the N.A.C.A. Propeller Research Tunnel have been made at moderate tip speeds with propellers of both plan forms, the actual blade thickness in each case being the same so that the tip sections of the wider propeller had lower values of  $TR$ . The efficiency was found to be about 1 per cent greater with the wide-tip plan form.

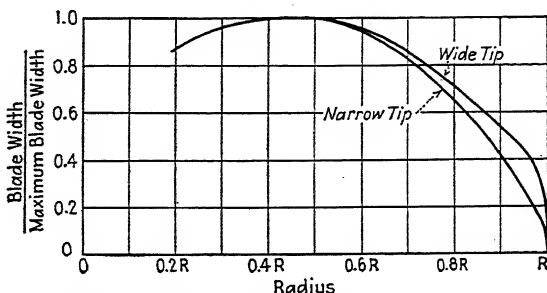


FIG. 71.—Plan forms of wide and narrow tip aluminum alloy propellers.

Sweepback and rake of the blades have no appreciable effect on the aerodynamic characteristics of a propeller, except that they affect the twist of the blades while operating, and therefore the pitch. The blades of wood propellers are often swept back (see tapered plan form in Fig. 70) in order to obtain smooth running qualities and to eliminate flutter.

**The Effect of Size.**—There appears to be very little scale effect with change in pure size from the ordinary 3-ft. wind tunnel models to the 6- to 12-ft. propellers used on aircraft. There is one difference, however, between model and full-scale wind tunnel tests which is noticeable even when they are run at nearly the same tip speeds. This is illustrated by a typical comparison of model<sup>1</sup> and full-scale<sup>2</sup> wind tunnel tests, the

<sup>1</sup> For the model tests see Comparison of Tests on Air Propellers in Flight with Wind Tunnel Model Tests on Similar Forms, by W. F. Durand and E. P. Lesley, N.A.C.A.T.R. 220, 1926.

<sup>2</sup> Full-scale Tests of Wood Propellers on a VE-7 Airplane in the Propeller Research Tunnel, by Fred E. Weick, N.A.C.A.T.R. 301, 1928.

efficiency curves of which are given in Fig. 72. Both propellers were tested in the presence of the same shaped bodies, and under as nearly as possible the same conditions. The full-size propeller has a higher  $V/nD$  for zero thrust and its maximum efficiency also occurs at a higher  $V/nD$ . In other words, the "dynamic" or zero thrust pitch of the full-size propeller is larger than that

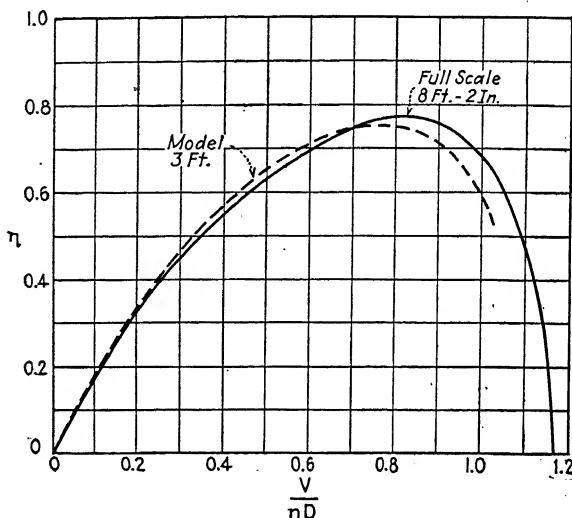


FIG. 72.—Effect of size on efficiency.

of the model, and the maximum efficiency is therefore slightly higher and occurs at a greater  $V/nD$ . This fact has also been indicated in flight tests but their lack of accuracy makes the results of dubious value. It is apparent, therefore, that if propellers are to be accurately designed to operate at a particular position on the efficiency curve, say at maximum efficiency, accurate full-scale test data must be available,



## CHAPTER VIII

### THE EFFECT OF TIP SPEED ON PROPELLER PERFORMANCE

As was shown in Chap. III, the aerodynamic force on an airfoil is a function of  $V/c$ , where  $c$  is the velocity of sound in air, or the rate of travel of any compression wave. While this compressibility function has been found to be unimportant in connection with airplane wings, which even in the fastest cases travel at velocities far below that of sound, the tip sections of propellers on modern aircraft engines often approach and in some cases exceed the velocity of sound.<sup>1</sup> In these cases in which the velocity approaches or exceeds that of sound, the effect of  $V/c$  is of vital importance, especially in regard to reduction of efficiency.

Three forms of experimental work have been carried on to gain information on the effect of tip speed on propeller performance coefficients. These are (1) tests on model airfoils at velocities up to and beyond that of sound; (2) wind tunnel tests on small model propellers run at tip speeds up to and beyond the velocity of sound; and (3) wind tunnel tests on full-scale propellers run throughout the same range of tip speeds.

The model airfoil and propeller tests have thrown a considerable amount of light on the subject, showing a great variation of coefficients with  $V/c$ , especially at high velocities. They are, however, limited by low Reynolds number, and in the airfoil tests by a questionable aspect-ratio effect, so that with our present limited knowledge the results have no quantitative value, and the more recent full-scale propeller tests are the only ones giving information which can be used for practical computations.

**Tests on Model Airfoils at High Speeds.**—The first model airfoil tests at velocities approaching that of sound were made in an open jet of air emerging from a standpipe with a nozzle

<sup>1</sup> The velocity of sound in air is independent of pressure but varies approximately as the square root of the absolute temperature. It is therefore independent of altitude except for a secondary temperature change. It varies from 1 050 ft per sec at 0°F to 1 160 ft per sec at 100°F

12¼ in. in diameter, an air stream having any velocity from 550 to 1,000 ft. per sec. being supplied by means of a large centrifugal compressor.<sup>1</sup> Model airfoils having a chord of 3 in. and extending entirely across the airstream were used. The aspect ratio effect is therefore questionable, especially at high angles of attack. Six airfoils were tested, all having standard propeller sections based on the R.A.F.-6 (see Fig. 19) but varying in thickness ratio from 0.10 to 0.20.

An extension of the above investigation was made in which the pressure distribution over the same six airfoil sections was measured on models of 1-in. chord extending entirely across a 2-in. air jet with velocities up to 1,250 ft. per sec.<sup>2</sup>

A still further extension was finally made in which force tests were made on 24 1-in. chord model airfoils in a 2-in. air jet.<sup>3</sup> The 24 airfoils included the original series of standard propeller sections with the addition of three thinner sections, the thinnest having a thickness ratio of 0.04. There were also five sections based on the Clark-Y, the ordinates all having been scaled up or down to give thickness ratios varying in even steps from 0.04 to 0.20, and a few other miscellaneous sections.

The results obtained for the same section in the three different ways do not agree in value, indicating that the aspect ratio effects and probably also the effect of Reynolds number at high speeds are very large. As pointed out by the authors of the reports, the results cannot be considered as having quantitative value, at any rate not until more is known regarding the effect of Reynolds number and regarding corrections for the aspect ratio condition occurring with a 1-in. chord airfoil extending entirely through a 2-in. jet of air. The tests no doubt have some qualitative value, however, for they all indicated the following effects:

1. The lift coefficient decreases with increase of velocity, very slightly for thin sections but rapidly for thick ones.

<sup>1</sup> Aerodynamic Characteristics of Airfoils at High Speeds, by L. J. Briggs, G. F. Hull, and H. L. Dryden, N.A.C.A.T.R. 207, 1925. An earlier investigation was made in a wind tunnel capable of air speeds up to about 600 ft. per sec., which is reported in Wind Tunnel Studies in Aerodynamic Phenomena at High Speed, by F. W. Caldwell and E. N. Fales, N.A.C.A.T.R. 83, 1920.

<sup>2</sup> Pressure Distribution over Airfoils at High Speeds, by L. J. Briggs and H. L. Dryden, N.A.C.A.T.R. 255, 1927.

<sup>3</sup> Aerodynamic Characteristics of Twenty-four Airfoils at High Speeds, by L. J. Briggs and H. L. Dryden, N.A.C.A.T.R. 210, 1926.



2. The drag coefficient increases with increase of velocity, the rate rising abruptly at a critical speed well below the speed of sound. The increase at the higher speeds is very great, especially for the thicker sections.

3. The center of pressure moves back with an increase of velocity.

4. The effects of high speed are less for thin than for thick sections.

5. The angle of zero lift decreases with increase of velocity up to a critical speed, after which it approaches zero degrees.

6. The last series of tests indicated that except for thin sections at high lift coefficients the Clark-Y series are somewhat better than the R.A.F.-6 series. Also, one section having a flat undersurface and a circular arc upper, with a thickness ratio of 0.08, was found to be better than any other section of the same thickness ratio at the higher speeds.

**Tests on Model Propellers at High Tip Speeds.**—Tests have been made in a 7-ft. wind tunnel at the Royal Aircraft Establishment in England on several 2-ft. model propellers run at tip speeds ranging from about half to somewhat over the speed of sound.<sup>1</sup> Very complete investigations were made including not only the usual force measurements of thrust and torque but also a measurement of the airflow through the propeller by means of total head pitot tubes and special yawmeters. The airflow measurements provided a basis for the computation of the thrust and torque grading curves, and, what is even more interesting, the airfoil lift and drag coefficients were calculated by means of the vortex blade-element theory. Thus the effect of high speeds on the computed lift and drag coefficients for the model propeller blade sections can be compared directly with the results of the model airfoil tests made in this country. In general they show the same tendencies, the effects shown by the computed propeller section characteristics being as follows:

1. The lift coefficient increases slightly with velocity up to about  $0.7c$ , after which it falls off rapidly. (The model airfoil tests showed a decrease throughout the entire range.)

<sup>1</sup> The Effects of Tip Speed on Airscrew Performances, by G. P. Douglas and R. McKinnon Wood, *British R. and M.* 884, 1923. Wind Tunnel Tests with High Tip-speed Airscrews, by G. P. Douglas and W. G. A. Perring, *British R. and M.* 1086, 1091, 1123, 1124, 1134, and 1198, published in 1927

2. The drag coefficient increases with increase of velocity, the rate rising abruptly at a critical speed of about  $0.6c$ .
3. The center of pressure moves back with an increase of velocity.
4. The effects of high speed are less for thin than for thick sections.

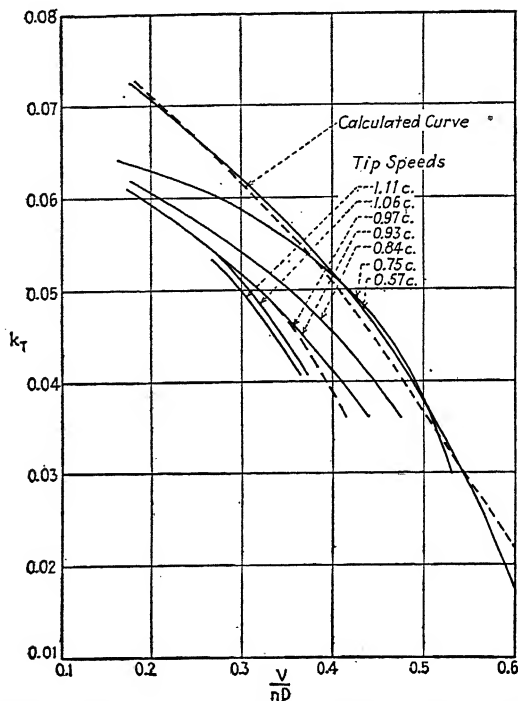


FIG. 73.—Thrust. Coarse pitch R.A.F.-31a airscrew. Curves of  $k_T$  measured at various tip speeds.

The results of the model propeller tests indicated that Reynolds number as well as  $V/c$  apparently had a large effect at high tip speeds. This was then proved by special model tests<sup>1</sup> and also by full-scale flight tests.<sup>2</sup> The same conclusion is indicated by a comparison of the model propeller test results with the results of wind tunnel tests on full-scale propellers. All of these

<sup>1</sup> Wind Tunnel Tests on High-speed Airscrews, by G. P. Douglas and W. G. A. Perring, British *R. and M.* 1174, 1928.

<sup>2</sup> Full-scale Determination of the Effect of High Tip Speeds on the Performance of an Airscrew, W. G. Jennings, British *R. and M.* 1173, 1928.

comparisons show that the effect of high speeds on the coefficients is less pronounced at high values of Reynolds number than at

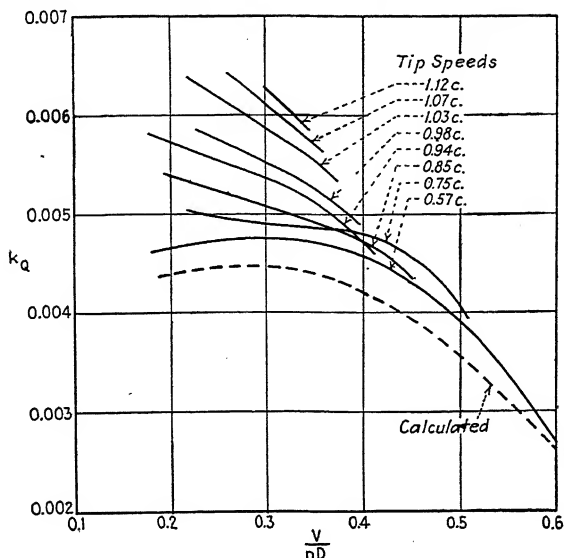


FIG. 74.—Torque. Coarse pitch R.A.F.-31a airscrew. Curves of  $k_q$  (measured) at various tip speeds.

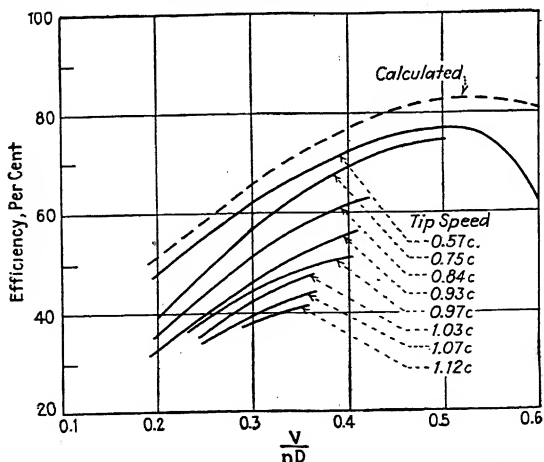


FIG. 75.—Efficiency. Coarse pitch R.A.F.-31a airscrew.

low. Unfortunately this complicates matters and makes full-scale tests necessary for obtaining quantitative results applicable to actual propeller problems.

In all of the model propeller tests the efficiency fell off as the tip speed was increased, throughout the entire range of the tests. The drop in efficiency was small at the lower tip speeds but became greater and of fairly constant rate at tip speeds above about  $0.75c$  or  $0.80c$ .

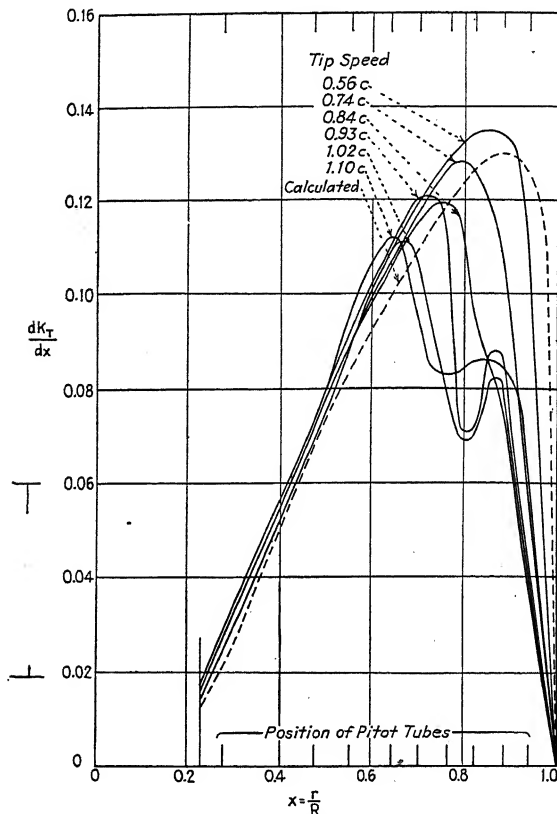


FIG. 76.—Thrust grading curves. Coarse pitch R.A.F.-31a airscrew.  $V/nD = 0.25$ .

Typical curves showing the thrust, torque, and efficiency coefficients at the different tip speeds are shown for one of the model propellers in Figs. 73, 74, and 75. (This propeller had R.A.F.-31a sections with a thickness ratio of 0.126 over the entire working portion of the blade.)

The thrust coefficient falls off and the torque coefficient becomes greater as the tip speed is increased. The dotted lines

represent coefficients calculated by means of the vortex theory from low-speed model airfoil tests. It is interesting to note that while the measured thrust coefficients for a tip speed of  $0.57c$  check the calculated values rather well, the measured torque coefficients for all tip speeds tested are substantially higher than the calculated.

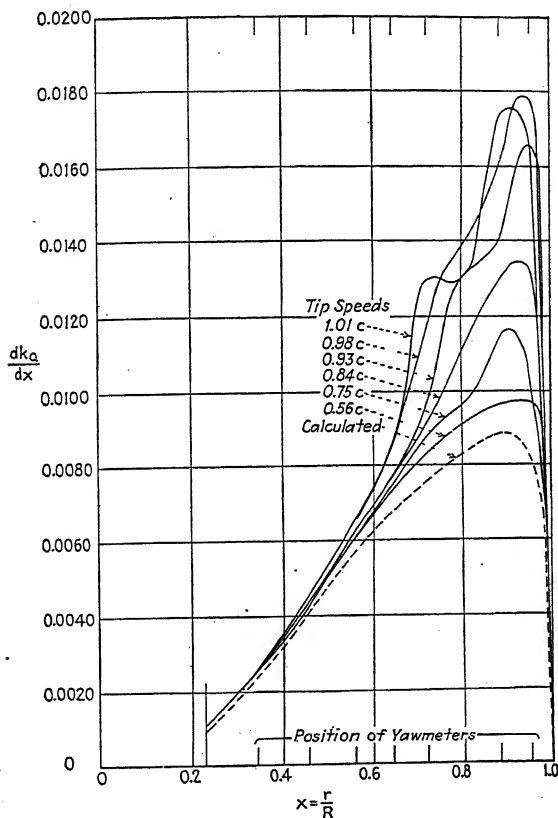


FIG. 77.—Torque grading curves. Coarse pitch R.A.F.-31a airscrew.  $V/nD = 0.25$ .

Thrust and torque grading curves as obtained for the same model propeller from the measured air flow through it are given for the various tip speeds in Figs. 76 and 77. These figures show very graphically the manner in which the thrust of the various sections decreases and the torque increases with increase of speed through the air. The tip sections are the first to be

influenced, the effect working in as the speed goes up. The values over the inner half of the blade are practically the same for all tip speeds, and they agree reasonably well with the calculated values.

**Wind Tunnel Tests on Full-scale Propellers at High Tip Speeds.**—The full-scale propeller tests were run on thin-bladed aluminum-alloy propellers in the N.A.C.A. 20-ft. Propeller Research Tunnel, at tip speeds from about 400 to 1,300 ft. per sec. ( $0.35c$  to  $1.15c$ ).<sup>1</sup>

Ten propellers in all were tested, four being of forms in common use and having diameters of 9 ft. and 9 ft. 6 in., and six also having diameters of 9 ft. 6 in. but being especially designed to afford a comparison of different airfoil sections and thickness

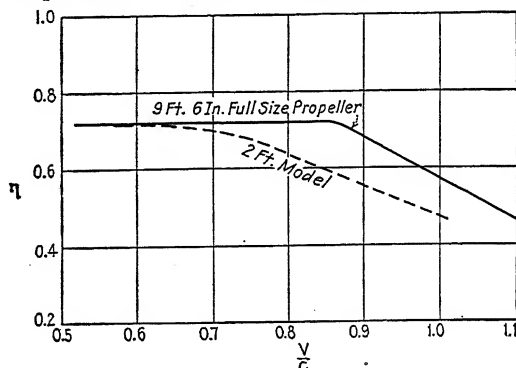


FIG. 78.—Comparison of tip-speed effect on typical model and full-scale propellers.

ratios. Of the six special propellers, three had standard propeller sections based on the R.A.F.-6 and the other three had sections based on the Clark-Y. In each case the three propellers made a series of different thicknesses, all of the sections in the outer half of the blade having thickness ratios of 0.06 in one propeller, 0.08 in another, and 0.10 in the third.

The full-scale tests gave results somewhat different from those of the model tests, although in both cases there was a great reduction of efficiency at the highest tip speeds. In the full-scale tests the efficiency was constant throughout the entire usual range of tip speeds, from the lowest at which the tests could be run, up to a critical speed of about  $0.9c$ . Above this critical

<sup>1</sup> Full-scale Tests on a Thin Metal Propeller at Various Tip Speeds, by Fred E. Weick, N.A.C.A.T.R. 302, 1928. Full-scale Tests of Metal Propellers at High Tip Speeds, by Donald E. Wood, N.A.C.A.T.R. 378, 1929.

tip speed the efficiency fell off rapidly at a constant rate of decrease. This is shown in Fig. 78, where a typical curve showing the maximum or peak efficiency of a full-scale propeller is plotted as a solid line against tip speed. The line, it will be noticed, has two straight portions connected by a short curve at the critical speed. The dashed line on Fig. 78 gives similar values from tests on a 2-ft. model. The efficiency falls off throughout the entire range. The critical speed is much lower and less definite than for the full-scale propeller. Beyond the critical speed the model efficiency line also becomes fairly straight, but its slope is not so great as that for the full-scale propeller.

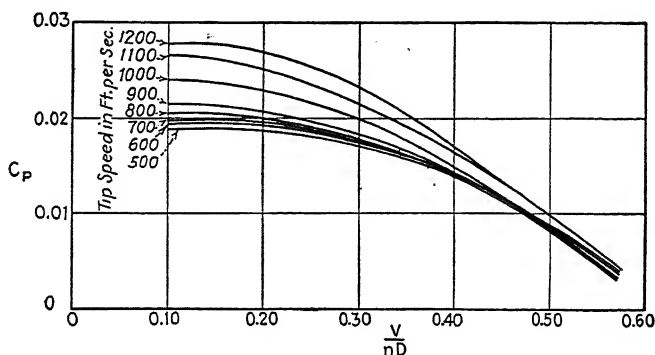


FIG. 79.—Power coefficient curves for a full-scale metal propeller at various tip speeds.

Figures 79 and 80 show curves of the power coefficients and efficiencies for the above full-scale metal propeller at various tip speeds. This propeller had a pitch-diameter ratio of 0.4 and Clark-Y type sections with a constant thickness ratio of 0.08 throughout the outer half of the blades.

The efficiency curves, it will be noticed, all lie within the experimental error of a single curve for the tip speeds under the critical, but above 1,000 ft. per sec. they drop off rapidly. The power coefficients also vary but slightly up to the critical speed, particularly at values of  $V/nD$  near maximum efficiency, as shown in Fig. 81. The variation which does occur below the critical speed can be accounted for by the deflection or twisting of the blades in operation, which was measured during the tests. This is a fortunate thing, for it means that the results of the regular full-scale wind tunnel propeller tests can be applied

directly to all ordinary cases of propeller operation where the tip speed is below the critical. At higher tip speeds, however, the power coefficient increases rapidly with increase in tip speed, and at a higher rate for the lower rate of advance and higher angles of attack of the blade sections.

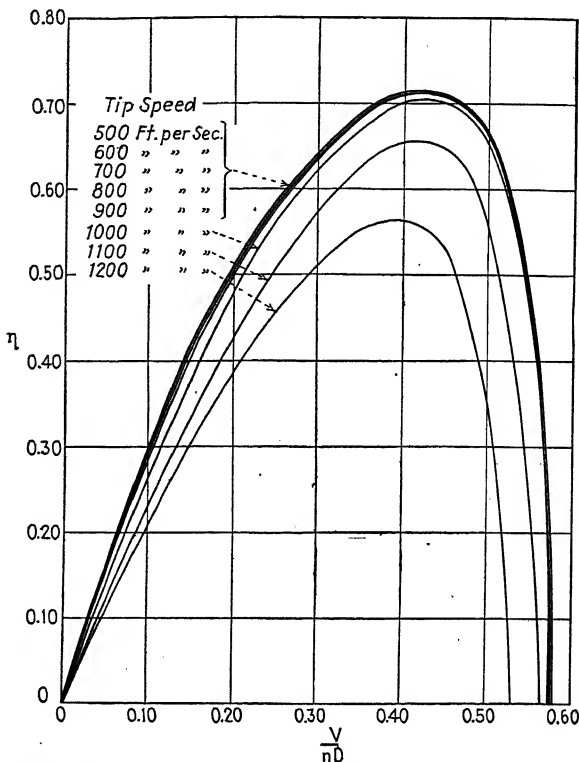


FIG. 80.—Efficiency curves for a full-scale metal propeller at various tip speeds.

Figure 82 shows the effect of section-thickness ratio on both the critical speed and the rate of decrease of efficiency beyond the critical speed. The ratio of the maximum efficiency at any tip speed to that at low tip speeds is plotted against tip speed for the series of three 9 ft. 6-in. propellers having Clark-Y type sections and thickness ratios of 0.06, 0.08, and 0.10. The critical tip speed for the 0.06 thickness ratio is 90 ft. per sec. higher than that for the 0.10 thickness ratio, and above the critical speed the maximum efficiency decreases at the rate of about 11 per cent per 100 ft. per sec. increase for the 0.06



thickness ratio as compared with 13 per cent for the 0.10. These results are in agreement with the indications of the model airfoil and model propeller tests which all showed a greater high speed or compressibility effect on thick than on thin airfoil sections.

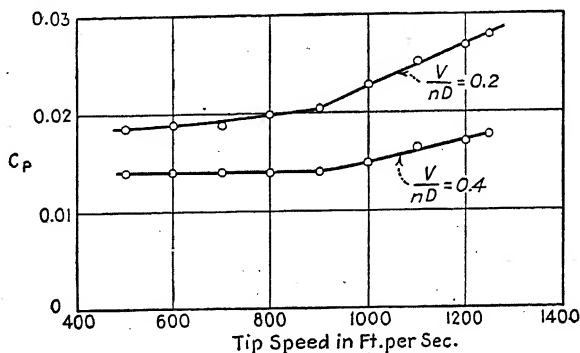


FIG. 81.—Variation of power coefficient with tip speed.

Since in the full-scale tests the critical speed varies only from about  $0.85c$  to  $0.95c$ , and since the velocity of the air passing just over the upper forward part of the airfoil is somewhat greater than the velocity of the section with respect to the air

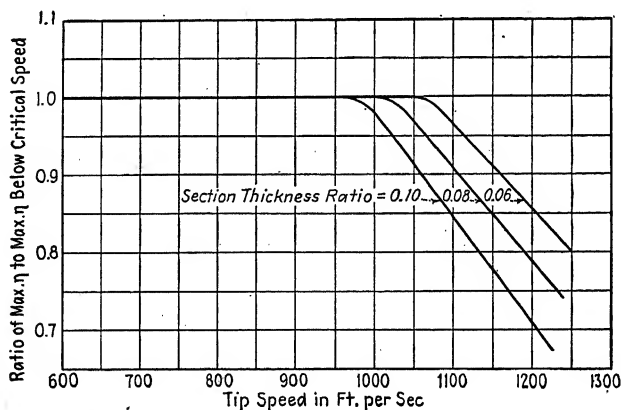


FIG. 82.—Effect of thickness ratio on loss of efficiency at high tip speeds.

in general, it seems quite likely that the critical speed is that at which the air flowing over the nose reaches the velocity of sound. This is substantiated to some degree by the fact that the critical tip speed is lower for the thicker sections which have

greater nose curvature and therefore greater air velocity over the nose portions.

As the tip speed is increased beyond the critical value, more and more of the blade runs above the critical speed and is affected by the compressibility factor. This effect is shown in Figs. 76 and 77 for a model propeller, but the model tests were apparently influenced by Reynolds number to a much greater extent than the full-scale tests, for they did not have such definite critical speeds.<sup>1</sup>

The propellers having Clark-Y type sections had slightly better efficiency below the critical tip speeds than the propellers of the same thickness ratio with R.A.F.-6 type sections, but the loss at the higher tip speeds was slightly greater. (This agrees with the results of the model airfoil tests.) It seems that since the reduction in efficiency at the higher speeds is accompanied by a more turbulent state of airflow, the better airfoils with smoother flow at low speeds suffer more at high speeds. The Clark-Y sections, however, are very slightly superior throughout the entire range covered in the tests.

**Practical Data for Correcting Efficiency for High Tip Speed.**—In both the full-scale and model propeller tests, in order to obtain high tip speeds with the wind tunnel and motive power equipment available, it was necessary to use propellers of rather low pitch. The tip-speed effects were therefore greater than for propellers of more ordinary pitch, and the results are not directly applicable to ordinary propellers of any pitch. As it affects efficiency, however, the tip-speed effect may be taken as a change of the  $L/D$  of the blade sections, and on this basis the results may be calculated for any pitch.

In the simple blade-element theory, the efficiency of a section is

$$\eta = \frac{\tan \phi}{\tan (\phi + \gamma)},$$

where  $\tan \gamma = D/L$  and  $\tan \phi$  is proportional to the effective pitch. By calculating the values of  $\gamma$  for various tip speeds from the propeller tests, the results can be applied by means of the

<sup>1</sup> The air flow through the propellers was measured in the full-scale propeller tests, and the thrust and torque grading curves as well as the section airfoil characteristics will be available when the computations are completed. Unfortunately they are still unfinished as this book goes to press.

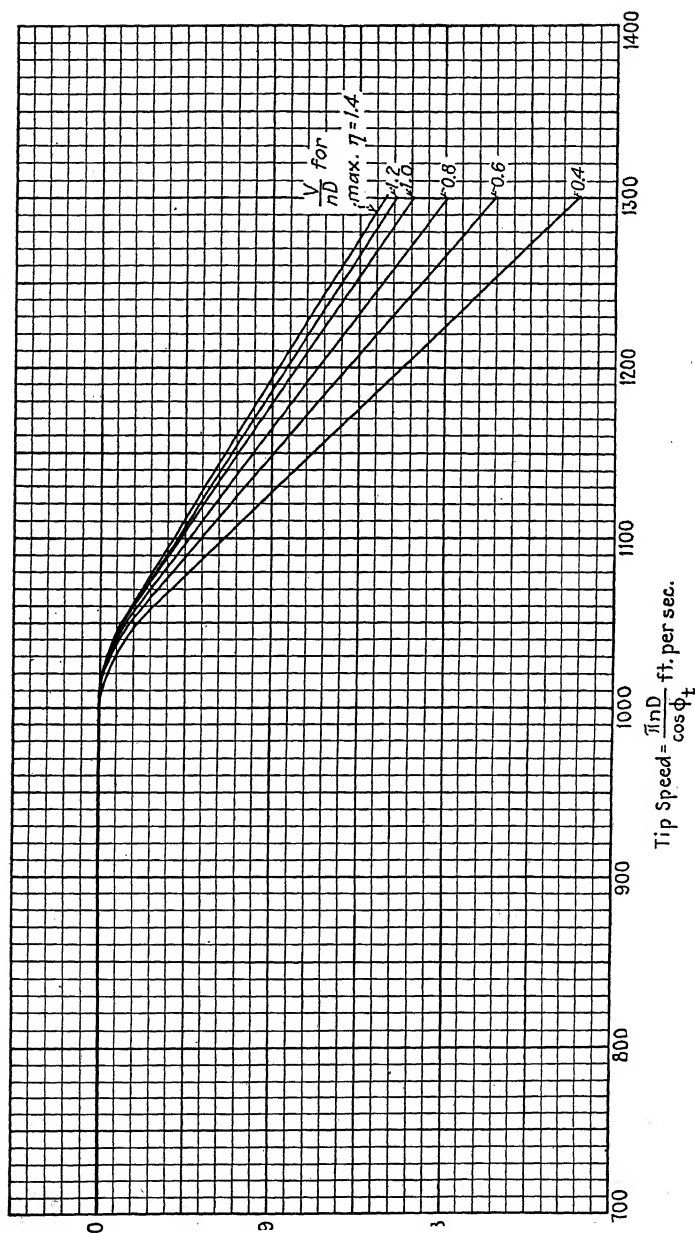


Fig. 83.—Correction factors for ordinary thin metal propellers operating at high tip speeds.

above relation to propellers operating at any effective pitch, or  $V/nD$ .

Figure 83 gives the correction factor to the maximum efficiency of ordinary thin-bladed metal propellers as computed by the above method from the average results of tests on four standard propellers. One is that shown in Fig. 176 for which test data are given in Figs. 51, 52, and 165 to 175. One of the others was geometrically similar to it but 9 ft 6 in. in diameter, and the other two were of the same general characteristics except for the plan form which was of the narrow-tip design shown in Fig. 71. Two of the propellers were tested at two different pitch settings, and the results give a satisfactory check on the method of computing the tip-speed correction factors for the other pitches.

Figure 83 gives the tip-speed correction factor to the efficiency of ordinary aluminum-alloy propellers with sufficient accuracy for performance computations. Fortunately the correction factor is approximately the same for a given propeller operating at various values of  $V/nD$ , so that while the values in Fig. 83 apply strictly to the region near maximum efficiency only, they can be used with fair accuracy for any flight condition.

It will be noticed that the tip speed in Fig. 83 is taken as

$$\text{tip speed} = \frac{\pi n D}{\cos \phi_t},$$

where the subscript  $t$  refers to the blade tip, and

$$\tan \phi_t = \frac{V}{\pi n D}.$$

This expression for the tip speed takes into account not only the peripheral speed in the plane of rotation but the speed of advance as well. Propellers operating at higher values of  $V/nD$  reach the critical tip speed at lower revolutions, assuming constant diameter. For convenience in computing the tip speed, Fig. 84 gives a curve from which the value of  $\cos \phi_t$  may be obtained for a propeller operating at any  $V/nD$ . Although the value of  $\cos \phi_t$  has practically no effect on the tip speed at low values of  $V/nD$ , its effect reaches a value of about 10 per cent or 100 ft. per sec. at high values of  $V/nD$ .

As an example showing the use of the tip-speed correction chart (Fig. 83), let us assume a metal propeller having a diameter of 10 ft. 6 in. operating at 2,100 r.p.m. on an airplane traveling at

110 m.p.h. (These figures represent an actual case, the Navy SC-1 three-purpose airplane.) For this combination

$$\begin{aligned}\frac{V}{nD} &= \frac{88 \times 110}{2,100 \times 10.5} \\ &= 0.44\end{aligned}$$

and from Fig. 84,  $\cos \phi_t = 0.99$ . Then the actual tip speed is

$$\begin{aligned}\text{T.S.} &= \frac{\pi n D}{\cos \phi_t} \\ &= \frac{\pi \times 35 \times 10.5}{0.99} \\ &= 1,167 \text{ ft. per sec.}\end{aligned}$$

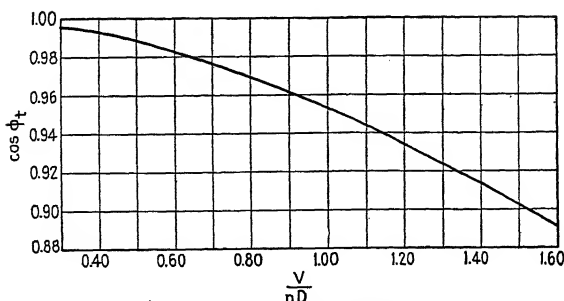


FIG. 84.—Curve for finding  $\cos \phi_t$ .

From Fig. 83, for a tip speed of 1,167 ft. per sec. and a  $V/nD$  of 0.44, the correction factor for efficiency is 0.86. The efficiency of our propeller operating at the above  $V/nD$  but with a tip speed under the critical would be, we shall say, 0.70. The efficiency at a tip speed of 1,167 ft. per sec. is then

$$\begin{aligned}\eta &= 0.70 \times 0.86 \\ &= 0.60.\end{aligned}$$

The high tip speed in this case causes a loss of 14 per cent in the useful or thrust power available.

As shown in Fig. 83, thin-bladed aluminum-alloy propellers of average form can be run at tip speeds up to 1,000 ft. per sec. without an efficiency loss due to high tip speed. Figure 85 shows directly the maximum propeller diameter which can be used at any revolutions and speed of advance to keep within the limit of 1,000 ft. per sec. and thereby avoid tip-speed loss.

In applying the tip-speed correction to airplane performance calculations, it should be kept in mind that with ordinary engines and propellers the maximum revolutions occur only at high speed, and the revolutions, and consequently the tip speeds also, are appreciably lower in taking off, in climbing, and in cruising flight. It is therefore quite possible to have a fairly large tip-speed loss at maximum horizontal speed, but if the tip speeds in climb and cruising are below the critical it is at the same time

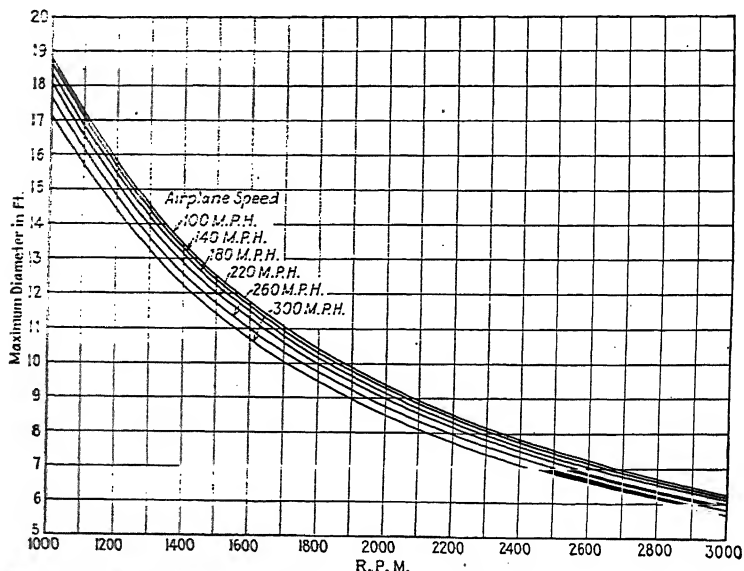


FIG. 85.—Maximum diameters for average metal propellers to operate without tip-speed loss.

possible to escape tip-speed loss in all performance excepting maximum speed. This, except in the case of racing and some military airplanes, is of little practical importance.

**Effect of Tip Speed on Noise.**—It has been noticed in all of the model and full-scale propeller tests mentioned in this chapter, as well as in electric whirling tests of propellers for strength determination, that the sound emitted increases with tip speed. As the tip speed is raised above 1,000 to 1,100 ft. per sec. or through the neighborhood of the speed of sound, the propeller noise suddenly increases in intensity, especially in or near the plane of rotation. During the full-scale tests in the N.A.C.A. Propeller

Research Tunnel, at tip speeds above the critical a pulsation was set up in the air which caused the hands and faces of the observers to tremble, indicating that violent compression waves were passing through the air.

Obviously, one way to reduce propeller noise is to reduce the tip speed.

## CHAPTER IX

### BODY AND PROPELLER INTERFERENCE

All propellers used on aircraft operate near other bodies, such as power plants, fuselages, or wings. In practically all cases, the propeller is attached directly to the power plant and is located within a few inches of it. Since both the propeller and body affect the flow of the air through which they are passing, but affect it in entirely different ways, each influences the aerodynamic characteristics of the other.

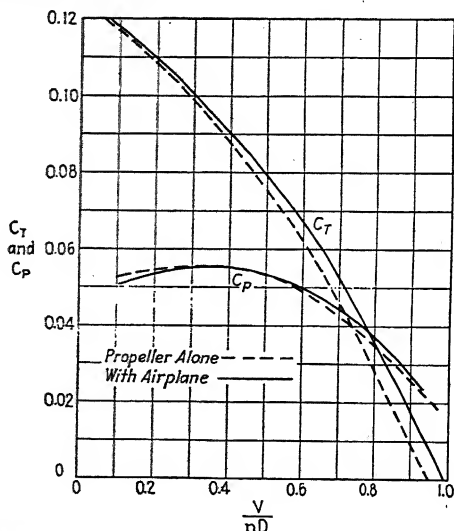


FIG. 86.—Comparison of thrust and power coefficient curves for a propeller alone and with a VE-7 airplane.

**Effect of Body on Propeller Characteristics.**—A body moving through the air has a resistance, and a certain amount of air is dragged or moved along with it. Also, even though the body were moving through a perfect non-viscous fluid, the velocity would be reduced near the nose. If a propeller is operating in the air affected by the body it will in effect be working at a lower rate of advance than if it were in free air. Thus with



respect to the local air in which it is working; it has in effect a lower  $V/nD$  and the blade elements work at higher angles of attack. Both the thrust and the torque are therefore greater than if the body were not present. This is shown in Fig. 86, in which curves of the propeller thrust and power coefficients are given for a model propeller alone, and also mounted in front of a model VE-7 airplane.<sup>1</sup>

The body does not have the effect of a change of velocity which is uniform throughout the entire plane of the propeller disc. With bodies of ordinary shape, having their longitudinal

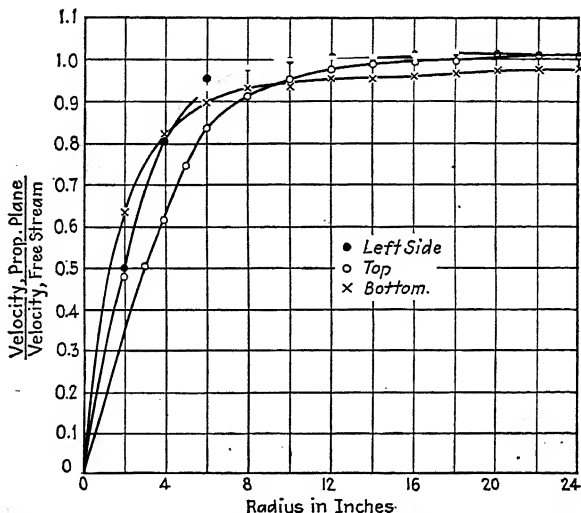


FIG. 87.—Survey of velocity in propeller plane. VE-7 model.

center lines in the neighborhood of the propeller shaft axis, the velocity of the air with respect to the body is reduced very greatly at the center but practically none out as far as the propeller tips. The velocity distribution in the propeller plane, but with the propeller removed, is shown in Fig. 87 for the VE-7 model airplane.<sup>2</sup> It will be noticed that due to the landing gear, the outer half of the propeller blades must work at lower effective

<sup>1</sup> Comparison of Tests on Air Propellers in Flight with Wind Tunnel Model Tests on Similar Forms, by W. F. Durand and E. P. Lesley, N.A.C.A.T.R. 220, 1926, model propeller B'.

<sup>2</sup> Tests of Five Metal Model Propellers with Various Pitch Distributions in a Free Wind Stream and in Combination with a Model VE-7 Fuselage, by E. P. Lesley and E. G. Reid, N.A.C.A.T.R. 326, 1929.

velocities of advance when the blades are down than when they are up. The average velocity at the propeller tip radius (18 in.) is the same as the free air velocity, but at the radius corresponding to the edge of the propeller hub the velocity has been reduced to one-half the free air value.

It is interesting to compare this velocity distribution in the propeller plane produced by the body alone with the velocity distribution caused by the propeller alone as shown in Figs. 57 and 58. Near the hub the velocity is reduced by both the body and the propeller. This means that they both set up resistance to the forward motion in the hub section, but fortunately when placed one close behind the other they cause a total resistance which is smaller than the sum of the two separate values when each is operating alone. Throughout the rest of the blade, or what is commonly called the working portion, the velocity is increased by the action of the propeller but decreased by the drag of the body. Also, due to its torque reaction the propeller gives the air back of it a twisting or rotational motion.

Unfortunately the mutual interference is too complicated for the individual effects of the propeller and body alone to be simply added together vectorially and the resultant velocity to be used as a basis for the computation of the propeller characteristics by means of the blade-element theory. Computations of this nature have been made by the author for a series of model propellers run in combination with the model VE-7 fuselage, but the results did not check the test results. Several methods of blade-element analysis including the effect of body interference have been published,<sup>1</sup> but none at the present time satisfactorily covers the problem.

**Effect of Propeller on Body Drag.**—If the body behind (or in front of) a propeller is not of extremely small size, it lies in the region of air which has been given an increase of axial velocity by the propeller, and the drag of the body is increased. This slipstream effect on body drag has been found from a large

<sup>1</sup> The Airflow round a Body as Affecting Airscrew Performance, by C. N. H. Lock, H. Bateman, and H. C. H. Townend, *British R. and M.* 956, 1925. Analysis of Experiments on an Airscrew in Various Positions within the Nose of a Tractor Body, by C. N. H. Lock, *British R. and M.* 1120, 1927. Influence of Fuselage on Propeller Design, by Theodor Troller, *N.A.C.A.-T. M.* 492.

number of tests to vary directly with the propeller thrust coefficient  $T_c$  in such a manner that

$$\begin{aligned}\frac{R}{R_0} &= a + bT_c \\ &= a + \frac{bT}{\rho V^2 D^2},\end{aligned}$$

where  $R$  is the resistance of the body when in the propeller slipstream,  $R_0$  is the resistance of the body alone at the free air velocity,  $T$  is the thrust of the propeller (or tension in the propeller shaft) when the body is present, and  $a$  and  $b$  are constants.

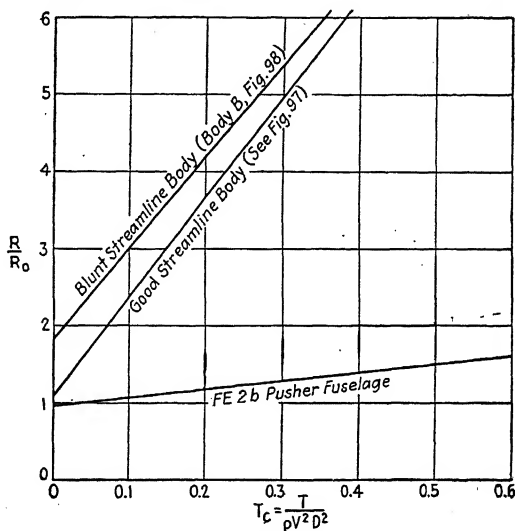


FIG. 88.—Increase of body drag with propeller thrust coefficient.

Theoretically  $a$  is equal to 1, and  $bT_c$  represents the ratio of the increase in drag due to the influence of the propeller. Actually, model tests show that for ordinary airplane fuselages the values of  $a$  are very close to 1. In one series of tests,<sup>1</sup> however, in which smooth streamline bodies having very blunt noses were used, the values of  $a$  ranged from 1 to nearly 2. This was very likely due to the propeller increasing the drag very considerably even at zero thrust, because of the disturbance of the air flow over the smooth body caused by the relatively poor

<sup>1</sup> Experiments with a Family of Airscrews Including Effect of Tractor and Pusher Bodies, Part II, by A. Fage, C. N. H. Lock, H. Bateman, and D. H. Williams. *British R. and M.* 830, 1922.

hub sections of the propeller. Values of  $b$  vary from about 1 to about 13, showing that the increased drag due to the slipstream varies greatly with different bodies. Curves of  $R/R_0$  plotted against values of  $T_c$  are given for various bodies in Fig. 88. It will be noticed that the increase in drag due to the propeller is much greater for good aerodynamic bodies of smooth form than for ordinary fuselage shapes. In fact, from the tests made to date it may be said that the greater the drag coefficient of the body the lower will be the value of  $b$ , or the relative increase in drag.

**Various Expressions for Efficiency.**—If the efficiency is found for a propeller acting near a body in the same manner as for the propeller alone, the higher thrust and torque of the propeller will be considered, but not the increased drag of the body. Thus the *apparent efficiency* is found by means of the same expression as the efficiency of a propeller in free air, or

$$\text{Apparent efficiency} = \frac{TV}{2\pi nQ},$$

where  $T$  and  $Q$  are measured for the propeller while running in the presence of the body. The thrust is increased more than the torque by the presence of the body, and the apparent efficiency is therefore always higher than the efficiency of the propeller alone at the same  $V/nD$ . Values of apparent efficiency of over 140 per cent have been measured in model propeller tests with blunt-nosed bodies, showing that this is not a true measure of the efficiency. It is therefore misleading and should not be used.

In another manner of computing the efficiency of a propeller with a body, the combination of propeller and body is looked upon as a complete propulsive unit. The *net thrust* is then considered the resultant horizontal force, or the propeller thrust minus the body drag, each measured in the presence of the other. The expression for *net efficiency* is then

$$\text{Net efficiency} = \frac{(T - R)V}{2\pi nQ}.$$

The net efficiency is always lower than the free propeller efficiency or the apparent efficiency, fairly typical curves of each being shown in Fig. 89. The net efficiency is useful for showing the effectiveness of engine-propeller units which are rather isolated from the rest of the aircraft, such as the power nacelles used on

dirigible airships. It is not useful, however, for cases where the propeller is near some essential part of the aircraft, such as a thick wing or a fuselage, which is more than merely a power-plant housing.

If the body in the presence of the propeller is considered a necessary part of the aircraft, such as a place in which to carry load, or a sustaining wing, then the drag  $R_0$  which it would have if the propeller were not near it should not be deducted from

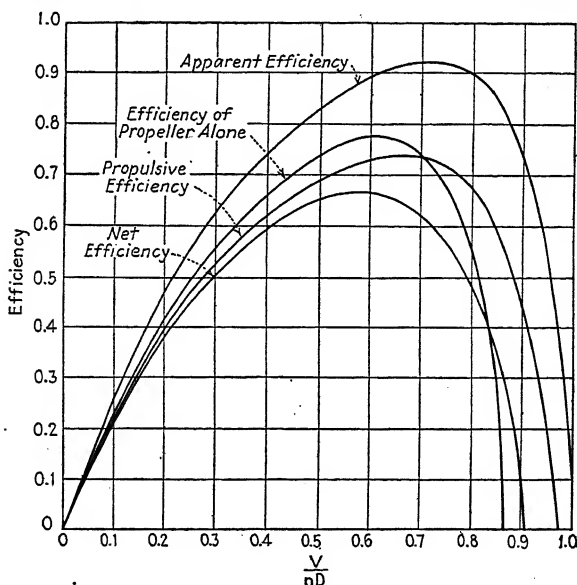


FIG. 89.—Various forms of efficiency for tractor body B, R. and M. 830.

the propeller thrust. The body under the influence of the propeller, however, has a higher drag  $R$  than it would have in free air. The thrust effective for propulsion is therefore the actual propeller thrust  $T$  in the presence of the body, minus the increase in body drag, or  $(R - R_0)$ , which is caused by the propeller. The efficiency based on this *effective thrust*  $T - (R - R_0)$  is called *propulsive efficiency* and is given by the equation

$$\text{Propulsive efficiency} = \eta = \frac{T - (R - R_0)}{2\pi nQ} V.$$

The symbol  $\eta$  is used to represent both propulsive efficiency and the efficiency of an isolated propeller, the context being sufficient to make clear which is meant.

The propulsive efficiency is a reasonable measure of the proportion of useful work done by a propeller in the presence of a body, and it is the only type of efficiency used for that purpose in this work.<sup>1</sup> If there is no body present, both  $R$  and  $R_0$  become zero and the expression becomes identical with the one given for the propeller alone. The propulsive efficiency curve is given in Fig. 89 along with the curves for the other forms of efficiency. It will be noticed that the propulsive efficiency is closer to the efficiency of the propeller alone than are the apparent or net efficiencies. As a matter of fact, with ordinary bodies the propulsive efficiency is usually only slightly below the corresponding isolated propeller efficiency, and under certain conditions it can even become slightly greater.

**Effect of Body Size.**—Model tests have been made in England<sup>2</sup> with three different-sized but similar bodies behind an average two-bladed propeller having a pitch-diameter ratio of 0.7. The bodies were circular in cross-section and had smooth low drag shapes but blunt nose portions. The three ratios of maximum body diameter  $d$  to the propeller diameter were 0.40, 0.60, and 0.75. The smallest 0.40 is about the average value found with most open cockpit fuselages on small airplanes, while 0.75 is larger than is ordinarily used in practice. In Fig. 90 the propulsive efficiency curves are shown for the propeller with each of the bodies along with the efficiency curve of the propeller alone. The maximum propulsive efficiency with the smallest body is only about 2 per cent less than the maximum efficiency of the propeller alone. This happens to be fairly typical for airplane fuselages of about the same size with respect to the propeller, although the shape of the body is not representative. The maximum efficiency is about 5 per cent less with the medium body and 7 per cent less with the largest body than the efficiency of the propeller alone.<sup>3</sup> These percentage differences in effi-

<sup>1</sup> In airplane performance computations the use of propulsive efficiency, instead of isolated propeller efficiency, eliminates the necessity for and the inaccuracies due to the correction for the extra drag of the parts in the slipstream.

<sup>2</sup> Experiments with a Family of Airscrews Including Effect of Tractor and Pusher Bodies, Part II, by A. Fage, C. N. H. Lock, H. Bateman, and D. H. Williams, *British R. and M.* 830, 1922.

<sup>3</sup> The percentage difference is based upon the ratios of the actual values of efficiency, not on the direct difference. Thus an efficiency of 0.75 is 6.25 per cent lower than an efficiency of 0.80.

ciency remain approximately the same throughout the whole flight range.

The fact that the propeller operates in slower air with the larger bodies is shown by the larger values of  $V/nD$  for both zero thrust and maximum efficiency with the larger bodies.

The above tests give a good idea of the manner in which the size of body and propeller affects the propulsive efficiency through a fairly wide range, but unfortunately the bodies used in the tests

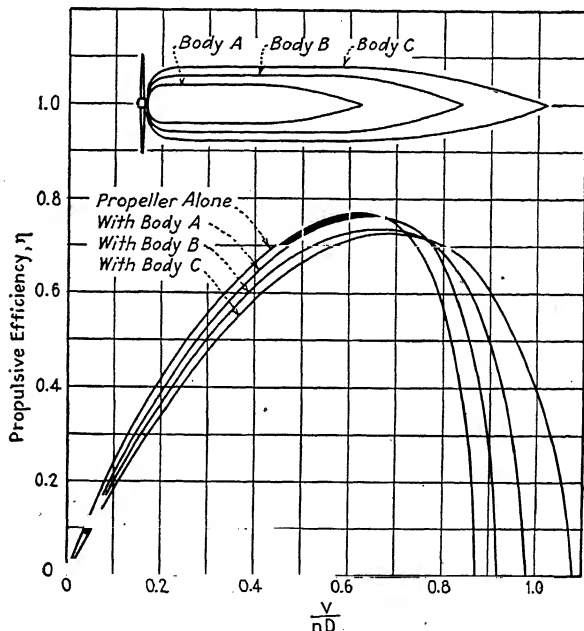


FIG. 90.—Propulsive efficiency of an average propeller with various sized bodies.

are quite different from ordinary aircraft body forms. Full-scale tests have been made, however, covering a smaller range of relative sizes but with an actual 200-hp. nine-cylinder air-cooled Wright J-5 engine in the nose of an average open-cockpit fuselage with an undercarriage. The tests were made in the 20-ft. Propeller Research Tunnel of the N.A.C.A.<sup>1</sup> The engine had normal cowling leaving the cylinder heads exposed, as shown in Fig. 91. Four metal propellers were tested, varying in diameter

<sup>1</sup> Full Scale Tests with a Series of Propellers of Different Diameters on a Single Fuselage by Fred F. Waick, N. A. C. A. T. R. 320, 1930

from 8 ft. 11 in. to 10 ft. 5 in. All were geometrically similar to the propeller shown in Fig. 176 and were set at a blade angle of 15.5 deg. at  $0.75R$ . The maximum cross-sectional area of the fuselage was 11 sq. ft., and assuming a circular cross-section having the same area, the tests were run at values of  $d/D$  from 0.36 to 0.42. The overall diameter of the engine was 45 in.

The results showed little difference in the characteristics of the four propellers tested, the only one of importance being an increase of propulsive efficiency of the order of 1 per cent for a 5 per cent increase of propeller diameter, or a 5 per cent decrease

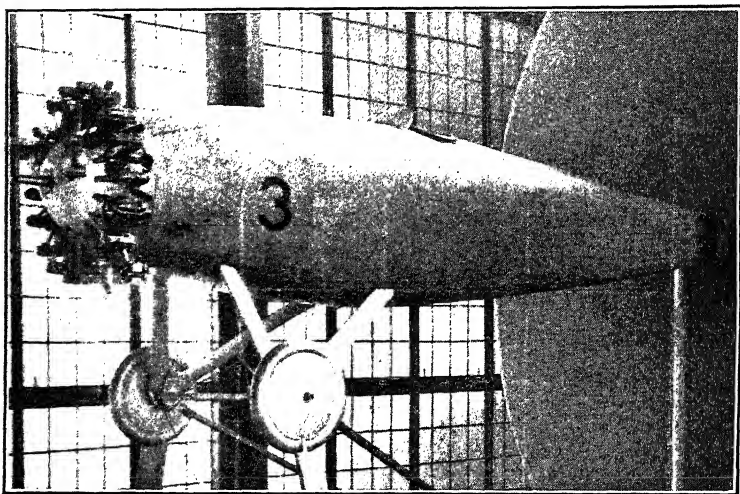


FIG. 91.—Open cockpit fuselage with Wright J-5 engine.

in the ratio  $d/D$  (see Fig. 92). This is the same general tendency as, but to a greater degree than, the results of the tests with the blunt-nosed model bodies which showed a variation of about 1 per cent in efficiency for a 10 per cent change of  $d/D$ . It is thought that the full-scale tests give good results for practical use within the limited range of the tests but that a mean value of 1 per cent change in efficiency with an 8 per cent change in diameter is probably a more accurate figure to use if the range is considerably larger.

**Effect of Body Shape and Drag.**—With the smooth blunt-nosed bodies used in the model tests shown in Fig. 90, the propulsive efficiency is lower with any of the bodies than the efficiency of the propeller alone. This is not necessarily the case with all



bodies, for tests have been made at Stanford University<sup>1</sup> in which with certain bodies the propulsive efficiency was found to be higher than the efficiency of the propeller alone. Figure 93 tabulates the results of some of the tests, in which a 3-ft. propeller having a pitch-diameter ratio of 0.9 was tested in front of a series of bodies all 1 ft. in diameter but with various amounts

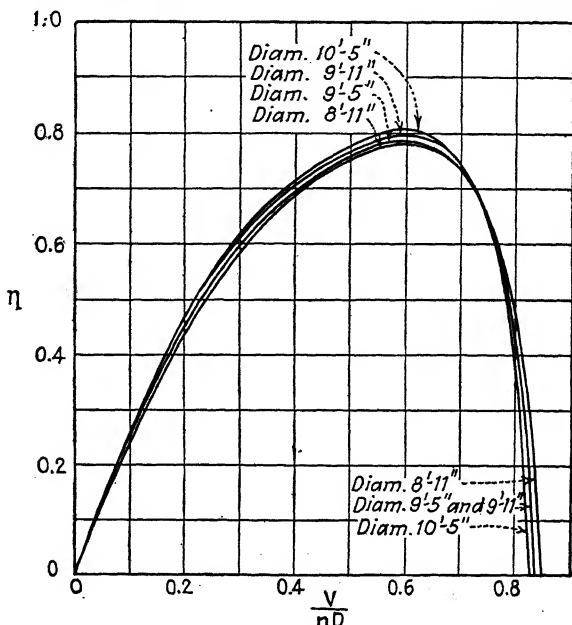


FIG. 92.—Propulsive efficiencies with different sized propellers on an average fuselage.

of taper at the propeller end. It will be noticed that with all of the bodies except that having the greatest taper, the propulsive efficiency is higher than the efficiency of the propeller alone. Also, for all of the bodies with a cylindrical portion the propulsive efficiency is greater for the bodies with greater resistance. This is partly because the bodies are small enough to be almost entirely in the central portion of the propeller where the poor propeller sections have the effect of decreasing rather than increasing the velocity of the air over the body, and partly because the poorer bodies close to the central portion of the propeller partially blank off or shield this poor portion of the propeller which

<sup>1</sup> The Effect of Slipstream Obstructions on Air Propellers, by E. P. Lesley and B. M. Woods, N.A.C.A.T.R. 177, 1924.

represents a loss rather than a gain when the propeller is operating alone.

It may be said that in general the propulsive efficiency is higher with bodies of poor aerodynamic shape than with those having low drag. To have a helpful influence on the propulsive

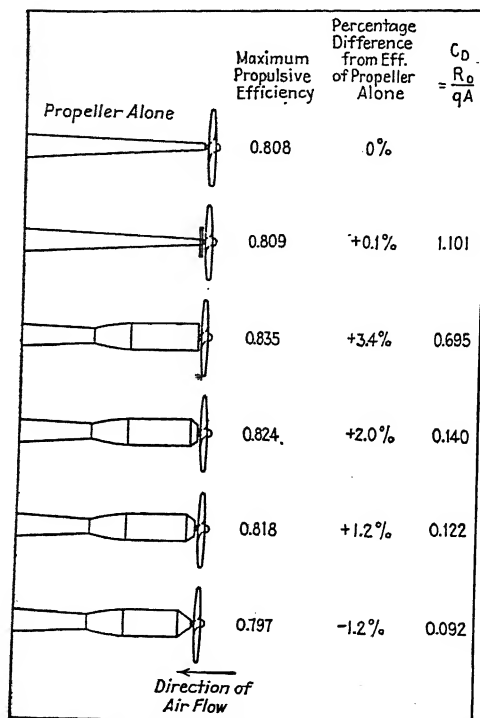


FIG. 93.—Some bodies with which the propulsive efficiency is higher than the efficiency of the propeller alone.

efficiency, however, the high drag must be due to a poor nose where the effect is close to the propeller. This is shown by some English tests in which a propeller was run with its poor hub portion enclosed in a spinner forming the nose of a good streamline body, and excrescences in the form of annular rings to increase the drag were added to the body at various distances from the nose.<sup>1</sup> All of these annular rings had the same amount of area.

<sup>1</sup> Experiments with a Family of Airscrews Including Effect of Tractor and Pusher Bodies, Part IV, by H. Bateman, H. C. H. Townend, and T. A. Kirkup, British R. and M. 1030, 1926.

The propulsive efficiency is less with the excrescences than with the smooth body, as tabulated in Fig. 94. Also, as would be expected, it is less with the smooth body than for the propeller alone. Considering only the cases in which the excrescences are present, however, the propulsive efficiency is higher if they are located nearer the nose, even though the drag also is higher.

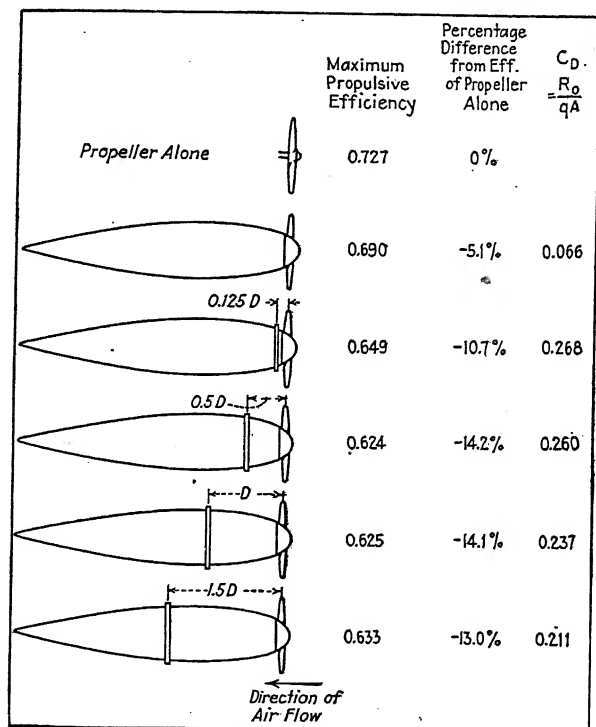


FIG. 94.—Effect of body excrescences on propulsive efficiency.

In fact, even the net efficiency is higher for the forward position of the annulus, indicating that if the body must be poor, say due to a radiator, it will improve the general effectiveness to put the poor portion at the nose and close to the propeller rather than back away from it.

The model tests referred to have been made with bodies which were either of nearly perfect streamline form or of some simple geometrical shape. Neither of these types is actually used on airplanes. A few tests have been made which show the effect of actual airplane shapes on propulsive efficiency. One of these

was on a model of the VE-7 airplane tested with several standard-type wood propellers.<sup>1</sup> The airplane is shown in Fig. 95. The propulsive efficiency with a propeller of pitch-diameter ratio

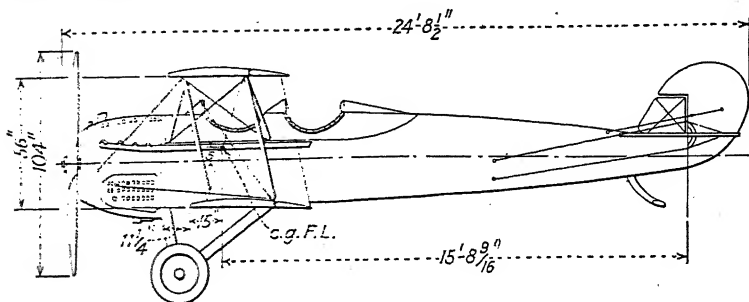


FIG. 95.—The VE-7 airplane.

0.7 is compared with the efficiency of the propeller alone in Fig. 96. The thrust coefficient  $C_T$  is here based on the effective thrust  $T - (R - R_0)$ , which may be called the tension in the propeller shaft minus the increase in body drag due to the

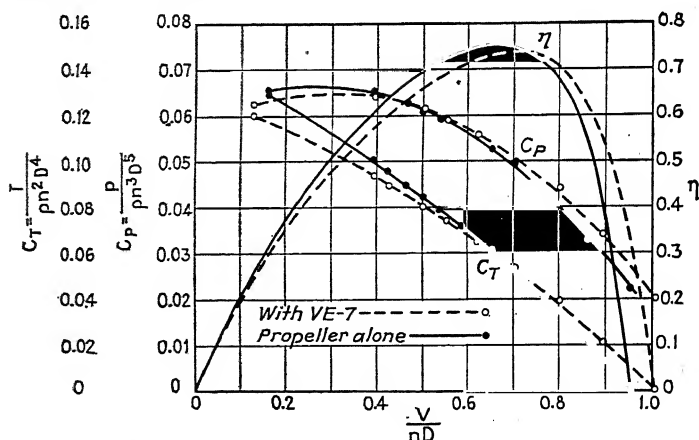


FIG. 96.—Comparison of propulsive efficiency with and without VE-7 airplane.

propeller. The maximum propulsive efficiency is about 2 per cent lower than the maximum efficiency of the propeller alone, and this is within one or two per cent of the reduction obtained

<sup>1</sup> Comparison of Tests on Air Propellers in Flight with Wind Tunnel Model Tests on Similar Forms, by W. F. Durand and E. P. Lesley, N.A.C.A.T.R. 220, 1926.

with most ordinary airplanes having either air-cooled or water-cooled engines in the nose of the fuselage. This is shown by many full-scale tests in the N.A.C.A. Propeller Research Tunnel, in which the same propellers have been tested on the VE-7 airplane and on both open-cockpit and cabin fuselages with both radial air-cooled and V-type water-cooled engines.<sup>1</sup> The propulsive efficiency is very nearly the same with all fuselages, it being highest for one with a radial air-cooled engine having complete or N.A.C.A.-type cowling, and lowest for a V-type water-cooled engine (Curtiss D-12) entirely enclosed in a smoothly rounded cowling. No radiator was in the airstream in the latter case, and the body had the lowest drag coefficient of any tested. The maximum propulsive efficiency ranged about 2 per cent less with this body than with any of the others, and about 4 per cent less than the one with N.A.C.A. cowling.

**Effect of Position of Propeller with Respect to Nose of Body.—**

The English tests referred to, in which an annular ring was located at various distances from the nose of a streamline body,<sup>2</sup> also included different positions of the propeller in the nose portion. Two bodies were used, one having a pointed nose and the other having a rounded nose, both being of good streamline shape, and both being the same back of the nose portion. The nose portion of the body formed a propeller spinner in each case, and three different locations of the propeller were selected with each body so that  $0.25D$ ,  $0.39D$ , and  $0.46D$  of the propeller were enclosed. The maximum propulsive efficiency and the reduction from the efficiency of the propeller alone are tabulated in Fig. 97.

With both shapes of bodies the efficiency is reduced as the propeller is moved back into the body, even though more of the inefficient hub section is enclosed. With the forward position the efficiency with the pointed nose is slightly higher than that

<sup>1</sup> Drag and Cooling with Various Forms of Cowling for a "Whirlwind" Radial Air-cooled Engine, Parts I and II, by Fred E. Weick, N.A.C.A.T.R. 313 and 314, 1929. Full Scale Wind Tunnel Tests of a Series of Metal Propellers on a VE-7 Airplane, by Fred E. Weick, N.A.C.A.T.R. 306, 1929. Working Charts for the Selection of Aluminum Alloy Propellers of a Standard Form to Operate with Various Aircraft Engines and Bodies, by Fred E. Weick, N.A.C.A.T.R. 350, 1930.

<sup>2</sup> Experiments with a Family of Airscrews, Including Effect of Tractor and Pusher Bodies, Part IV, by H. Bateman, H. C. H. Townend, and T. A. Kirkup. British R. and M. 1030. 1926.

with the blunter rounded nose, probably because with the pointed nose the propeller is located farther forward of the main portion of the body. For the two rear positions the efficiency is greater with the rounded nose.

The same tendency of the propulsive efficiency to become greater as the propeller is moved forward with respect to the body has been shown to be true for actual fuselage shapes, by

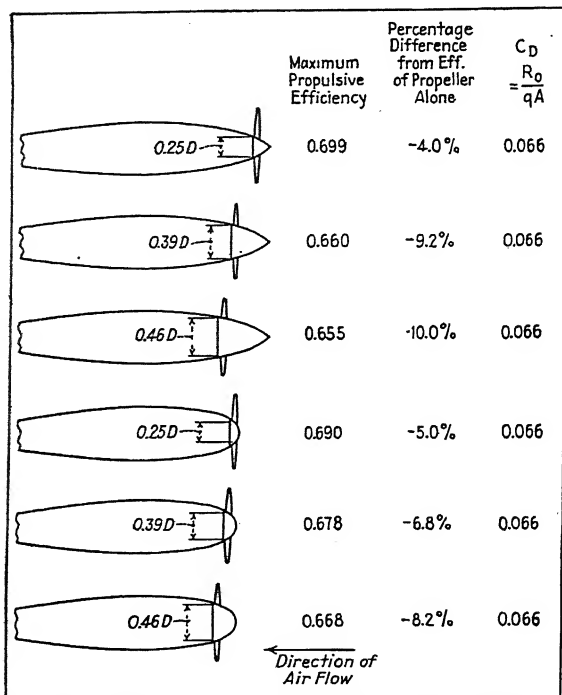


FIG. 97.—Effect of position in nose on propulsive efficiency.

both model and full-scale tests. The model tests were made at Stanford University with a 3-ft. propeller and a model DH-4 fuselage.<sup>1</sup> The DH-4 airplane had a water-cooled Liberty engine with a large flat-nosed radiator and no spinner. Moving the propeller from  $\frac{3}{8}$  to 4 in. ahead of the radiator increased the propulsive efficiency 4 per cent with a propeller having a pitch-diameter ratio of 0.7, and 5 per cent with one of 0.9.

<sup>1</sup> Interaction between Air Propellers and Airplane Structures, by W. F. Durand, NACA TR 235, 1926

The full-scale tests were made in the N.A.C.A. Propeller Research Tunnel with an open-cockpit fuselage having a radial air-cooled Wright J-5 engine with ordinary cowling as shown in Fig. 91.<sup>1</sup> The same 10 ft. 5 in. metal propeller was tested on the fuselage with a direct-drive engine and also with a geared engine of the same type, the propeller being located 7.5 in. farther forward in the latter case. The propulsive efficiency was found to be 4.4 per cent greater with the propeller in the forward position. This is probably an extreme case due to the high drag but small body interfering with the central portion of a large propeller.

**Comparison of Tractor and Pusher Arrangements.**—In the British tests with the smooth blunt bodies previously referred to,<sup>2</sup> three pusher arrangements were tested as well as the three tractor. The same propellers were used with all of the bodies, and each of the pusher bodies had the same diameter as one of the tractor bodies. The pusher bodies had the bluff portion at the rear and consequently had higher drag coefficients.

The maximum propulsive efficiencies are given in Fig. 98 for both the pusher and tractor bodies. Within the limits of experimental error there is no difference between the propulsive efficiencies obtained with the pusher and tractor bodies having the same diameter. In both cases it is lower with the larger bodies. With the particular bodies tested the net efficiencies are higher for the tractor than for the pusher arrangements, due to the greater drag of the pusher bodies. This is likely to be the case in practice also because of the desirability of keeping the propeller close to the engine, but it is not necessarily so for there have been a few cases in which the propeller was mounted some distance from the engine on an extended shaft.

**Mutual Interference between Propellers and Wings.**—Very little experimental work has as yet been done on the mutual interference between propellers and wings,<sup>3</sup> although some model

<sup>1</sup> The Effect of Reduction Gearing on Propeller-body Interference, as Shown by Full-scale Wind Tunnel Tests, by Fred E. Weick, N.A.C.A.T.R. 338, 1930.

<sup>2</sup> Experiments with a Family of Airscrews Including Effect of Tractor and Pusher Bodies, Part II, by A. Fage, C. N. H. Lock, H. Bateman, and D. H. Williams, British R. and M. 830, 1922.

<sup>3</sup> A rather complete series of tests with a 4-ft. propeller mounted with a nacelle in a large number of positions with respect to a wing having a span of 16 ft. is now underway in the N.A.C.A. 20-ft. Propeller Research Tunnel.

tests showing the general effect of a propeller on a wing have been made at the Göttingen Aerodynamics Laboratory in Germany.<sup>1</sup> These tests indicate that if the propeller is above the wing, it increases the natural circulation and therefore also the lift. Conversely, if the propeller operates below the wing, the lift is reduced somewhat. The effect on lift is, however, ordinarily quite small.

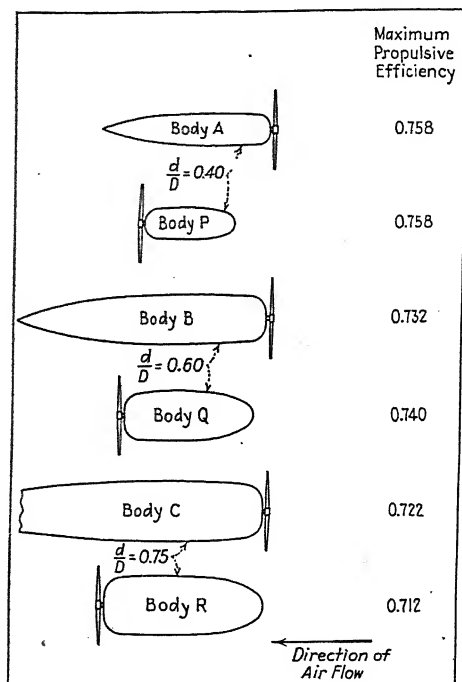


FIG. 98.—Comparison of propulsive efficiency with pusher and tractor bodies.

The wing also has an effect on the propeller characteristics, for if the propeller is above the wing it is in a region of faster-moving air, and its thrust and power coefficients are less than in free air at the same  $V/nD$ . Again, if the propeller is below the wing the effect is the opposite. If the propeller axis is near the chord line of the wing, the lift and drag of the wing increase due to the increased velocity in the slipstream, and the propeller thrust and torque increase because the wing drag reduces the air velocity.

<sup>1</sup> Mutual Influence of Wings and Propeller, by L. Prandtl, N.A.C.A. T.N. 74, 1921.



With most present-day airplanes, and particularly the single-engined ones, the effect of the wings on the propeller characteristics is small. Full-scale tests have been made in the N.A.C.A. Propeller Research Tunnel in which five different single-engined airplanes having monoplane and biplane wings were tested both with and without the wings.<sup>1</sup> The propulsive efficiency was

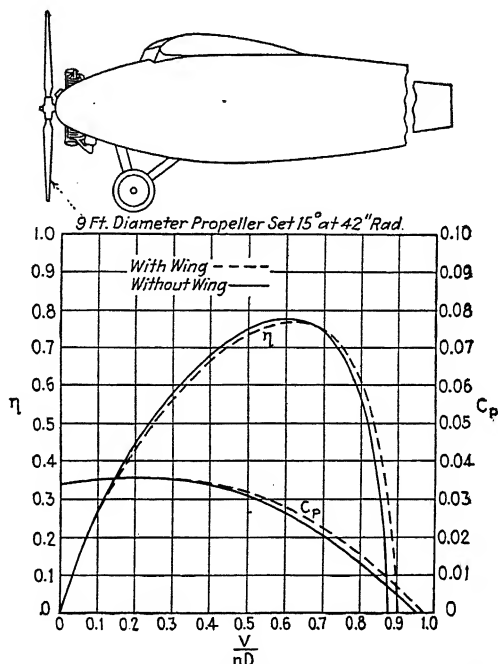


FIG. 99.—Effect of wing on propulsive efficiency with a single-engined airplane.

reduced from 1 to 3 per cent by the presence of the wings, the loss being about the same for the biplane and monoplane wings tested. The loss was slightly greater with high-pitch than with low-pitch propellers.

Typical curves of propulsive efficiency and power coefficient are given in Fig. 99 for a cabin monoplane with and without the wing. The power coefficient  $C_P$  is slightly greater with the wing

<sup>1</sup> The Effect of the Wings of Single Engine Airplanes on Propulsive Efficiency as Shown by Full-scale Wind Tunnel Tests, by Fred E. Weick and Donald H. Wood, N.A.C.A.T.N. 322, 1929. Full-scale Tests of Wood Propellers on a VE-7 Airplane in the Propeller Research Tunnel, by Fred E. Weick, N.A.C.A.T.R. 301, 1929.

in place, indicating that the wing reduces the velocity through the propeller plane even though the leading edge is more than half the propeller diameter to the rear.

The VE-7 airplane was tested both with and without the tail surfaces, and there was no measurable difference in the propeller characteristics.

The effect of an exceptionally large wing on propulsive efficiency has been tested at Stanford University.<sup>1</sup> The wing chord was 2.37 times the propeller diameter and the thickness was

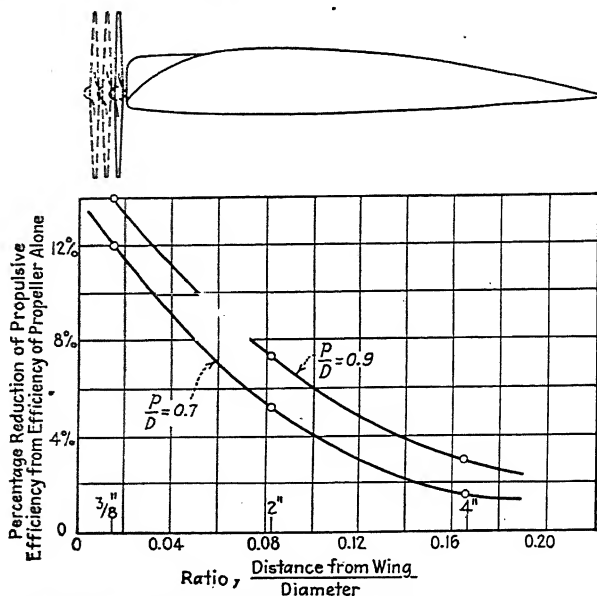


FIG. 100.—Effect of large wing on propulsive efficiency.

0.42D. The tests were made with two propellers having pitch-diameter ratios of 0.7 and 0.9, and with each propeller located at three different distances in front of the wing. Figure 100 shows the percentage loss in propulsive efficiency compared with the efficiencies of the propellers alone. It will be noticed that while the loss is great if the propeller is very close to the wing, there should even in this extreme case be little loss if the propeller were located at a distance of  $D/5$  or more ahead of the leading edge. As in the case of the smaller wings and most bodies, the loss in

<sup>1</sup> Interaction between Air Propellers and Airplane Structures, by W. F. Durand, N.A.C.A.T.R. 235, 1926.

propulsive efficiency is slightly greater with the propeller having the higher pitch.

The above tests represented the case of a wing engine installation for a proposed Army night bomber, the central fuselage and nose engine arrangement of which was also tested. As shown in Fig. 101, due to the great size of the body and wing, and the machine gun turret in the nose, this probably represents the most extreme case of body and propeller interference tested to date. The projected area of the body covers almost the entire propeller disc area. The loss in propulsive efficiency was 25 per cent for both the 0.7 and 0.9 pitch-ratio propellers close to the body, but

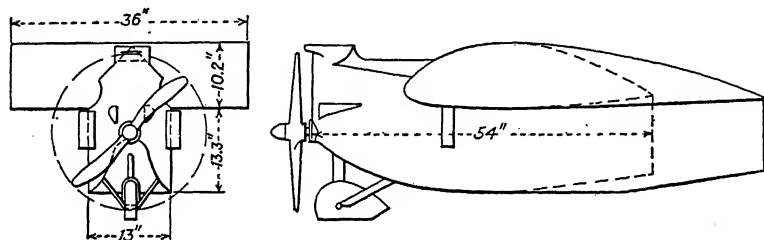


FIG. 101.—Central section of proposed night bomber with extreme propeller interference.

if the results are extrapolated it seems that a very small loss might be expected if the propeller were placed at least  $D/2$  ahead of the body.

**Effect of Propeller Pitch Distribution.**—As shown by Fig. 87, the effect of an ordinary type of body located near the center of the propeller disc is to reduce the velocity of the air passing through the propeller, this reduction being great at the hub and little, if anything, at the blade tips. Tests have been made with five model propellers having different pitch distributions, operating both alone and with a model VE-7 airplane.<sup>1</sup> The model propellers were of metal and, except for the blade angles, were all geometrically similar to the typical metal propeller shown in Fig. 177. Model A had a uniform pitch over the entire blade with a pitch-diameter ratio of 0.7. The others all had the same average pitch, but the pitch of B increased from  $0.6R$  to the tip, that of C decreased over the same range, while that of D increased and E

<sup>1</sup> Tests of Five Metal Model Propellers with Various Pitch Distributions in a Free Wind Stream and in Combination with a Model VE-7 Fuselage, by E. P. Lesley and E. G. Reid, N.A.C.A.T.R. 326, 1929.

decreased from  $0.6R$  to the hub. Curves showing the distribution of pitch along the radius for the various models are given in Fig. 102, along with values of the maximum efficiencies of the propellers alone and the maximum propulsive efficiencies with the model airplane.

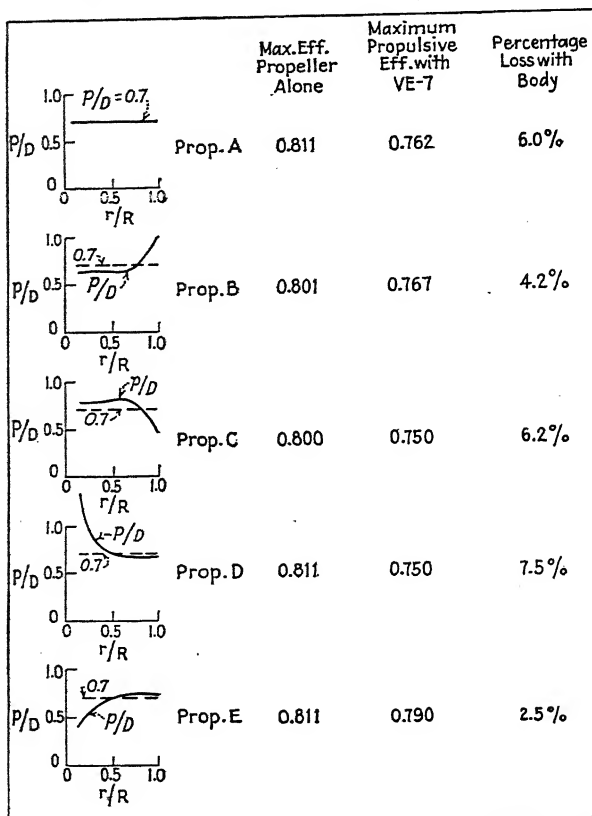


FIG. 102.—Effect of pitch distribution on propulsive efficiency with VE-7 body.

The maximum efficiencies of the propellers alone are all surprisingly near the same value. Models *A*, *D*, and *E* all had maximum efficiencies of 0.811. These models all had a uniform or nearly uniform pitch over the outer portions of the blades, and the results indicate that without a body present the sections near the hub are relatively unimportant. Propellers *B* and *C* had efficiencies about one per cent lower.

With the model airplane, the propellers had propulsive efficiencies in the order in which their pitch distributions fitted the flow conditions set up by the body (as shown in Fig. 87). Propeller *E* had a propulsive efficiency of 0.79, which was noticeably better than any of the others. This propeller had a pitch distribution of such a nature that the angles of attack at maximum efficiency, as calculated by the simple blade-element theory on the basis of the average velocity given in Fig. 87, were practically the same over the entire blade. The pitch distribution therefore fitted the flow conditions caused by the body remarkably well. Propeller *B*, which also had the pitch increasing from hub to tip but did not fit the airflow so well, was next with a propulsive efficiency of 0.767. Model *D*, in which the pitch increased toward the hub, had as high an efficiency as any when tested alone but as low an efficiency as any when tested with the airplane, giving it the greatest loss. This indicates that the sections near the hub are more important when the propeller is working with a body.

It is also interesting that the loss in efficiency with the uniform-pitch propeller *A* in front of the VE-7 model was 6 per cent, while the average loss with five uniform-pitch model wood propellers in front of the same model airplane<sup>1</sup> was only 4 per cent. The smaller loss with the wood propellers is probably due to their thicker and therefore less efficient sections near the hub, for the poorer sections would have less to lose by being forced to work at poor angles by the body interference.

**Practical Use of Body Interference Data.**—The simplest and most accurate method of taking body interference into account in designing a propeller is to base the design on wind tunnel tests made with the particular design of body and propeller desired. This is of course not ordinarily possible, but a selection can be made from the results of full-scale tests made in the N.A.C.A. Propeller Research Tunnel with series of typical metal propellers tested at various pitch settings and with several typical forms of bodies. Since there is fortunately little difference in the interference effects on either propulsive efficiency or power absorbed with moderate changes in body form, the results of the above tests can be used directly for selecting a

<sup>1</sup> Comparison of Tests on Air Propellers in Flight with Wind Tunnel Model Tests on Similar Forms, by W. F. Durand and E. P. Lesley, N.A.C.A.-T.R. 220, 1926.

suitable propeller of the type tested to operate with any ordinary form of single-engined tractor airplane.<sup>1</sup> Corrections for different relative propeller and body sizes can be based on the information given in this chapter.

For bodies which do not fall within the range of the above tests, or for propellers of different forms, the results of the various tests which have been made can be used indirectly to show the approximate effect to be expected. For example, although few tests have been made with pusher installations, the results of the few which have been made show that the effect on propulsive efficiency and power absorbed is about the same as for tractor installations having about the same size and resistance of the body. A pusher propeller can therefore often be satisfactorily obtained by selecting it to fit an equivalent tractor installation.

<sup>1</sup> The test results are given in convenient form for this purpose in Working Charts for the Selection of Aluminum Alloy Propellers of a Standard Form to Operate with Various Aircraft Engines and Bodies, by Fred E. Weick, N.A.C.A.T.R. 350, 1930. The charts are also given in Chap. XVII.

## CHAPTER X

### THE EFFECT OF PROPELLER CHARACTERISTICS ON AIRPLANE PERFORMANCE

In calculating the performance of an airplane, it is usual to compute first the power required for horizontal flight at various air speeds. The performance at any speed is then found from the relation between the power required and that available.

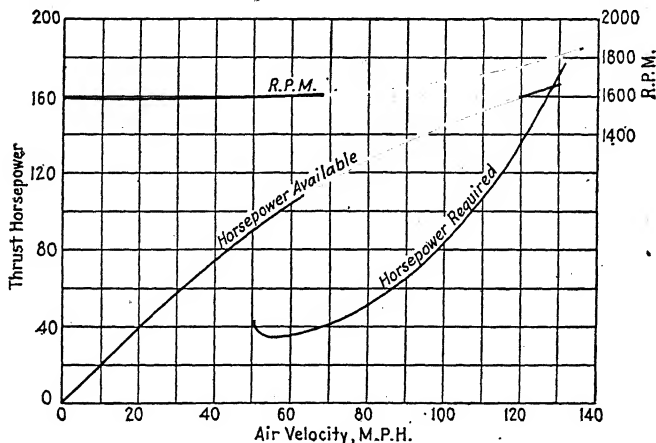


FIG. 103.—Curves of power required, power available, and revolutions; 8.17-ft. metal propeller.

The curves of power required vs. air speed are of more or less similar form for all airplanes.<sup>1</sup> For showing the effect of propeller characteristics on airplane performance it is convenient to take as an example a typical airplane having a normal performance, such as the Vought VE-7. The curve of power required<sup>2</sup> vs. airspeed for the VE-7 is given in Fig. 103.

<sup>1</sup> The manner of obtaining the power required may be found in books on airplane design, such as "Airplane Design—Aerodynamics," by E. P. Warner, or "Engineering Aerodynamics," by Walter S. Diehl.

<sup>2</sup> The curve was obtained from flight tests reported in *Characteristics of Five Propellers in Flight*, by J. W. Crowley, Jr., and R. E. Mixson, N.A.C.A.T.R. 292, 1928.

**Power Available.**—The power available under various conditions depends upon the characteristics of the power plant and propeller. With the gasoline engine, as used in airplanes today, the full-throttle torque is very nearly constant throughout the working range of revolution speeds, although it drops off slightly with increased revolutions.

A typical curve of full-throttle horsepower at sea level *vs.* revolutions per minute is given in Fig. 104 for an engine rated at 200 hp. at 1,800 r.p.m. In ordinary practice, if 1,800 r.p.m.

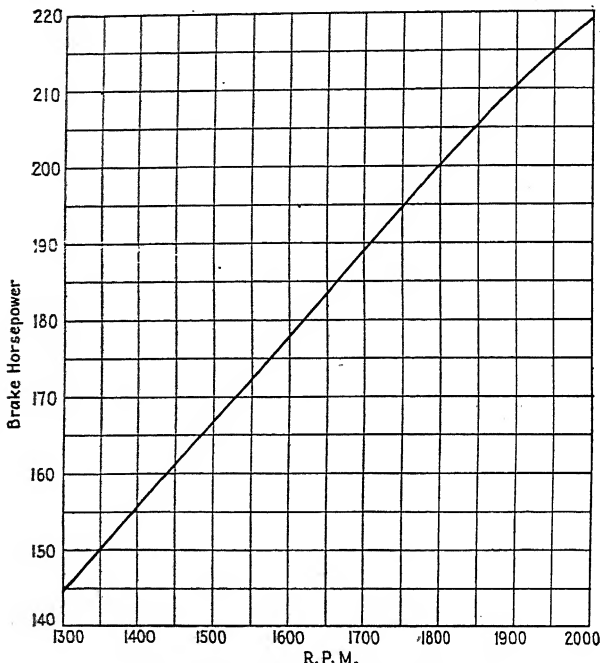


Fig. 104.—Full-throttle horsepower *vs.* r.p.m.

is specified by the engine manufacturer as the maximum revolution speed for service use, the propeller is designed so as to absorb the full engine power (200 hp.) at the maximum horizontal sea-level speed and 1,800 r.p.m. These are often called the maximum horsepower and revolution speed, although they are actually merely the maximum specified for safety.

The useful or thrust horsepower available at maximum speed at sea level is the product of the maximum brake horsepower and the propulsive efficiency of the propeller.



As an example, let us select from the series of metal propellers whose aerodynamic characteristics are given in Figs. 51, 52, and 56 the one which will give the highest possible sea-level speed. This will, of course, be the propeller having the highest efficiency under the high-speed conditions. We find, either by means of the method of the speed-power coefficient  $C_s$  or with the Eiffel logarithmic diagram, that the highest speed is obtained with the propeller having a diameter of 8.17 ft. and a blade-angle setting of 22 deg. at  $0.75R$ . ( $p'/D = 0.95$ , where  $p' = p$  at  $0.75R$ ).<sup>1</sup>

Neglecting the effect of the relative size of propeller and body, this propeller gives a propulsive efficiency of 0.833 at maximum speed. That efficiency was obtained, however, from tests with a 9-ft. propeller on the VE-7 airplane, and as shown in Chap. IX, our 8.17-ft. propeller will give a slightly lower efficiency due to the effect of body interference. Taking the effect on the efficiency to be 1 per cent for an 8 per cent difference in propeller diameter, the actual propulsive efficiency with our 8.17-ft. propeller will be  $0.833 \times 0.989$  or 0.824, giving a thrust horsepower of 164.8 and a maximum speed of 128.5 m.p.h.

It is now desirable to find the useful power available at lower speeds so that we can draw a curve of power available *vs.* airspeed. Since the torque coefficient of the propeller increases as the advance per revolution becomes less (see Figs. 47 and 48), but the engine torque remains essentially constant, a decrease in airplane speed will cause the engine to slow down to the point where the torque of the engine and that of the propeller are equal.

To find the full-throttle r.p.m. corresponding to any other than the maximum speed, the curves of  $V/nD$  *vs.*  $C_s$  (Fig. 51 or 52) can be used. We shall proceed to find the r.p.m. at which our 8.17-ft. metal propeller will turn at an air speed of 80 m.p.h. First, we shall assume three revolution speeds which are likely to cover the range desired, say 1,700, 1,600, and 1,500 r.p.m., and find the value of  $C_s$  for each at 80 m.p.h. and the reduced power corresponding to each revolution speed. (The latter is obtained from Fig. 104.) This gives us three points through which we

<sup>1</sup> To find this it is first necessary to assume a trial value for the propulsive efficiency, from which the approximate thrust horsepower is calculated and an approximate value of the maximum speed obtained from the power-required curve of Fig. 103. This speed is then used in selecting the propeller. If the efficiency does not check that assumed, the process is repeated.

can draw a curve of r.p.m. vs.  $C_s$  (curve 1, Fig. 105). Now, for each of the above three values of  $C_s$ , we can find from Fig. 51 or 52 the value of  $V/nD$  for our propeller, which has a blade-angle setting of 22 deg. at  $0.75R$ , and then, knowing  $V/nD$ ,  $V$ , and  $D$ , we can solve for the revolutions. This gives us another set of values of r.p.m. vs.  $C_s$ , which when plotted give curve 2, Fig. 105. At the intersection of the two curves, r.p.m. = 1,618 and  $C_s = 0.939$ , which are the values for our propeller at full throttle and 80 m.p.h.<sup>1</sup> At 1,618 r.p.m. the engine develops

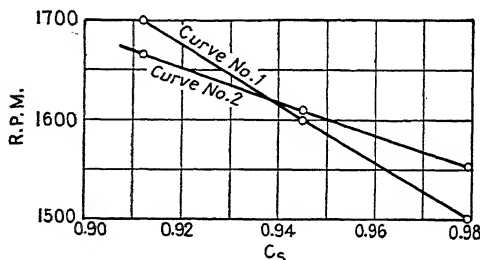


Fig. 105.

179.9 hp. (Fig. 104), and for  $C_s = 0.919$  the propulsive efficiency is  $0.715 \times 0.989 = 0.707$  (Fig. 51 or 52). The useful or thrust power available at 80 m.p.h. is therefore

$$179.9 \times 0.707 = 127.2 \text{ hp.}$$

Following the same procedure, the revolutions and the power available have been found for several air speeds and the curves drawn in Fig. 103. The maximum horizontal speed is shown by the intersection of the curves of power required and power available. The vertical distance between the power-required and power-available curves shows the excess of power available above that required for horizontal flight, and this excess can be used for climbing. At speeds higher than the maximum horizontal speed (higher speeds can be attained by diving) the

<sup>1</sup> The tests on which these figures are based were made with the propeller axis parallel to the direction of airflow, whereas in actual flight the propeller axis assumes angles as high as 10 or 12 deg. with respect to the flight path. Full-scale tests in the 20-ft. Propeller Research Tunnel of the N.A.C.A. have shown, however, that the propeller characteristics are practically unaffected within that range. Other tests confirming this conclusion are reported in Experimental Investigation of Aircraft Propellers Exposed to Oblique Air Currents, by O. Flachsbart and G. Kröber, N.A.C.A.T.M. 562, 1930.

full-throttle revolutions will go above the maximum permissible, and the engine should be throttled.

For the purpose of showing the effect on the performance of the VE-7 of using other propellers of our metal series, the power-available curves have also been computed for propellers having blade-angle settings at  $0.75R$  of 20, 17.5, 15, and 12.5 deg. (The corresponding values of  $p'/D$  are 0.86, 0.74, 0.63, and 0.52.) The propeller with a setting of 17.5 deg. operates at the peak

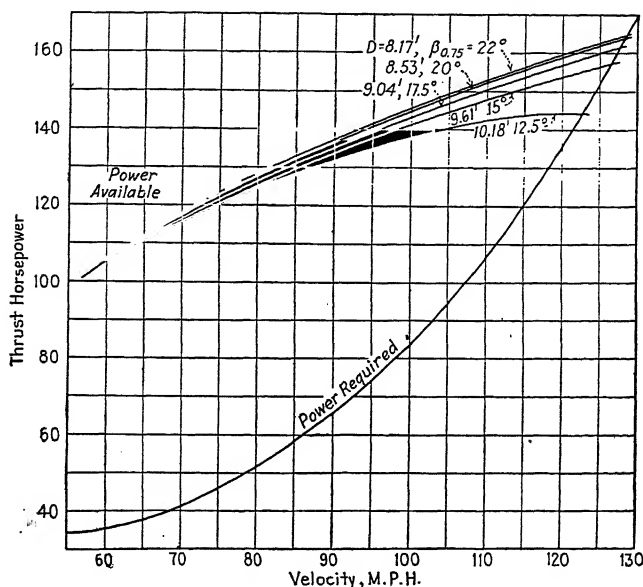


FIG. 106.—Curves of power available with metal propellers of various diameters and pitches.

of its efficiency curve at the maximum horizontal speed. The power-available curves for these propellers, along with that for our original "high-speed" propeller having a setting of 22 deg., are given in Fig. 106.

**Effect of Propeller Characteristics on Maximum Speed.**—Since the engine revolutions and power are specified for the high-speed condition of flight, the propeller must conform to the engine requirements. In our example this means that it must absorb 200 hp. at 1,800 r.p.m. at the maximum speed of the airplane, and since the brake horsepower is determined, the propulsive efficiency is the only factor in the propeller design affecting the

thrust horsepower at maximum speed, and therefore the speed itself.

The high-speed performance with the five metal propellers is tabulated below:

Blade angle at $0.75R$ , deg .....	22.0	20.0	17.5	15.0	12.5
$p'/D$ .....	0.95	0.86	0.74	0.63	0.52
Diameter, ft. ....	8.17	8.53	9.04	9.61	10.18
Propulsive efficiency .....	0.833	0.828	0.810	0.780	0.710
Body correction factor .....	0.989	0.994	1.001	1.010	1.017
Corrected efficiency .....	0.824	0.822	0.811	0.788	0.721
Max. speed, m.p.h. ....	128.5	128.4	127.8	126.6	122.7

It is noteworthy that even wide extremes of pitch ratio and diameter do not have a great effect on the high speed. The propeller operating at its peak efficiency (17.5 deg. at  $0.75R$ , 9.04-ft. diameter) is the one which in the past has been generally

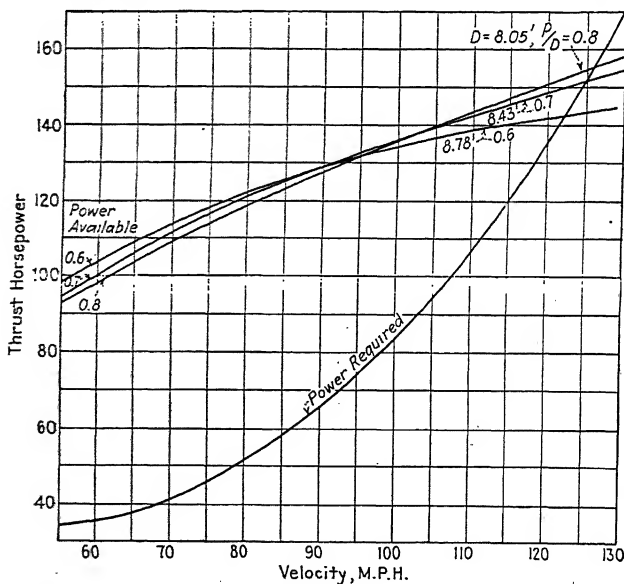


FIG. 107.—Curves of power available with wood propellers.

used as a propeller for all-around service on airplanes of this power and speed. It gives a maximum speed only 0.7 m.p.h. lower than that with the best high-speed propeller.

The propeller having the lowest pitch setting, which setting is considerably lower than would ordinarily be used in practice,

also has the lowest efficiency at high speed. The maximum speed with this propeller is 122.7 m.p.h., which is 5.8 m.p.h. less than the best obtained. It is interesting to note that a reduction in propulsive efficiency from 0.824 to 0.721 or 12.5 per cent reduces the maximum speed of the airplane only 4.5 per cent.

The curves of power available for three typical wood propellers, having pitch ratios of 0.6, 0.7, and 0.8, are shown in Fig. 107. The data for these propellers, as well as for the metal propellers, have been obtained from full-scale tests in the N.A.C.A. 20-ft. Propeller Research Tunnel at Langley Field.<sup>1</sup> The high-speed performance with the wood propellers is as follows:

$p/D$ .....	0.8	0.7	0.6
Diameter, ft.....	8.0	8.43	8.78
Propulsive efficiency <sup>1</sup> .....	0.768	0.758	0.710
Max. speed, m.p.h.....	125.5	124.9	122.1

<sup>1</sup> These propellers had approximately the same diameter calculated, and so the body interference factor is automatically taken into account.

The propeller with a pitch ratio of 0.8 has approximately the best pitch ratio for high speed. It is interesting to note that the diameter is nearly the same as that of the metal propeller giving the highest speed and, also, that the maximum speed obtained with the best metal propeller is 3 m.p.h. or 2.4 per cent higher than that with the best wood propeller. This difference would of course be greater if the propellers were operating at high tip speeds.

A simple rule for finding the effect on the maximum speed of ordinary differences in propulsive efficiency is that *the percentage variation in velocity is one-third that in efficiency*, although this usually underestimates the velocity variation by about 10 per cent and it is somewhat more accurate to use 0.37 instead of one-third. This rule, while of course of a very approximate nature, is quite useful for making preliminary estimates and is usually sufficiently accurate for designing propellers to fit their conditions.

**Effect of Propeller Characteristics on Rate of Climb.**—When the power available is greater than the power required, as is the case for an airplane flying between its minimum and maximum

<sup>1</sup> Full-scale Tests of Wood Propellers on a VE-7 Airplane in the Propeller Research Tunnel, by Fred E. Weick, N.A.C.A.T.R. 301, 1928. Full-scale Wind Tunnel Tests of a Series of Metal Propellers on a VE-7 Airplane, by Fred E. Weick, N.A.C.A.T.R. 306, 1928.

horizontal speeds, the excess power available may be used for climbing (see Figs. 106 and 107). The rate of climb in feet per minute is given by the relation

$$\text{Rate of climb} = \frac{EHP \times 33,000}{W},$$

where *EHP* is the excess horsepower available over that required for horizontal flight and *W* is the weight of the airplane in pounds. Obviously the greatest rate of climb for a given airplane is obtained at the speed at which the vertical distance between the power-available and power-required curves is the greatest. This speed is usually in the neighborhood of 0.6 of the maximum speed with modern airplanes.

Because its torque coefficient becomes greater as the advance per revolution decreases, the propeller holds the engine to a lower revolution speed than that at the maximum velocity of the airplane, even though the throttle is left wide open. As a result the thrust or useful power at climbing speed is less than that at the maximum horizontal speed, both because the engine delivers less power at the lower revolutions and because the propulsive efficiency is less at the lower rate of advance per revolution at climbing speed.

With a given airplane and engine, the propeller which will give the highest thrust horsepower at climbing speeds will give the highest rates of climb. Referring to the power-available curves for the three wood propellers in Fig. 107, it is seen that the curves cross, and that while the highest-pitch propeller is the best for maximum speed, it is also the poorest for climb, and the one having the lowest pitch gives the greatest power available for climbing.

In Fig. 108 are curves of the rate of climb *vs.* air speed for our VE-7 at sea level, the total weight of the airplane being 2,200 lb. Each curve shows the climb for one of the wooden propellers. The one having a pitch ratio of 0.6 gives a maximum rate of climb of 1,095 ft. per min., the one with a pitch ratio of 0.7 gives 1,062, and the best speed propeller with a pitch ratio of 0.8 gives only 1,020.

It will be noticed that on Fig. 106 the curves of power available for the thin-bladed metal propellers do not cross above the speed for maximum climb, so that *the propeller giving the highest horizontal speed also gives the greatest thrust horsepower available at*

climbing speeds and consequently the best climb! The curves of rate of climb vs. air speed for our series of five metal propellers

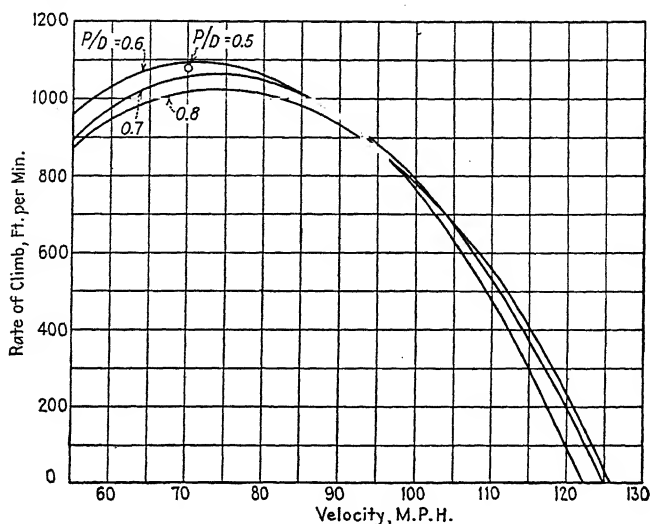


FIG. 108.—Rates of climb vs. air speed with wood propellers.

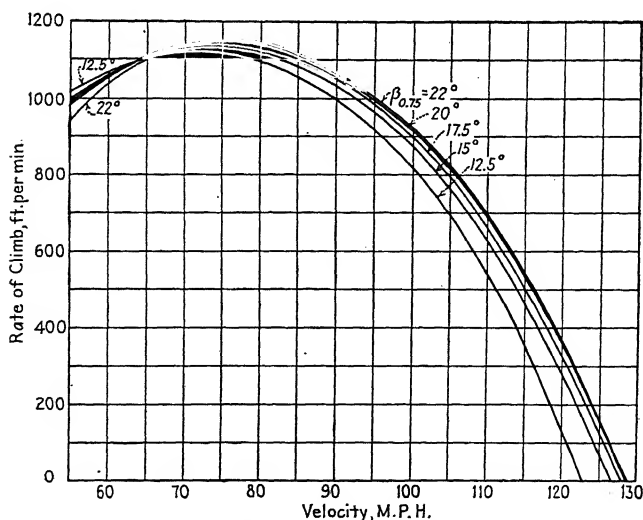


FIG. 109.—Rates of climb vs. air speed with metal propellers.

on the VE-7 are shown in Fig. 109. These curves show that for these propellers the lower the pitch the lower is the maximum

climb, which is the reverse of the case with the wood propellers. Another interesting point is that there is a difference of only 30 ft. per min. between the best and the poorest maximum rates of climb.

The reason for this difference in climb between the performance of the wood propellers and the metal propellers is made clear by a study of the curves in Fig. 110. The top set of curves shows the

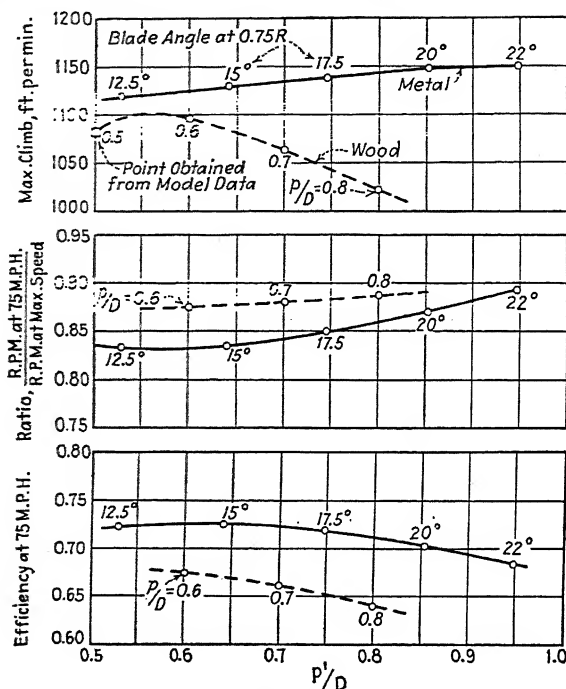


FIG. 110.

maximum rates of climb obtained with both the wood and metal propellers with the various pitch ratios. Unfortunately, the lowest-pitch wood propeller tested was not low enough to give the maximum possible climb with that type of propeller, and so the point for  $p/D = 0.5$  has been calculated from tests on model propellers of similar form. The wood propeller giving the maximum climb would from the top set of curves of Fig. 110 have a pitch ratio of about 0.56 and would give a rate of climb of 1,100 ft. per min. The metal propeller giving both the highest speed and the best climb gives a rate of climb of 1,150 ft. per min., which is about 5 per cent better than that with the wood pro-



PELLER giving the best climb and about 13 per cent better than with the best high-speed wood propeller.

The middle set of curves on Fig. 110 shows the reduction of engine revolutions at a speed of 75 m.p.h., which is about the average speed for maximum climb with all of the propellers being investigated. The ratio of the r.p.m. at 75 m.p.h. to the r.p.m. at maximum horizontal speed is plotted against pitch ratio. Since the engine torque is approximately constant, the ratio of the revolutions is also an indication of the fraction of the maximum permissible brake horsepower which is being used at climbing speed. With both the wood and the metal propellers the reduction in revolutions is less for the propellers of high than low pitch, but the variation with pitch is much more pronounced with the metal propellers. The highest-pitch metal propeller makes use of a larger portion of the maximum horsepower than any of the wood propellers, and the lower-pitch metal propellers make use of considerably less than any of the wood propellers. Thus the high-pitch metal propeller has a great advantage over the lower-pitch metal propellers in the amount of engine power used in climb, while the high-pitch wood propeller has but a very slight advantage over the lower-pitch wood propellers.

The bottom set of curves in Fig. 110 shows the variation of propulsive efficiency with pitch ratio at a climbing speed of 75 m.p.h. The metal propellers are decidedly more efficient in climb than the wood propellers. From the curves in Fig. 110, it is seen that in climbing flight the drop in engine revolutions is less for the higher-pitch propellers but that the efficiency is greater with the lower-pitch propellers. Since with the wood propellers the change in efficiency with pitch ratio is greater than the variation in revolutions, the low-pitch wood propellers are better in climb. Conversely, since with the metal propellers the variation of revolutions is greater than that of efficiency, the higher-pitch metal propellers are better in climb.

A simple and useful formula for quickly finding the effect of changes in propeller characteristics on the rate of climb is as follows:

A one-point change (*i.e.*, from 0.71 to 0.72) in either the propulsive efficiency or the fraction of the maximum revolutions results in a change in the rate of climb, in feet per minute, of

$$\frac{330 \times HP_{max.}}{W}, \text{ or } \frac{330}{\text{power loading}}.$$

This shows that in the case of a single-seater fighter type of airplane, in which the weight per horsepower is very low, the propeller can influence the absolute rate of climb more than with a heavily laden transport airplane. Due to the much greater climb of the fighter type, however, variations in the propeller characteristics will have a larger relative effect on the climb of the transport type. As an example of this difference suppose that we have a typical 600-hp. fighter airplane weighing 3,000 lb. and having a maximum rate of climb of 3,000 ft. per min., and also a 600-hp. transport weighing 9,000 lb. and having a rate of climb of 400 ft. per min. A total difference of five points in efficiency and fraction of maximum revolutions, which as can be seen from Fig. 110 is easily obtainable, will cause a difference in the rate of climb of the fighter of 330 ft. per min. and a difference in that of the transport of only 110 ft. per min. The climb of the fighter, however, is changed only 11 per cent, while that of the transport is changed 27.5 per cent.

In special cases where the climb of an airplane far outweighs in importance the other performance characteristics such as the high-speed and cruising performance, the propeller can be designed to absorb the full permissible power of the engine at climbing speed. The pilot is then relied upon to throttle the engine at all higher air speeds.

**The Effect of Propeller Characteristics on Take-off.**—The take-off distance, or the length of the run of a land plane between the time of starting and the time of leaving the ground, depends on the accelerating force, which is the excess of thrust over the resistance. The thrust becomes less as the speed increases, and the resistance, which is partly due to rolling friction, varies widely with different fields, making it practically impossible to calculate the take-off distance accurately. An approximate idea of the relative take-off qualities with different propellers can be obtained, however, by comparing the average thrusts over the take-off period. The average thrust can be found with sufficient accuracy by taking the average of the thrusts at zero advance<sup>1</sup> (called static thrust), at the take-off speed or

<sup>1</sup> The static thrust can be conveniently found by means of the equation

$$T = \frac{QC_T}{DC_Q} \quad \text{or} \quad T = \frac{2\pi QC_T}{DC_P},$$

where  $Q$  is the full-throttle engine torque, which is substantially constant.

slightly higher, and at a third speed halfway between the other two.

The various thrusts obtained with our metal and wood propellers on the VE-7 airplane are tabulated below for speeds of 0, 30, and 60 m.p.h.

Material	Diameter, ft.	Blade angle at 0.75R or pitch ratio	Static thrust, lb.	Thrust at 30 m.p.h., lb.	Thrust at 60 m.p.h., lb.	Average thrust lb.	Approximate take-off run, ft.
Metal	8.17	22.0 deg.	731	713	656	700	364
	8.53	20.0 deg.	860	755	664	759	336
	9.04	17.5 deg.	962	803	660	806	316
	9.61	15.0 deg.	1,050	809	656	836	305
	10.18	12.5 deg.	1,080	815	656	850	300
Wood	8.05	0.8	930	761	616	769	332
	8.43	0.7	950	780	628	786	325
	8.78	0.6	970	801	650	807	316

In the last column approximate take-off distances are given for an average field and no wind. These distances were obtained from an average value by varying the distances for the various propellers in inverse proportion to their average thrusts. This is not, of course, strictly correct, but since the average resistance is very small compared with the average thrust, the distances are not greatly in error relative to one another.<sup>1</sup>

It will be noted that the best wood propeller in climb, *i.e.*, that having a pitch ratio of 0.6, is also the best of the wood propellers in take-off. Also, the lowest-pitch metal propeller gives the best take-off of all, and the highest-pitch metal propeller, which

<sup>1</sup> Flight tests have been made by the author which give an interesting check on the performances calculated for the VE-7 with the five metal propellers. A Stearman biplane with a 200-hp. Wright J-5 engine was tested with four metal propellers of different diameters, all being geometrically similar to the ones used for the VE-7 calculations. In each case the pitch setting was adjusted to give 1,900 r.p.m. at maximum speed. The performances measured were as follows:

Diameter, ft.....	8	8.5	9	9.5
Max. speed, m.p.h.....	114.5	114.5	114.0	112.0
Max. climb, ft./min.....	850	850	850	850
Take-off time, sec.....	10.5	8.3	8.2	8.0

gave the highest speed and the best climb, gives the poorest take-off. The shortest distance, however, is only 18 per cent less than the longest, which in this case makes a difference of only 64 ft. This is practically negligible with ordinary airplanes operating from average fields but might, of course, become important in the special cases of small fields or heavily laden airplanes.

The problem of a seaplane taking off from the water is somewhat different from that of a land plane, for the resistance of the water rises to a very large value at a speed called the "hump" speed which is usually in the neighborhood of one-half the take-off speed. It is often difficult to get sufficient propeller thrust to push over the hump speed with heavily loaded seaplanes, and sometimes it is necessary to design the propeller to absorb the maximum permissible power of the engine at the hump speed. In that case, as in the case where the full power is used in climb, the pilot is relied upon to throttle the engine at higher air speeds.

**Effect of Propellers on Cruising Performance.**—After an airplane has taken off and climbed to a reasonable altitude it is usually flown at reduced throttle, both because it is easier on the engine, which has a limited life, and because the fuel consumption is lower and the range and endurance are greater.

A reasonable cross-country cruising speed for our VE-7, which, with the 8.17-ft. propeller has a maximum speed of 128.5 m.p.h. at 1,800 r.p.m., would be about 100 m.p.h. The power required for horizontal flight at 100 m.p.h. is found from Fig. 103 to be 83.2 hp. Assuming that the propulsive efficiency is the same at cruising speed as at high speed (the reason for this assumption will appear later), the brake or engine power required is  $83.2/0.824 =$  approximately 100 hp.

The revolution speed to which the engine is throttled to give 100 hp. at 100 m.p.h. can be found in the same manner as for full-throttle flight at reduced speeds, *i.e.*, by (1) assuming three revolution speeds which cover the likely range, say 1,300, 1,400, and 1,500; (2) computing the value of  $C_s$  for each; (3) from the curves of  $C_s$  vs.  $Vn/D$  finding the value of  $V/nD$  corresponding to each value of  $C_s$ ; (4) calculating the r.p.m. corresponding to each  $V/nD$ ; (5) plotting curves similar to those of Fig. 105 of both the original and final values of r.p.m. vs.  $C_s$ ; and (6) finding the actual values of r.p.m. and  $C_s$  at the intersection of the two curves. The values for cruising at 100 m.p.h. with

100 hp. are r.p.m. = 1,420 and  $C_s = 1.39$ . The efficiency for  $C_s = 1.39$  is 0.821, which checks the assumption of 0.824 closely enough so that another trial would still give 1,420 r.p.m.

It will be noticed that the  $C_s$  for cruising, 1.39, is nearly the same as that for high speed, 1.42. This is also true of the values of  $V/nD$  at high speed and cruising, for the drop in revolutions is very nearly proportional to the drop in air speed. The most efficient propeller at high speed is therefore also very nearly the most efficient at cruising speeds. Actually, the most efficient of our series of metal propellers for cruising at 100 m.p.h. with the engine throttled to 100 hp. at 1,420 r.p.m. would have a diameter of 8.20 instead of 8.17 ft., a blade angle at  $0.75R$  of  $21.9$  instead of  $22$  deg., and an efficiency about one-tenth per cent greater, which is negligible.

At a cruising speed of 80 m.p.h., the 8.17-ft. propeller would be throttled to 1,193 r.p.m., and its propulsive efficiency would be 0.818 as compared with 0.820 for the most efficient propeller under the same conditions.

The revolutions of all of our five metal and three wood propellers would be nearly enough the same at any cruising speed so that the wear on the engine can be considered the same for all. The more efficient ones would actually turn a little more slowly, for they would require less engine power to give the same thrust power. The fuel consumption is also less in about the proportion that the efficiency is greater.

The VE-7 cruising at 100 m.p.h. requires approximately 100 hp. from the engine, and except for the limitations imposed by the propeller, it would be possible to obtain this at any r.p.m. above that at which the engine is held down to delivering 100 hp. at full throttle, or in this case from 900 to 1,800 r.p.m., the latter being the upper limit for safety. A curve of the specific fuel consumption in pounds per horsepower per hour for our 200-horsepower engine developing 100 hp. at various revolutions is given in Fig. 111.<sup>1</sup> The specific consumption with the 8.17-ft. metal propeller throttled to 1,420 r.p.m. is 0.524 lb. per hp. per hr. With a propeller which would absorb the 100 hp. at 1,050 r.p.m. or below, the fuel consumption would be reduced to 0.495 lb. per hp. per hr. There would be no advantage in going lower

<sup>1</sup> This figure was drawn from data given in *Cruising Performance of Airplanes*, by E. E. Wilson and B. G. Leighton, Navy Dept. Bur. Aeronautics *Tech. Note* 133, 1924.

than 1,050 r.p.m., for the fuel consumption would not be any less and it would be harder on the engine.

The metal propeller of our family having the highest efficiency while absorbing 100 hp. at 1,050 r.p.m. and a cruising speed of 100 m.p.h. would have a diameter of 9.65 ft., a blade angle at  $0.75R$  of 24 deg., and a propulsive efficiency on the VE-7 of  $0.851 \times 1.010 = 0.859$ . The actual fuel consumption at 100 m.p.h. with this propeller, considering its higher efficiency as well as the lower specific consumption at 1,050 r.p.m., is 9.5 per cent better than with the best cruising propeller throttled to 1,420 r.p.m.

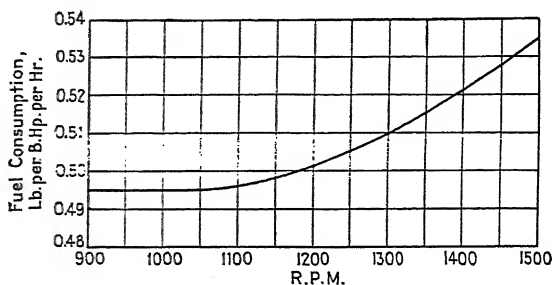


FIG. 111.—Fuel consumption of engine rated at 200 hp. at 1,800 r.p.m., when developing 100 hp. at various revolutions.

The large propeller would, however, entail great disadvantages which would practically prohibit its use. The high-speed full-throttle r.p.m. would be only 1,150, so that only 131 hp. instead of the full 200 would be taken from the engine, and the high speed would consequently be only 111 m.p.h. instead of 128.5. For the same reason the maximum rate of climb would be reduced to less than half of its normal value. Also, it is probably harder on the engine to develop 100 hp. at 1,050 than at 1,420 r.p.m., due to the higher explosion pressures and temperatures.

**Range and Endurance.**—Both the range and the endurance are directly proportional to the propulsive efficiency and inversely proportional to the specific fuel consumption. It is therefore advantageous, of course, to have a high propulsive efficiency at cruising speeds and a low fuel consumption, but the importance of these may be outweighed by other factors where the maximum range or endurance are desired without regard to the other performance. In these cases it is also advantageous to have a propeller which will enable the airplane to take off with the

largest possible fuel load, and the best propeller is a compromise which must be worked out for each individual case.

**Performance at Altitude.**—The density of the air decreases with altitude, as shown for standard atmosphere in Fig. 112, where  $\rho_0$  is the density at sea level, or 0.002378 slug per cu. ft.

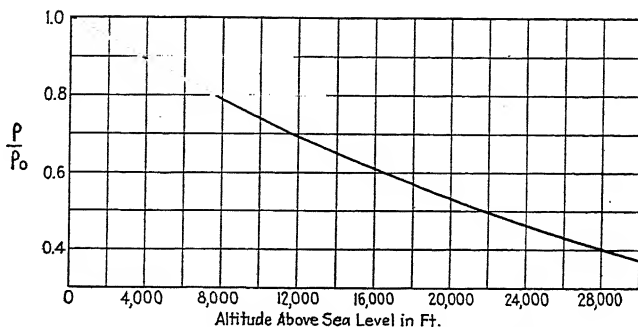


FIG. 112.—Variation of air density with altitude.

With an airplane flying horizontally at any angle of attack, the following equation shows the relation of lift, density, and velocity:

$$L = \frac{1}{2} \rho V^2 C_L S,$$

$$= \rho V^2 \times \text{constant}.$$

Since the lift is equal to the weight, which remains constant (fuel loss with time being neglected), the airplane must fly faster in the lighter air encountered at altitudes above sea level, in order to maintain level flight at the same angle of attack. Using the subscript zero to denote sea level, the necessary speed at altitude is given by the equation

$$V = V_0 \sqrt{\frac{\rho_0}{\rho}}.$$

If the angle of attack does not change, the  $L/D$  remains the same regardless of altitude, and since  $L$  remains constant,  $D$  does also. The thrust horsepower required at the new altitude and speed is then

$$HP_r = \frac{DV}{550}$$

$$= \frac{DV_0}{550} \sqrt{\frac{\rho_0}{\rho}}$$

$$= HP_{r_0} \sqrt{\frac{\rho_0}{\rho}},$$

where  $HP_{r_0}$  is the thrust horsepower required at sea level.

The power required curve for our VE-7 at an altitude of 10,000 ft. has been calculated by means of the above relations and is given in Fig. 113 along with the curve for sea level.

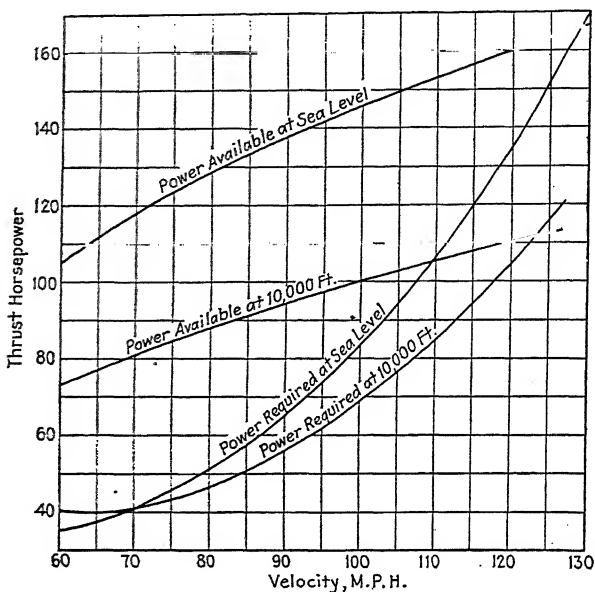


FIG. 113.—Power available and power required curves for sea level and 10,000 ft. with 8.17-ft. metal propeller.

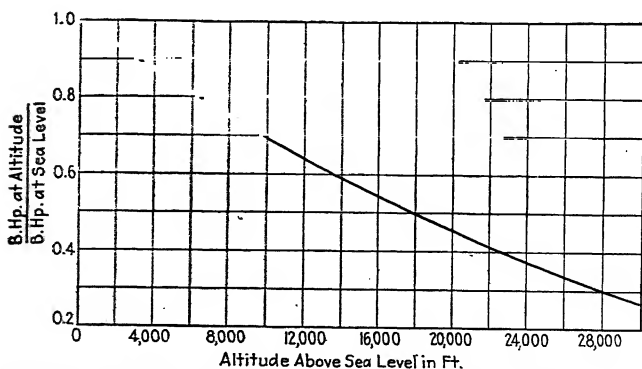


FIG. 114.—Variation of engine power with altitude, at constant r.p.m.

The power available depends on the effect of altitude on both the engine power and the propeller characteristics. As shown in Chap. VI and also by the blade-element theory, the thrust,



torque, and power of a propeller vary directly with the density of the air, but the efficiency is independent of the density, remaining the same for the same advance per revolution ( $V/nD$ ) regardless of altitude.

The power output of the engine also falls off with altitude, but the decrease is greater than the decrease in density. Figure 114<sup>1</sup> shows the decrease with altitude of the ratio  $HP/HP_0$ , where  $HP$  is the horsepower at any altitude and  $HP_0$  is that developed at sea level at the same revolutions.

The curve of power available at 10,000 ft. with our 8.17-ft. metal propeller is shown in Fig. 113 along with that for sea-level and the power-required curves. The power-available curve at altitude is found in the same manner as that for sea level except that the lower density and power must be considered. The formula for  $C_s$  is

$$C_s = \sqrt[5]{\frac{\rho V^5}{P n^2}}$$

It will be noticed that  $P$  and  $\rho$  are both in the expression to the one-fifth power. The simplified formula for sea-level density and in terms of engineering units was given in Chap. VI as

$$C_s = \frac{0.638 \times MPH}{HP^{1/5} RPM^{2/5}}$$

For altitudes this may be changed to

$$C_s = \frac{0.638 \times MPH}{\left(\frac{HP}{\rho/\rho_0}\right)^{1/5} \times RPM^{2/5}}$$

where  $HP$  is the actual horsepower developed at altitude and  $\rho/\rho_0$  is obtained from Fig. 112. The one-fifth power of the whole factor  $\frac{HP}{\rho/\rho_0}$  may be found from the  $HP$  scale in Fig. 53 (Chap. VI).

The performance of the VE-7 with the 8.17-ft. propeller is tabulated below for an altitude of 10,000 ft. and also for sea level:

<sup>1</sup> Figure 114 is based on data from 'The Variation in Engine Power with Altitude Determined from Measurements in Flight with a Hub Dynamometer, by W. D. Gove, N.A.C.A.T.R. 295, 1928; and The Determination of the Horsepower Height Factor of Engines from the Results of Type Trials of Aircraft, by J. D. Coales and A. L. Lingard, British R. and M. 1141, 1927.

	10,000 ft.	Sea level
Max. horizontal speed, m.p.h.....	122.8	128.5
R.p.m. at max. speed.....	1,748	1,800
Brake hp. at max. speed.....	137.4	200
$C_s$ at max. speed.....	1.40	1.42
$\eta$ at max. speed.....	0.822	0.824
Max. rate of climb, ft./min.....	613	1,150
Air speed for max. climb, m.p.h....	78	75

The value of the  $C_s$  for high speed is very nearly the same for 10,000 ft. as for sea level, from which it follows that the propeller giving the greatest efficiency at the maximum sea-level speed will also give approximately the highest efficiency at maximum horizontal speed at 10,000 ft. Also, the maximum revolutions at 10,000 ft. are only 3 per cent lower than at sea level, so that very nearly all of the permissible engine power is used at 10,000 ft. Our example therefore leads to the conclusion, which is fortunately true in practically all cases, that with an unsupercharged engine the best propeller for a given purpose (high speed or climb) at sea level is also the best for that purpose at altitudes.

The ceiling, or the altitude at which the rate of climb is zero, is about 21,000 ft. for our VE-7 with the 8.17-ft. metal propeller. Ordinarily, the propeller giving the greatest rate of climb at sea level will give the best climb at all altitudes and also the highest ceiling.

**Performance at Altitude with Supercharged Engine.**—In order to overcome the loss of power at high altitudes, engines are sometimes fitted with superchargers, or blowers which supply air to the carbureter at sea-level pressure, up to a certain "critical" altitude. Above the critical altitude the power falls off in about the usual manner.

We shall now consider the performance of the VE-7 on the assumption that the engine is fitted with a supercharger having a critical altitude of 20,000 ft. ( $\rho/\rho_0 = 0.5327$ ). We shall assume for convenience that the sea-level power curve (Fig. 104) also applies at 20,000 ft., although this is not strictly true, for the actual sea-level conditions are not reproduced. At altitudes lower than the critical, it is usually necessary to reduce the amount of supercharging to avoid excessive cylinder pressures and temperatures, so that approximately the same power is

obtained from sea level to the critical altitude. The effective power is reduced somewhat by the power absorbed by the supercharger, but we shall neglect this factor in our calculations.

With these assumptions, our 8.17-ft. metal propeller still gives the best air performance at sea level. At 20,000 ft., however, with full supercharging and full throttle, it would allow the engine to turn up 2,350 r.p.m., and at this revolution speed the engine would develop about 240 hp. If the motor could be run under these conditions, which are of course far beyond the specified safe limits, the airplane would attain a maximum horizontal speed of 168 m.p.h. at 20,000 ft. Actually, however, the engine should be throttled to the specified safe limit of 1,800 r.p.m., and if this is done the performance is about the same as if no supercharger were used. It is evident, therefore, that our 8.17-ft. propeller is not suitable for use with a supercharged engine at high altitudes.

The best high-speed propeller selected from our metal series to absorb 200 hp. at 1,800 r.p.m. at 20,000-ft. altitude has a diameter of 9.15 ft. and a blade angle at  $0.75R$  of 23.6 deg. The propulsive efficiency and maximum horizontal speed at 20,000 ft. are 0.849 and 159.5 m.p.h., respectively. With this propeller a fine performance is obtained at altitudes in the neighborhood of 20,000 ft. and above, and a ceiling of 30,000 to 40,000 ft., depending somewhat on the properties of the supercharger and engine. At sea level, however, even assuming that the engine develops a full 200 effective hp. at 1,800 r.p.m., the propeller holds the engine down to 1,320 r.p.m., at maximum speed, the engine develops only 117 brake hp., and the maximum horizontal speed is only 116.5 m.p.h. as compared with 128.5 with the unsupercharged engine. Also, the maximum rate of climb at sea level with this propeller, neglecting the additional weight due to the supercharger installation, is only 690 as compared with 1,167 ft. per min. without a supercharger.

These examples serve to show that the same propeller is not suitable for both high and low altitudes when a supercharged engine is used. If a fixed propeller is used, the performance must be sacrificed at one end or the other, or a compromise of some kind must be made. Usually when a supercharger is used the main interest is in the high-altitude performance, and the performance at low altitude is sacrificed.

## CHAPTER XI

### THE VARIABLE-PITCH PROPELLER

Chapter X brought out the fact that no one propeller of fixed shape and size gives the best results for all conditions of flight with an airplane. If the propeller is designed for one condition, say maximum speed at sea level, the full permissible engine power and best propulsive efficiency are not obtained at the other conditions such as take-off and climb. With a supercharged engine, the loss of performance at low altitudes is very serious if the propeller is designed for a high altitude, and *vice versa*.

**Performance with Variable Propellers.**—Curve 1 of Fig. 115 shows the power available for our VE-7 at sea level, based on the assumption that at each speed the full 200 hp. is absorbed at 1,800 r.p.m. by the most efficient metal propeller of our series for the speed, power, and revolutions. This would require a propeller whose size and pitch could be independently varied in flight. No such propeller is available at the present time, but propellers have been made and successfully tested<sup>1</sup> in which the pitch can be varied in flight at the will of the pilot or, in one case, automatically. In all of these propellers the pitch is varied, as in the case of the adjustable-blade metal propellers, by turning the entire blade in the hub.

If the pitch of our 8.17-ft. metal propeller were varied in such a manner that it would absorb the full 200 hp. at 1,800 r.p.m. at all air speeds, the power available would be as shown by curve 2 of Fig. 115. Curve 3 shows the power available with the 8.17-ft. propeller when the blade angle is fixed at 22 deg. at 0.75*R*.

The difference between curves 2 and 3 shows that the power available when the full allowable power is used throughout the

<sup>1</sup> Although several designs of variable-pitch propellers have been successfully flight tested, none has been used after the tests. Apparently the extra weight and complications, including in most cases an added control for the pilot to attend to, have overshadowed the advantages of the variable-pitch feature in the propellers so far designed. The construction of a few of these propellers is explained in Chap. XIV.

entire speed range is materially greater than the power available with a fixed propeller except at maximum speed. A variable-pitch propeller cannot, of course, increase the maximum speed over that obtained with the best fixed high-speed propeller. Above 80 m.p.h. it makes practically no difference whether the pitch alone is varied or whether both the best pitch and diameter

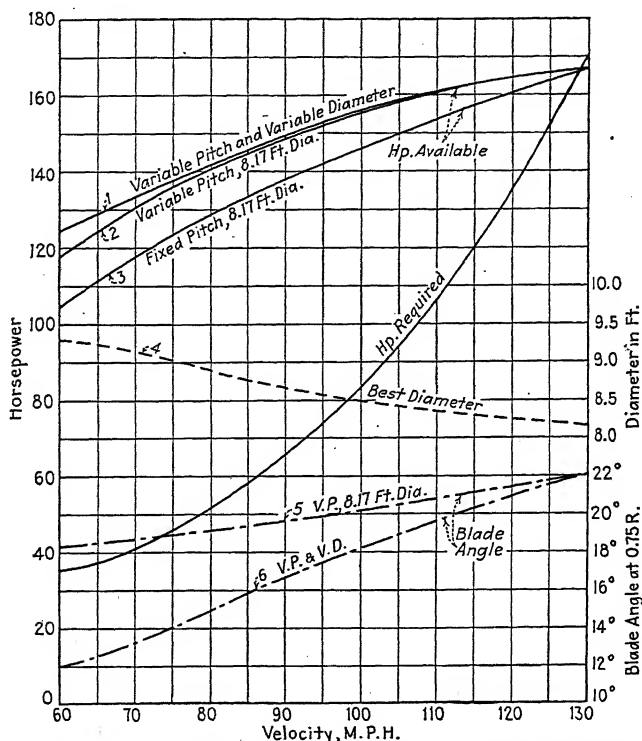


FIG. 115.—Power available with variable pitch and diameter propellers.

are used at each speed to give the highest efficiency obtainable with the particular series of propellers used. At maximum speed the best diameter is 8.17 ft., and there is no difference between curves 1 and 2. Below 80 m.p.h., however, it is markedly advantageous to have a diameter greater than 8.17 ft.

Curves 4 and 6 of Fig. 115 show the variation in diameter and blade angle required to give the highest efficiency at each speed while absorbing the full 200 hp. at 1,800 r.p.m., resulting in power-available curve 1. Curve 5 shows the variation in blade

angle of the 8.17-ft. variable-pitch propeller to absorb 200 hp. at 1,800 r.p.m. at each speed and give power-available curve 2.

Curves of the rate of climb at sea level *vs.* airspeed are given for all three propellers in Fig. 116. The climb with the 8.17-ft. variable-pitch propeller is practically as high as that with the hypothetical variable-pitch and variable-diameter propeller except at low speeds. It is decidedly better than that with the fixed propeller at all speeds below maximum, and the maximum rate of climb is 193 ft. per min. or 16.5 per cent better.

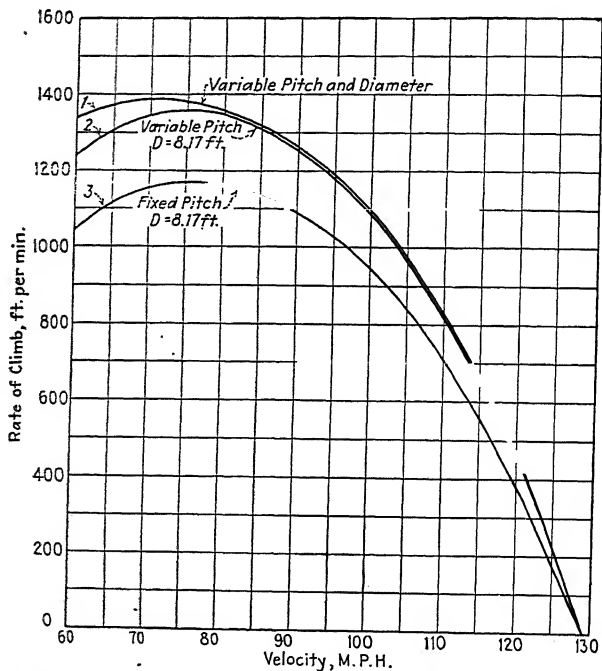


Fig. 116.—Rates of climb with variable pitch and diameter propellers.

This difference is appreciable with the VE-7, but with the heavily loaded transport airplane mentioned in Chap. X having a rate of climb of 400 ft. per min. with 600 hp. and a total weight of 9,000 lb., the same relative increase in power available with a variable-pitch propeller would result in an increase of 145 ft. per min. or 36.2 per cent.

As shown by Fig. 116, a propeller of larger diameter than that which is best for high speed would increase the rate of climb still

more, and, what is also important, the maximum rate of climb would occur at a lower forward speed, resulting in greater angle of climb.

The propulsive efficiency with the three propellers—(1) the hypothetical variable-pitch and variable-diameter propeller; (2) the 8.17-ft. variable-pitch propeller; and (3) the fixed 8.17-ft. propeller—is shown as solid lines on Fig. 117. It is noteworthy that there is very little difference between the efficiency curves of the three propellers, except at very low speeds where the variable-pitch and -diameter propeller is noticeably better than the other two.

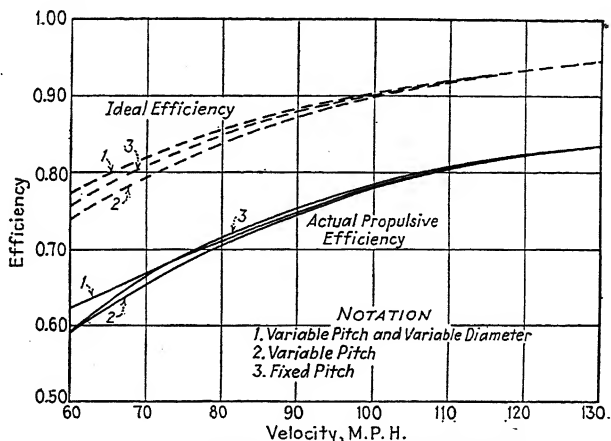


FIG. 117.—Comparison of actual and ideal efficiencies.

It is interesting, also, that from the speed for maximum climb (75 m.p.h.) to the maximum speed the fixed propeller has the highest efficiency of the three.

One of the advantages often claimed for variable-pitch propellers is that at climbing speeds, where the  $V/nD$  is low, the blade angles of the variable-pitch propeller are reduced and the sections therefore work at more nearly their best  $L/D$  than those of fixed-pitch propellers which have necessarily been designed with the maximum speed in mind also. Since the propeller sections operate at more nearly the angle of attack for maximum  $L/D$ , it is concluded that the propeller efficiency is higher. The same conclusion may easily be drawn from an incautious study of a series of efficiency curves plotted on a basis of  $V/nD$  for a number of propellers varying in pitch (see Fig. 60), for at the

lower values of  $V/nD$ , the low-pitch are more efficient than the high-pitch propellers. Ordinarily, however, as in the case of our example (illustrated by curves 2 and 3 in Fig. 117), the opposite is true—the efficiency of the variable-pitch propeller is lower than that of the fixed-pitch propeller throughout practically the entire flying range. In our case the efficiency of the fixed propeller is even higher than that of the variable-pitch and -diameter propeller, between the maximum speed and the speed for maximum climb.

Two useful conclusions may be drawn from the above discussion and a study of Fig. 117:

1. Any gain in climbing performance at sea level with a variable-pitch propeller will usually be entirely due to the use of greater engine power than can be obtained with a fixed propeller designed to hold the engine down to the specified maximum revolutions at high speed; also, the variable-pitch propeller will usually be slightly handicapped by a slightly lower efficiency;

2. While propeller characteristics plotted on a basis of  $V/nD$  are satisfactory for showing the comparative values of the characteristics themselves, the  $V/nD$  basis is unsatisfactory and in many cases misleading when used for showing the relative performances of propellers on aircraft.

It is interesting to compare the ideal efficiencies of the three propellers according to the momentum theory. This may be obtained from the expression (explained in Chaps. II and VII)

$$\frac{\eta^3}{1 - \eta} = \frac{\pi(V/nD)^3}{2C_P} = \frac{\pi C_s^5}{2(V/nD)^2}.$$

The curves of ideal efficiency for the three propellers are shown as dotted lines in Fig. 117. It will be noted that the ideal efficiency of the fixed propeller, curve 3, is also greater than that of the variable-pitch propeller, curve 2. This is due to the lower  $V/nD$  and the greater power input with the variable-pitch propeller. With the best possible propeller of the metal series, however, in which the diameter is varied as well as the pitch, the ideal efficiency is higher than for either of the other two.

**Effect on Take-off.**—In order to see the effect of the variable-pitch propellers on the take-off run, we shall find the best of our metal propellers for producing static thrust while absorbing the



full 200 hp. at 1,800 r.p.m. To do this it is convenient to make use of the relation

$$\frac{TD}{Q} = \frac{2\pi C_T}{C_P},$$

which is plotted for the various propellers of our series at zero advance in Fig. 118. The diameter corresponding to each angle setting or pitch, as obtained from the relation,

$$C_P = \frac{P}{\rho n^3 D^5} = \frac{200 \times 550}{0.002378 \times (30)^3 D^5},$$

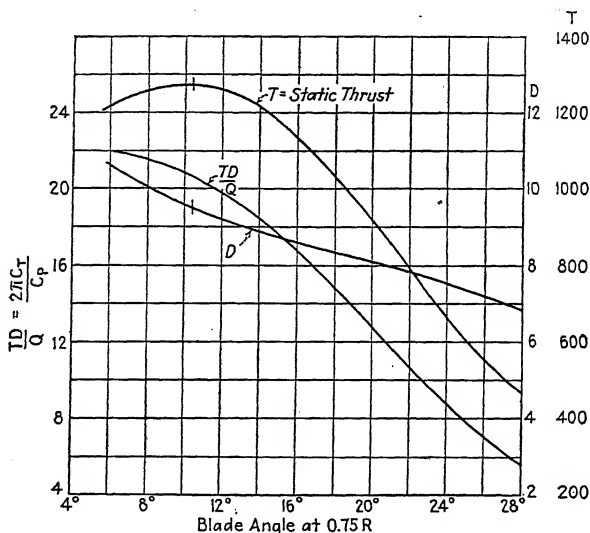


FIG. 118.—Static thrust for various blade-angle settings.

is also given in Fig. 118. The torque of our 200-hp. engine at 1,800 r.p.m. is 584 lb.-ft. Then, since for any blade angle  $D$ ,  $Q$ , and  $TD/Q$  are known, it is easy to solve for  $T$ . The static thrust obtained in this manner is also plotted in Fig. 118. The maximum static thrust is obtained with a 9.5-ft. propeller set to 10.4 deg. at  $0.75R$ .<sup>1</sup> This maximum static thrust is 1,275 lb. as compared with 950 lb. for the 8.17-ft. variable-pitch propeller set to 19.4 deg. (from Fig. 118) and 731 lb. for the

<sup>1</sup> The fact that the static thrust decreases with diameters greater than 9.5 ft. and blade settings lower than 10.4 deg. is partly due to the poor pitch distribution of these propellers at very low pitches. With propellers having uniform pitch the diameter for the best static thrust would be somewhat larger.

8.17-ft. propeller with its pitch angle fixed at 22 deg. at  $0.75R$ . The thrusts at 0, 30, and 60 m.p.h. and the corresponding take-off runs are tabulated below for the three propellers:

	Static thrust, lb.	Thrust at 30 m.p.h., lb.	Thrust at 60 m.p.h., lb.	Average thrust, lb.	Approximate take-off run, ft.
Prop. having best diameter & pitch.....	1,275	1,000	779	1,018	250
Variable-pitch prop., 8.17-ft. dia.....	950	840	738	842	302
Fixed pitch prop., 8.17-ft. dia..	731	713	656	700	364

The take-off run with the 8.17-ft. variable-pitch propeller is about the same as with the best fixed-pitch propeller for take-off (Chap. X). The fixed-pitch propeller, however, has a very poor performance in climb, high speed, and cruising. With our hypothetical variable-pitch and -diameter propeller, for which the diameter is 9.5 ft. for 0 and 30 m.p.h. and 9.29 ft. for 60 m.p.h., the take-off run is reduced to approximately 250 ft.

**Effect on Cruising Economy.**—We found in the section on cruising in Chap. X that the most economical propeller for cruising at 100 m.p.h. would hold the engine down to 1,050 r.p.m. while absorbing approximately 100 hp. The diameter of this propeller is 9.65 ft. and the blade angle at  $0.75R$  is 24 deg. If the pitch of the 8.17-ft. propeller is increased to absorb 100 hp. at 1,050 r.p.m., a blade angle of about 33 deg. is required, an efficiency of only 0.77 is obtained as compared with 0.851 with the 9.65-ft. propeller, and the fuel consumption is actually greater than with the 8.17-ft. fixed-pitch propeller with the engine throttled to 1,420 r.p.m.

The best fuel consumption with the 8.17-ft. propeller is obtained at 1,270 r.p.m. (blade setting at  $0.75R = 26$  deg.,  $\eta = 0.829$ , specific fuel consumption = 0.507), in which case the fuel consumption is 5 per cent higher than with the best propeller at 1,050 r.p.m. and 3.3 per cent lower than with the fixed propeller at 1,420 r.p.m.

**Summary of the Effect of a Variable-pitch Propeller on Performance with an Unsupercharged Engine.**—With an unsupercharged engine, the increase in performance at altitudes with a

variable-pitch propeller is very much the same as that at sea level. A slight increase in high speed over that with a fixed propeller is also obtained at altitudes, however, due to the fact that the power corresponding to the maximum permissible revolutions can be taken from the engine.

The final performances obtained with our three propellers are compared in the first three columns of the following table:

	8.17-ft. fixed pitch	8.17-ft. variable pitch	Variable pitch & diameter	Best diam- eter, ft.	9.00-ft. variable pitch
Max. speed, m.p.h.....	128.5	128.5	128.5	8.17	127.8
Max. rate of climb, ft./min...	1,167	1,360	1,387	9.11	1,380
Take-off run, ft.....	364	302	250	9.5	255
Relative effectiveness, cruising at 100 m.p.h., based on best.	0.92	0.95	1.00	9.65	0.99

It is evident that even with a variable-pitch propeller the best possible performance in all conditions of flight cannot be obtained with a single propeller of constant diameter, and the propeller must at best be a compromise. If it is desired to obtain a high maximum speed, the 8.17-ft. propeller is the best. If any of the other items is more important, a propeller of larger diameter is required for the best performance.

If a compromise propeller 9 ft. in diameter is used, the performance is given by the figures in the last column of the table above. The high speed, climb, and economy in cruising at 100 m.p.h. with this 9-ft. variable-pitch propeller are all within 1 per cent of the maximum obtainable with a variable-pitch and -diameter propeller, and the take-off run is only 2 per cent longer.

The performance with this 9-ft. variable-pitch propeller (and 9 ft. may be taken as about the best compromise diameter) is appreciably better than the performance with a fixed propeller in climb, take-off, and cruising. It is not, however, sufficiently better to warrant a large increase in weight (which has been neglected in our computations) and in cost and complication.

**Performance with Variable-pitch Propeller and Supercharged Engine.**—It was shown in Chap. X that a fixed propeller was not

suitable for both high and low altitudes when used with a supercharged engine. If reasonable advantage of the supercharger is to be obtained it is necessary to use a propeller having changeable characteristics.

We found in Chap. X that the best high-speed propeller for the supercharged VE-7 at the critical altitude of 20,000 ft. had a diameter of 9.15 ft. and a blade angle at  $0.75R$  of 23.6 deg. This diameter is nearly the same as that of our 9-ft. compromise variable-pitch propeller for all-around sea-level performance. As a matter of fact, a variable-pitch propeller having a diameter of either 9 or 9.15 ft. would make a satisfactory all-around propeller for all altitudes. If the climb at 20,000 ft. and above were important, it would be advisable to use a slightly larger diameter, say 9.5 ft., sacrificing about 2 m.p.h. more in maximum speed at sea level.

The supercharger is very limited in usefulness with a fixed propeller, for the performance is either mediocre at all altitudes or very poor at high or low altitudes, but the variable-pitch propeller and the supercharger make a happy combination for high-altitude flying without sacrificing low-altitude performance. The supercharger enables the engine to develop full power at altitudes, and the variable-pitch propeller makes it possible to use the full power under all flying conditions. It must not be forgotten, however, that they add both weight and complication and also extra duties for the pilot. Since the pilot already has much to absorb his attention, it is highly desirable that the control of the variable-pitch propeller be made automatic but subject to control by the pilot if necessary or desired.

**Other Uses for Variable-pitch Propellers.**—Some variable-pitch propellers are constructed in such a manner that the pitch can be reversed for the purpose of giving a braking action or backward thrust. This is particularly advantageous in the maneuvering of lighter-than-air craft such as dirigibles while landing or taking off.

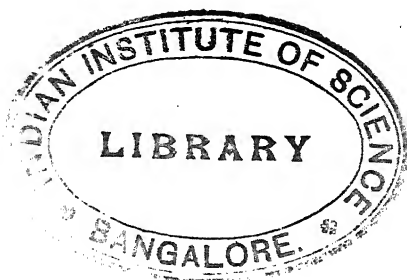
The effectiveness of the reversible-pitch propeller as an air-brake to shorten the landing distance of an airplane has been experimented with by both the Army and the Navy in this country. There is no doubt that the reverse thrust substantially reduces both the gliding angle and the distance run on the ground before stopping. Difficulty was experienced, however, with the effect on the controllability, both in the air and on the ground, where it

was very difficult to hold the airplane straight and keep it from ground looping. These tests were made several years ago, and it is likely that the ground looping could be overcome by the use of modern individually operating wheel brakes.

With reversible propellers, it is advisable to have the engine throttle connected with the pitch-changing mechanism in such a manner that the throttle is closed while the propeller blades are passing through zero pitch. If this is not done and the throttle is accidentally opened when the pitch is at or near zero, the engine will race and may destroy itself.

Often dirigible airships, and sometimes multi-engined airplanes, cruise with one or more engines cut out. Sometimes the engine and propeller stop, and sometimes the propeller acts as a windmill with sufficient torque to keep the engine rotating. In either case, and particularly in the latter, the drag is high and could be reduced appreciably if the propeller blades could be turned fore and aft so that their average pitch was infinite.

With multi-engined airplanes having fixed propellers, if one engine fails the speed of the airplane is reduced and the other propellers do not allow their engines to turn at full revolutions and deliver full power. The condition is similar to that of a normal airplane in climb, and variable-pitch propellers would improve the performance in the same way as in normal climb.



## CHAPTER XII

### THE GEARING OF PROPELLERS

Due to the fact that the power output of gasoline engines is directly proportional to the revolutions as well as the mean effective pressure, one obvious way to cut down the weight per horsepower of the engine is to increase the revolution speed. Unfortunately this reduces the value of  $C_s$  at which the propeller operates, and the propeller has a lower pitch and a lower maximum efficiency. The knowledge of this fact has been influential in more or less limiting the maximum revolutions of aircraft engines, but in spite of it there has been a gradual tendency toward higher maximum engine revolutions.

There is also a tendency toward engines delivering more and more power, and this too decreases the value of  $C_s$  and therefore the maximum possible propeller efficiency. In addition, the combined high powers and revolutions are accompanied by high tip speeds and the consequent efficiency losses which may be very great. Due to the losses accompanying one or more of these items it has in some cases been found advisable to mount the propeller on a separate shaft which is geared to turn more slowly than the engine crankshaft. This, of course, increases the weight, the complication, and the cost.

**Factors Affected by Reduction Gearing.**—The question of the desirability of reduction gearing is an involved one because of the many factors affected. The advantages and disadvantages which must be balanced against each other may be summarized briefly as follows:

#### Advantages:

1. Increase in propulsive efficiency and consequently in airplane performance, due to
  - a. Greater propeller pitch ratio.
  - b. Larger size of propeller with respect to body.
  - c. Elimination of tip-speed loss, if any.
2. Less propeller noise due to lower tip speed.

#### Disadvantages:

1. Loss of power in gear

2. Extra weight of propeller, gearing, and structure.
3. Possible effect of greater propeller diameter on landing gear height, engine location, etc.
4. Greater number of moving parts requiring lubrication and service.
5. Greater cost.

The problem is further complicated by the effect of the gain in propulsive efficiency on the various items of airplane performance, such as high speed, cruising speed, take-off, climb, and cruising economy. Due to the number of factors involved, no simple general rule can be made to cover all cases, but each case should be worked out individually and in detail. Two examples follow which show the nature of the results to be expected in rather extreme cases, as well as a method in which the problem can be attacked for any given case by airplane, engine, or propeller designers.

**Example 1.**—For our first example we shall take the case of an express or mail transport airplane powered with a single engine delivering 800 hp. at 2,000 r.p.m.<sup>1</sup> We shall assume that our engine is water cooled with a nose radiator and that with a direct-drive propeller the mutual propeller-body interference is the same as with the VE-7. The gross weight will be 12,000 lb., with a wing loading of 15 lb. per sq. ft. and a power loading of 15 lb. per hp. With a direct-drive propeller the maximum speed at sea level will be 130 m.p.h. and the stalling speed 65 m.p.h. The power-required curve is shown in Fig. 119.

The propeller characteristics and the resultant power-available curves are calculated for the direct-drive condition and also for gear ratios of 5:4, 5:3, and 5:2, the corresponding maximum propeller revolutions being 2,000, 1,600, 1,200, and 800. The computations are made in the same manner as those in Chap. X, based on the full-scale metal-propeller test data given in Figs. 51, 52, and 167. The form of these propellers is shown in Figs. 176 and 177. Owing to the high power and revolutions, the direct-drive propeller will have an efficiency loss due to the high tip speed which is inevitable at full throttle and maximum speed. The propeller diameter for the direct-drive installation is therefore selected as that which just escapes a tip-speed loss when cruising at 1,750 r.p.m. It then also escapes this loss in

<sup>1</sup> There is now one water-cooled engine, the Packard 1 A-2500, which is manufactured to this particular rating, and it is likely that there will be both air- and liquid-cooled engines of about the same power in the near future.

the take-off condition and in climbing at very low air speeds, all of which are more important in this type of airplane than the maximum speed. A compromise diameter of 11 ft. gives about the best results.

The three geared propellers are selected, considering take-off, climb, and high cruising speed, so as to have diameters halfway between those for the best high-speed propeller and the propeller operating at the peak of its efficiency curve at maximum speed.

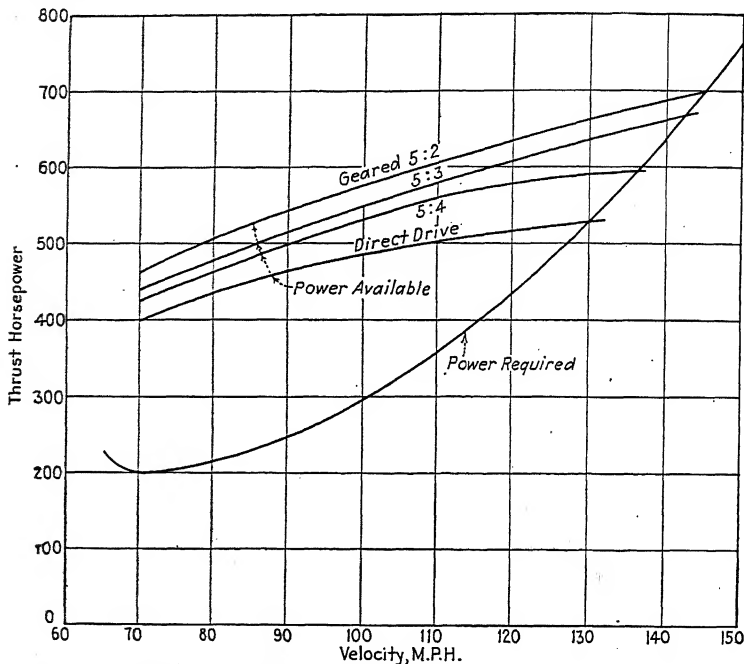


FIG. 119.—Power available with various gear ratios. Transport airplane.

A 2 per cent loss in power in the gears is assumed for all ratios. This value is not the result of accurate measurements, which are difficult to make, but seems reasonable from data on gears and also from the comparative measured power outputs of direct-drive and geared engines of the same design.

In regard to body interference, it is assumed that the data from the VE-7 tests are correct for the direct-drive propeller and that for the geared propellers the propulsive efficiency is 1 per cent higher for each 8 per cent increase in propeller diameter (see Chap. IX).



The main characteristics of the four propellers are tabulated below, and the power-available curves obtained with them, assuming that the full-throttle engine torque is constant within the range of revolutions required, are given in Fig. 119.

Gear ratio.....	Direct	5:4	5:3	5:2
Max. r.p.m.....	2,000	1,600	1,200	800
$C_s$ .....	1.040	1.183	1.408	1.670
$V/nD$ .....	0.520	0.589	0.728	0.922
Diameter, ft.....	11.00	12.68	14.42	17.31
$\beta_{0.75}$ , deg.....	15.9	16.2	19.7	24.7
$\eta$ , with VE-7.....	0.756	0.784	0.828	0.855
Tip speed, ft./sec.....	1,168	1,080	930	770
T.S. correction factor....	0.873	0.954		
Body interference factor...	.....	1.016	1.030	1.045
Corrected $\eta$ .....	0.660	0.760	0.853	0.893
Thrust hp. at max. speed..	528	596	669	700
Max. speed, m.p.h.....	130.0	136.3	142.5	145.0

The effect of gearing on the maximum speed is surprisingly great, it being 15 m.p.h. higher with the 5:2 gear ratio than with direct drive. Nearly half of this effect is due to the large tip-speed loss with the direct-drive propeller, and it will be noticed that there is a substantial tip-speed loss even with the 5:4 reduction gear.

The variation of propeller diameter and weight with gear ratio is shown in Fig. 120. Regarding the limitations on propeller diameter with our transport airplane, the landing gear would ordinarily be sufficiently high to give the required 9 in. of ground clearance in flying position<sup>1</sup> with a 14-ft. propeller diameter, this landing gear height being necessary to give the wings the proper angle of attack in landing. If the regular two-blade propellers of our calculations are used, it will be necessary to increase the landing-gear height for gear ratios greater than about 5:3. For the 5:2 ratio this increase would be about 20 in. The drag and weight would also be increased somewhat, but this factor we shall neglect. If the gearing happened to be of the spur type with the propeller axis above the crankshaft axis, a larger diameter, probably at least 15 ft., could be used without increasing the landing-gear height.

With our transport airplane the effect of the gearing on cruising speed is of more interest than the effect on maximum speed.

<sup>1</sup> This is the present Department of Commerce requirement.

Assuming that the cruising is done at two-thirds full power, the engine revolutions will be 1,750, and there will be no appreciable tip-speed loss even with the direct-drive propeller. The cruising speeds obtained with the engine turning 1,700 r.p.m. are plotted along with the maximum speeds for the various gear ratios in Fig. 121. Without the tip-speed losses in the direct drive, the gain with reduction gearing is not so great in cruising speed as in high speed, but it is nevertheless quite

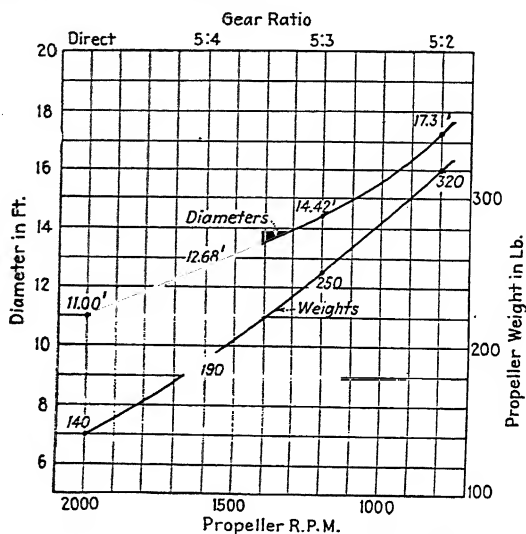


FIG. 120.—Variation of propeller diameter and weight with gear ratio. Transport airplane.

substantial, being nearly 8 m.p.h. with the 5:2 ratio. The cruising economy and range are also better at the higher cruising speed by the percentage increase in speed, and they are much better at the same cruising speed.

The stalling speed is of course affected by the extra weight with gearing and a larger propeller diameter. The propeller diameters and weights with the various gear ratios are given in Fig. 120. For our calculations of stalling speed, climb, and take-off it is assumed that the extra engine weight due to the gearing is about 130 lb. for all ratios. With this and the added weight due to the larger propeller, and also a reasonable increase in the weight of the structure supporting the engine and propeller, the total increased weight is about 200 lb. for the 5:4 ratio, 300 lb. for the

5:3 ratio, and 400 lb. for the 5:2 ratio. The resultant stalling speeds given in Fig. 121 show an increase of about 1 m.p.h. with the 5:2 ratio.

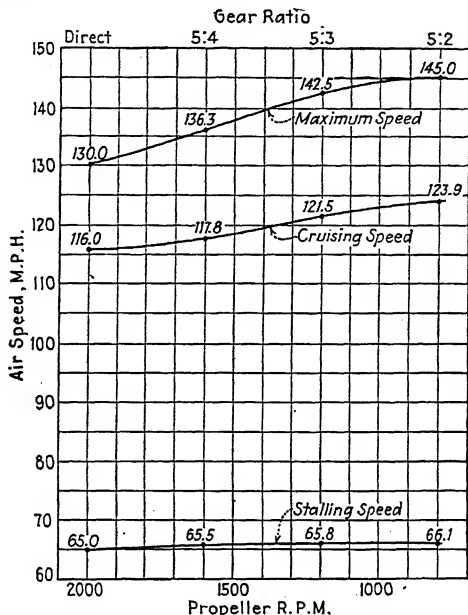


FIG. 121.—Variation of maximum speed, cruising speed, and stalling speed with gear ratio. Transport airplane.

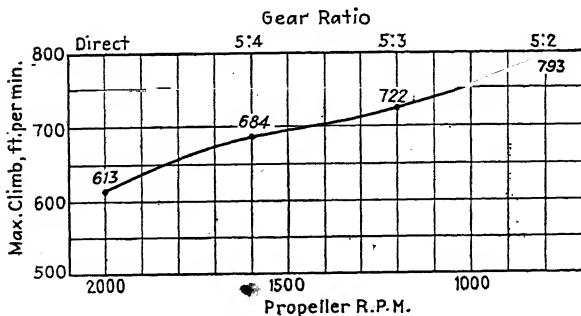


FIG. 122.—Variation of maximum rate of climb with gear ratio. Transport airplane.

It is apparent from the power-available curves of Fig. 119 that the rate of climb is noticeably greater with the larger gear reductions. The maximum rates of climb obtained with the

various reduction ratios are given in Fig. 122, the extra weight with gearing being allowed for. The maximum rate of climb with the 5:2 ratio is 180 ft. per min. or approximately 30 per cent greater than that with the direct drive, and apparently with greater gear reduction the climb would increase at an even greater rate.

In order to calculate the relative take-off distance obtained with the different gear ratios, the static thrust is obtained by means of the curve of  $TD/Q$  given in Fig. 118. As is apparent from this curve, the static thrust is very low for the highest-pitch

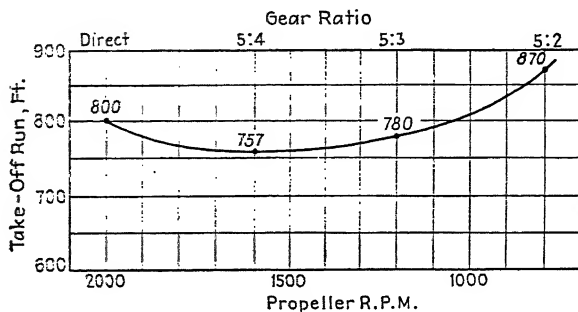


FIG. 123.—Effect of various gear reductions on take-off run. Transport airplane.

propellers, and this tends to limit the gear reductions which can be satisfactorily used. Assuming a take-off run of 800 ft. with the direct-drive propeller, the lengths of run required with the various gear reductions are calculated in the manner shown in Chap. X and are given in Fig. 123. The shortest take-off run is obtained with a propeller having a maximum revolution speed of about 1,500, and with less than 1,100 r.p.m. the take-off is poorer than with direct drive.

An examination of Figs. 120 to 123 shows that for the case of our example, gearing the propeller increases the performance to an extent which would more than justify the additional cost and weight. Just what gear ratio is best is difficult to say, but it would probably be between 5:3 and 5:2. The 5:3 ratio escapes all tip-speed loss and gives an increase in all of the performance items considered excepting stalling speed. The 5:2 ratio gives slightly larger gains in most items but gives a loss in take-off, and with greater reductions this loss would become prohibitive. Also, the propeller size has approached, if not exceeded, the

practical limit. Everything considered, the ratio of 2:1 giving the propeller 1,000 r.p.m. is probably the maximum gear reduction advisable in this case.

With a reduction of 2:1, the propeller diameter is 15.6 ft., and an increase in landing-gear height of about 9 in. is necessary. Neglecting the effect of this,

- a. The high speed is increased 14 m.p.h.
- b. The cruising speed is increased 7 m.p.h.
- c. The maximum rate of climb is increased 140 ft. per min. or 23 per cent.

Against these gains we have the very slight disadvantages that

- a. The take-off distance is increased 2.5 per cent.
- b. The stalling speed is 1 m.p.h. higher.

In case the diameter of the two-blade propeller is considered too great, a three-blade propeller could be used. This would have a diameter of about 14 ft. and the original landing gear could be used unchanged, but the weight would be approximately 70 lb. more than with the 15.6-ft. two-blade propeller. The propulsive efficiency would be only about 2 per cent less at maximum speed, and the all-around performance only a trifle less than with the two-blade propeller.

The three-blade feature has one distinct advantage where very large propellers are used. It is noticeably smoother running in turns and in yawing flight. This is due to the fact that in turns the gyroscopic moments are balanced and uniform with three-blade but not with two-blade propellers. Also, both in turns and in yawing or slipping flight the air loads on the blades vary during each revolution, and with two-blade propellers one blade has its greatest loading at the same time that the other has its lightest, while with three-blade propellers as each blade gets its extreme loading it is balanced by two others with medium loadings. Unless large, slow-turning two-blade propellers are mounted on very rigid structures, the vibrations they cause in sharp turns may be severe enough to make the use of three or more blades advisable.

If the above example were a flying boat instead of a land airplane, almost all of the performance items excepting take-off would be affected in the same manner by gearing. It is likely that there would be no difficulty in getting the seaplane above the "hump" speed with any of our gear ratios. Assuming this to be true, the best and most certain take-off would be

given by the combination having the greatest thrust at the take-off speed, or about 65 to 70 m.p.h. As is evident from Fig. 119, this is the propeller having the largest diameter and the greatest gear reduction.

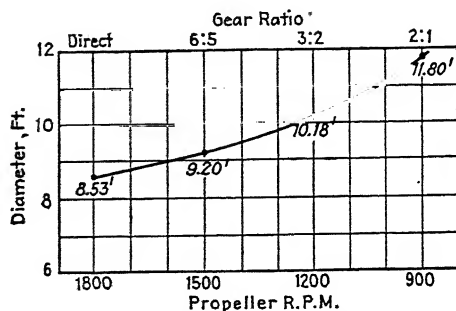


FIG. 124.—Variation of propeller diameter with gear ratio. VE-7 example.

**Example 2.**—The foregoing example represents a rather extreme case where gearing is not only advisable but practically necessary. For another example we shall take a smaller and lighter airplane, our VE-7 airplane dealt with in Chap. X, having

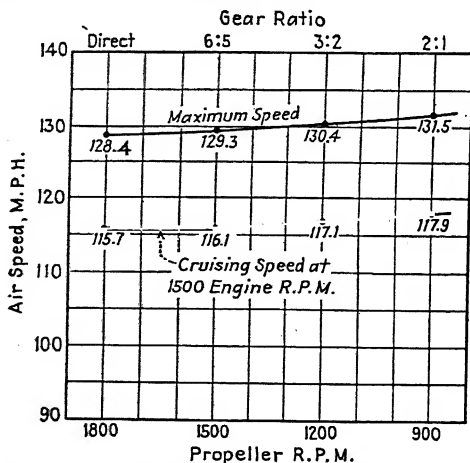


FIG. 125.—Effect of various gear ratios on maximum speed and on cruising speed. VE-7 example.

an engine delivering 200 hp. at 1,800 r.p.m. We shall take the 8.53-ft. direct-drive propeller of Chap. X, having a blade-angle setting of 20.0 deg. at 0.75R, and select the geared propellers to operate at the same relative portion of their efficiency curves.

The propeller diameters with various gear reductions are shown in Fig. 124. The original VE-7 will have proper clearance for only a 9-ft. propeller, and the landing-gear height must be increased if any reasonable gear ratio is to be used.

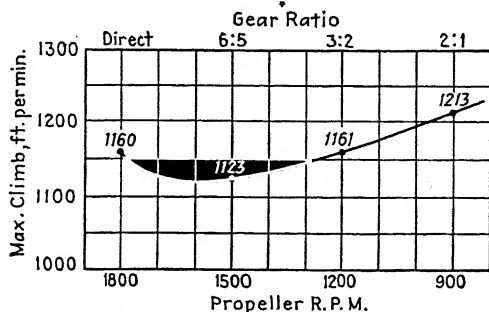


Fig. 126.—Effect of gear reductions on maximum climb. VE-7 example.

The high speed, cruising speed, climb, and take-off distance, calculated in the same manner as for the previous example, are shown for various gear ratios in Figs. 125, 126, and 127. With the VE-7, which with direct drive has no high tip-speed loss but has a reasonably high value of  $C_s$  ( $C_s = 1.42$  as compared with

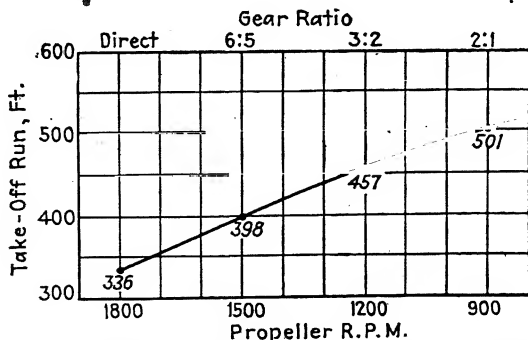


Fig. 127.—Effect of gear reductions on take-off distance. VE-7 example.

1.04 for the transport example), the gains in both maximum speed and cruising speed are very slight even with large gear reductions. They would be even less than shown if the necessary increased landing-gear height were considered.

The maximum climb is less with small gear reductions than with direct drive, due to the power loss in the gears and the extra

weight. With this example there is no appreciable gain in climb with any reasonable gear reduction.

The take-off run is longer with any gear reduction than with direct drive, and it becomes worse as the reduction ratio is increased. This is due to the fact that even the direct-drive propeller has a reasonably high pitch and the higher-pitched geared propellers have greatly reduced static thrust.

Obviously, with no appreciable increase in any performance, and with a definite loss in take-off and possibly in climb, gear reduction of any amount is not desirable for the VE-7 example, even neglecting such items as cost.

**General.**—As shown by these examples, the problem of whether or not gearing is desirable, and if so what reduction ratio will give the best results, is a complicated one because of the many factors involved. Obviously in cases where the maximum speed is important, such as in racing airplanes, it is important that there be no appreciable loss due to too high tip speed, and gearing can be used to eliminate this loss if it exists with direct drive. Also, if the efficiency with direct drive is low, due to a combination of high power and high revolutions, gearing will probably help.

Since increasing either the horsepower or the revolutions decreases the value of  $C_s$ , and since the value of  $C_s$  is directly connected with the maximum efficiency obtainable, a value of  $C_s$  may be used as a criterion for the desirability of gearing. In general it may be said that if with direct drive the value of  $C_s$  is higher than about 1.3, and if the tip speed is under the critical, gearing is undesirable. If, however, the value of  $C_s$  is lower than 1.3 or if there is a tip-speed loss, gearing may substantially improve the performance. In order to find the best gear ratio and whether or not the increase in performance is worth the cost, performance computations considering all of the factors affected should be made, after the manner of the examples given.



## CHAPTER XIII

### TANDEM PROPELLERS

In some multiple-engined airplanes, two engines, each driving its own propeller, are placed in tandem. The rear propeller, which is a pusher, operates in the slipstream of the front propeller, which is a tractor.

Since the propellers are usually spaced about one diameter apart, the front propeller is not influenced to an appreciable extent by the action of the rear one, and it may be considered as if it were working alone. The rear propeller, however, works in a twisting slipstream which has been given both an additional axial velocity and a rotational velocity by the front propeller.

If both propellers absorb the same power and turn in opposite directions, the rear propeller will produce a rotation which is equal and opposite to that produced by the front propeller, and there will be no general rotation in the final slipstream back of the rear propeller. This condition is obtained with the usual tandem arrangement in which two similar engines are used end to end, one pointing forward and one to the rear. This tandem arrangement, therefore, does not suffer the usual loss of efficiency due to the rotation in the slipstream.

**Calculation of Slipstream Velocities in which Rear Propeller Operates.**—The velocity in the slipstream of the front propeller (neglecting the rear propeller) can be found by applying the momentum theory to one annulus at a time. Thus:

$$\begin{aligned} dT &= \text{mass per unit time} \times \text{velocity imparted} \\ &= 2\pi r dr V(1 + a)\rho 2aV. \end{aligned}$$

The symbols are the same as in the momentum and blade-element theories (Chaps. II and V), and from any of the forms of the blade-element theory,  $dT$  for an annulus also has the value

$$dT = \frac{1}{2}\rho V^2 BT_c dr,$$

where  $T_c$  is calculated from the air forces on a blade element. Equating both expressions for  $dT$ ,

$$2\pi r dr V(1 + a)\rho 2aV = \frac{1}{2}\rho V^2 BT_c dr$$

from which, if  $V_1$  is the axial component of the full slipstream velocity,

$$\frac{V_1}{V} = 1 + 2a = 2\sqrt{\frac{BT_c}{8\pi r}} + \frac{1}{4}$$

and

$$V_1 = 2V\sqrt{\frac{BT_c}{8\pi r}} + \frac{1}{4}$$

The rotational component of the slipstream velocity is found in like manner from the equation for angular momentum,

$$\begin{aligned} dQ &= \text{mass per unit time} \times \text{tangential velocity} \times \text{radius} \\ &= 2\pi r dr V(1 + a)\rho 2wr, \end{aligned}$$

where  $w = a'(2\pi rn)$  is the interference tangential velocity at the plane of the front propeller, as in the induction or vortex theory.

From the blade-element theory  $dQ$  also has the value,

$$dQ = \frac{1}{2}\rho V^2 BQ_c dr,$$

and equating both expressions for  $dQ$ ,

$$2\pi r dr V(1 + a)\rho 2wr = \frac{1}{2}\rho V^2 BQ_c dr$$

from which the tangential velocity in the final slipstream is

$$\begin{aligned} 2w &= 2a'(2\pi rn) = \frac{VBQ_c}{4\pi r^2(1 + a)} \\ &= \frac{VBQ_c}{4\pi r^2\left(\sqrt{\frac{BT_c}{8\pi r}} + \frac{1}{4} + \frac{1}{2}\right)} \end{aligned}$$

**Calculation of the Air Forces on the Elements of the Rear Propeller.**—The regular blade-element theory equations for the thrust, torque, and efficiency of the elements can be applied to the rear propeller of the tandem arrangement by substituting  $V_1 = V(1 + 2a)$  in place of  $V$  and  $(2\pi rn)_1 = (2\pi rn) + 2a'(2\pi rn)$  in place of the ordinary tangential velocity  $2\pi rn$ .

It is interesting to examine the difference in the expressions for the efficiency of an element of the front and rear propellers according to the vortex blade-element theory. The efficiency of an element of the front propeller, which is the same as for an isolated propeller, is

$$\begin{aligned} \eta &= \frac{dT V}{dQ(2\pi rn)} \\ &= \frac{(1 - a') \tan \phi_0}{(1 + a) \tan(\phi_0 + \gamma_0)}. \end{aligned}$$

The useful work performed per second by an element of the rear propeller is the thrust times the velocity of advance of the airplane, the latter being less than the velocity of the slipstream in which the rear propeller works. With the subscript 1 pertaining to the rear propeller, the efficiency of an element of the rear propeller, when the propellers are turning in opposite directions, is

$$\begin{aligned}\eta &= \frac{dT_1 V}{dQ_1 (2\pi r n)} \\ &= \frac{(1 + 2a')(1 - a'_1) \tan \phi_{01}}{(1 + 2a)(1 + a_1) \tan (\phi_{01} + \gamma_{01})}\end{aligned}$$

Thus the efficiency of the element of the rear propeller is increased by the rotational velocity factor  $2a'$  and decreased by the axial velocity factor  $2a$ . Ordinarily, and especially in take-off or climbing flight, the value of  $a$  is much larger than that of  $a'$ , and the net result is a loss in the efficiency of the rear propeller.

Since the area of the slipstream is not constant but becomes smaller back of the propeller, there is some radial flow and the air passing the front propeller at a given radius may (and usually does) pass the rear propeller at a different radius. This complicates the use of the blade-element theory for tandem propellers, but with an ordinary body housing the two engines between the propellers, the slipstream is spread so that it is not far wrong for the main working portions of the blades to assume that the same air passes both propellers at the same radius.

**Model Tests with Tandem Propellers.**—Only a few isolated tests<sup>1</sup> have been made with tandem propellers, and the only systematic investigation of sufficient size to throw much light on the subject was made by Eiffel in 1919.<sup>2</sup> In his investigation, Eiffel tested two main series of tandem propellers, one in which both propellers were of the same diameter and form, but of opposite hand, and one in which the rear propellers were 12.5 per cent smaller in diameter. Both series were made up of propellers of several pitch ratios, and the blades of the rear propeller were adjustable as to pitch. The pitch of the rear propeller was in every case adjusted so as to make it absorb the

<sup>1</sup> Some Experiments with Tandem Combinations of Airscrews, by A. Fage and H. E. Collins, British *R. and M.* 421, 1918. Some Further Experiments on Tandem Airscrews, by A. Fage and H. E. Collins, British *R. and M.* 605, 1918.

<sup>2</sup> Tandem Propellers, by G. Eiffel, published in the French magazine *L'Aéronaute*. November, 1919.

same power at the same revolutions as the front propeller, at the speed for the maximum efficiency of the front propeller.

The pitch required by the rear propeller of like diameter to absorb the same power as the front propeller is shown for various pitch ratios by the dotted line in Fig. 128. It is interesting that with propellers of the form tested having pitch ratios higher than 1.0, the rear propeller requires less pitch than the front one, showing that at high rates of advance per revolution the rotational

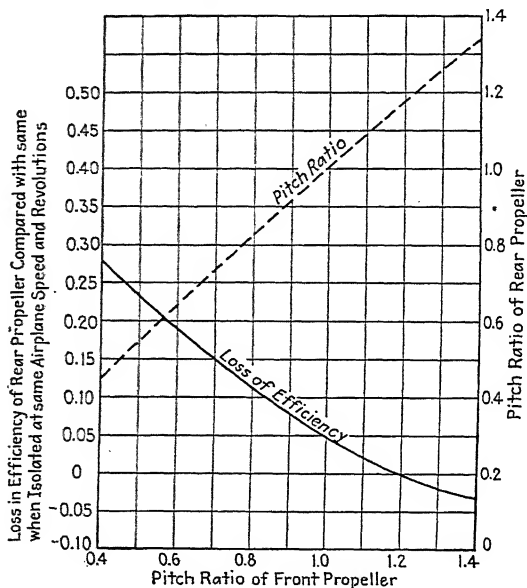


FIG. 128.

component of the slipstream has a greater influence on the pitch of the rear propeller than the axial component. The solid line in Fig. 128 shows the loss of efficiency of the rear propeller as compared to its efficiency at the same airplane speed and revolutions when isolated. The loss is large for the low pitches, but it is smaller for the higher pitches and actually becomes a gain for pitch ratios higher than 1.2. The tandem sets with the smaller rear propellers show the same general tendencies.

While Eiffel's tests could have been more complete, especially regarding the operating régimes corresponding to climb and take-off, they, along with the other tests referred to, tend to illustrate the following points:

1. With propellers of normal proportions having a spacing of about one diameter, the front propeller is not appreciably affected by the rear propeller with regard to power, but with high power coefficients and low pitches the efficiency of the front propeller may be reduced as much as 2 or 3 per cent.

2. The efficiency of the rear propeller is greater if the propellers rotate in opposite rather than like directions.

3. It is advantageous as regards efficiency for tandem propellers to have high pitch ratios.

Since the tandem arrangement is ordinarily used on highly powered but rather slow airplanes, propellers of high pitch ratio can usually be obtained only by gearing the propellers to run at lower revolution speeds than the engines. Gearing is also advantageous in that the larger diameters of geared propellers enable them to work on a larger mass of air with consequent higher ideal efficiencies. This is particularly desirable with tandem propellers, for their greatest disadvantage is their low efficiency at take-off and climbing speeds due to the fact that both propellers work on the same air.

**The Diameter of the Rear Propeller.**—It has been the practice of some designers, especially in England, to make the rear propeller markedly smaller (in the neighborhood of 20 per cent) in diameter than the front one, mainly to make certain that the rear propeller always operates entirely within the slipstream of the front one. In climbing flight the slipstream does not follow the propeller axis, and the rear propeller is consequently not in the center of the slipstream of the front propeller; so it is necessary to make the diameter of the rear propeller quite small if it is always to work entirely within the slipstream of the front one. In order to obtain a reasonable pitch with the small diameter, it has usually been found necessary to use four blades on the rear propeller. The small rear propeller has the disadvantage that if the front engine fails in flight the rear propeller has a comparatively low efficiency at the low speeds possible with one engine.

The diameter of the rear propeller is naturally somewhat smaller than that of the front if both propellers are of the same general form and are selected to give the highest efficiency, for the rear propeller works at higher effective velocity and revolutions. When it is remembered that (1) due to the body between the two propellers, the slipstream of the front propeller is spread

so that it retains approximately the full diameter of the front propeller;<sup>1</sup> (2) the transition from the full slipstream velocity to the velocity of the outside air is not sudden; and (3) the velocity is far from constant within the slipstream, varying greatly with radius at climbing speeds and also being of a pulsating nature, there seems to be no good reason why the rear propeller should not have so large a diameter as the front propeller as far as operating conditions and smooth running qualities are concerned. There is a variation of the air load on any propeller in climb due to the angle between the propeller axis and the flight path and the consequent greater angles of attack of the blade elements going down than those going up. For a rear tandem propeller in climb, to this load variation is added that due to the operation in the pulsating and varying velocity of the slipstream of the front propeller, and the conditions are apparently as good for a propeller the size of the front one as for a smaller one. There is therefore no apparent advantage in using a rear propeller which is smaller than that giving the best efficiency.

**A Method of Dealing with Tandem Propellers in Which Each Propeller Is Treated as a Complete Unit.**—It is usually more convenient to deal with a propeller as a whole than to deal with each section separately and then sum them all up. For this purpose the average axial and rotational velocities in the slipstream of the entire front propeller are used, the rotational velocity being considered as an increment in the revolutions of the rear propeller. (It is an increment only if the propellers rotate in opposite directions.) The revolutions of the rear propeller are then in effect (relative to the air in which it works) higher than the engine revolutions, just as the forward velocity is in effect higher than that of the airplane, due to the axial component of the slipstream from the front propeller. If  $V_1$  and  $N_1$  are the velocity and revolutions (in m.p.h. and r.p.m.) of the rear propeller with respect to the air in the slipstream of the front propeller, and  $V$  and  $N$  are the airplane velocity and the engine revolutions, the relations between them are given by the following empirical equations:

$$\frac{V_1}{V} = \left( \frac{1.25C_T}{(V/nD)^2} + 0.25 \right)^{\frac{1}{2}} + 0.50$$

<sup>1</sup> Investigation of Slipstream Velocity, by J. W. Crowley, Jr., N.A.C.A.T.R. 194, 1924.

or

$$\frac{V_1}{V} = \left( \frac{1.25(V/nD)^2\eta}{C_s^5} + 0.25 \right)^{\frac{1}{2}} + 0.50,$$

and

$$\frac{N_1}{N} = \frac{C_P}{5(V/nD)} + 1$$

or

$$\frac{N_1}{N} = \frac{(V/nD)^4}{5C_s^5} + 1.$$

The coefficients  $C_T$ ,  $C_P$ ,  $\eta$ ,  $C_s$ , and  $V/nD$  apply, of course, to the entire front propeller.

If  $\eta_1$  is the efficiency of the rear propeller with respect to  $V_1$  and  $N_1$ , the actual efficiency of the rear propeller is

$$\eta = \frac{V}{V_1} \times \frac{N_1}{N} \times \eta_1.$$

**Examples.**—Let us take as an example an airplane having a maximum sea-level speed of approximately 120 m.p.h. with two engines in tandem, each developing 500 hp. at 1,800 r.p.m.

From the front propeller, which is treated as if alone,  $C_s = 1.10$ ; and from Fig. 51 or 52 (we shall choose our propellers from the metal series tested on the VE-7 airplane and assume that the nose of our engine nacelle is similar to that of the VE-7), the  $V/nD$  for the propeller having the highest efficiency for the above  $C_s$  is found to be  $V/nD = 0.573$ . The diameter is then 10.23 ft., the blade angle at  $0.75R$  is  $18.0^\circ$ , and the propulsive efficiency is 0.778.

The ratios of the velocity and revolutions in the slipstream to those of the airplane and engine are

$$\begin{aligned} \frac{V_1}{V} &= \left( \frac{1.25(V/nD)^2\eta}{C_s^5} + 0.25 \right)^{\frac{1}{2}} + 0.50 \\ &= 1.170 \end{aligned}$$

and

$$\begin{aligned} \frac{N_1}{N} &= \frac{(V/nD)^4}{5C_s^5} + 1 \\ &= 1.0135. \end{aligned}$$

The velocity and revolutions of the rear propeller with respect to the air in which it works are therefore

$$\begin{aligned} V_1 &= 1.170 \times 120 \\ &= 140.4 \text{ m.p.h.} \end{aligned}$$

and

$$\begin{aligned} N_1 &= 1.0135 \times 1,800 \\ &= 1,824 \text{ r.p.m.} \end{aligned}$$

Then for the rear propeller  $C_{s1} = 1.28$ , and assuming that the curves of Figs. 51 and 52 apply also to pushers, which is true within practical limits, we find that  $(V/nD)_1 = 0.687$ ,  $D = 9.86$  ft., the blade angle at  $0.75R$  is  $20.5^\circ$ , and  $\eta_1 = 0.816$ . The actual efficiency of the rear propeller is then

$$\begin{aligned} \eta &= \frac{1.0135}{1.170} \times 0.816 \\ &= 0.707, \end{aligned}$$

and the average efficiency of the front and rear propellers is 0.742. This is a trifle higher than the best efficiency which can be obtained with a single propeller of the same family absorbing the whole 1,000 hp. at 1,800 r.p.m. and 120 m.p.h.

Since the efficiency of the rear propeller is greatly reduced by the axial velocity added by the front propeller, it might reasonably be thought that the overall efficiency could be increased by using a front propeller of greater diameter, thereby reducing the slipstream velocity. A small gain would result if the diameter could be increased by the use of narrower blades. If, however, the larger diameter is obtained by the use of lower pitch, as would normally be done, the efficiency of the front propeller drops more than the ratio  $V_1/V$ , so that the overall efficiency is reduced slightly.

The thrust horsepower available at various air speeds has been computed for the above tandem propellers, on the assumption that the full-throttle engine torque is constant, and plotted in Fig. 129. The front propeller yields from 10 per cent more useful power at 120 m.p.h. to 22 per cent more at 60 m.p.h.

It is interesting to compare the tandem arrangement with a side-by-side arrangement having two engine-propeller units similar to the front one. The thrust horsepower available with two propellers similar to the front one is shown by the top curve in Fig. 129. This does not make a fair comparison with the tandem arrangement, however, for the side-by-side arrangement would necessitate the use of two engine nacelles instead of one. Taking the difference between the drag of two nacelles and that of one long nacelle housing both engines as being 150 lb. at 100 m.p.h., which appears to be a reasonable value for this sized



installation, another curve has been plotted on Fig. 129 in which allowance has been made for this difference in drag. If this curve is compared with that for the tandem installation, it is seen that the tandem propellers give a higher thrust power at speeds above 100 m.p.h. and therefore are better for high speed

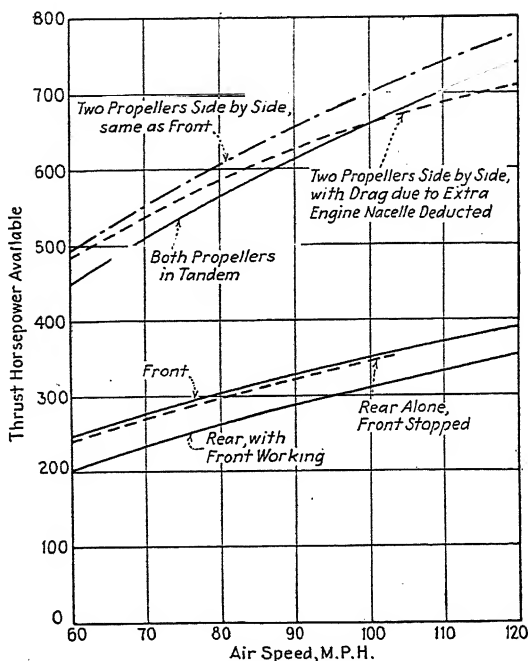


FIG. 129.—Thrust horsepower available with direct-drive tandem propellers.

and cruising, but the side-by-side propellers give greater thrust power below 100 m.p.h. and are therefore better for take-off and climb. The differences, however, are not large.

It is sometimes argued that one disadvantage of the tandem arrangement is that if the front engine fails, the rear propeller, which is designed to operate in the relatively high velocity of the slipstream, will hold the engine down to a low revolution speed and consequently give a very low thrust horsepower. As a matter of fact, the rotation in the slipstream ordinarily affects the engine revolutions slightly more than the added axial velocity, so that with propellers of ordinary form, the full-throttle revolutions of the rear propeller are very slightly greater

with the front propeller stopped than with it running at full power. The efficiency is slightly lower than that of the front propeller, due to the higher pitch and the low speeds obtainable with one engine, and so the thrust horsepower available with the rear propeller running alone is very slightly lower than that for the front propeller alone, as shown by the lower dotted curve in Fig. 129.

With side-by-side engines, if one stops, the thrust power of the other is the same as for the front engine of the tandem set, but the thrust is to one side of the center of resistance of the airplane, which increases the difficulty of control and also the drag.

All things considered, the tandem arrangement seems slightly superior to the side-by-side in case either engine stops.

Eiffel's model test indicated that the loss in efficiency of the rear propeller is less for propellers of high than low pitch. The pitch of the propellers of our example could be increased by gearing the propellers to turn more slowly than the engines. Larger diameters would then be necessary, which would also be advantageous especially at take-off and climbing speeds.

Assuming that our two 500-hp. engines are geared so that the propellers turn at half the crankshaft speed, and assuming a gear loss of 2 per cent so that the actual brake horsepower delivered to the propellers is 490 hp. at 900 r.p.m., the best front propeller for 120 m.p.h. has a value of  $C_s$  of 1.46, a diameter of 14.7 ft., a blade angle at  $0.75R$  of 22.7 deg., and an efficiency of  $0.838 \times 1.038 = 0.869$ .<sup>1</sup> Then  $V_1/V = 1.092$  and  $N_1/N = 1.0122$ , and the best rear propeller has a diameter of 14.42 ft., a blade angle at  $0.75R$  of 24.0 deg., and a value of  $\eta_1$  of  $0.852 \times 1.038 = 0.884$ . The actual efficiency of the rear propeller is

$$\eta = \frac{1.0122}{1.092} \times 0.884 = 0.819,$$

and the average efficiency for the two geared propellers neglecting gear losses is 0.844 as compared with 0.742 for the direct-drive installation.

Curves of thrust horsepower available, similar to those for the direct-drive propellers, are given for the geared propellers in Fig. 130. A 2 per cent gear loss has been allowed for in these curves. It will be noticed that the loss for the rear propeller

<sup>1</sup> This value for the efficiency is obtained by considering that due to body interference the propulsive efficiency increases 1 per cent with an 8 per cent reduction of  $d/D$ .

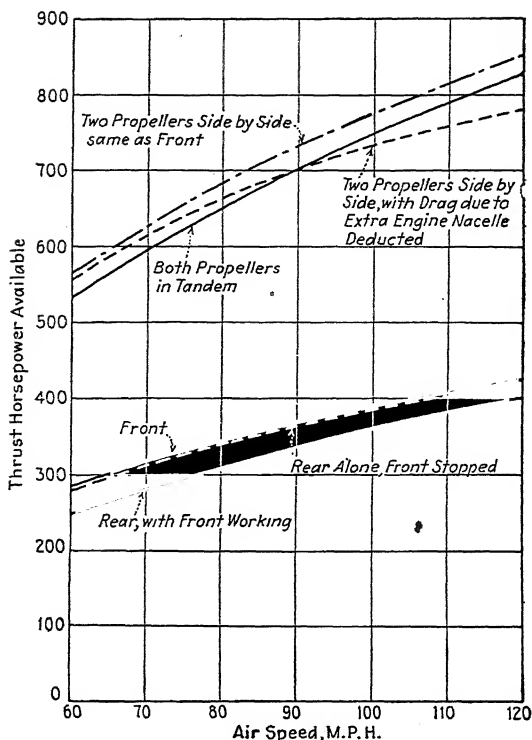


FIG. 130.—Thrust horsepower available with geared tandem propellers.

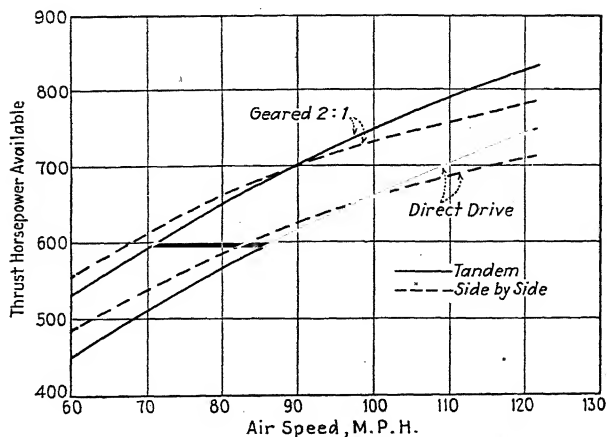


FIG. 131.—Comparison of tandem and side-by-side, geared and direct-drive

is less for the geared installation. Also, at high speed the geared tandem arrangement has more advantage over the side-by-side than is the case with the direct drives, and the geared side-by-side arrangement has less advantage over the geared tandem in climb and take-off.

In Fig. 131 the geared tandem and side-by-side arrangements are compared with the direct-drive tandem and side-by-side arrangements. Both geared sets are better than either of the direct-drive ones throughout the entire range.



## CHAPTER XIV

### MATERIALS AND FORMS OF CONSTRUCTION

Propellers are subject to two main types of loads, those due to centrifugal forces and those due to air forces. Since the centrifugal force is greater for heavy than light materials, a low weight per unit volume is advantageous. The strength should of course be high, particularly the fatigue strength, which is the stress which may be repeated indefinitely without causing failure.

The air loads fluctuate somewhat with time due to gustiness, unsymmetrical conditions, and the elasticity of the propeller blades, and the fluctuating tends to set up vibrations in the blades. Hysteresis, or internal friction, is therefore advantageous in a material for damping vibrations.

A good propeller material should also hold its shape in various climates and under varying weather conditions and should be able to withstand impact with seaplane spray, raindrops, and small pebbles without appreciable damage.

**Wood Propellers.**—In some ways wood is almost an ideal material for aircraft propellers, but in others it is not well suited. Its best qualities are a high strength-weight ratio, a high fatigue strength, and great internal friction. Tensile stresses up to 5,000 or 6,000 lb. per sq. in. and compressive stresses up to 3,000 lb. per sq. in. are permissible with most propeller woods, the fatigue strength being almost as high as the fiber stress at the elastic limit. Thus the ratio of tensile fatigue strength to weight is higher for wood than for any other successfully used propeller material. The disadvantages of wood, however, in most cases outweigh the advantages, and although in 1922 it was universally used, at the present time it has been replaced by other materials for all propellers subject to severe service.

Wood propellers warp with varying climatic conditions, especially in tropical climates. In order to minimize this warping and twisting, wood propellers are built up of several layers or laminations, all glued together. The laminations are from  $\frac{1}{2}$  in. thick, the normal value being  $\frac{3}{8}$  in. and all of the lamina-

tions of the same propeller having the same thickness, except possibly the two outer ones. The laminations are placed parallel to the plane of rotation so that a section through the propeller

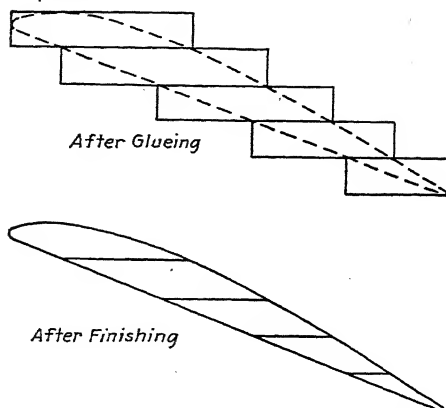


FIG. 132.—Section through blade of laminated wood propeller.

blade appears as shown in Fig. 132.<sup>1</sup> Wood does not satisfactorily withstand the impact of pebbles, rain, or seaplane spray. In fact, one-half hour of running in hard rain is sufficient to ruin the leading edge entirely.

For this reason wood propellers are usually sheathed with metal at the tip and part way along the leading edge. Three forms of metal tipping are illustrated in Fig. 133. The Navy tip, which is for propellers subjected to severe seaplane spray, is a complete tip of brass 0.022 in. thick, fastened on with brass wood screws where the blade is over  $\frac{1}{2}$  in. thick and with copper rivets where it is thinner.

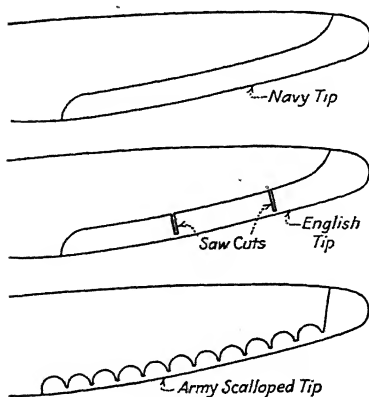


FIG. 133.

In England a similar tip is used excepting that saw cuts are put in the metal as shown. This provides a certain amount of freedom which keeps the tipping from cracking at other places,

<sup>1</sup> For a description of the process of manufacture of wood propellers, see "The Propeller," published by the War Department in 1920.

as is common with the Navy tip, especially on flexible propellers. Some American manufacturers use a somewhat similar arrangement in which the tip is made up of a number of overlapping sections. The Army uses a scalloped tipping of terne plate which is expected to crack between scallops.

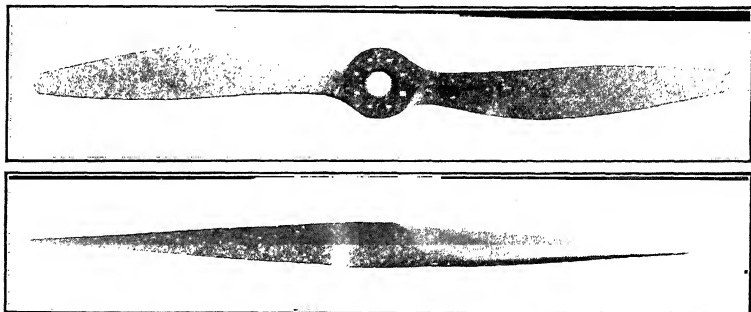


FIG. 134.—Typical fabric-sheathed wood propeller.

The best propeller woods are walnut, birch, oak, and Honduras mahogany. Walnut is probably the best all-around wood and has the special advantage of holding its shape well. Birch is the toughest and is best used in experimental propellers of doubtful

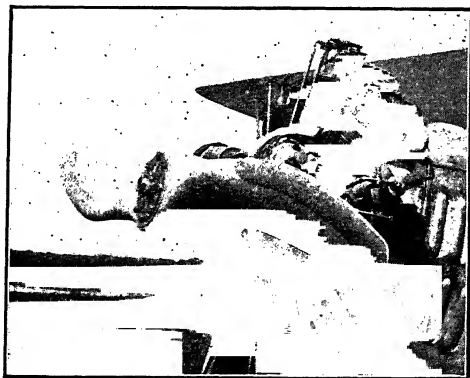


FIG. 135.—Wood propeller with Navy tips.

strength. It is a better propeller wood than walnut except for a greater tendency to warp. Oak is used by the Navy because of its ability to withstand seaplane spray better than the others. It wears away without splitting. Mahogany is lighter than the others and it holds its shape well.

While wood is strong in tension it is weak in longitudinal torsion and splits easily along the grain. For this reason the blades of wood propellers are often sheathed with fabric. The fabric is glued on and increases both the torsional strength and stiffness. A typical fabric-sheathed wood propeller of Navy form is shown in Fig. 134. A similar propeller with a Navy-type metal tip is shown in Fig. 135, and a typical four-bladed propeller in Fig. 136. The latter two pictures show the metal-flanged hubs



FIG. 136.—Four-bladed wood propeller.

with through bolts commonly used with wood propellers.

**Micarta Propellers.**—A material called micarta has been developed by the Westinghouse Electric and Manufacturing Company and has been applied by the same company, in cooperation with the Army, to aircraft propellers.<sup>1</sup> As used in propellers, micarta is a composition formed of layers of cotton-duck fabric impregnated with a synthetic resin binder and baked under pressure. The propeller is

formed of laminations of cotton-duck micarta and is finished as it comes from the mold, except for slight trimming at the parting line and curing for about 20 hr. at a temperature of 100°C.

The hub is fitted with a steel bushing having large splines extending into the micarta, the bushing fitting directly on the engine shaft. The propeller is balanced by locating the bushing at the center of gravity. A micarta propeller with hub bushing is shown on a balancing stand in Fig. 137. Micarta propellers are also made with detachable blades held in a steel hub in much the same manner as the aluminum-alloy blades described later.

Micarta is not affected to an appreciable extent by climatic changes, and it withstands rain, cinders, and pebbles somewhat better than wood. It does not withstand them with entire satisfaction, however, and the latest micarta propellers are

<sup>1</sup> For a detailed account of the materials, methods of construction, and design see *Micarta Propellers, Parts I to IV*, by F. W. Caldwell and N. S. ...



being tipped with metal in much the same manner as wood propellers.

The properties of micarta depend largely on the fabric used for the laminations. With an ordinary good grade of cotton duck, as usually used in propellers, an ultimate tensile strength of from 9,000 to 10,000 lb. per sq. in. and a longitudinal shearing strength of about 4,000 lb. per sq. in. are obtained. With a special fabric having 90 per cent of the total weight of the cloth in the warp, which is placed lengthwise of the propeller blade, a tensile strength of 26,000 lb. per sq. in. has been obtained. Ordinary propeller micarta weighs approximately 0.05 lb. per cu. in.

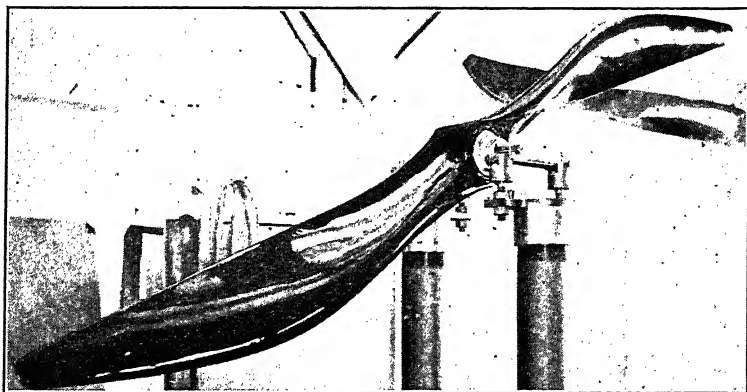


Fig. 137.—Micarta propeller for Liberty Engine. (Photograph from N.A.C.A. T.N. 199.)

Like wood, micarta has a high degree of internal friction, and the fatigue strength is apparently fairly high. Unlike wood, however, micarta has no tendency to split, and micarta propellers often run satisfactorily under conditions which have proved too severe for wood propellers and certain types of metal propellers, conditions such as that of a wing propeller operating partially in the slipstream of a nose propeller, with a consequent highly fluctuating air load on the blades. Due to the non-splitting properties of micarta, micarta blades can be made from 20 to 40 per cent thinner than wood blades, resulting in slightly greater efficiency. At the present time the cost of micarta propellers is high and they are used but little.

**Steel Propellers.**—Many steel propellers have been designed and built in a large variety of both solid and hollow forms of

construction, but only one type, the Leitner-Watts, has proved sufficiently satisfactory to be used in service. This type is made with detachable blades which fit in a two-piece split-steel hub. The blades are hollow and are built up of thin laminated sheets of mild steel pressed to form. The number of laminations decreases from hub to tip, giving the material in effect a tapering cross-sectional area. A section showing the construction of the

blade root is shown in Fig. 138. The shapes of the blades and the laminations, which are terminated in a sort of tapered fork so that the change in cross-sectional area is not abrupt, are shown in Fig. 139. The blades are pressed in

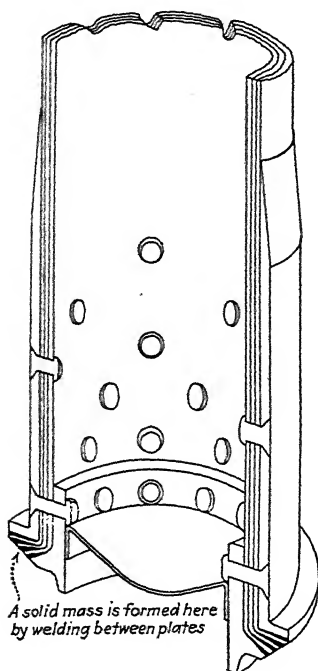


FIG. 138.—Section showing construction of blade root of Leitner-Watts propeller. (From catalogue of Metal Airscrew Company, Ltd.)

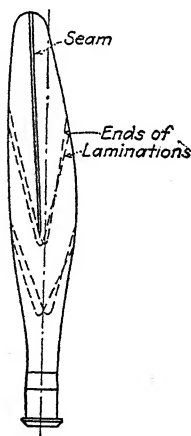


FIG. 139.—Leitner-Watts laminated steel blade.

halves, and the two halves are fastened together by welding along the edges. In order to stiffen the flat face a seam is put in it and internal spacers are riveted in between the two faces.

Under fluctuating loads the friction between the laminations tends to damp out vibrations, which, in the opinion of the writer, is the reason for the success of the Leitner-Watts propellers when all other steel propellers have failed. Steel has very little internal friction if stressed below the elastic limit, and steel propellers,

have repeatedly failed, probably because the vibrations build up to the extent that they cause stresses above the fatigue limit.

The Leitner-Watts propellers were the first to be made with a limited number of standard-sized blades and with two-, three-, and four-bladed hubs to take the blades, making it possible to take blades and hub from stock to fit any ordinary aircraft engine. The hubs are made with removable bushings which fit the various engine shafts.

The Leitner-Watts propellers are made no thinner than wooden propellers, and they are consequently no more efficient aerodynamically. They are not being widely used at this time, for they are more expensive and less efficient than the thinner solid aluminum-alloy propellers which have been developed during the last few years. They still have a field, however, in very large-sized propellers, especially for airships, where they can be made lighter than the present solid aluminum-alloy propellers.

**Aluminum-alloy Propellers.**—Aluminum alloy has now been used for propellers for several years and its use is rapidly increasing. It has already displaced wood in the high-power high-revolution range, and it is gradually displacing it in the low-power range.

The composition and physical properties of all aluminum alloys used for propellers are practically the same, although they are made by various manufacturers and bear different trade names.<sup>1</sup> There are slight variations in the alloys and the methods of heat treating, but all are made up of approximately 95 per cent aluminum, 4 per cent copper, and 1 per cent other ingredients and impurities. In propellers, the alloys are used in the rolled or forged state, and all of the alloys, after heat treatment, have approximately the following physical properties:

Ultimate strength.....	55,000 to 60,000 lb. per sq. in.
Fatigue strength.....	10,000 to 15,000 lb. per sq. in.
Modulus of elasticity.....	10,000,000 to 11,000,000 lb. per sq. in.
Weight per cubic inch.....	0.100 to 0.103 lb.

The aluminum alloys have no definite yield point or elastic limit, although the yield point is often arbitrarily considered as from 30,000 to 40,000 lb. per sq. in. The material does not have a straight-line stress-strain curve, the deflection not being exactly

<sup>1</sup> Aluminum Company of America, 25S; Baush, duralumin; Vickers (England), duralumin; Schneider and Company (France), alferium; Metallgesellschaft and M. G. (Germany), Aerop.

proportional to the load applied even with comparatively low loads. This indicates a hysteresis or internal friction in the material which is helpful in damping out vibrations. Stresses up to the fatigue limit, which is usually considered about 12,000 lb. per sq. in., can be repeated indefinitely without failure, and it is the aim in designing propellers to keep the stresses, including those due to vibrations and fluctuations, below this value.

Aluminum, although it has a slight grain structure when rolled or forged, has very nearly the same strength in all directions. Due to this homogeneity, and also to the stiffness of the aluminum alloys, propellers of this material can be made with very thin sections which are advantageous as regards efficiency, especially at high tip speeds.

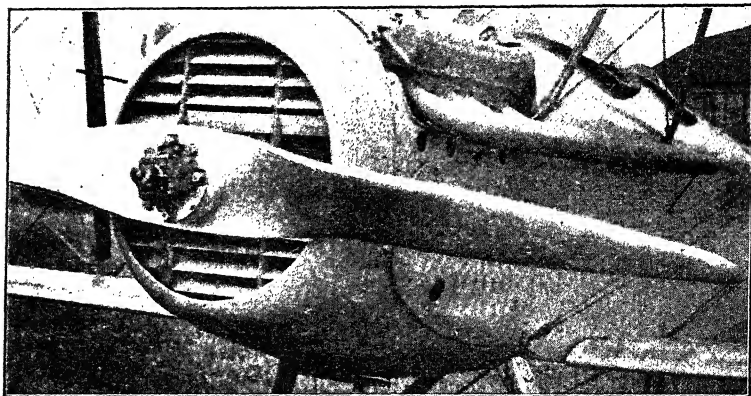


FIG. 140.—Reed twisted-slab type of aluminum-alloy propeller.

The first aluminum-alloy propellers to be used were of the Reed twisted-slab type. Propellers of this type are made from flat slabs of aluminum alloy, the blades being machined and hand filed to the form of a flat tapered airfoil and then twisted to the proper pitch angles. The center portion is fitted to the ordinary flanged hub for wooden propellers by means of filler blocks, as shown in Figs. 140 and 141. The twisted-slab type of propeller was rather widely used a few years ago but during the last few years its use has declined greatly.

The twisted-slab type of construction with filler blocks was considered by the inventor a temporary expedient for adapting wood propeller hubs, and it has been replaced

propellers are made of a single forged piece of aluminum alloy and look very much like wooden propellers except that the sections are thinner, especially at the hub and blade roots, as shown in Fig. 142. A steel bushing, much like that used in the

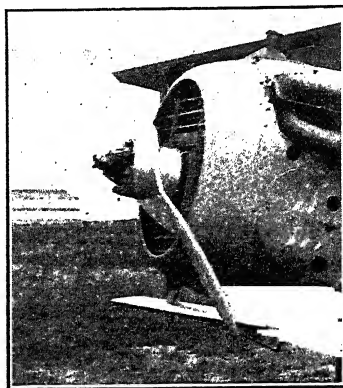


FIG. 141.—Reed twisted-slab propeller showing twist and hub blocks.

one-piece micarta propeller, fits on the engine shaft and has large splines projecting into the aluminum alloy.

Since 1923, aluminum-alloy propellers have also been made with detachable blades which can be turned in the hub and

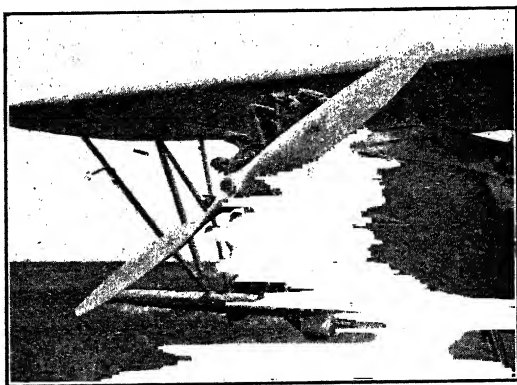


FIG. 142.—Reed forged aluminum-alloy propeller, type R.

adjusted to various pitch angles. A typical detachable-blade aluminum-alloy propeller is shown in Fig. 143. The hubs are made of high-strength alloy steel, usually chrome nickel or chrome manganide, having an ultimate strength of at least 130,000

lb. per sq. in. On the first propellers of this type the blades screwed into the hub with buttress screw threads, and they were

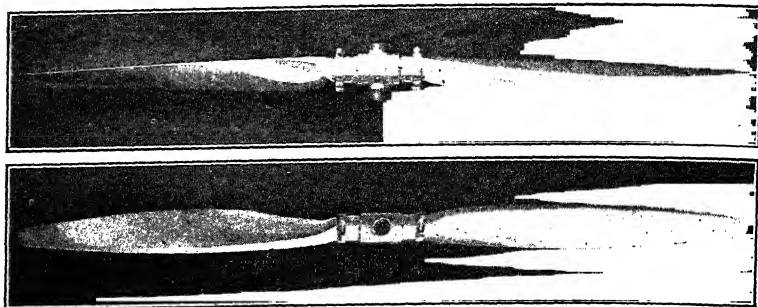


FIG. 143.—Typical detachable-blade aluminum-alloy propeller.

held against turning or chattering by a split-steel wedge ring forced between the blade shank and the hub by a screw collar, as shown in Fig. 144. This type of hub has now been abandoned

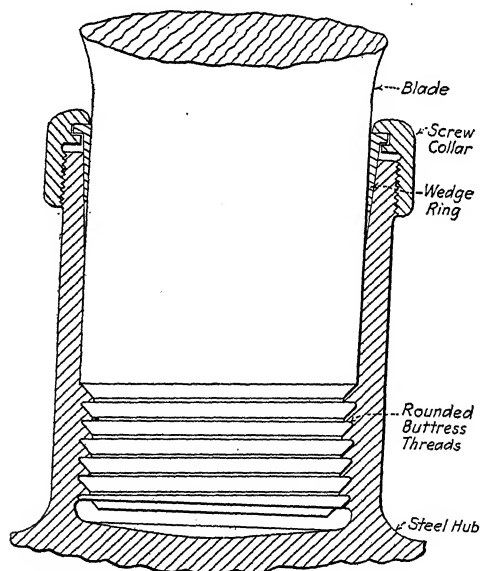


FIG. 144.—Section through screw-type hub for aluminum-alloy propeller.

for the cheaper split hub, which can be forged in two halves and is easier to manufacture. The parts of a split hub for a three-bladed propeller are shown in Fig. 145. The two halves of the

hub are squeezed tightly down around the blade shanks by means of clamp rings, which are shown separately in Fig. 145 and on a

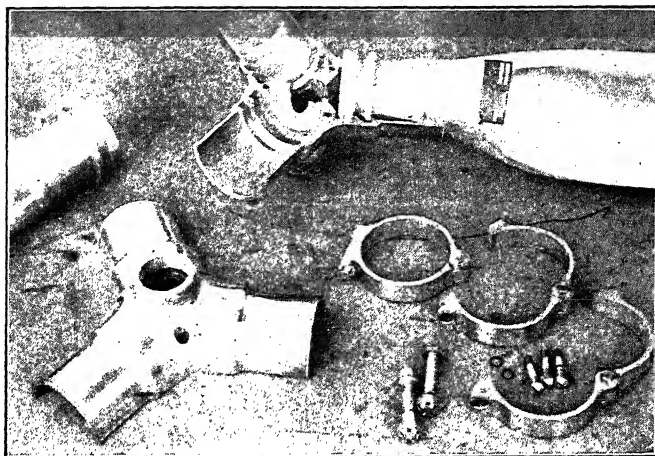
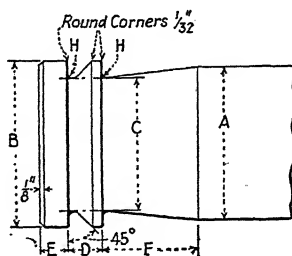


FIG. 145.—Parts of split-type hub for three-bladed propeller.

propeller in Fig. 143. The dimensions of the blade roots recommended by the Department of Commerce and standard for the Army and Navy are given in Fig. 146.



STANDARD BLADE END NO.	A	B	C	D	E	F	H
NO.00-0 TO 50 HP.	2.250 $\begin{smallmatrix} +0.000 \\ -0.003 \end{smallmatrix}$	2.435 $\begin{smallmatrix} +0.000 \\ -0.003 \end{smallmatrix}$	2.000 $\begin{smallmatrix} +0.010 \\ -0.010 \end{smallmatrix}$	0.500 $\begin{smallmatrix} +0.002 \\ -0.000 \end{smallmatrix}$	0.4375 $\begin{smallmatrix} +0.010 \\ -0.010 \end{smallmatrix}$	1.312 $\begin{smallmatrix} +0.010 \\ -0.010 \end{smallmatrix}$	$\frac{3}{32}$
NO.0-50 TO 250 HP.	3.000 $\begin{smallmatrix} +0.000 \\ -0.003 \end{smallmatrix}$	3.250 $\begin{smallmatrix} +0.000 \\ -0.003 \end{smallmatrix}$	2.625 $\begin{smallmatrix} +0.010 \\ -0.010 \end{smallmatrix}$	0.6675 $\begin{smallmatrix} +0.002 \\ -0.002 \end{smallmatrix}$	0.562 $\begin{smallmatrix} +0.010 \\ -0.010 \end{smallmatrix}$	1.687 $\begin{smallmatrix} +0.010 \\ -0.010 \end{smallmatrix}$	$\frac{1}{8}$
NO.1-250 TO 500 HP.	3.875 $\begin{smallmatrix} +0.000 \\ -0.003 \end{smallmatrix}$	4.245 $\begin{smallmatrix} +0.000 \\ -0.003 \end{smallmatrix}$	3.375 $\begin{smallmatrix} +0.010 \\ -0.010 \end{smallmatrix}$	0.875 $\begin{smallmatrix} +0.002 \\ -0.000 \end{smallmatrix}$	0.750 $\begin{smallmatrix} +0.010 \\ -0.010 \end{smallmatrix}$	2.375 $\begin{smallmatrix} +0.010 \\ -0.010 \end{smallmatrix}$	$\frac{5}{32}$
NO.2-500 TO 800 HP.	4.500 $\begin{smallmatrix} +0.000 \\ -0.003 \end{smallmatrix}$	4.995 $\begin{smallmatrix} +0.000 \\ -0.003 \end{smallmatrix}$	3.875 $\begin{smallmatrix} +0.010 \\ -0.010 \end{smallmatrix}$	1.250 $\begin{smallmatrix} +0.002 \\ -0.000 \end{smallmatrix}$	1.000 $\begin{smallmatrix} +0.010 \\ -0.010 \end{smallmatrix}$	3.125 $\begin{smallmatrix} +0.010 \\ -0.010 \end{smallmatrix}$	$\frac{5}{32}$

FIG. 146.—Department of Commerce standard ends for detachable blades for aluminum-alloy propellers.

The blades of these propellers are forged solid, and when a particular design is made in large quantities, they are drop

forged with dies which leave them within about  $\frac{1}{16}$  in. of their final size. They are then machined to the proper dimensions, largely by means of hand grinding with flexible disc grinders and hand filing. Usually each blade is balanced against a master

blade kept for that purpose only.

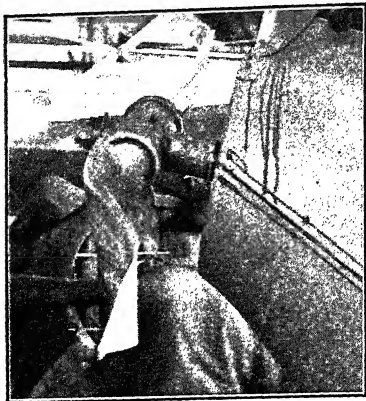


FIG. 147.—Aluminum-alloy propeller bent in an accident.

Propellers made of aluminum alloy are, including the steel hub, of about the same weight as micarta propellers for the same purpose and are usually (but not necessarily) slightly heavier than wood propellers for the same purpose.

Aluminum alloy is not only well fitted for use in propellers but also has the additional advantage over any other material used to date that a propeller damaged in an air-

plane accident (Fig. 147) can be straightened and heat treated by the manufacturer at nominal cost and used again.

Aluminum alloy resists the erosion of rain, pebbles, and seaplane spray better than wood or micarta, but it will not satisfactorily withstand severe seaplane spray. In one extremely severe taxiing test made by the Navy, in which the writer participated, approximately one-fourth inch of the leading edge of an aluminum-alloy propeller was eroded off in ten minutes. After the smooth edge has been partially eaten into, the impact of the spray and occasional solid waves tears the metal off rapidly in irregular pieces. For ordinary seaplane service the conditions are not so severe, and aluminum-alloy propellers usually give reasonably satisfactory service if they are kept smooth by rubbing with crocus cloth and, when the blades become slightly rough or pitted, an occasional filing. If the propellers are operated near salt water it is advisable to protect them from corrosion by wiping them with oil after each flight.

**The Construction of Variable-pitch Propellers.**—Although variable- or controllable-pitch propellers have not yet progressed beyond the experimental stage, it seems certain that in the near future they will be used, at any rate on supercharged airplanes,



and it is therefore of interest to describe the construction of a few of the most promising types.

One of the greatest problems with the early variable-pitch propellers was to provide a suitable way of attaching the wooden blades to the hub in such a manner that the full strength of the wood was obtained. This was finally worked out in a fairly

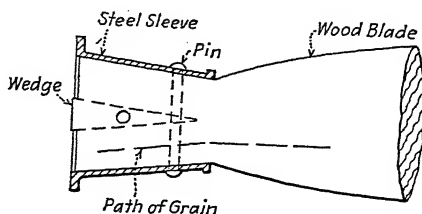


FIG. 148.—Sleeve for fastening wood blade in metal hub.

satisfactory way for low powers, by fitting the blade root in a tapered-steel sleeve as shown in Fig. 148. With micarta, or aluminum alloy, standard or nearly standard detachable blades can be used, and the blade fastening is not a difficult problem.

In all of the variable-pitch propellers which have been flight tested on airplanes, the centrifugal force on the blades is taken on ball or roller thrust bearings in order to make the friction

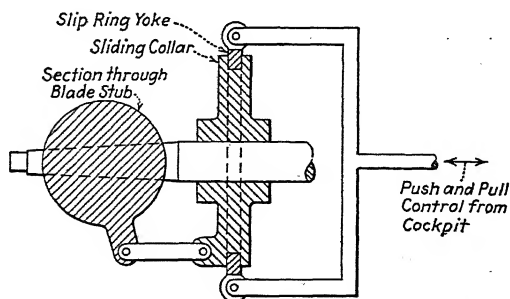


FIG. 149.—Principle of operating mechanism of Hart variable-pitch propeller.

against turning as low as possible. In order to keep the weight within reason it is usually necessary to use bearings which are very highly loaded. It is therefore important that the blades be made as light as is practicable. The air loads, which put a side force on the blades, are not so great and are often taken on plain radial bearings.

The Hart variable-pitch propeller was one of the first to be built and tested in this country. The pitch control is manually operated, the blade angles being set to any desired value by means of a lever in the pilot's cockpit. The operating mechanism, which is quite simple, is diagrammed in Fig. 149. This shows a cross-section of the root of one blade having an arm extending out to one side and projecting through a slot in the hub casing. This arm is connected by a link to a collar which rotates with the propeller and can slide back and forth along the axis of the engine shaft. Each position of the collar corresponds to a certain propeller pitch angle. The collar has a groove fitted with a yoke, the position of which is controlled by a lever in the cockpit.

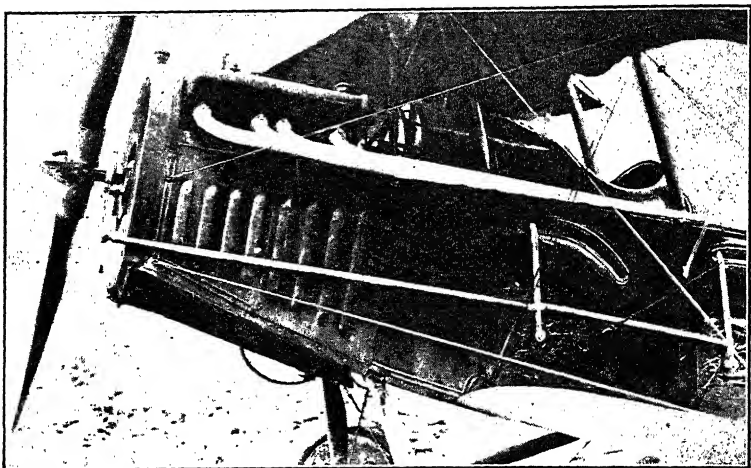


FIG. 150.—Hart variable-pitch propeller with counterweights and micarta blades. (Photograph from *N.A.C.A. T.N. 200*.)

Due to the fact that the blades are not symmetrical about a radial center line, the centrifugal force produces a twisting moment which is much larger than and opposite to that produced by the air force and which tends to turn the blades in the hub, making it necessary to apply an undesirably large force to change the pitch in one direction. To overcome this the Army, which has undertaken the development of the Hart-type propeller, has designed small counterweights which project forward from the blade roots near the hub and which produce twisting moments due to centrifugal force approximately balancing those on the blades themselves. These are shown in Fig. 150, which is a

view of a Hart variable-pitch propeller with micarta blades, on a JN-4H airplane with pitch control from both cockpits.

Another form of variable-pitch propeller is that invented and developed by Spencer Heath, in which engine power is used to change the pitch. The principle of operation is shown diagrammatically in Fig. 151, which represents a brake drum connected through a gear train to each blade of the propeller. If the brake drum is allowed to revolve freely, it will turn with the crankshaft, all gears will remain stationary, and the pitch will remain the same. If, however, the brake drum is held stationary, the gears will be put into action, and the pitch angle will change as long as the braking force is applied. In order to change the pitch in the opposite direction, a second brake drum is connected to the worm shaft through an idler which reverses the direction of rotation. During normal flying none of these gears is operating, and the blades are locked in position by the worm gears which are irreversible.

In actual construction the mechanism is complicated by the necessity for a large gear reduction, entailing several extra gear wheels, and also by the necessity for a pitch-angle indicator which entails many small continuously operating gears. It has the advantages, however, that the pitch can be changed by a light pull or push on a button on the end of the brake-control rod, that the angular range of the blades is unlimited, and that there are no running gears or slip joints in the pitch-changing mechanism.

Another promising variable-pitch propeller is that designed by R. W. Turnbull of Canada and tested by the Royal Canadian Air Force. In the Turnbull propeller the pitch is changed by a small electric motor which is located in a spinner at the front of the hub and is geared to the blades.

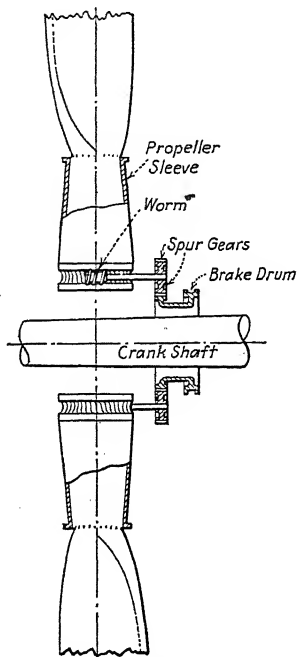


FIG. 151.—Diagram showing operation of Heath variable-pitch propeller. (From N.A. C.A. T.M. 70.)

The most recent and perhaps the most promising variable-pitch propeller is the hydraulically and automatically operated Hele-Shaw Beacham. This propeller has a double-acting hydraulic ram or piston which is located in a spinner in front of the hub and operates a sliding collar similar to the one in Fig. 149, which in turn changes the pitch angle of the blades through a link and arm. The whole mechanism revolves with the propeller. The piston is moved back and forth by oil pressure, the oil being brought in through the engine shaft, which must be drilled and fitted with a rotating oil-tight joint, from a variable-stroke pump driven by the engine. The stroke of the pump is controlled by a governor, also driven by the engine, which can be set by the pilot for any desired engine revolutions. If the revolutions fall below the set value, the governor acts on the pump in such a manner as to increase the oil pressure on the side of the piston which decreases the pitch, and *vice versa*. Thus the action is entirely automatic but can be over controlled by the pilot by merely changing the revolution setting, which is a highly desirable feature, especially in high-altitude and acrobatic flying. If the hydraulic gear should fail, a spring returns the blades to a predetermined "normal" pitch, and the flight is completed with what is in effect an ordinary fixed propeller.<sup>1</sup>

If variable-pitch propellers are used as brakes for landing airplanes or for reversing an airship, the pitch angles must pass through zero. If the throttle were kept open while the blades passed through zero pitch, the engine would race and very likely destroy itself. To eliminate this possibility, the pitch-control mechanism is connected to the throttle, usually by means of a cam of some kind, in such a manner that the throttle is closed as the blades are moved through the zero pitch position.

Although all of the variable-pitch propellers described have apparently been successfully flight tested, none has been used further in service. The Gloster Hele-Shaw Beacham propeller, however, is new and is apparently being given service trials by the British Government. All of the propellers are quite heavy, but there is a possibility of reducing the weight materially by refinement of design.

<sup>1</sup> The Gloster Hele-Shaw Beacham variable-pitch propeller is thoroughly described in a paper by the inventors, published in the July, 1928, issue of the *Journal of the Royal Aeronautical Society*.

## CHAPTER XV

### THE STRENGTH OF PROPELLERS

The calculation of the stresses in propellers, which have both a non-uniform shape and a varying load, is a complex problem, and no strictly correct method of calculating the stresses has been devised. The ordinary theory of bending is used as the best practical method, but it is based upon assumptions which are of very doubtful value when applied to a body with as complex a shape as that of a propeller.<sup>1</sup>

**The Loads on a Propeller Blade.**—There are three main types of loads which act on propeller blades in operation:

1. The load due to air forces.
2. The load due to centrifugal forces.
3. The load due to gyroscopic forces and to other inertia forces due to unsteady motion.

In our analysis of propeller stresses we shall limit the case to steady rectilinear flight, so that only aerodynamic and centrifugal loadings need be considered.<sup>2</sup>

The propeller blade may be looked upon as a cantilever beam, in which case the stresses at any given cross-section depend on the loads on the portion of the blade from the section in question to the tip. It is not a cantilever beam in the ordinary sense, for the centrifugal force tends to hold the blade straight out after the manner of a tie.

A section of a propeller blade is shown in Fig. 152, where the direction of rotation is given by  $OA$ , the direction of translation by  $OB$ , and  $OC$  represents the radial axis through the center of gravity of the section  $O$  perpendicular to the plane of the section.

<sup>1</sup> See Some Notes on the Calculation of the Working Stresses of an Air-screw, by A. Fage and H. E. Collins, British *R. and M.* 420, 1918. These notes contain the basis of the method of stress analysis given in this chapter.

<sup>2</sup> Loads due to gyroscopic and other inertia forces are small compared with the air and centrifugal loads, and a propeller which is strong enough to endure the latter two types of loads for an indefinite period of time is also strong enough to stand the slightly higher total loading during the relatively short periods in which the gyroscopic and other inertia forces act.

The loading on the section due to the air forces on the portion of the blade between the section and the tip may be represented by:

1. A bending moment which may be represented by the two components
  - a.  $M_T$ , due to thrust, about the axis  $OA$ .
  - b.  $M_Q$ , due to torque forces, about the axis  $OB$ .
2. A twisting moment  $M_A$  about the axis  $OC$ , due to the fact that the resultant air forces for the various sections along the blade do not pass through the axis  $OC$ .
3. A shearing force across the section.

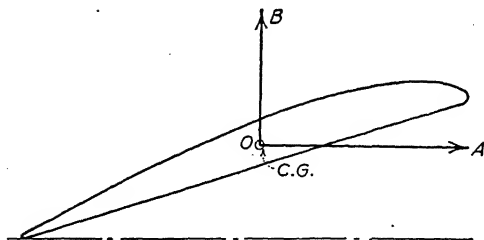


FIG. 152.

The centrifugal loading on the section for the general case where the centers of gravity of all of the blade sections do not lie on a straight radial line perpendicular to the axis of rotation may be represented by

1. A bending moment which may be resolved into the two components
  - a.  $M_T'$ , about the axis  $OA$ .
  - b.  $M_Q'$ , about the axis  $OB$ .
2. A twisting moment  $M_A'$  about the axis  $OC$ , which is due partially to the fact that the centers of gravity of the sections are not all on a straight radial line and partly to the fact that the sections are airfoils of unsymmetrical shape.
3. A tensile force  $CF$  acting radially outward along  $OC$ .
4. A longitudinal shear perpendicular to the plane of the section.

The shearing forces are small and are ordinarily neglected even in wood propellers, which are particularly weak in longitudinal shear. It should be kept in mind, however, that the cross-shear due to the air load also results in a longitudinal shear and that when the air load fluctuates, as it usually does,

the resultant varying longitudinal shear has a tendency to cause working and deterioration of the glue joints.

The twisting moments also cause an unimportant shear in the blades and are usually neglected. In wood propellers, large twisting moments tend to split the blades lengthwise and should be avoided. The most important effect of the twisting moments is more aerodynamic than structural, for the accompanying angular deflection affects the propeller pitch.

In computing stresses the loading at a section is therefore considered as made up only of a tensile force  $CF$ , the centrifugal bending moments  $M_T'$  and  $M_Q'$ , and the air-load bending moments  $M_T$  and  $M_Q$ . The combined resultant bending moment on the section is then

$$M = \sqrt{(M_T + M_T')^2 + (M_Q + M_Q')^2}.$$

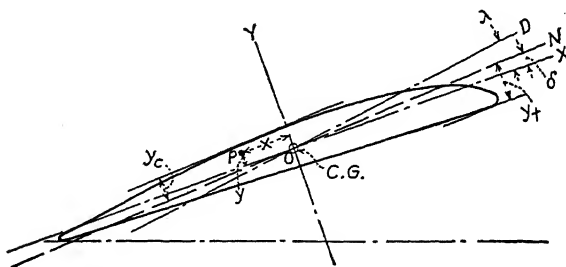


FIG. 153.

**Calculation of the Maximum Stresses at a Section.**—The typical propeller section shown in Fig. 153 has the principal axes  $OX$  and  $OY$ . The resultant bending moment  $M$  is about the axis  $OD$ , which is at an angle  $\lambda$  with the minor principal axis  $OX$ .

The neutral axis  $ON$  is found as follows: The resultant bending moment  $M$  is resolved into two components:  $M \cos \lambda$  about the minor principal axis  $OX$ ; and  $M \sin \lambda$  about the major principal axis  $OY$ . Then if  $I_x$  and  $I_y$  are the moments of inertia about the minor and major principal axes, respectively, at any point  $P$  (Fig. 153), which is a distance  $x$  from  $OY$  and a distance  $y$  from  $OX$ , the stress according to the ordinary theory of bending is

$$S = \frac{yM \cos \lambda}{I_x} - \frac{xM \sin \lambda}{I_y}.$$

The stress at all points on the neutral axis is zero, and so by equating the above expression to zero the equation of the neutral axis is found to be

$$y = x \frac{I_x}{I_y} \tan \lambda.$$

The neutral axis (Fig. 153) is inclined to the minor principal axis  $OX$  by an angle  $\delta$ , where

$$\tan \delta = \frac{y}{x} = \frac{I_x}{I_y} \tan \lambda.$$

The bending moment about the neutral axis is then

$$M \cos (\lambda - \delta),$$

and the moment of inertia about the neutral axis is

$$I = I_x \cos^2 \delta + I_y \sin^2 \delta.$$

The maximum tensile and compressive stresses in the section occur at the points farthest from the neutral axis ( $y_t$  and  $y_c$ , Fig. 153). The maximum stresses due to bending are then

$$S_t = \frac{M \cos (\lambda - \delta) y_t}{I},$$

$$S_c = \frac{M \cos (\lambda - \delta) y_c}{I}.$$

If  $A$  is the area of the section, the uniform tensile stress across the section due to the centrifugal load is

$$S_t = \frac{CF}{A}.$$

The total maximum tensile and compressive stresses at the section are then

$$\text{Total } S_t = \frac{M \cos (\lambda - \delta) y_t}{I} + \frac{CF}{A}$$

and

$$\text{Total } S_c = \frac{M \cos (\lambda - \delta) y_c}{I} - \frac{CF}{A}.$$

There is at present no way of knowing the accuracy of the stress calculated in this way, for there is no strictly rigorous method to compare with.

**Calculation of Loads.**—The air forces are calculated by means of the blade-element theory, the unit resultant force for each section being obtained from the thrust and torque per unit radius.



The centrifugal force acting on any given particle in the propeller is represented by the equation

$$CF = \frac{W}{g} \omega^2 r,$$

where  $W$  is the weight of the particle,  $g$  is the acceleration due to gravity,  $\omega$  is the angular velocity in radians per second, and  $r$  is the perpendicular distance between the particle and the axis of rotation. In engineering units the angular velocity  $\omega$  becomes  $2\pi \times \text{RPM}/60$  and the equation takes the form

$$CF = \frac{Wr}{g} \left( \frac{2\pi \times \text{RPM}}{60} \right)^2.$$

The propeller blade is usually divided into elements spaced either 6 in. or 0.15  $R$  apart along the radius. The weight  $W$  of an element per inch of radius becomes

$$W = Aw,$$

where  $A$  is the cross-sectional area of the section in square inches and  $w$  is the specific weight of the material in pounds per cubic inch. The centrifugal force on an element is given by

$$\frac{d(CF)}{dr} = Ar \frac{w}{g} \left( \frac{2\pi \times \text{RPM}}{60} \right)^2.$$

**Variation of Stresses with Tip Speed in Geometrically Similar Propellers.**—As can be seen from the above equation the centrifugal force is proportional to  $n^2 D^4$ , and the blade-element theory shows that for any one value of  $V/nD$  the air forces also are proportional to  $n^2 D^4$ . Both the centrifugal and air-load bending moments are therefore proportional to  $n^2 D^5$ , and

$$\text{Bending stress} \sim \frac{My}{I}.$$

Since  $I/y$  is proportional to  $D^3$ , the above expression may be written,

$$\begin{aligned} \text{Bending stress} &\sim \frac{n^2 D^5}{D^3} \\ &\sim n^2 D^2. \end{aligned}$$

Also, since the uniform tensile stress due to centrifugal force is given by the expression  $CF/A$ , and since  $A \sim D^2$ ,

$$\begin{aligned} \text{Centrifugal stress} &\sim \frac{n^2 D^4}{D^2} \\ &\sim n^2 D^2. \end{aligned}$$

Thus at any one value of  $V/nD$ , and neglecting scale effect, all of the stresses in geometrically similar propellers of like material vary as  $n^2D^2$  and therefore as the *square of the tip speed*.

**An Approximate Method of Stress Analysis.**—The above method of stress analysis is very laborious as well as of doubtful accuracy. An approximate method, which for all practical purposes is as accurate as the more complete method, will now be given, based on the following simplifications:

1. The resultant air force is assumed to be perpendicular to the chord at all sections. This is essentially true and causes negligible errors.
- \* 2. The chords of all sections are assumed to lie in a plane, so that the resultant air forces also lie in a plane. This neglects the change of blade angle along the radius and results in the cal-

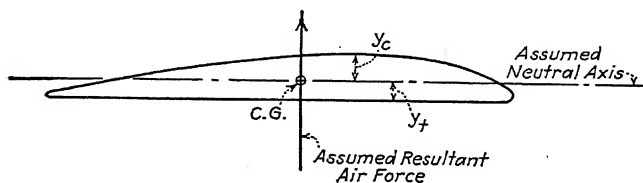


FIG. 154.

culated stress being slightly too high, an error on the safe side. The error is negligible in propellers of ordinary and low pitch and is never likely to be greater than 5 or 10 per cent even in the worst case of the hub sections of a very high-pitch propeller.

3. The neutral axis is assumed to be parallel to the chord (Fig. 154). This, as shown by calculations in *R. and M.* 420, causes no error in the maximum compressive stresses, but the computed maximum tensile stresses due to bending are 25 to 30 per cent low for the ordinary range of angles between the actual neutral axis and the assumed one parallel to the chord. The tensile stresses due to bending as found by this approximate method are therefore multiplied by the factor 1.30.

4. Twisting forces are neglected.

**Example of Approximate Stress Analysis.**—We shall make an approximate analysis of the stresses in the standard aluminum-alloy propeller shown in Fig. 176 (Navy Bureau of Aeronautics Drawing 4412, set at 15 deg. at the 42-in. radius, giving a medium pitch). The blades have standard propeller sections based on the R.A.F.-6 airfoil (Fig. 19). The blade widths, thicknesses,

and angles are given in the first part of Table IV. The centers of gravity of all of the blade sections lie on a straight radial line perpendicular to the axis of rotation, and so, neglecting deflection in operation, there are no bending moments due to centrifugal force. The areas and the locations of the centers of gravity of the standard (R.A.F.-6) propeller sections may be found from Fig. 155.

We shall analyze the stresses for the case where the propeller is absorbing 170 brake hp. at 1,700 r.p.m. and 82 m.p.h.

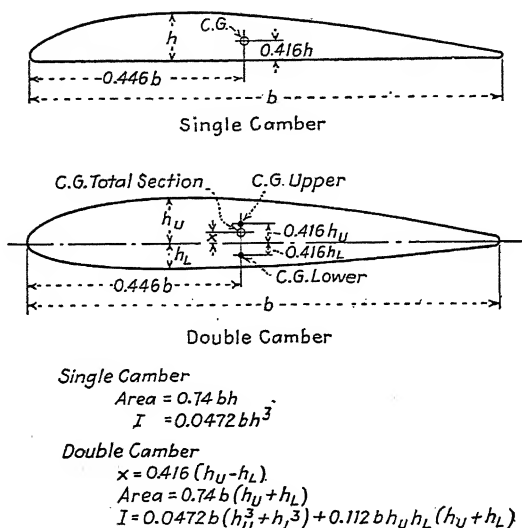


FIG. 155.—Centers of gravity, areas, and moments of inertia of standard propeller sections based on R.A.F.-6 (see Fig. 19).

For the section at  $0.45R$  the cross-sectional area (Fig. 155) is

$$\begin{aligned} A &= 0.74 bh_u \\ &= 0.74 \times 7.25 \times 0.86 \\ &= 4.62 \text{ sq. in.} \end{aligned}$$

The centrifugal force per foot radius is

$$\begin{aligned} \frac{d(CF)}{dr} &= \frac{12rAw}{g} \left( \frac{2\pi \times \text{RPM}}{60} \right)^2 \\ &= \frac{12 \times 2.01 \times 4.62 \times 0.101}{32.2} \left( \frac{2\pi \times 1,700}{60} \right)^2 \\ &= 11,100 \text{ lb. per ft.} \end{aligned}$$

The centrifugal force per foot radius is found in like manner for all of the sections and is plotted against radius in Fig. 156. The area under the curve from any section to the tip, proper consideration being given the scales, represents the total centrifugal force acting on the section. This area for the 0.45R or

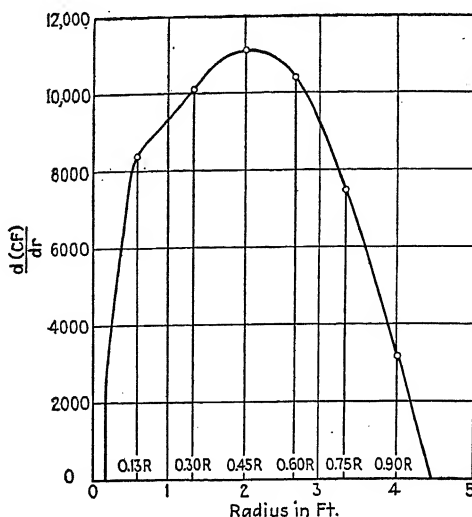


FIG. 156.—Centrifugal-force loading curve.

2.01-ft. section, as found by means of a planimeter, is 8.86 squares, and the centrifugal force acting on the section is

$$\begin{aligned} CF &= 2,000 \times 8.86 \\ &= 17,700 \text{ lb.} \end{aligned}$$

The uniform tensile stress due to the centrifugal force is then

$$\begin{aligned} S_t &= \frac{CF}{A} \\ &= \frac{17,700}{4.62} \\ &= 3,830 \text{ lb. per sq. in.} \end{aligned}$$

The thrust and torque grading curves for one blade of the propeller are shown in Fig. 157, having been computed by means of the blade-element theory and modified slightly to agree with

an actual full-scale test on the propeller operating under the given conditions in the N.A.C.A. Propeller Research Tunnel at Langley Field. From the thrust and torque, the resultant unit

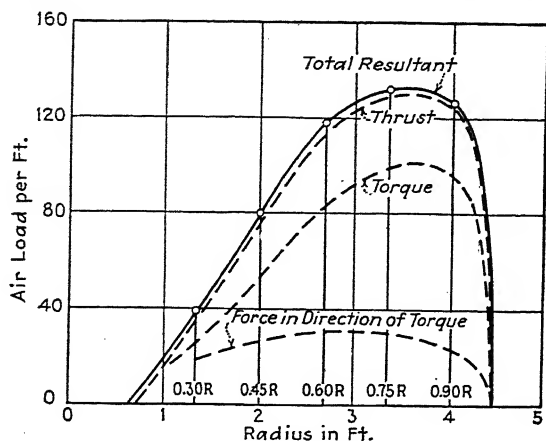


FIG. 157.—Air-loading curves.

air load is found at each section, and this is also shown in Fig. 157.

The shear at each section is then found from the area under the curve of the resultant air loading. For the section at  $0.45R$

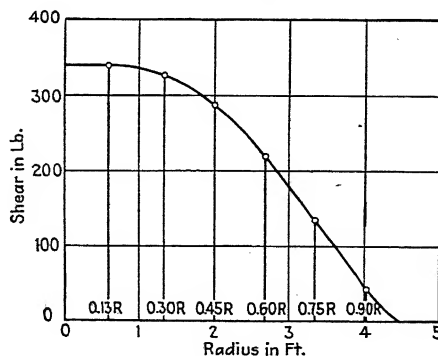


FIG. 158.—Shear curve.

this area is 7.18 squares and the shear is  $40 \times 7.18 = 287$  lb. The shear for each section is then plotted against radius (Fig. 158), and the integration of this curve gives the bending moment. Thus for the  $0.45R$  section, the area under the shear curve

between  $0.45R$  and  $R$  is 3.58 squares, and the bending moment at  $0.45R$  due to the air load is

$$\begin{aligned} M &= 100 \times 3.58 \\ &= 358 \text{ ft.-lb.} \\ &= 4,290 \text{ in.-lb.} \end{aligned}$$

From Fig. 155,

$$\begin{aligned} y_t &= 0.416h_u \\ &= 0.416 \times 0.86 \\ &= 0.36 \text{ in.} \end{aligned}$$

and

$$y_c = 0.50 \text{ in.}$$

Also, from Fig. 155,

$$\begin{aligned} I &= 0.0472 bh_u^3 \\ &= 0.0472 \times 7.25 \times 0.86^3 \\ &= 0.217 \text{ in.}^4 \end{aligned}$$

The maximum stresses at the  $0.45R$  section due to the bending moment caused by the air load are

$$\begin{aligned} S_t &= \frac{1.3 My_t}{I} \\ &= \frac{1.3 \times 4,290 \times 0.36}{0.217} \\ &= 9,250 \text{ lb. per sq. in.} \end{aligned}$$

and

$$\begin{aligned} S_c &= \frac{My_c}{I} \\ &= \frac{4,290 \times 0.50}{0.217} \\ &= 9,900 \text{ lb. per sq. in.} \end{aligned}$$

The total maximum tensile stress at the section, which occurs on the face near the leading edge, is then

$$\begin{aligned} S_t &= S_t \text{ (bending)} + S_t \text{ (centrifugal)} \\ &= 9,250 + 3,830 \\ &= 13,080 \text{ lb. per sq. in.,} \end{aligned}$$

and the total maximum compressive stress at the section is

$$\begin{aligned} S_c &= S_c \text{ (bending)} - S_t \text{ (centrifugal)} \\ &= 9,900 - 3,830 \\ &= 6,070 \text{ lb. per sq. in.} \end{aligned}$$

The maximum tensile stress at each section is plotted as curve 1 in Fig. 159, showing that the maximum for the whole blade occurs at the  $0.45R$  section.

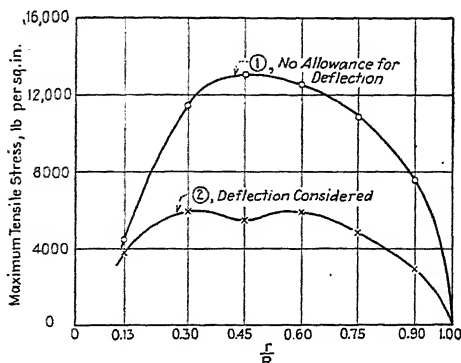


FIG. 159.—Maximum tensile stress at each section.

**The Effect of Deflection on the Stresses.**—The centers of gravity of the sections of this propeller all lie on a straight radial line perpendicular to the axis of rotation, so that if the deflection of the blades under load is neglected, and this has been the accepted practice and was done in our example above, there are in this case no bending moments due to centrifugal force.

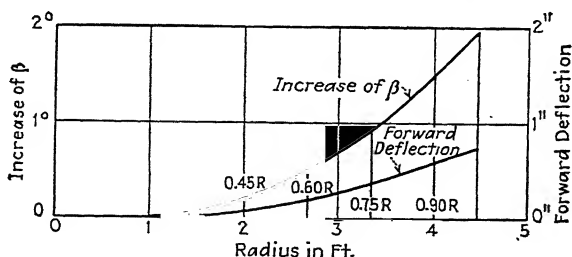


FIG. 160.—Deflection of propeller in operation.

With the propeller operating under the above conditions (*i.e.*, 170 hp., 1,700 r.p.m., and 82 m.p.h.) in the Propeller Research Tunnel, however, both a forward deflection and a twist were measured, as shown in Fig. 160. The change of blade angles affects the pitch (this was allowed for in the thrust and torque computations) and the forward deflection brings in bending moments due to centrifugal force which are opposed to the air-

TABLE IV.—COMPUTATIONS FOR STRESS ANALYSIS OF STANDARD ALUMINUM-ALLOY PROPELLER, NEGLECTING DEFLECTION

## Bu-Aero Propeller 4412

$D = 8 \text{ ft. } 11 \text{ in.}$	Hp. = 170	R.p.m. = 1,700			M.p.h. = 82	
$r/R$ .....	0.133	0.30	0.45	0.60	0.75	0.90
$r$ (ft.).....	0.594	1.34	2.01	2.68	3.34	4.02
$b$ (in.).....	3.87	7.00	7.25	6.88	5.71	3.90
$h_T$ (in.).....	Circular section	1.22	0.86	0.64	0.44	0.23
$h_L$ (in.).....	.....	0	0	0	0	0

## Centrifugal Force Loads

$$\frac{d(CF)}{dr} = 12Ar \frac{v}{g} \left( \frac{2\pi N}{60} \right)^2 = Ar \times \frac{12 \times 0.101}{32.2} \left( \frac{2\pi \times 1,700}{60} \right)^2$$

$$= 1,195 Ar$$

$A = 0.74bh_u$ .....	11.78	6.32	4.62	3.26	1.86	0.66
$Ar$ .....	7.00	8.46	9.29	8.74	6.21	2.65
$d(CF)/dr$ .....	8,350	10,100	11,100	10,420	7,430	3,160
C. F. (lb.).....	32,200	25,100	17,700	10,500	4,500	780

## Air-load Bending Moments

Thrust per ft. (lb.).....	0	34.0	75.5	113.7	128.8	124.8
Torque per ft. (ft.-lb.)..	0	26	53	83	99	96
Torque force, per ft., (lb.).....	0	19	26	31	30	24
Resultant air load, per ft., (lb.).....	0	39	80	118	131	127
Shear (lb.).....	340	327	287	220	135	44
$M$ (in.-lb.).....	9,840	6,830	4,290	2,270	828	108

## Stresses

$y_t$ (in.).....	1.94	0.51	0.36	0.27	0.18	0.10
$y_c$ (in.).....	1.94	0.71	0.50	0.37	0.26	0.13
$I$ (in. <sup>4</sup> ).....	11.08	0.600	0.217	0.085	0.023	0.0022
$S_t$ , bending.....	1,720	7,540	9,250	9,370	8,400	6,400
$S_c$ , bending.....	1,720	8,100	9,900	9,900	9,300	6,400
$S_t$ , direct centrifugal...	2,730	3,970	3,830	3,220	2,420	1,180
$S_t$ , total.....	4,450	11,510	13,080	12,590	10,820	7,580
$S_c$ , total.....	.....	4,130	6,070	6,680	6,880	5,220



force bending moments; thus the stresses are actually lower than the values found by assuming no deflection.

The unit bending moment at the  $0.45R$  section due to the centrifugal loading at the  $0.60R$  section is the loading at the latter section (Table IV) multiplied by the difference in forward

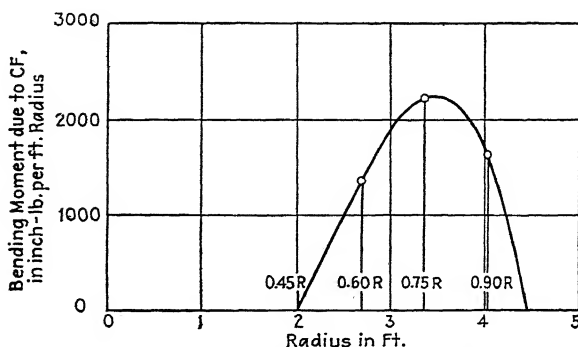


FIG. 161.—Bending moment at  $0.45R$  due to centrifugal force.

deflection at the two sections (it being assumed that the forward deflections are the same as those in the assumed plane of the resultant air loading), or

$$\begin{aligned}\frac{dM'}{dr} &= \frac{d(CF)}{dr} (\text{deflection at } 0.60R - \text{deflection at } 0.45R) \\ &= 10,420 (0.20 - 0.07 \text{ in.}) \\ &= 1,355 \text{ in.-lb. per ft. radius.}\end{aligned}$$

This is plotted in Fig. 161 along with the corresponding values for the  $0.75R$  and  $0.90R$  sections, and the area under the curve represents the total bending moment at the  $0.45R$  section due to centrifugal force. The area is 3.55 squares, and the bending moment at the  $0.45R$  section due to centrifugal force is

$$\begin{aligned}M' &= -1,000 \times 3.55 \\ &= -3,550 \text{ in.-lb.}\end{aligned}$$

The value is negative because it is opposite to the air-load bending moment, which was taken as being positive. The bending moments due to centrifugal force have been found in like manner for the other sections and are given in Table V, along with the moments due to the air load.

TABLE V.—STRESSES CONSIDERING DEFLECTION

$r/R$ .....	0.133	0.30	0.45	0.60	0.75	0.90
$M$ , air load.....	9,840	6,830	4,290	2,270	828	108
$M'$ , centrifugal.....	-5,050	-5,050	-3,550	-1,610	-590	-78
$M + M'$ .....	4,790	1,780	740	660	238	30
$S_b$ , bending.....	840	1,960	1,600	2,720	2,420	1,780
$S_c$ , bending.....	840	2,110	1,710	2,880	2,670	1,780
$S_t$ , direct centrifugal.....	2,730	3,970	3,830	3,220	2,420	1,180
$S_t$ , total.....	3,570	5,930	5,430	5,940	4,840	2,960
$S_c$ , total.....					250	600

The maximum tensile stress at  $0.45R$  due to bending is now found to be

$$\begin{aligned}
 S_t &= \frac{1.3(M + M')y_t}{I} \\
 &= \frac{1.3(4,290 - 3,550) \times 0.36}{0.217} \\
 &= 1,600 \text{ lb. per sq. in.}
 \end{aligned}$$

as compared with 9,250 lb. per sq. in. when the deflection was neglected. Thus it is obvious that neglecting the deflection gives an entirely erroneous idea of the bending stress, and in this case a value of the tensile stress which is several hundred per cent too great, and an apparent compressive stress along the whole blade with a value as high as 6,880 lb. per sq. in., while when the deflection is considered there is no compressive stress except for a negligible quantity near the tip (Table V). Curve 2 of Fig. 159 shows the total maximum tensile stress found along the blade when the deflection is taken into account. It will be noted that the maximum is about 6,000 lb. per sq. in., less than half of that found when the deflection was neglected. In the propeller under consideration, therefore, and the same applies to most propellers, it is hopeless to get even a reasonably accurate approximation to the actual stresses without a fairly accurate knowledge of the deflections under load.

The fact that the forward deflection of the blades in operation reduces the bending stresses suggests the possibility of eliminating the bending stresses entirely by so inclining the blade to start with that the bending moments due to centrifugal force just balance those due to the air load. This can be done for one set of operating conditions (*i.e.*, one value of  $V/nD$ ) only, but if average conditions are taken the stresses in the propeller can be

substantially reduced, and clever designers have for years taken advantage of this fact. It is more important with thick rigid propellers than with relatively thin and flexible propellers which tend to take the proper inclination when operating.

These stresses were found for the propeller turning 1,700 r.p.m. which corresponds to a tip speed of 795 ft. per sec. Since the stresses vary as the square of the tip speed (at constant  $V/nD$ ), and since the fatigue limit of the aluminum alloy used is in the neighborhood of 12,000 to 15,000 lb. per sq. in., it should be safe according to the stress analysis to run geometrically similar propellers at the same  $V/nD$ , at tip speeds up to about

$$795 \sqrt{\frac{12,000}{6,000}} = 1,125 \text{ ft. per sec.,}$$

which corresponds to about 2,400 r.p.m. with our particular 8 ft. 11-in. propeller. Actually, due partly to the fact that the air load fluctuates, partly to the fact that vibrations may increase the stresses, and partly to the questionable accuracy of the stress analysis, the safe limit for indefinitely long operation is probably somewhat less than the tip speed of 1,125 ft. per sec. indicated.

The stress analysis of our example was made under the condition of full-throttle climbing flight. At higher full throttle air speeds the revolutions, and consequently the centrifugal force, would be higher, but the air load would be lower, while at lower speeds the reverse is true. The maximum calculated stresses are therefore not ordinarily greatly different at the various full-throttle speeds, although the case of full power at zero advance seems the most severe in practice.

**Flutter and Weave of Propeller Blades.**—Flutter is a form of severe vibration of the propeller blades. It is usually considered a torsional vibration in which the blade angles increase and decrease rapidly, but it may be connected with bending, for fore-and-aft deflections are ordinarily accompanied by a change of angle also. Flutter is accompanied by an unpleasant increase in noise which is sometimes of a rapid hammering nature. It sometimes sets up uncomfortable pulsations in the air for some little distance from the propeller. Both tests and practical experience show that severe flutter is accompanied by a sufficiently great stress, or variation of stress, to cause failure if

Weave is a form of comparatively slow waving backward and forward of the propeller blades while turning. It is much less severe than flutter but is also accompanied by a stress variation of some magnitude. This is apparent from our stress-analysis example, in which a forward deflection of about  $\frac{1}{2}$  in. at the tip changed the maximum fiber stress from 13,080 to 6,000 lb. per sq. in. A weaving motion of only  $\frac{1}{8}$ -in. total amplitude would therefore be accompanied by a change in stress in the neighborhood of 1,500 to 2,000 lb. per sq. in. in this propeller.

There are also vibrations other than those associated with flutter and weave. Propellers, like all elastic bodies, have natural periods of vibration, and the vibrations may build up to alarming proportions if the natural frequency corresponds to some frequency of impulse of the engine or airplane, such as that of the torque impulses. The natural frequency of geometrically similar propellers has been found by both theory and experiment<sup>1</sup> to vary inversely as the diameter. If the frequency of the propeller and that of the torque vibrations coincide, a propeller of smaller diameter might be used, in which case if the diameter were small enough the vibration frequency would be above the range of the torque impulses, thus preventing resonance.

Vibrations are also caused by (1) unbalance of the centrifugal and air loads which is present if one blade is heavier than the other and the propeller does not balance statically, or if angles and shape of both blades are not the same so that one blade carries more air load than the other or others; (2) periodically varying air loads which occur because of unsymmetrical air flow about the axis of rotation due to the proximity of unsymmetrical fuselages, wings, and landing gears;<sup>2</sup> (3) periodically varying air loads due to the inclination of the axis of rotation to the flight

<sup>1</sup> The investigation of vibration periods was made by the Army Air Corps at McCook Field, Dayton, Ohio.

<sup>2</sup> One particularly bad case of periodic fluctuation of the air load has been found in large airplanes having three side-by-side engines, the center engine being located somewhat ahead of the two wing engines, and the wing-engine propellers operating partly in the slipstream of the center engine. Even if the overlapping is not large, severe pulsations are set up in the side propellers when they get into phase with the center propeller, and few propellers last long under such conditions, micarta being about the best because of the combination of high fatigue limit with homogeneity. Other cures for the situation have been to use a three-bladed center propeller and two-bladed

path, particularly in climbing flight, for as a blade goes up it has a smaller angle of attack than normal and as it goes down it has a larger one; (4) irregular variations of the air, such as gusts.

Since the propeller axis is seldom exactly parallel with the direction of flight, and also since the air is seldom free from gusts and currents, propellers practically always operate under more or less fluctuating loads, and therefore the fatigue limit of the material should not be exceeded even by the peak stresses if a propeller is to run indefinitely without failure. Unfortunately with present methods it is not possible to calculate the stress fluctuations, propellers usually being designed so that the calculated stresses are well under the fatigue limit. The only final criterion of strength is actual operation over an extended period of time, although a fairly satisfactory substitute is an overload whirling test for a period of several hours. After propellers of a certain form have been thoroughly tested and their real strength and endurance are known, it is fairly safe to apply the ordinary stress analysis to new propellers of generally similar form, but it cannot be applied with any assurance to new forms.

**Fatigue Failures.**—Most of the few failures of conventional forms of aluminum-alloy propellers are fatigue failures which started at some flaw or irregularity in the surface. It is well known that fatigue failures due to fluctuating stresses are likely to start in cracks or irregularities, such as sharp internal corners, even though the actual stresses are very low. Figure 162 shows an example of fatigue failure in the blade root of an aluminum-alloy propeller caused by a sharp internal corner just outside the steel hub. The blade had been hand filed to fit a hub to which it did not belong, and a small but sharp internal corner was left in it. The failure started as a crack (at top of the photograph) which gradually worked its way in toward the middle until the effective area was reduced to a point where the centrifugal force pulled the blade off. It will be noticed that at the top of the picture the metal is bright, due to rubbing. The hole in the center was filled with lead for purposes of balance.

Even lettering stamped on a propeller blade has caused complete failure due to the notch effect in the surface. The surface of all propeller blades should be smooth and fair with no sharp curvatures along the blades and no irregularities of any kind.

Since fatigue failures start as small cracks which gradually

propellers after every 100 hr. or so of service and to examine them for cracks. The blades are swabbed with, or preferably immersed in, a 10 to 20 per cent solution of commercial caustic soda of the same temperature as the propeller, for from two to six minutes. They are then rinsed in water and swabbed with or immersed in a 5 per cent solution of nitric acid until bright, after which they are thoroughly washed with water and dried. The surface is carefully inspected for cracks, preferably with a low-power

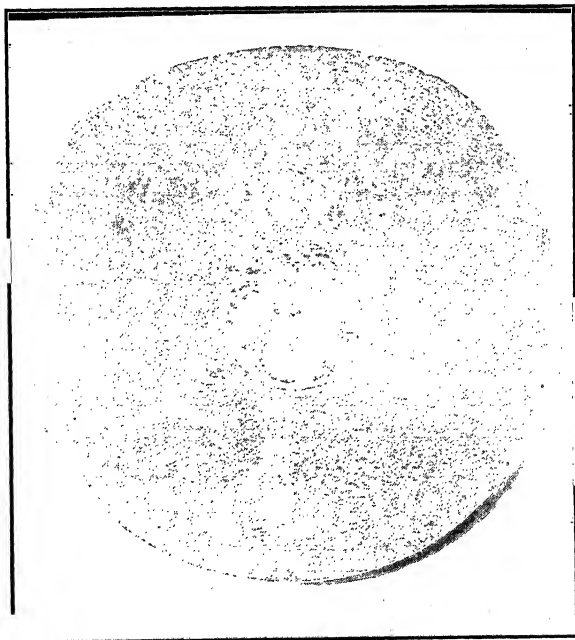


FIG. 162.—Example of fatigue failure in blade root of aluminum-alloy propeller.

magnifying glass. At any cracks or flaws found the surface is sanded off a little and given a deeper local etch. Small longitudinal seams which are rolled into the material are not important, but cracks across the blade which penetrate under the surface are usually a sign of impending fatigue failure and are cause for rejection.

**Failures of Wood Propellers.**—Good propeller woods have great toughness, and the fatigue limit is very near to the ultimate strength. Practically no wood propellers of reasonably normal form fail in direct tension or compression, and of those few that

do, the failure can usually be traced to a poor grade of material. Wood is not so uniform in its properties as metal, and it is not so easily tested, so that occasionally even with rigorous inspection some poor wood will creep in.

Usually wood propellers fail by the blade splitting longitudinally near the tip. Because of their grain structure, wood propellers are weak in torsion, and so large twisting moments should be avoided. Flutter in wood propellers will nearly always cause longitudinal splitting if continued long enough. A slight amount of sweepback has been found to make for smooth running without flutter and is usually used with wood propellers.

If wood propellers are thick and heavy enough to be reliable and hold their shape under various weather and operating conditions, and also to withstand normal handling, they are usually sufficiently strong for ordinary requirements with tip speeds up to about 900 ft. per sec.

**Destructive Whirling Tests.**—Due to the effect of flutter and fluctuating air loads, as well as to the complicated nature of the stresses in propellers and the inability to calculate them with a reasonable assurance of accuracy, the only real criterion of propeller strength and endurance is actual operation and use. This not only takes considerable time under ordinary operating conditions, but also it may be highly dangerous since a serious propeller failure in flight, in which either one whole blade or a substantial part of a blade breaks off, always results in the remaining unbalanced force tearing the whole or a large part of the engine completely out of the aircraft.

It has therefore been the practice to test the strength and endurance of propellers by whirling them by means of electric motors in armored stands or on an oversized gasoline engine. The stands for the electric motors are usually completely enclosed to the ground, making the air flow past the propeller unsymmetrical, the propeller consequently being subjected to a fluctuating air load. Instead of testing a propeller for several hundred hours at the maximum power for which it is designed, it is whirled at an overload for a shorter period of time. The usual test is ten hours without failure of any kind at 100 per cent power overload for metal propellers and at 50 per cent power overload for wood propellers. If the propeller develops a violent flutter at any speed, it is run for an additional ten hours at that speed.

Nearly all of the electric whirling tests made in this country have been made by the Army Air Corps at Dayton, Ohio. New whirling equipment is now being completed at Wright Field near Dayton, on which propellers up to 40 ft. in diameter can be tested while absorbing up to 6,000 hp., and ordinary-sized propellers can be turned as high as 5,000 r.p.m.

If propellers are whirled with an oversized airplane engine, the requirement is usually ten hours at 75 per cent power overload for metal propellers and 40 per cent for wood propellers.





## CHAPTER XVI

### SUMMARY OF FACTORS TO BE CONSIDERED IN THE DESIGN OF A PROPELLER

Before undertaking the actual design of a propeller to give a certain performance, it is well to summarize the pertinent factors which have been considered in detail in the previous chapters.

**Particular Airplane Performance Desired.**—As shown in Chap. X, an airplane will have somewhat different performance characteristics if equipped with different propellers of the same geometric form, the diameter and pitch only being varied in such a manner that the revolutions at maximum speed remain the same. A certain combination of diameter and pitch will give the highest maximum speed, and certain others will give the best climb, angle of climb, take-off, cruising economy, etc.

**High Speed.**—Ordinarily the design of a propeller for a racing airplane represents the simplest and most straightforward case, for the only requirement is that the propeller should be that giving the highest possible propulsive efficiency at the maximum speed condition. In most cases the performance in take-off and climb will be reasonably satisfactory. There have been a few cases, however, in which racing seaplanes have been unable to leave the water with propellers designed to give the maximum possible speed. The condition is difficult, for with engines delivering over 1,000 hp., the propeller must turn at a reasonably low revolution speed to avoid a high tip-speed loss, and with airspeeds of over 300 m.p.h., a very high-pitch propeller is required, resulting in a very low static thrust and poor take-off qualities. The best solution of the propeller phase of the problem, assuming that the revolutions are fixed and that a fixed-pitch propeller is to be used, is probably to increase the diameter and blade-width ratio and decrease the pitch as much as is necessary to get a satisfactory take-off.

**Rate of Climb.**—The propeller giving the highest rate of climb, if it is one of a family of given form, can be selected by calculating the performance for a series of pitches and diameters, each hold-

ing the engine to the same full-throttle revolutions at maximum speed, as was done in Chap. X for a series of metal and a series of wooden propellers. With the relatively thin-bladed metal propellers the pitch and diameter giving the maximum rate of climb are approximately the same as those giving the greatest high speed. All combinations of pitch and diameter throughout quite a large range will, however, give very nearly the same rates of climb.

With the thicker wood propellers the best climbing propeller is not the one which also gives the greatest speed but is one having a considerably larger diameter and smaller pitch. In our example of Chap. X, the wooden propeller giving the greatest rate of climb would have had a pitch-diameter ratio of about 0.56 and a value of  $V/nD$  at high speed of about 0.65, from which

$$1 - S = \frac{V/nD}{P/D} = \frac{0.65}{0.56} \\ = 1.16,$$

and the nominal slip  $S$  would have a negative value of 16 per cent. A negative slip of 10 per cent would give practically the same climb, and this value may be taken as an approximate one to which good climbing wooden propellers of ordinary pitch ratios may be designed.

*Take-off and Angle of Climb.*—Good take-off characteristics and a steep angle of climb are of great importance, and in practically all commercial and the majority of military airplanes, these characteristics overshadow the rate of climb. In fact, when a "good climbing propeller" is ordered, what is almost always desired is a propeller which will give a short take-off run and a steep angle of climb and not a high rate of climb. It happens that with both wood and metal propellers, the ones having the largest diameters and the lowest pitches which will give a reasonable high speed give both the quickest take-off and the greatest angle of climb.

*Cruising Speed.*—The propeller which will give the highest cruising speed is within all practical limits the same as that giving the highest full-throttle speed in level flight. This is due to the fact that as the motor is throttled in level flight, the air speed is reduced in very nearly the same proportion as the revolutions. In fact, if the maximum speed and revolutions of an airplane are known, the cruising speed at any revolution speed is

easily and quite accurately obtained from the relation that a 10 per cent decrease in revolutions results in an 11 per cent decrease in air speed, a 20 per cent decrease in revolutions resulting in a 22 per cent decrease in air speed. The propeller in cruising flight therefore works at about the same values of  $C_s$  and  $V/nD$  as it does at maximum speed, and with the revolutions at maximum speed fixed, the propeller giving the highest full-throttle speed will also give the highest cruising speed at any particular revolutions.

*All-around Performance.*—If, as is ordinarily the case, good take-off and angle of climb are considered as having about equal importance with high maximum and cruising speeds, a compromise or general service propeller is selected. This will of course have a larger diameter and smaller pitch than the best high-speed propeller but a smaller diameter and greater pitch than the propeller giving the shortest take-off and the steepest climb. Fortunately a propeller about halfway between the two extremes will give a speed very nearly as high as the best high-speed propeller and at the same time give a take-off nearly as short as the best take-off propeller. The compromise or general service propeller, whether of wood or metal, may be taken as being the one which operates at its maximum or peak efficiency at the high-speed condition of flight. The efficiency here referred to is the propulsive efficiency of the full-scale propeller operating with body interference. With wood propellers this peak efficiency usually occurs at a nominal slip value between zero and negative 5 per cent, while with metal propellers it comes between zero and positive 10 per cent.

*Special Performances.*—For special performances not mentioned above, such as high-altitude flying with a supercharged engine, no simple general rules are available and it is usually preferable to calculate the performance with a series of at least three propellers, as was done in Chap. X, and then choose the best.

The above discussion has applied only to airplane propellers. The problem of designing propellers to give maximum performance on lighter-than-air craft is simpler, for only the high-speed condition need be considered. In this case, where there is no induced drag due to dynamic lift to be considered, the forward speed varies directly with the revolutions when the engines are throttled, so that the propeller works at exactly the same values

of  $C_s$  and  $V/nD$  at all steady speeds. The best high-speed propeller is therefore the best at all throttled speeds. If thin metal propellers are used the same propeller is also the best, even though some of the engines on an airship are shut down and the ship is cruised with the remaining ones running at or near full throttle, as is sometimes done to improve the fuel economy.

**Limitations Imposed by Airplane and Engine.**—The diameter of a propeller is often limited by insufficient ground clearance, interference with a part of the structure such as a seaplane float, or interference with another propeller or its slipstream on a multi-engined airplane. The present Department of Commerce requirement for ground clearance on a landplane is 9 in. in flying position, and on a seaplane the propeller is required to have 18 in. clearance from the surface of the water. One inch is given as the minimum allowable distance between the propeller tips and a body such as a fuselage, boat hull, or float, and more is desirable. In cases where propellers are operating side by side in the same plane with no body between them, they should clear each other by a minimum of about 6 in.

Where side propellers are located somewhat to the rear of a center propeller, as is usually the case with airplanes having three engines, care should be taken that they have sufficient clearance to be essentially free of the slipstream of the front propeller. If there is an appreciable amount of overlap the blades of the side propellers are subjected to a severe periodic fluctuation of air load which is almost certain to cause failure sooner or later. In this connection it should be remembered that although the slipstream of an isolated propeller necks down behind the plane of rotation, the center propeller is likely to be working on the nose of a rather large body which actually spreads the slipstream somewhat. It is therefore desirable that the projected propeller discs have a few inches' clearance between them.

In the cases where the diameter is limited, there are several courses which may be followed. If take-off is not of great importance, a small high-pitch high-speed propeller may be satisfactory. If take-off is important it may be advisable to use a propeller with extra-wide blades or, in extreme cases, with three or four blades.

**Choice of the Number of Blades.**—Two-bladed propellers are used in all ordinary cases, for the fewer the blades the lighter,

cheaper, simpler, and more efficient will be the propeller; and two is the smallest number of blades with which proper balance of mass and air forces can be obtained. Three or four blades are used if the diameter is limited to a size where a two-bladed propeller is unsuitable, or in cases where the operation is not smooth with a two-bladed propeller due to unsymmetrical body interference or the slipstream of another propeller. If there is an unsymmetrical airflow through a two-bladed propeller, ordinarily one blade is at its highest angle of attack and load at the same time that the other is at its lowest, and this is likely to cause undesirable vibrations. With three or more blades the uneven load distribution is spread more evenly around the propeller disc and the vibrations are greatly reduced. Vibrations are also set up in two-bladed propellers when the airplane is turning, due to the varying gyroscopic moment of the two-bladed arrangement and, when the airplane is sideslipping, due to the uneven air loading. These effects are too small to be noticed in ordinary installations, but with very large and slowly turning geared propellers the pulsations may become so great as to necessitate the use of three or more blades, which will remedy the situation. Vibration difficulties considered, it is usually advisable to have three or more blades in the rear propellers of tandem series, in large geared propellers, in propellers operating very close to a body which is far from symmetrical about the axis of rotation, and in propellers which operate partially in the slipstream of other propellers.

Metal propellers are seldom made with more than three blades, but wooden propellers are usually made with either two or four, due to the ease of construction.

**Résumé of Factors Affecting Propulsive Efficiency.**—In order to collect the various factors, such as the geometric proportions of propellers, which are directly connected with the propulsive efficiency, the important ones are given briefly here.

**Pitch Ratio.**—For a series of propellers differing only in pitch, the maximum or peak efficiencies become greater as the pitch is increased, within the range of present-day aircraft practice. Since the propeller must operate reasonably near its peak efficiency range at the maximum speed of the airplane, the pitch depends largely on the relative values of the maximum air speed, the revolutions, and the power absorbed by the propeller, all of which are conveniently combined in the coefficient  $C_p$ .

The higher the value of  $C_s$ , again within the range of present-day practice, the greater is the maximum possible efficiency obtainable.

After the speed, power, and revolutions are fixed, and these are usually fixed by the airplane and engine designers, the propeller designer still may select from a fairly large pitch range to stress the particular kind of airplane performance desired, as outlined in the foregoing sections on performance.

*Pitch Distribution.*—If the pitch of a propeller operating on a body is smaller near the hub than at the tip, a somewhat higher propulsive efficiency is obtained than if the pitch is uniform over the entire blade. The maximum difference is of the order of three or four per cent with average metal propellers.

*Blade Width and Number of Blades.*—The total width of all the blades of a propeller is the critical factor affecting the performance, regardless of the number of blades or the width of each. Thus a four-bladed propeller will have the same performance as an otherwise similar two-bladed propeller if the blades of the two-bladed one are twice as wide, making the total width the same. With blades of average width ( $WR = 0.053$ ), the maximum efficiency of a two-bladed propeller is ordinarily about 3 per cent greater than that of a three-bladed propeller of the same diameter and about 7 per cent greater than that of a four-bladed one. A two-bladed propeller having extremely narrow blades ( $WR = 0.02$ ) is about 2 per cent more efficient than the average one. These differences are somewhat less for high-pitch propellers and greater for low-pitch propellers. Also, they are slightly greater at the climbing range than at the high-speed or maximum efficiency range.

The above values are for propellers of the same diameter and pitch. Actually if a four-bladed propeller replaces a two-bladed propeller on the same airplane and engine, it will have about the same pitch but a smaller diameter and consequently a higher pitch ratio. This higher pitch ratio is accompanied by an increase in maximum efficiency which partly offsets the decrease due to the greater width ratio.

*Thickness Ratio.*—Ordinary aluminum-alloy propeller blades have thickness ratios about one-half as great as those of ordinary wood propellers, and if the R.A.F-6 type sections are used, the thinner metal propellers are from 4 per cent (with high pitches) to 7 per cent (with low pitches) more efficient than the wooden

ones. If Clark-Y type sections are used the effect of thickness is less pronounced.

*Blade Section.*—Of the two airfoil sections most commonly used in propellers, the Clark-Y type gives somewhat better efficiencies at low angles of attack while the R.A.F-6 type is superior at high angles of attack. This gives the Clark-Y type an advantage in low-pitch propellers in which high angles of attack are not reached but gives the R.A.F-6 type an advantage in high-pitch propellers with which it has a much better take-off and climbing efficiency. Also, in the high-pitch propellers the maximum efficiencies are practically the same with either type of section. All-around performance being considered, it may be said that the Clark-Y type sections are better with low-pitch propellers while the R.A.F-6 type are better with high-pitch propellers.

*Plan Form.*—If the blades are given some taper and the tip is rounded, the exact shape or degree of taper has no appreciable effect on the propulsive efficiency. The same is true of sweep-back and rake or forward tilt.

*Tip Speed.*—Ordinary thin-bladed aluminum-alloy propellers can be operated at tip speeds up to about 1,000 ft. per sec. without loss of propulsive efficiency, but as the tip speed exceeds this critical value the efficiency drops off very rapidly. With the thicker wooden propellers the critical speed is lower and the loss above it greater.

*Body Interference.*—The propulsive efficiency, which includes the increase of body drag due to the propeller as well as the effect of the body on the propeller, ranges for ordinary bodies from the same as to about 7 per cent less than the efficiency of the isolated propeller. For most bodies the value is about 2 or 3 per cent. Roughly, the lower the drag of the body the worse will be the effect on the propulsive efficiency. It is advantageous to have a large propeller diameter with respect to the mean body diameter, and for the average case it may be said that the propulsive efficiency increases about 1 per cent for an 8 per cent increase of the ratio of the propeller diameter to the body diameter.

*Strength.*—One of the most important and difficult problems in designing a propeller of a new shape or form of construction is to establish thoroughly its ability to operate indefinitely without failure. This usually requires careful stress analyses and overload whirling tests. With geometrically similar propellers of

proved form, however, since the stresses vary as the square of the tip speed regardless of the size, a limiting tip speed can be found below which any propeller of the family can be operated safely. This may even be applied to different pitch settings with reasonable accuracy if the actual tip speed at maximum air speed is used, and not merely the tip speed in the plane of rotation. For the commonly used family of aluminum-alloy propellers shown in Figs. 176 and 177, the limiting tip speed below which the calculated stresses will not exceed the fatigue strength is about 1,100 ft. per sec. For ordinary routine design procedure it is more satisfactory to use the more conservative value of 1,000 ft. per sec. Thus if a propeller of this form operates under the critical tip speed for efficiency loss at the maximum speed of the aircraft, it should be safe from the strength point of view. It should also, however, operate smoothly, without flutter or excessive vibration.



## CHAPTER XVII

### DESIGN PROCEDURE, WITH CHARTS AND EXAMPLES

In this chapter a simple method of design procedure is given along with accurate working charts which may be used for the selection of metal propellers of a standard form. An approximate method is also given for using the same charts for propellers of different form. The use of the methods to select propellers for various performances is shown by means of examples.

**Information Furnished Propeller Designer.**—The primary data required for the design of a propeller are of course the correct brake horsepower, the revolutions at which that power is obtained, and the maximum air speed. One of the most difficult problems of the propeller designer has been to obtain accurate values of the power and air speed for new engines and airplanes, due partially to a lack of accurate tests on the new types and partially to the optimistic results usually expected by the makers. If the engine actually delivers less power than the propeller is designed to absorb, the propeller will hold the revolutions down to a lower value than desired, which in turn cuts down the horsepower output and consequently the airplane performance. The lower high speed obtained causes a further reduction in revolutions which tends further to reduce the speed. The same conditions occur if the airplane fails to make the speed designed for, even though the engine power is up to standard. It is therefore necessary to get accurate power and speed data if the propeller is to perform satisfactorily.

It is better to design the propeller from the power-required curve of the airplane than merely the anticipated maximum speed, for with it and the propulsive efficiency of the particular propeller designed, the power available and power required can be balanced and the high speed determined more accurately. An accurate power-required curve is not, however, ordinarily available.

One method, and usually the most satisfactory one, of finding accurate values of the power and speed is to run high-speed tests

of the airplane in question, with a propeller of known characteristics. The speed is then accurately determined over a timed course and the engine power can be calculated from the propeller characteristics.

The propeller designer should also know the kind of performance desired from the airplane, the form of the body and engine and the relative location of the propeller, and any limitations, such as the maximum permissible diameter.

**A Simple System for Selecting Propellers of a Standard Form.**—Due to the limitations imposed by the material used, including such factors as weight, strength, and satisfactory smooth operation, all propellers made of one particular material will naturally fall within a fairly small range of blade width and thickness ratios, for any ordinary performance required. Since small changes in the width and thickness ratios have no important effect on the propulsive efficiency, it is quite reasonable to give the same blade form to all ordinary propellers of a given material. Thus both the designing and manufacturing operations are greatly simplified.

A convenient method of selecting propellers of a given family to operate under any particular performance conditions is the one based on the coefficient  $C_s$ ,<sup>1</sup> which is outlined in Chap. VI.

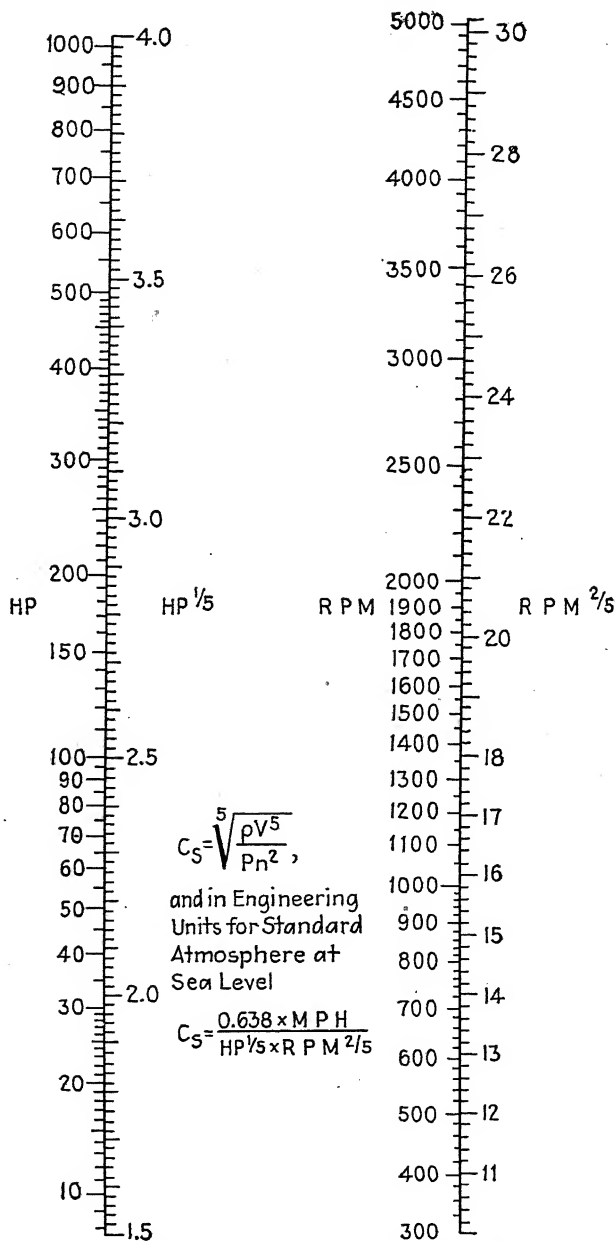
The coefficient  $C_s$  involves only the conditions under which the propeller must operate—i.e., the power, revolutions, air speed, and air density—but has no connection with the dimensions of the propeller itself. The value of  $C_s$  can, therefore, be computed from the desired performance factors alone. In engineering units and for standard sea-level density its value may be easily found from the equation

$$C_s = \frac{0.638 \times MPH}{HP^{1/3} \times RPM^{2/3}},$$

the values of  $HP^{1/3}$  and  $RPM^{2/3}$  being obtained from scales given in Fig. 163 (also Fig. 53).

Working charts, in which curves of  $V/nD$  and propulsive efficiency are plotted against  $C_s$  for even blade-angle settings, are given for a standard form of aluminum-alloy propeller operating with six different engine and fuselage combinations in

<sup>1</sup> The Eiffel logarithmic diagram is also convenient for this purpose but requires the use of simple drawing equipment.


 FIG. 163.—Scales for finding  $HP^{1/5}$  and  $RPM^{2/5}$ .

Figs. 164 to 175. These charts are drawn from full-scale wind tunnel test data published by the N.A.C.A.<sup>1</sup>

A drawing of the blade of the 9-ft. propeller used in all of the tests is given in Fig. 176, and the blade form is given in non-dimensional ratios which can be applied to any diameter, in Fig. 177. Airfoil sections based on the R.A.F.-6 are used. The various pitches were obtained by merely turning the whole blade in the hub, the pitch being approximately uniform for a pitch-diameter ratio of 0.5. As shown in Chaps. VII and IX, this

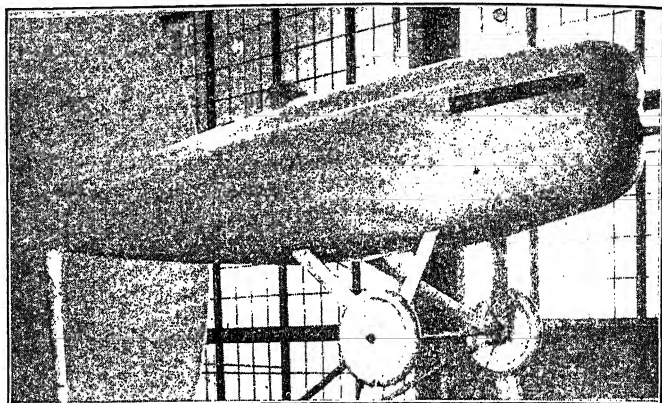


FIG. 164.—Open-cockpit fuselage with 400 hp. Curtiss D-12 engine. No radiator (corresponds to case with wing radiators). Smoothly faired nose. Maximum cross-sectional area, 11.6 sq. ft. Data in Fig. 165.

combination gives very close to the best pitch distribution for operation with an ordinary body over a large range of pitches. In fact, propellers of this standard form will give efficiencies which are within ordinary practical limits as high as can be obtained with any form capable of filling the same strength and performance requirements.

*Torsional Deflection of Blades.*—As was brought out in Chap. XV, propellers deflect and twist under load, so that the pitch of an operating propeller is often quite different from the pitch of

<sup>1</sup> Working Charts for the Selection of Aluminum-alloy Propellers of a Standard Form to Operate with Various Aircraft Engines and Bodies, by Fred E. Weick, N.A.C.A.T.R. 350, 1930. For a method of selecting wood propellers of a standard form, see Propeller Design—III: A Simple System based on Model Propeller Test Data, by Fred E. Weick, N.A.C.A.T.N. 237, 1926. Also, Simplified Propeller Design for Low-powered Airplanes, by Fred E. Weick, N.A.C.A.T.N. 212, 1925.

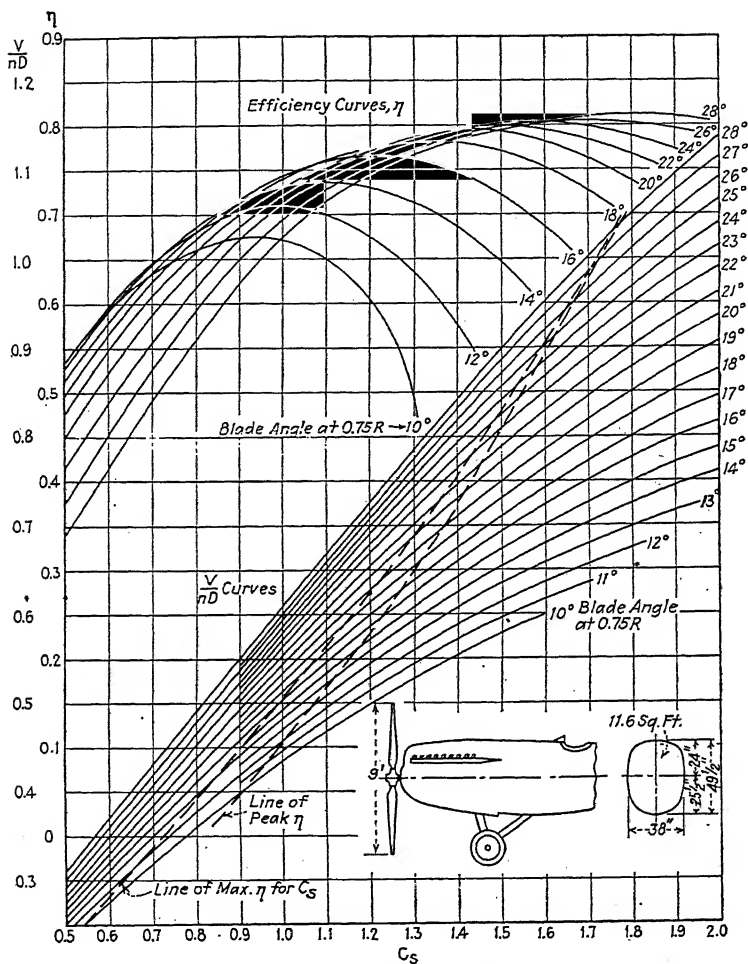


FIG. 165.—Open-cockpit fuselage with D-12 engine. Propeller 4412.

the same propeller in the static condition where there is no load. It was found in the test with the 400-hp. D-12 engine installation shown in Fig. 164 that the deflection was not sufficient to affect the propeller characteristics to an appreciable extent for powers up to 200 hp., but above that amount the power and thrust coefficient become greater for a given  $V/nD$ , and the efficiency drops off slightly. In order to make the results of the tests with all engines and bodies comparable, the tests from which the working-chart data were taken were run with the D-12 engine throttled to 200 hp., which was approximately the power of the other engines.

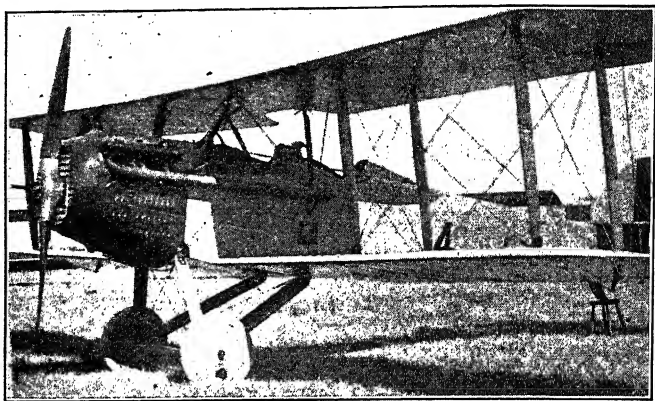


FIG. 166.—Complete VE-7 airplane with wings and tail surfaces. Open-cockpit fuselage with 180 hp. Wright E-2 water-cooled engine and nose radiator. Maximum cross-sectional area of fuselage 9.6 sq. ft. Data in Fig. 167.

The change in propeller characteristics which occurred at the higher powers can be accounted for by considering that the blades twisted to increase their pitch. This increased pitch is substantiated by the fact that the thrust and efficiency coefficients obtained with the high powers are about the same as those obtained with lower powers but at slightly higher pitch settings. Also, deflection measurements which were taken during the tests show that the blade angles increased with increase of power, but the measurements were unfortunately not sufficiently accurate to use as a basis for showing the exact variation.

Considering the variation of the propeller coefficients with power as being due entirely to deflection, the working charts can be satisfactorily used for engines of all powers if only the deflection

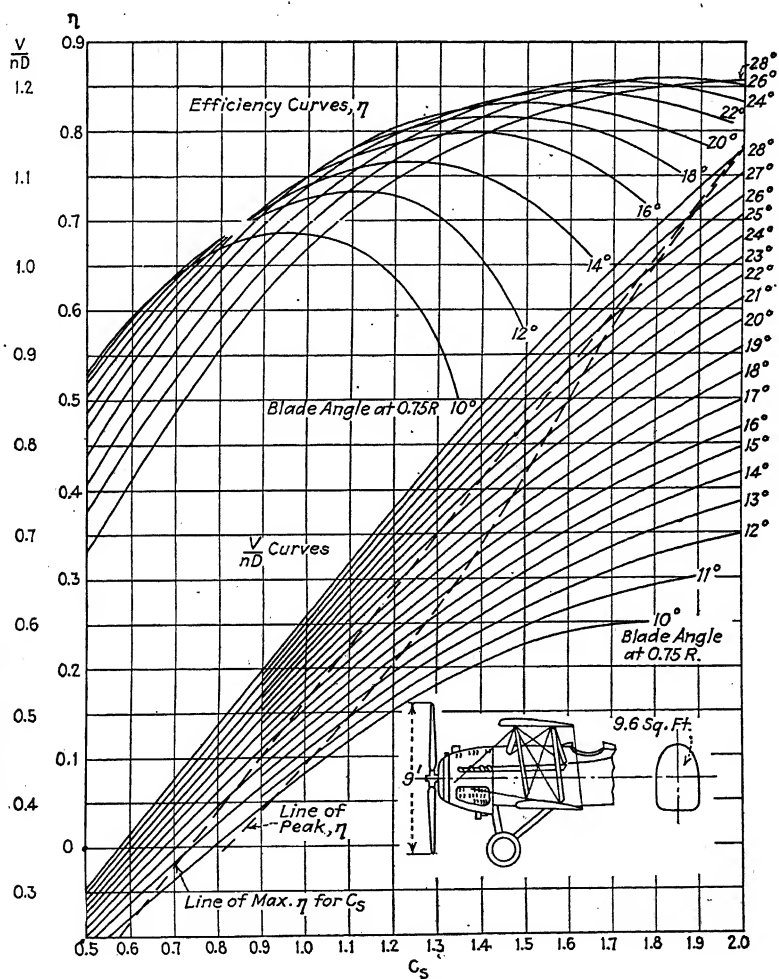


FIG. 167.—VE-7 open-cockpit biplane. Propeller 4412.

in operation is known. It is necessary only to consider the blade angles as those existing under operating instead of static conditions.

Although accurate deflection data covering a large range of powers, bodies, and propellers are not available, a useful approximate rule for direct-drive propellers similar to the design used in these tests has been based on the data obtained with the D-12 engine. This rule is that the working charts may be used without considering deflection in operation for powers up to 200 hp., but above 200 hp., the average blade angle increases at the

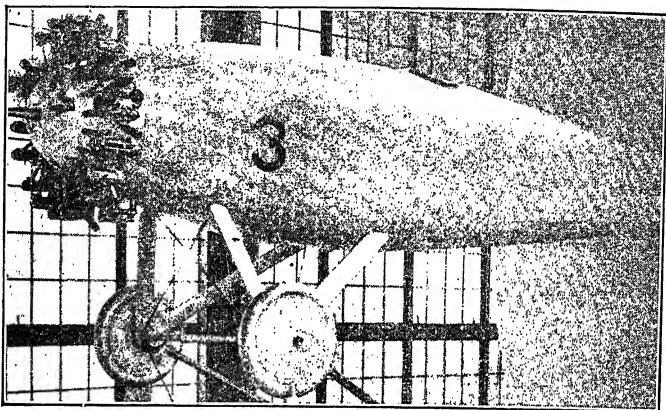


Fig. 168.—Open-cockpit fuselage with J-5 engine and conventional cowling. Maximum cross-sectional area of fuselage, 11.0 sq. ft. Data in Fig. 169.

rate of  $\frac{1}{2}$  deg. for each increase of 100 hp. This makes an increase of 0.5 deg. for an engine of 300 hp., 1.0 deg. for 400 hp., and 1.5 deg. for 500 hp.

This approximate rule has worked quite satisfactorily in selecting hundreds of direct-drive propellers to fit commercial airplanes. For propellers geared to run at one-half the engine revolutions the angular deflection is in the neighborhood of half as large.

*Use of Working Charts.*—In order to find the diameter and pitch setting of a propeller of this form for any particular set of operating conditions, it is merely necessary to

1. Calculate the value of  $C_s$  for the conditions under which the propeller is to operate.

2. Choose the pitch setting for the propeller operating at the desired portion of its efficiency curve (depending on the airplane performance desired) and the above  $C_s$ .



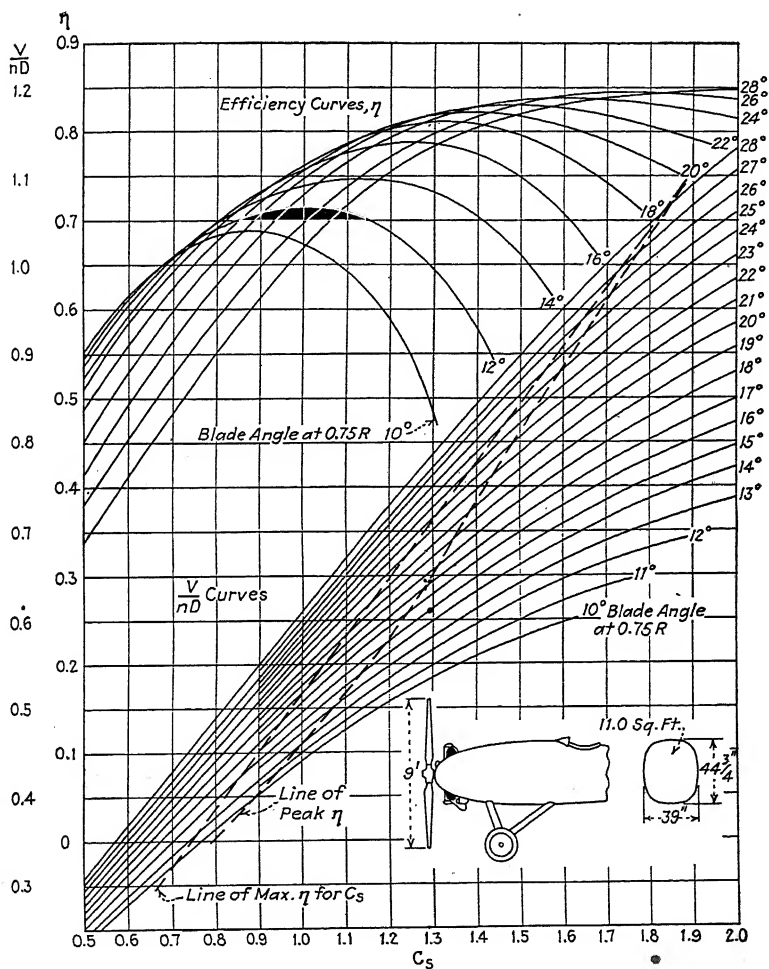


FIG. 169.—Open-cockpit fuselage with J-5 engine. Propeller 4412.

3. Find the  $V/nD$  for the above  $C_s$  and pitch setting, from the lower curves.

4. Knowing  $V/nD$ ,  $n$ , and  $V$ , calculate  $D$ .

If the diameter of the propeller is fixed to start with,  $V/nD$  is also fixed, and the pitch setting can be found directly from the curves of  $V/nD$  vs.  $C_s$ .

**Examples.**—Several typical examples showing the use of this system for the selection of propellers of this standard form are given here.

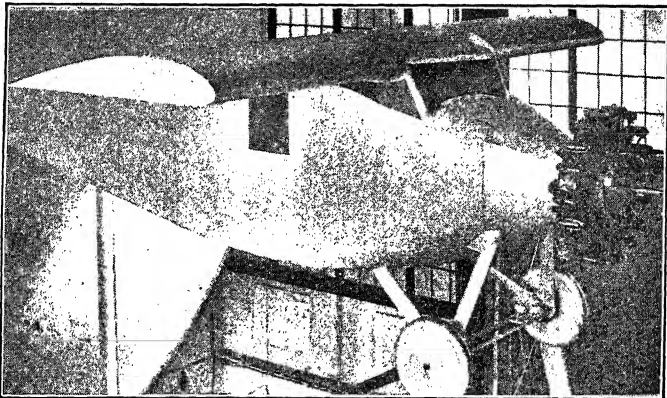


FIG. 170.—Cabin monoplane with J-5 engine. No cowling over cylinders or crankcase. Maximum cross-sectional area of fuselage alone, 21.3 sq. ft. Data in Fig. 171.

*Example 1.*—For our first example we shall select a propeller for a small open-cockpit sport airplane, with a conventionally cowled radial air-cooled engine, delivering 150 hp. at 2,000 r.p.m. The maximum speed expected is 115 m.p.h. High speed is of greater importance than the other performance characteristics, but a fair take-off is also desired.

First solving for  $C_s$ , we find that

$$\begin{aligned} C_s &= \frac{0.638 \times \text{MPH}}{\text{HP}^{1/2} \times \text{RPM}^{1/2}} \\ &= \frac{0.638 \times 115}{2.72 \times 21.0} \\ &= 1.29, \end{aligned}$$

the values of  $150^{1/2}$  and  $2,000^{1/2}$  having been obtained from Fig. 163.

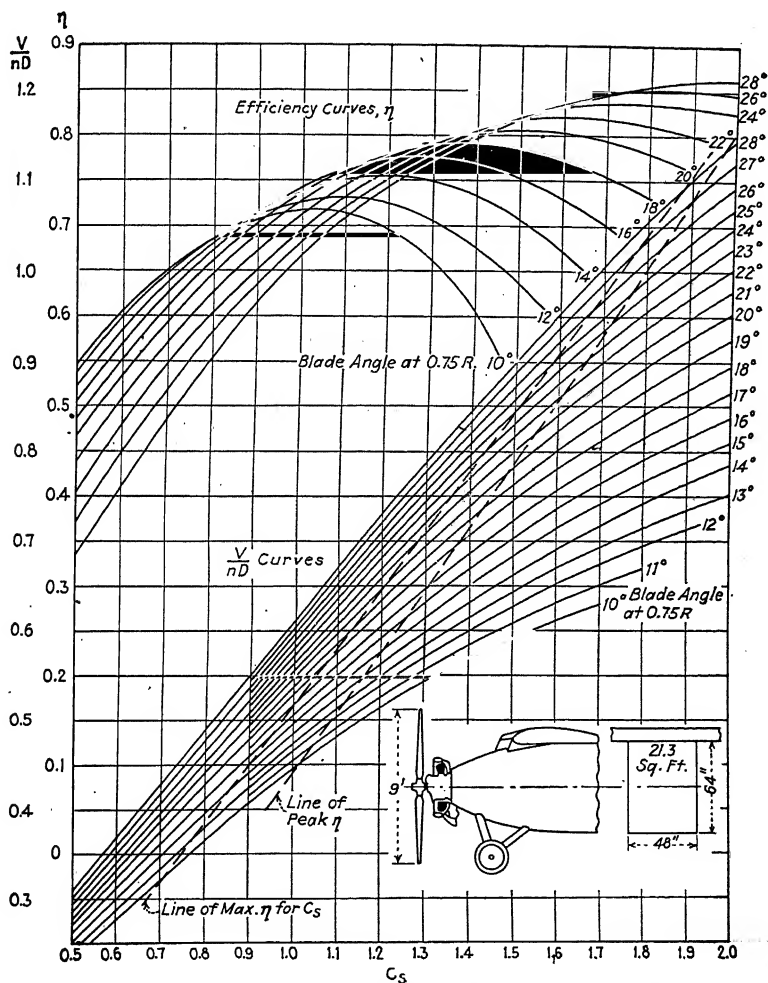


FIG. 171.—Cabin monoplane with J-5 engine. Propeller 4412.

Then from Fig. 169, which is the working chart based on body conditions similar to those specified, we find that the maximum possible efficiency, and therefore the highest speed, will be obtained for a  $C_s$  of 1.29 with a propeller operating at a  $V/nD$  of 0.705. This will, however, give a poor take-off, as was shown in the example in Chap. X. A good average take-off would be obtained with a propeller operating at the peak of its efficiency curve at the high-speed condition, but this would mean a slight sacrifice of speed. The  $V/nD$  for the propeller operating at

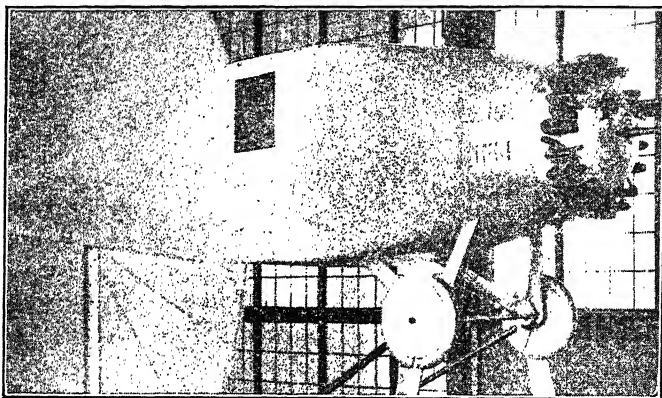


FIG. 172.—Cabin fuselage with J-5 engine. Large amount of conventional cowling, leaving only the top portions of the cylinder heads and valve gear exposed. Maximum cross-sectional area, 21.3 sq. ft. Data in Fig. 173.

the peak of its efficiency curve and at a value of  $C_s$  of 1.29 would be 0.645 (also from Fig. 169). Now it happens that with a propeller about halfway between these two the take-off will be very nearly as good as with the peak-efficiency propeller, while at the same time the maximum speed will be within all practical limits (about 0.1 m.p.h.) as high as with the best-speed propeller. We shall therefore choose a propeller with a maximum speed  $V/nD$  about halfway between 0.645 and 0.705, or 0.675. Then from Fig. 169 the blade angle at  $0.75R$  is 19.7 deg.

Knowing the  $V/nD$ , the revolutions, and the velocity,

$$\begin{aligned} D &= \frac{88 \times \text{MPH}}{\text{RPM} \times (V/nD)} \\ &= \frac{88 \times 115}{2,000 \times 0.675} \\ &= 7.50 \text{ ft.} \end{aligned}$$

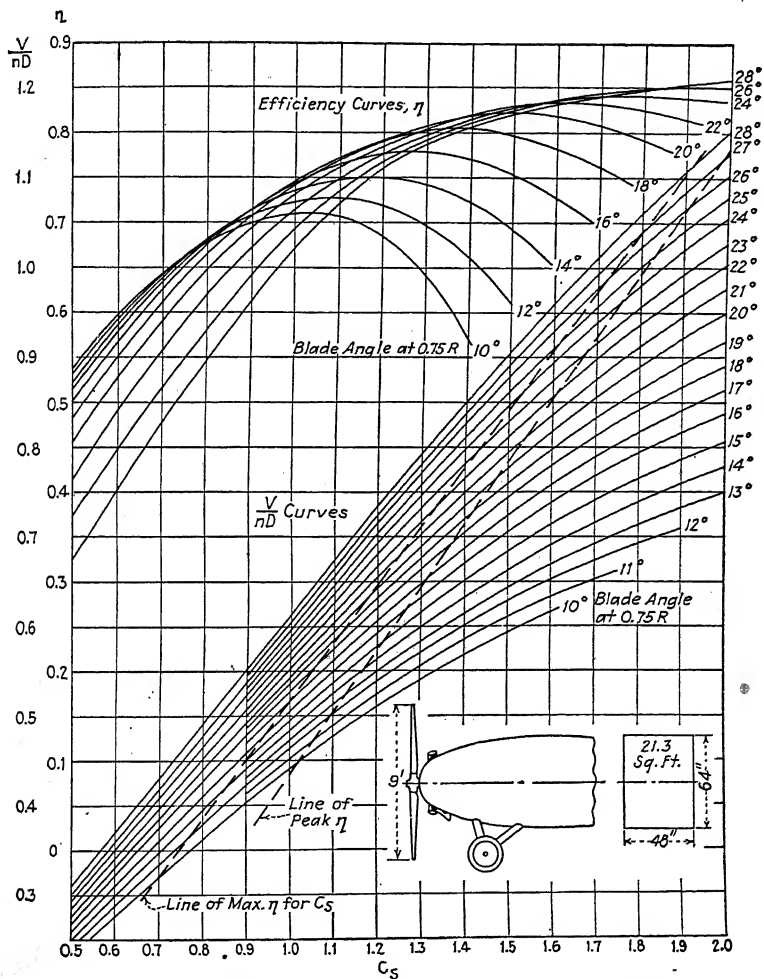


FIG. 173.—Cabin fuselage with J-5 engine. Propeller 4412.

Thus our propeller will have a diameter of 7 ft. 6 in., a blade angle of 19.7 deg. at 75 per cent of the tip radius, and from the upper curves of Fig. 169 the propulsive efficiency is 0.818 for the airplane without wings. With ordinary biplane wings this would be reduced, as shown in Chap. IX, to about 0.805.

Also, from Fig. 179 the weight with an average hub will be 35 lb., and from Fig. 178 the blade angle at the 42-in. radius, which is used as a standard,<sup>1</sup> is found to be 17.3 deg.

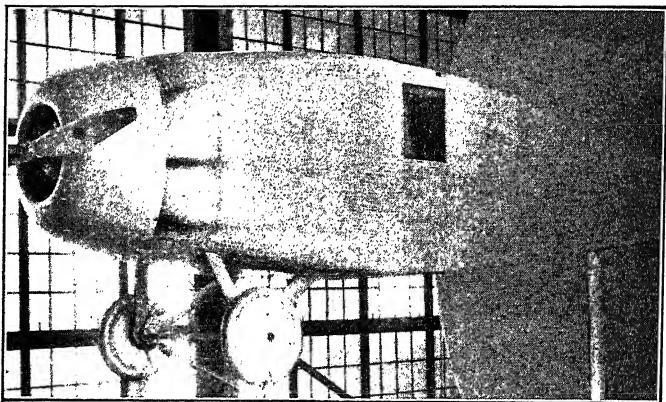


Fig. 174.—Cabin fuselage with J-5 radial air-cooled engine and N.A.C.A. type complete cowling. Maximum cross-sectional area 21.3 sq. ft. Data in Fig. 175.

If a propeller giving the best possible take-off and angle of climb were desired without a large sacrifice of high speed, a propeller of greater diameter and lower pitch would be selected. As shown by the example in Chap. X, a propeller with an angle setting 2 or 3 deg. lower than that of the propeller operating at the peak of its efficiency curve at maximum speed will give just about as good a take-off as can be obtained with any, while at the same time it represents about the limit in the low-pitch direction if a substantial decrease in high speed is to be avoided. Now from Fig. 169, the propeller operating at the peak of its efficiency curve at  $C_s = 1.29$  has a blade angle at  $0.75R$  of 17.4 deg. Our take-off propeller will therefore have an angle of, say,

<sup>1</sup> For propellers under 8 ft. in diameter it is better to use a smaller radius, preferably the even 6-in. station nearest  $0.75R$ .

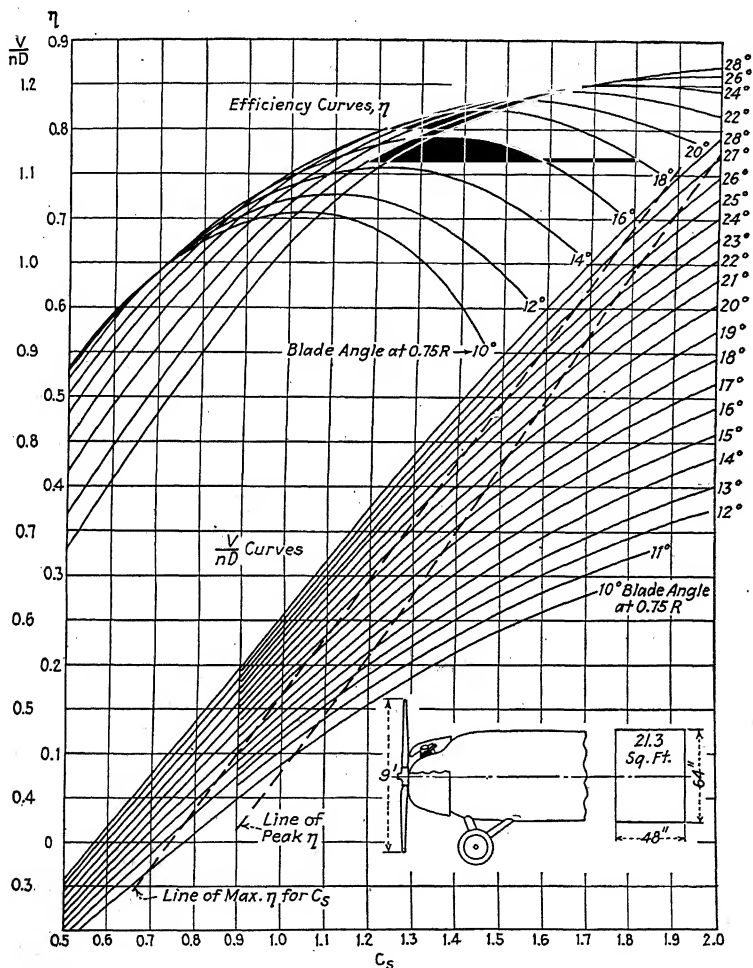


FIG. 175.—Cabin fuselage with completely cowled J-5 engine. Propeller 4412.

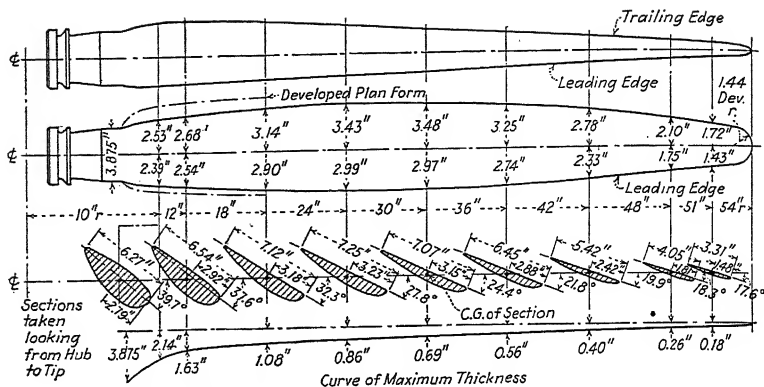


FIG. 176. Metal blade for 9-ft. diameter standard propeller 4412.

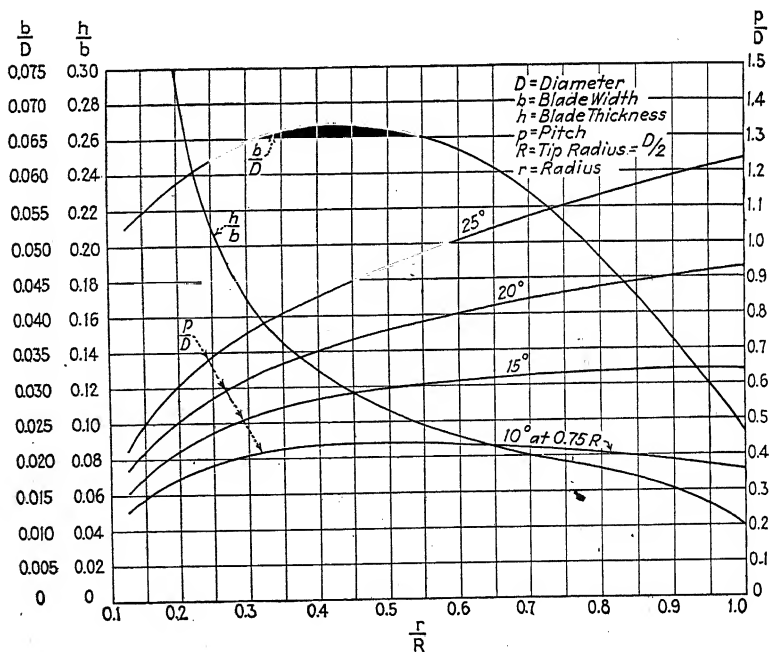


FIG. 177.—Blade-form curves for standard propeller.



15.0 deg. at  $0.75R$ , the  $V/nD$  (from Fig. 169) is 0.61, and the diameter is

$$D = \frac{88 \times 115}{2,000 \times 0.610}$$

$$= 8.30 \text{ ft.}$$

The propulsive efficiency at maximum speed is about 5 per cent less with this propeller than with the other, and if the maximum

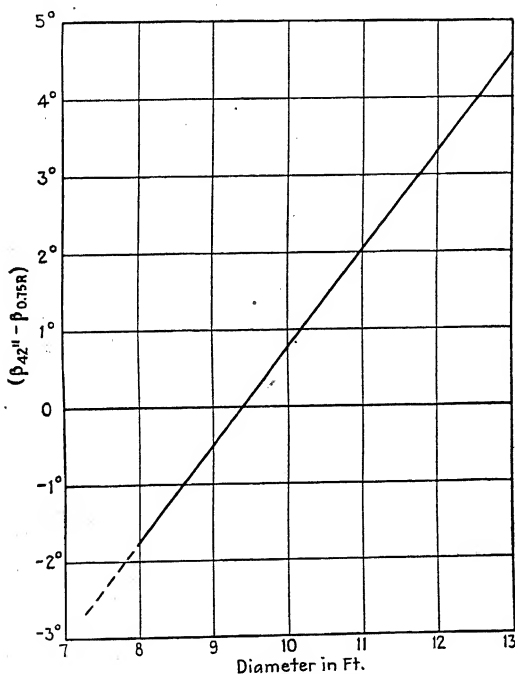


FIG. 178.—Difference between the blade angle at a radius of 42 in. and that at 75 per cent of the tip radius, for propellers of the form shown in Figs. 176 and 177.

speed of 115 m.p.h. is obtained with the first propeller, the speed with the take-off propeller would be about  $0.37 \times 5$  per cent = 1.9 per cent less (see Chap. X), or about 113 m.p.h. Using this maximum speed the value of  $C_s$  is 1.26, and for a blade angle of 15 deg. at  $0.75R$  the  $V/nD$  is 0.600, and the diameter is

$$D = \frac{88 \times 113}{2,000 \times 0.600}$$

$$= 8.30 \text{ ft.}$$

Thus a difference of only 2 m.p.h. does not make an appreciable difference in the propeller selected.

The tip speeds of these two propellers, as can be seen from Fig. 85, are both well below the critical speed of 1,000 ft. per sec., and so they will have no tip-speed loss and should be satisfactory in regard to strength.

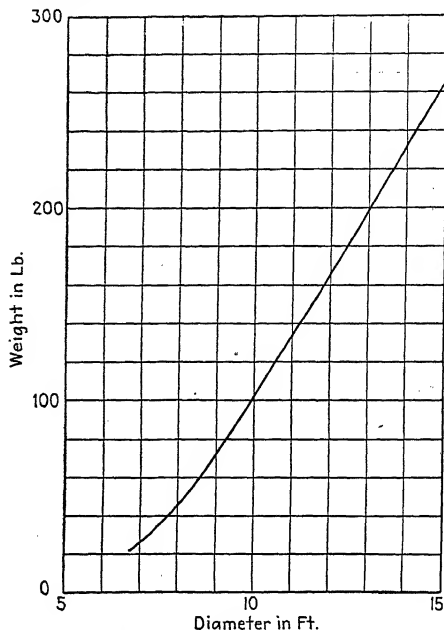


FIG. 179.—Approximate weights of two-bladed aluminum-alloy propellers of the form shown in Figs. 176 and 177; based on actual propellers with hub and blade root sizes most likely to be used.

*Example 2.*—A propeller is desired for a load-carrying transport monoplane having a maximum speed of 135 m.p.h. with an uncowled radial air-cooled engine delivering 575 hp. at 1,950 r.p.m. It is important that the airplane be given as short a take-off as possible as well as the highest possible cruising speed.

Solving for  $C_s$ , we get

$$C_s = \frac{0.638 \times 135}{3.57 \times 20.7} = 1.17.$$

Then from Fig. 171 we find that for the propeller operating at its peak efficiency at maximum speed, and this is about the best

compromise propeller giving both a good take-off and a good cruising speed, the  $V/nD$  is 0.557 and the blade angle at  $0.75R$  is 14.2 deg. The diameter is

$$D = \frac{88 \times 135}{1,950 \times 0.557} \\ = 10.93 \text{ ft.}$$

The tip speed of this propeller at maximum speed is 1,135 ft. per sec., the efficiency factor due to tip-speed loss is found from Fig. 83 to be 0.905, and the actual efficiency at maximum speed is  $0.759 \times 0.905 = 0.687$ . Although there is a 9.5 per cent tip-speed loss at high speed, at cruising speeds below about 119 m.p.h., the revolutions will be not over 1,720, the tip speed not over 1,000 ft. per sec., and there will be no tip-speed loss. The propulsive efficiency at cruising speeds will therefore be about 0.759. Also due to the fact that the revolutions are under 1,720 in take-off and in climb, there will be no tip-speed loss in those conditions. Since there is no tip-speed loss except at high speed, which is unimportant in a transport airplane, the propulsive efficiency is considered satisfactory.

The 575-hp. propeller will have a twist in operation increasing the average blade angle about  $1.9^\circ$ , so that when the propeller is not operating the blade angle at  $0.75R$  is  $14.2^\circ - 1.9^\circ = 12.3^\circ$ . Then, from Fig. 178,  $\beta_{42 \text{ in.}} - \beta_{0.75R} = 1.9^\circ$ , and the setting at the 42-in. radius is  $12.3^\circ + 1.9^\circ = 14.2^\circ$ .

The weight of this 10.93-ft. propeller, as shown by Fig. 179, would be about 131 lb. Actually, due to the fact that the tip speed is higher than the conservative limit of 1,000 and even slightly higher than the maximum safe limit found for a similar propeller in Chap. XV, it would undoubtedly be advisable to make the propeller somewhat heavier and stronger. In fact, the loading of this propeller is severe enough to warrant a careful overload whirling test.

*Example 3.*—In order to show the effect of altitude on the design system, we shall take as our next example a propeller for an airplane intended for high-altitude cross-country flying, and powered with a radial air-cooled engine having a gear-driven blower in the intake manifold, which gives a certain amount of supercharging. The engine thus equipped develops 400 hp. at 2,000 r.p.m. at a standard altitude of 8,000 ft. Above this altitude the power falls off in about the usual manner, as

shown in Fig. 114, while below it the engine may have to be partially throttled to avoid overstressing. We shall therefore, design the propeller to absorb 400 hp. at 2,000 r.p.m. and 8,000 ft. altitude, under which conditions the maximum horizontal speed is expected to be 170 m.p.h.

As was shown in Chap. X, we can write the engineering unit form of the equation for  $C_s$  as

$$C_s = \frac{0.638 \times MPH}{\left(\frac{HP}{\rho/\rho_0}\right)^{1/2} \times RPM^{3/2}},$$

where  $HP$  is the actual horsepower developed at the altitude being considered,  $\rho$  is the air density at that altitude, and  $\rho_0$  is the density of standard air at sea level. The ratio  $\rho/\rho_0$  can be obtained from Fig. 112, and for an altitude of 8,000 ft. we find that the value is 0.79. Then

$$\begin{aligned} C_s &= \frac{0.638 \times 170}{(400/0.79)^{1/2} \times (2,000)^{3/2}} \\ &= \frac{0.638 \times 170}{3.48 \times 21.0} \\ &= 1.48. \end{aligned}$$

We shall assume that this airplane has a large fuselage and that the engine is fitted with complete N.A.C.A. cowling, making the body conditions similar to those in Figs. 174 and 175. Assuming further that high cruising speed and rate of climb are the performance characteristics to be favored, we shall select the propeller halfway between that giving maximum possible speed and that working at the peak of its efficiency curve. From Fig. 175, the  $V/nD$  for this condition is about 0.80, the corresponding blade angle at  $0.75R$  is  $21.7^\circ$ , and the diameter is

$$\begin{aligned} D &= \frac{88 \times 170}{2,000 \times 0.80} \\ &= 9.35 \text{ ft.} \end{aligned}$$

The blade angle with 400 hp. is  $1.0^\circ$  greater in operation than for the static condition, and from Fig. 178 we find that  $\beta_{42 \text{ in.}} - \beta_{0.75R} = -0.1^\circ$ . The angle setting at the 42-in. radius is therefore  $21.7^\circ - 1.0^\circ - 0.1^\circ = 20.6^\circ$ .

The tip speed at maximum air speed is 1,006 ft. per sec., which is just about the maximum for no appreciable tip-speed loss and also for a conservative strength allowance.

*Example 4.*—Propellers having three blades can be satisfactorily selected with the working charts for two-bladed propellers by means of an approximate rule. A two-bladed propeller will always absorb just about 70 per cent of the power that a propeller having three of the same blades will absorb, regardless of the pitch or rate of advance. If we wish to select a three-bladed propeller to absorb a certain horsepower, we may therefore simply select a two-bladed propeller to absorb 70 per cent of this horsepower at the same speed and revolutions and then provide the same blades and settings for the three-bladed propeller. The efficiency of the three-bladed propeller will be about 3 per cent less at the peak and 4 per cent less in the climbing range than that of the hypothetical two-bladed propeller having the same blades.

To illustrate this method we shall find the proper three-bladed propeller for a seaplane having a water-cooled engine delivering 300 hp. at 1,800 r.p.m. and a maximum speed of 135 m.p.h. The airplane has a nose radiator similar to that shown in Fig. 166, but there is not sufficient clearance for a two-bladed propeller giving a satisfactory take-off. A general service propeller (one operating at the peak of its efficiency curve at maximum speed) is desired.

We shall select a hypothetical two-bladed propeller to absorb  $0.70 \times 300$  or 210 hp. The value of  $C_s$  for this propeller is

$$\begin{aligned} C_s &= \frac{0.638 \times 135}{2.91 \times 20.1} \\ &= 1.47. \end{aligned}$$

Then from Fig. 167, for the propeller operating at the peak of its efficiency curve at a value of  $C_s$  of 1.47, we find the  $V/nD$  is 0.740, the blade angle at  $0.75R$  is 19.0 deg., and the diameter is

$$\begin{aligned} D &= \frac{88 \times 135}{1,800 \times 0.74} \\ &= 8.92 \text{ ft.} \end{aligned}$$

Our three-bladed propeller will therefore have a diameter of 8.92 ft. The blades have the same loading as those of the two-bladed propeller which absorbs about 200 hp., and so the deflection in operation may be considered negligible. The actual blade angle at the 42-in. radius will be, from Fig. 178,  $19.0^\circ - 0.6^\circ = 18.4^\circ$ .

The efficiency at maximum speed will be about 3 per cent less than that of the two-bladed propeller, or  $0.97 \times 0.825 = 0.80$ .

The maximum tip speed is well below 1,000 ft. per sec., so that there is no tip-speed loss and the strength is satisfactory.

**Method of Using Charts for Propellers of any Form.**—As has been shown previously,<sup>1</sup> the blade section at  $0.75R$  best represents the average of the thrust- and torque-grading curves of most propellers. By considering that the section at  $0.75R$  represents the whole propeller, and then making allowances for the differences in width ratio, thickness ratio, and airfoil section between the  $0.75R$  section of the propeller in question and that of the standard propeller used for the charts, a fairly accurate approximate method is developed for using the charts for the selection of propellers of any reasonably conventional form. The plan form, taper in thickness, and pitch distribution are all of secondary importance, and the section at  $0.75R$  gives a good average for them all.

Any difference in blade-width ratio from that of our standard propeller (0.053) may be handled in the same manner as the problem of selecting a three-bladed propeller, which has been shown in the previous section. For differences in blade width up to about 20 per cent or so, it is permissible to assume that the power absorbed varies directly with the width ratio. Then if we wished to use the charts for a propeller having a width ratio of 0.06 to operate on an engine developing 200 hp., we should select a standard propeller for the proportionate power which it would absorb if it had the same diameter and pitch. The standard propeller would therefore be selected to absorb  $200 \times \frac{0.0530}{0.060}$

$= 177$  hp. If the difference in blade width is greater than about 20 per cent, the ratio of powers, and also the approximate effect on the maximum efficiency, can be obtained from Fig. 66.

If the thickness ratio of the airfoil section at  $0.75R$  is different from the standard value of 0.076, approximately the same effect may be produced by giving the standard propeller a different blade angle of such an amount that the aerodynamic pitches are the same. The thrust and power coefficients will then be very nearly the same over the range near maximum efficiency. This

<sup>1</sup> See also Propeller Design—I: Practical Application of the Blade-element Theory, by Fred E. Weick, N.A.C.A.T.N. 235, 1926.

is easily understood when it is recalled that the slope of the lift-coefficient curve *vs.* angle of attack is practically the same for all airfoil sections regardless of thickness. If plotted on a basis of the angle from zero lift, the lift curves will all lie in essentially the same place for the low and medium lift coefficients. The drag coefficients of course vary widely, but they are small and have only a very slight effect on the power absorbed by a propeller.

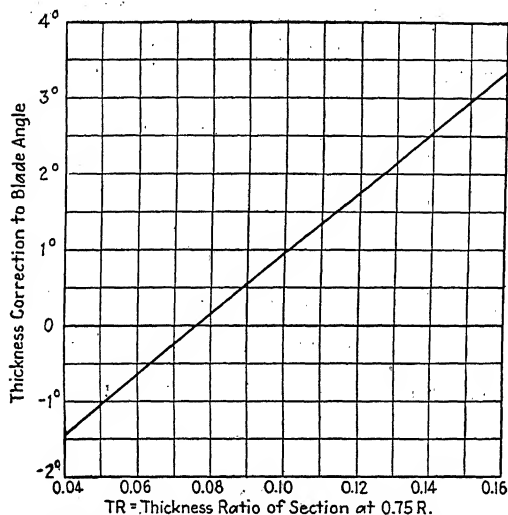


FIG. 180.—Correction to blade angle for section thickness ratio at 0.75R. Blade angle of standard propeller to be greater than that of special propeller by above amount. Suitable for R.A.F.-6 or Clark-Y type sections.

The angle of attack for zero lift can be obtained from airfoil tests made in wind tunnels, or they can be calculated with equal accuracy by means of a very simple method devised by Dr. Max M. Munk.<sup>1</sup> The corrections of the blade angle due to R.A.F.-6 or Clark-Y type sections of various thickness ratios may be found from Fig. 180.

The effect of different airfoil sections may be taken into account in the same manner as the different thickness ratios, *i.e.*, by considering only the difference between their angles of zero lift. Fortunately the two airfoils most commonly used in propellers in this country, the R.A.F.-6 and the Clark-Y types, happen to have the same angles of zero lift for sections of the

<sup>1</sup> The Determination of the Angles of Attack of Zero Lift and of Zero Moment, Based on Munk's Integrals, by Max M. Munk, N.A.C.A.T.N. 122, 1923.

same thickness ratio. Either section may therefore be replaced by the other without affecting the power absorbed.

All of the above factors apply to the power absorbed by the propeller, but not to the efficiency. The efficiency can usually be obtained with a fair degree of accuracy by using the efficiency of the standard propeller as a basis, the secondary factors being largely a matter of good judgment.

*Example 5.*—As an example of the design procedure showing the use of the charts with a propeller of different form, we shall assume a form having a width ratio of 0.062, a thickness ratio of 0.084, and Clark-Y type airfoils (for the propellers with which the charts were obtained,  $WR = 0.053$ ,  $TR = 0.076$ , and the sections were based on the R.A.F.-6). A general performance propeller is needed for a cabin monoplane having a maximum speed of 140 m.p.h. with an uncowed radial air-cooled engine developing 400 hp. at 1,900 r.p.m.

First considering the difference in blade widths, we shall select one of our standard propellers to absorb  $400 \times \frac{0.053}{0.062} = 342$  hp. at the above revolutions and air speed. For this the value of  $C_s$  is

$$\begin{aligned} C_s &= \frac{0.638 \times 140}{3.21 \times 20.5} \\ &= 1.36. \end{aligned}$$

From Fig. 171, for the propeller operating at the peak of its efficiency curve the  $V/nD$  is 0.688, the blade angle at  $0.75R$  is 17.9 deg. and the diameter is

$$\begin{aligned} D &= \frac{88 \times 140}{1,900 \times 0.688} \\ &= 9.43 \text{ ft.} \end{aligned}$$

Now from Fig. 180 we find that our special propeller having a thickness ratio of 0.084 will have a blade-angle setting 0.3 deg. lower than that of the standard propeller. No correction is necessary for the Clark-Y type airfoil. Our correction for twist in operation we shall take as being approximately the same as with the standard propeller, or  $1.0^\circ$  for 400 hp. The pitch distribution of the special form of propeller must be known in order to get the angle at 42 in. Assuming it to be the same as standard, we find from Fig. 178 that  $\beta_{42 \text{ in.}} - \beta_{0.75R} = 0^\circ$ . The



actual blade-angle setting of our 9.43-ft. special propeller will then be  $17.9^\circ - 0.3^\circ - 1.0^\circ + 0^\circ = 16.6^\circ$ .

The tip speed of this propeller is well below 1,000 ft. per sec., and so there will be no danger of tip-speed loss. While this also indicates that the strength will very likely be satisfactory, the safety should be assured by comparison with tests of other propellers of the same form or by special tests on the particular design to be used.

*Example 6.*—Let us now suppose we have on hand a 9-ft. propeller with a width ratio of 0.062 and a thickness ratio of 0.084 and that we wish to find the suitability of this propeller for the airplane in the above example. The value of  $C_s$  for a standard 9-ft. propeller will be the same as in the previous example, or 1.36, but since the diameter is now fixed the  $V/nD$  is also fixed at

$$\begin{aligned}\frac{V}{nD} &= \frac{88 \times 140}{1,900 \times 9.00} \\ &= 0.721.\end{aligned}$$

Now from Fig. 171, for  $C_s = 1.36$  and  $V/nD = 0.721$  we find that the blade angle at  $0.75R$  is  $20.0^\circ$ , and that the propeller is about halfway between that giving the highest possible efficiency and that operating at the peak of its efficiency curve. Thus the high speed, cruising speed, and rate of climb will be slightly better than with the all-around propeller, but the take-off and angle of climb a little poorer.

The blade thickness and twist corrections to the blade angle are the same as before, or  $0.3^\circ$  and  $1.0^\circ$ , respectively. For our 9-ft. propeller, assuming the standard pitch distribution,  $\beta_{42 \text{ in.}} - \beta_{0.75R} = -0.5^\circ$ . The blade angle at the 42-in. radius is therefore  $20.0^\circ - .3^\circ - 1.0^\circ - .5^\circ = 18.2^\circ$ .

*Example 7. Analysis of Flight Tests.*—It is often desired to analyze the results of flight tests made with one propeller in order to find the horsepower developed by the engine and to use this value for the design of another propeller. This is one of the best methods of finding the horsepower to use in designing a propeller to fit accurately a particular airplane, for any errors which may be in the design system will cancel out. For our example we shall find the power developed by a radial air-cooled engine in a full-throttle flight test in which it turned its propeller at 2,050 r.p.m., with the airplane, which was a cabin monoplane, making



# INDEX

## A

- Adjustable-pitch propellers, 221
- Aerodynamic tests on propellers, 82
- Aeron, 219
- Air, variation of density with altitude, 175
- Air-brake, variable-pitch propeller, 188
- Air-loading curves, 237
- Airflow through propeller, 77
- Airfoil, characteristics, compressibility effects, 28
  - effects of scale, 28
  - methods of plotting, 16
  - from propeller tests, 58
  - chart for, 61
  - plan form, effect of, 22
  - propeller, area of, 235
  - center of gravity of, 235
  - moments of inertia of, 235
  - section, effect on efficiency, 114, 255
  - effect with different pitch, 115
  - sections, Clark-Y vs. R.A.F-6, 115
  - suitable for propellers, 29
  - shape, effect of, 19
  - effect of lower camber, 21
  - position of maximum ordinate, 21
  - upper camber, 20
  - tests at high speeds, 119
  - theory, 23
- Airfoils, effect of high speed, 119
  - forces on, 13
  - pressure distribution over, 18
  - for propellers, 11
- Airplane performance, 249
  - effect of propeller characteristics, 159
- Airscrew, 2
- Airship propellers, 251
- Alferium, 219
- All-around performance propellers, 251
- Altitude, effect on airplane performance, 175
  - on design of propellers, 275
  - on engine power, 176
  - performance with supercharger, 178
  - relation with density, 175
- Aluminum-alloy propellers, erosion of, 224
  - etching of, 245
  - repair of, 224
  - weight of, 224
- Aluminum alloys, properties of, 219
- Analysis of flight test data, 281
- Angle of climb, best propellers for, 250
- Apparent efficiency, 140
- Approximate stress analysis, 234
  - example of, 234
- Area of R.A.F-6 propeller sections, 235
- Army tip, 214
- Aspect ratio, 3
  - effect, 65
- Attachment of wood blades, 225
- Automatic variable-pitch propeller, 228
- Axes, neutral, 231
  - principal, 231

## B

- Balance, 244
  - weights, variable-pitch propeller, 226
- Balances, test, 83
- Balancing, against master blade, 224

- Bearings, variable-pitch propeller, 225
  - Bending, moments on propeller blades, 230
    - theory of, 229
  - Birch, 215
  - Blade, angle, relation with pitch ratio, 94
    - deflection, 239
    - detachable, 221
    - elements, independence of, 79
    - interference, simple blade-element theory, 42
    - section, effect of, 114
      - on efficiency, 255
    - shape, effect of, 105
    - thickness, effect on efficiency, 254
    - twist, measurement of, 85
    - width, effect of, 111
      - on efficiency, 254
    - measure of, 110
  - Blade-element theory, comparison of forms of, 77
    - independence of elements, 38
    - induction or vortex theory, 64
      - check with tests, 77
      - direct procedure, 69
      - example, 74
      - Glauert's procedure, 69
      - limitations of, 72
      - tabular form, 76
    - modifications of, 51
    - with multiplane interference, 55
      - comparison with test data, 64
      - example, 59
      - limitations of, 57
      - tabular form, 63
  - résumé, 77
  - simple, 37
    - accuracy of, 43
    - comparison with test data, 48
    - example, 44
    - limitations of, 41
    - scale effect, 43
    - tabular form, 47
    - tip loss, 43
    - use in design, 282
  - Blades, choice of number, 252
    - number of, 112
  - Body, drag, effect on propulsive efficiency, 144
    - effect on airflow, 137
    - interference, 136
      - data, practical use of, 157
    - effect of body on propeller, 136
    - effect on efficiency, 255
    - effect of propeller on body, 138
    - size, effect on efficiency, 142
  - Boss, 3
  - Brake, horsepower, 160
    - effect of variable pitch, 184
  - state, 105
  - variable-pitch propeller, 188
  - Brass tipping, 214
  - Bushings, engine shaft, 219
- C
- Caustic soda, 246
  - Center of pressure, 15
    - chart of, 18
  - Centers of gravity of R.A.F-6 sections, 235
  - Centrifugal force, loads due to, 230
  - Charts, design type, 93, 99, 257
    - use of, 95
    - working, 257
    - examples, 266
    - use of, 264
  - Chrome-nickel steel, 221
  - Chrome-vanadium steel, 221
  - Clamp rings, hub, 223
  - Clark-Y airfoil, 33
    - propeller efficiency with, 115
  - Climb, best propeller for, 166, 249
    - calculation of rate of, 166
    - effect of pitch, 166
      - of propeller, 165
      - of reduction gearing, 195, 199
      - of variable pitch, 182
    - maximum, speed for, 166
    - metal *vs.* wood propellers, 168
    - tandem *vs.* side-by-side propellers, 209
  - Coefficient, power, 90
    - speed-power, 91
      - fifth root of, 92
    - use of in curves, 93
    - in design, 95

Coefficient, thrust, 87  
torque, 88  
Coefficients, airfoil, conversion factors for, 15  
basis of, 87  
lift and drag, 13  
propeller, 86  
Combined theory, 51  
application of, 52  
limitations of, 54  
Compressibility effect, 12, 119  
Consumption, effect of variable pitch, 186  
fuel, 173  
at cruising speed, 173  
Controllable-pitch propellers, 180  
construction of, 224  
Convex lower camber, 31  
effect on lift, 33  
Corrosion, protection against, 224  
Counterweights, variable-pitch propeller, 226  
Cracks, shown by etching, 246  
surface, effect on fatigue failures, 245  
Critical tip speed, 126  
chart for, 134  
Cross shear, 230  
Cruising speed, best propellers for, 250  
effect of propeller on, 172  
fuel consumption at, 173

## D

Damaged propellers, repair of, 224  
Data, working, from full-scale tests, 260  
Deflection, blade, measured, 239  
effect on stresses, 241  
in twist, 260  
approximate rule for, 264  
Design, with blade-element theory, 282  
charts, 93, 94, 99, 257  
examples, 266  
use of, 95, 264  
simple method, 258  
Destructive whirling tests, 247

Detachable-blade propellers, 221  
Diameter, front propeller of tandem series, 208  
limitations, 252  
propeller, 2  
rear propeller of tandem series, 205  
Disc area, effective, 53  
Distribution of pitch, 108  
best, 110  
effect of body, 155  
Downwash, 65  
angle, 23  
multiplane interference, 55  
effect on inflow, 51  
Drag, induced, 24  
equations for, 25  
profile, 24  
equations for, 25  
Drzewiecki theory, 37  
Duralumin, 219  
Dynamical similarity, principle of, 12

## E

Effective thrust, 141  
Efficiency, apparent, 140  
of blade element, maximum, 41  
simple blade-element theory, 40  
comparison of actual with ideal, 107  
correction for high tip speed, 130  
effect of airfoil section, 255  
axial interference, 68  
blade thickness, 112  
blade width, 254  
body interference, 140, 255  
high tip speeds, 123, 126, 128  
number of blades, 112, 254  
pitch, 106  
distribution, 108, 254  
ratio, 253  
plan form, 116, 255  
profile drag, 68  
propeller-wing interference, 151  
rotational interference velocity, 68  
scale, 118  
size, 117

Efficiency, effect of thickness ratio, 254  
tip speed, 255  
variable pitch, 183  
factors affecting, 253  
ideal, 7  
computation of, 7  
effect of diameter, thrust, and forward velocity, 9  
usefulness of, 8  
induction or vortex theory, 68, 73  
inflow theory, 54  
metal vs. wood propellers, 113  
methods of plotting, 93  
multiplane interference theory, 57  
net, 140  
propeller, 90  
propulsive, 141  
effect of body shape, 144  
of body size, 142  
of propeller location, 149  
tandem propellers, 203, 207  
various expressions for, 140  
with body interference, effect of pitch distribution, 155  
Eiffel logarithmic diagram, 97  
explanation of, 98  
use of, 100  
Element, blade, air forces on, 39  
Elements, blade, independence of, 38  
Endurance, flight, 174  
Engine power, effect of altitude, 176  
English coefficients, 89  
Erosion, by seaplane spray, 224  
Etching of propellers, 245

## F

Fabric sheathing, 216  
Failures, fatigue, 245  
photo of, 246  
of wood propellers, 246  
Fan, wind tunnel, 85  
cast aluminum alloy, 86  
Fatigue failures, 245  
photo of, 246  
strength, 213  
Filler blocks, for twisted-slab propellers, 220  
Finishing of blades, 224

Flight tests, analysis of data, 281  
on propellers, 82  
Flow through propeller, 77, 101  
measurements of, 102  
periodic nature of, 79  
Fluctuating air loads, 244  
Fluid, perfect, 11  
resistance, 11  
Flutter, 243  
Forging of blades, 223  
Form of a standard metal blade, 272  
Four-bladed propellers, when used, 253  
Frequency, natural, effect of size, 244  
Froude momentum theory, 5  
Fuel consumption, 173  
effect of variable pitch, 186  
Full-scale propeller tests, 85  
Fuselage, effect on air flow, 137

## G

Geared propellers, effect on static thrust, 196  
on weight, 193  
example, transport airplane, 191  
VE-7 airplane, 198  
factors affected, 190  
gyroscopic vibrations, 253  
when desirable, 200  
Gearing, with tandem propellers, 210  
Glauert theory, 64  
Glide tests, 82  
Gloster Hele-Shaw Beacham variable-pitch propeller, 228  
Governor, for variable-pitch propeller, 228  
Grading curves, integration of, 46, 48  
Grinding of blades, 224  
Gyroscopic forces, 229  
moments, effect of three blades, 253

## H

Hart variable-pitch propeller, 226  
Heath variable-pitch propeller, 227

Hele-Shaw Beacham variable-pitch propeller, 228  
 High speed, effect of airfoil section, 121, 130  
   effect on airfoil characteristics, 28, 120  
     on angle of zero lift, 121  
     on drag coefficient, 121  
     on lift coefficient, 120  
 propeller for, 97, 249  
   tandem *vs.* side-by-side, 209  
 section thickness, 121, 129  
 High tip speeds, 119  
   full-scale propeller tests, 126  
   model propeller tests, 121  
   practical corrections for, 130  
 Horsepower, maximum, 160  
 Hub, 3  
   detachable-blade propeller, 221  
     screw type, 222  
     split type, 223  
   drag, 78  
 Hubs, for micarta propellers, 216  
   split, 219, 222  
   for wood propellers, 216  
 Hydraulic variable-pitch propeller, 228  
 Hysteresis, 213

## I

Ideal efficiency, 7  
   computation of, 7  
   effect of diameter, thrust, and forward speed on, 9  
   usefulness of, 8  
 Inclined propeller axis, effect of, 162  
 Independence of blade elements, 79  
 Induced drag, 24  
   calculation of for rectangular plan form, 25  
   example, 26  
 Induction theory, 64  
 Inertia, forces, 229  
   moments of, 231  
 Inflow, 65  
   axial, 52  
   calculation of, 52  
   empirical factors for, 51

Inflow, rotational, 52  
   simple blade-element theory, 42  
   theory, 51  
     expressions for thrust, torque, and efficiency, 53  
     limitations of, 54  
 Information furnished designer, 257  
 Instantaneous velocity, 80  
 Interference, angle, 69  
   chart for solution of, 71  
   relation to downwash, 70  
 blade, downwash correction chart, 60  
   lift correction chart, 59  
 body, 136  
   effect of body on propeller, 136  
     of propeller on body, 138  
 data, practical use of, 157  
 effect on efficiency, 255  
 factor, effect on efficiency, 68  
   rotational, 66  
 flow, 52  
   axial, 69  
   calculation of, 65  
   chart for solution of, 72  
   definition of, 65  
   rotational, 66  
 propeller and wing, 151  
   extreme example of, 155  
 velocity, 80

## L

Laminations, metal propellers, 218  
   wood propellers, 213  
 Leitner-Watts propellers, 218  
 Lift coefficient, engineering, 14  
   English, 14  
   N.A.C.A., 14  
   coefficients, conversion factors for, 15  
 Lighter-than-air craft propellers, 251  
 Limitations of blade-element theories, 41, 54, 57, 72  
   to diameter, 252  
 Loading curve, air, 237  
   centrifugal force, 236  
 Loads on propeller blades, 229  
   calculation of, 232

Logarithmic diagram, Eiffel, 97  
 explanation of, 98  
 use of, 100  
 Longitudinal shear, 230  
 Lower camber, effect on airfoil  
 characteristics, 21

## M

Machining of blades, 224  
 Mahogany, 215  
 Major principal axis, 231  
 Master blades, 224  
 Maximum airplane speed, effect  
 of propeller, 163  
 of variable pitch, 181  
 horsepower, 160  
 revolutions, 160  
 Metal propellers, 217  
 efficiency of, *vs.* wood, 113  
 Micarta propellers, construction of,  
 216  
 strength of, 217  
 thickness of, 217  
 Minor principal axis, 231  
 Miscellaneous propeller forms, use  
 of design charts for, 278  
 Model propeller tests, pressure dis-  
 tribution, 49  
 propellers, 84  
 tests, correct scale for, 12  
 Moment coefficient, airfoil, 15  
 of inertia of R.A.F-6 propeller  
 sections, 235  
 Moments, bending, 230  
 of inertia, 231  
 twisting, 230  
 Momentum theory, 5  
 Multiplane effect, 42  
 interference, 55  
 chart for downwash correction, 60  
 chart for lift correction, 59  
 effect of lift, 56  
 of profile, 55  
 of solidity factor, 56  
 of spacing, 55

## N

Narrow-tip plan form, 117  
 Natural frequency, effect of size, 244

Navy tip, 214  
 Net efficiency, 140  
 Neutral axis, 231  
 Nitric acid, 246  
 Noise, effect of tip speed, 134  
 Nomenclature, 2  
 Number of blades, 112  
 choice, of, 252

## O

Oak, 215  
 One-piece forged propellers, 221  
 Outflow, 65

## P

Performance, airplane, 159, 249  
 all-round, propellers for, 251  
 effect of altitude, 175  
 with variable pitch, 180  
 Periods of vibration, 244  
 Pitch, definition of, 2  
 distribution, best, 110  
 effect, 108  
 of body interference, 155  
 on efficiency, 254  
 effect on efficiency, 105  
 on ideal efficiency, 107  
 on power, 108  
 on thrust, 108  
 effective, 3  
 experimental, 3  
 geometrical, 3  
 ratio, effect on efficiency, 253  
 relation with blade angle, 94  
 relation to speed-power coefficient,  
 107  
 variable, 180  
 Plan form, effect of, 116  
 on efficiency, 255  
 forms commonly used, 117  
 Polar diagram, 17  
 Power, accurate values for, 257  
 available, computation of, 161  
 effect of altitude, 176  
 of pitch, 163  
 of reduction gearing, 192  
 coefficient, 90  
 effect of tip speed, 127, 129  
 effect of pitch, 108



Power, excess, 166  
  required, 159  
    effect of altitude, 175  
Prandtl theory, 23  
Pressure distribution, over airfoils, 18  
  on model propeller, 49  
Principal axes, 231  
Profile lift and drag, 24  
Propeller gearing, 190  
  sections, based on R.A.F-6, 29, 30  
  test data, 260  
Propulsive efficiency, 141  
  effect of body size, 142  
    of body shape, 144  
    of propeller location, 149  
  factors affecting, 253  
Pusher arrangement, 4  
  effect on efficiency, 151

## R

R-type propeller, 220  
R.A.F-6 airfoil, efficiency with, 115  
R.A.F-6-type propeller sections, air-  
  foil characteristics of, 31-35  
  ordinates of, 30  
Racing airplanes, propellers for, 249  
Rain, erosion due to, 224  
Rake, 4  
  effect on stresses, 242  
Range, effect of propeller on, 174  
Rankine theory, 5  
Rate of climb, best propellers for,  
  249  
Rear propellers of tandem series, 201  
  diameter of, 205  
  effect of pitch, 204  
  efficiency of, 203  
Reed propellers, 220  
Repair of metal propellers, 224  
Resistance, fluid, 11  
Reversible-pitch propellers, use as  
  brakes, 188  
Revolutions, computation of for  
  various air speeds, 161  
  maximum, 160  
  reduction of by gearing, 190  
Reynolds number, 12  
  effect of, 28, 122  
  at high tip speeds, 126

Right-hand propeller, 4  
Rings, hub clamp, 223  
Root, blade, 3  
  standard for aluminum-alloy pro-  
    pellers, 223  
Rotation of slipstream, 202, 207  
Rotational velocity, computation  
  of, 66  
Run before take-off, effect of pro-  
  peller, 170

## S

Safety, structural, 255  
Scale effect, 117  
  terms of, 12  
Seaplane service, 224  
Selection charts, types, 93, 94, 99  
  use of, 95  
  of propellers, 257  
Shape of blades, effect of, 105  
Shear curve, 237  
Shearing forces, 230  
Sheathing, wood propeller, 214  
Side-by-side propellers, comparison  
  with tandem, 208  
Simple blade-element theory, 37  
  computation of efficiency, 40  
  of thrust, 39  
  of torque, 40  
  limitations of, 41  
Simple design method, 258  
Simpson's rule, 46  
Size, effect on coefficients, 117  
Slab, twisted propeller, 220  
Slip, function, 87  
  nominal, 87  
Slipstream, dissipation of, 104  
  effect on body drag, 139  
  measurement of, 102  
  size of, 102, 104  
  velocities, calculation of, 201, 206  
Solid forged propellers, 220  
Solidity factor, multiplane inter-  
  ference, 56  
Sound, velocity of in air, 119  
Special performances, propellers for,  
  251

Speed, accurate values of, 257  
 as affected by gearing, 191, 195, 198  
 cruising, 172  
 high, effect of on airfoil characteristics, 119  
 practical corrections for, 130  
 maximum airplane, effect of propeller, 163  
 of pitch, 164  
 propeller for, 249  
 variation with propulsive efficiency, 165  
 tandem *vs.* side-by-side arrangements, 209

Speed-power coefficient, 91  
 with altitude term, 177  
 use of, 91, 95

Split hubs, 219, 222

Splitting, of wood propellers, 247

Spray, erosion due to, 224

Standard form, use of, 258  
 metal blade, 272

Static balance, 244  
 thrust, 170  
 effect of variable pitch, 185

Steel propellers, 217  
 failures of, 218

Strength, 229, 255  
 fatigue, 213  
 of wood, 213

Stress, analysis, accuracy of, 232  
 approximate, 234  
 example, 234  
 effect of flutter, 243  
 of weaving, 244  
 when safe to apply, 245

Stresses, calculation of, 231  
 effect of deflection, 241  
 of rake or tilt, 242  
 variation with tip speed, 233

Strobometer, 79

Supercharged engines, 178  
 propeller requirements, 179  
 use with variable-pitch propellers, 187

Surface irregularities, effect on fatigue failures, 245

Sweepback of wood propeller blades, 247

Symbols, list of, xi

## T

Take-off, best propellers for, 250  
 effect of propeller on, 170  
 of pitch and diameter on, 171  
 of reduction gearing on, 196, 199  
 of variable pitch on, 184  
 of tandem *vs.* side-by-side arrangements on, 209

Tandem propellers, 201  
 air forces on rear propeller, 202  
 comparison with side-by-side, 198  
 diameter of front propeller, 208  
 effect of gearing, 210  
 efficiency of rear propeller, 203, 207  
 example calculations, 207  
 flow at rear propeller, 202, 206  
 model tests, 203  
 simple method of design, 206

Taper of blade, effect of, 116  
 on efficiency, 255  
 of plan form (airfoil), 23

Tensile force, 230

Terms, propeller, 2

Terne-plate tipping, 215

Test results, coefficients used, 86  
 methods of plotting, 86

Tests, model propeller, 83  
 on propellers, 82  
 flight tests, 82  
 whirling, 247

Theory, airfoil, 23  
 Glauert, 64  
 induction, 64  
 momentum, 5  
 Prandtl, 23  
 résumé of blade-element theories, 77  
 vortex, 64

Thickness, blade, effect of, 112  
 ratio, 112  
 angle correction for, 278  
 blade, 4  
 effect on efficiency, 254

Three-bladed propellers, use of design charts with, 277  
when used, 253  
Thrust, coefficient, 87, 89  
effect of high tip speed, 122, 124  
of pitch, 108  
effective, 141  
grading curves, 46  
comparison of calculated and measured, 78  
horsepower, computation of, 161  
induction or vortex theory, 67  
inflow theory, 53  
multiplane interference theory, 56  
simple blade-element theory, 40  
static, 170  
Tilt, 4  
effect on stresses, 242  
Tip, loss, 78  
simple blade-element theory, 43  
speed, computation of, 132  
corrections for efficiency, example, 132  
data, effect of pitch, 130  
effect of, 119  
on efficiency, 255  
model vs. full size, 126  
on noise, 134  
limiting value for allowable stress, 243  
loss, practical data, 130  
relation to stresses, 233  
Tip speeds, high, 119  
full-scale propeller tests, 126  
model propeller tests, 121  
Tipping of wood propellers, 214  
Torque coefficient, 88, 89  
effect of high tip speed, 123, 125  
gasoline engine, 160  
induction or vortex theory, 68  
inflow theory, 53  
multiplane interference theory, 57  
simple blade-element theory, 41  
Torsional deflection, 239, 260  
approximate rule for, 264  
vibration, flutter, 243  
Total width ratio, TWR, 4, 112  
Tractor, 4

Tractor, comparison with pusher, 151  
Turnbull variable-pitch propeller, 227  
Twist, propeller blade, 239, 260  
approximate rule for, 264  
measurement of, 85  
Twisted-slab propellers, 220  
Twisting moment due to centrifugal force, 226  
moments on propeller blades, 230  
Two-dimensional airfoil characteristics, use of, 65

## U

Upper camber, effect on airfoil characteristics, 20

## V

Variable diameter, 180  
Variable-pitch propellers, 180  
compromise diameter for, 187  
construction of, 224  
Hart, 226  
Heath, 227  
Hele-Shaw Beacham, 228  
Turnbull, 227  
effect on climb, 182  
on cruising economy, 186  
on efficiency, 183  
on engine power available, 184  
on speed, 181  
on take-off, 184  
use, as brake, 188  
with supercharger, 187  
Velocity of sound, 119  
Vibration, 244  
Vortex blade-element theory, 64  
limitations of, 72

## W

Wake, 65  
Wall effect, wind tunnel, 27  
Walnut, 215  
Warping, of wood, 213  
Weave, 243  
Weight, standard metal propellers 274  
Whirling tests, 247  
Wide-thin plan form, 117

- Speed, accurate values of, 257  
 as affected by gearing, 191, 195, 198  
 cruising, 172  
 high, effect of on airfoil characteristics, 119  
     practical corrections for, 130  
     maximum airplane, effect of propeller, 163  
     of pitch, 164  
     propeller for, 249  
     variation with propulsive efficiency, 165  
 tandem vs. side-by-side arrangements, 209  
 Speed-power coefficient, 91  
     with altitude term, 177  
     use of, 91, 95  
 Split hubs, 219, 222  
 Splitting, of wood propellers, 247  
 Spray, erosion due to, 224  
 Standard form, use of, 258  
     metal blade, 272  
 Static balance, 244  
     thrust, 170  
     effect of variable pitch, 185  
 Steel propellers, 217  
     failures of, 218  
 Strength, 229, 255  
     fatigue, 213  
     of wood, 213  
 Stress, analysis, accuracy of, 232  
     approximate, 234  
     example, 234  
     effect of flutter, 243  
     of weaving, 244  
     when safe to apply, 245  
 Stresses, calculation of, 231  
     effect of deflection, 241  
     of rake or tilt, 242  
     variation with tip speed, 233  
 Strobometer, 79  
 Supercharged engines, 178  
     propeller requirements, 179  
     use with variable-pitch propellers, 187  
 Surface irregularities, effect on fatigue failures, 245  
 Sweepback of wood propeller blades, 247  
 Symbols, list of, xi  
 T  
 Take-off, best propellers for, 250  
     effect of propeller on, 170  
     of pitch and diameter on, 171  
     of reduction gearing on, 196, 199  
     of variable pitch on, 184  
     of tandem vs. side-by-side arrangements on, 209  
 Tandem propellers, 201  
     air forces on rear propeller, 202  
     comparison with side-by-side, 208  
     diameter of front propeller, 208  
     effect of gearing, 210  
     efficiency of rear propeller, 203, 207  
     example calculations, 207  
     flow at rear propeller, 202, 206  
     model tests, 203  
     simple method of design, 206  
 Taper of blade, effect of, 116  
     on efficiency, 255  
     of plan form (airfoil), 23  
 Tensile force, 230  
 Terms, propeller, 2  
 Terne-plate tipping, 215  
 Test results, coefficients used, 86  
     methods of plotting, 86  
 Tests, model propeller, 83  
     on propellers, 82  
     flight tests, 82  
     whirling, 247  
 Theory, airfoil, 23  
     Glauert, 64  
     induction, 64  
     momentum, 5  
     Prandtl, 23  
     résumé of blade-element theories, 77  
     vortex, 64  
 Thickness, blade, effect of, 112  
     ratio, 112  
     angle correction for, 278  
     blade, 4  
     effect on efficiency, 254

- Three-bladed propellers, use of design charts with, 277
    - when used, 253
  - Thrust, coefficient, 87, 89
    - effect of high tip speed, 122, 124
      - of pitch, 108
    - effective, 141
    - grading curves, 46
      - comparison of calculated and measured, 78
    - horsepower, computation of, 161
    - induction or vortex theory, 67
    - inflow theory, 53
    - multiplane interference theory, 56
    - simple blade-element theory, 40
    - static, 170
  - Tilt, 4
    - effect on stresses, 242
  - Tip, loss, 78
    - simple blade-element theory, 43
  - speed, computation of, 132
    - corrections for efficiency, example, 132
    - data, effect of pitch, 130
    - effect of, 119
      - on efficiency, 255
      - model *vs.* full size, 126
      - on noise, 134
    - limiting value for allowable stress, 243
    - loss, practical data, 130
    - relation to stresses, 233
  - Tip speeds, high, 119
    - full-scale propeller tests, 126
    - model propeller tests, 121
  - Tipping of wood propellers, 214
  - Torque coefficient, 88, 89
    - effect of high tip speed, 123, 125
      - gasoline engine, 160
    - induction or vortex theory, 68
    - inflow theory, 53
    - multiplane interference theory, 57
      - simple blade-element theory, 41
  - Torsional deflection, 239, 260
    - approximate rule for, 264
    - vibration, flutter, 243
  - Total width ratio, TWR, 4, 112
  - Tractor, 4
    - Tractor, comparison with pusher, 151
    - Turnbull variable-pitch propeller, 227
    - Twist, propeller blade, 239, 260
      - approximate rule for, 264
      - measurement of, 85
    - Twisted-slab propellers, 220
    - Twisting moment due to centrifugal force, 226
      - moments on propeller blades, 230
    - Two-dimensional airfoil characteristics, use of, 65
- U
- Upper camber, effect on airfoil characteristics, 20
- V
- Variable diameter, 180
  - Variable-pitch propellers, 180
    - compromise diameter for, 187
    - construction of, 224
      - Hart, 226
      - Heath, 227
      - Hele-Shaw Beacham, 228
      - Turnbull, 227
    - effect on climb, 182
      - on cruising economy, 186
      - on efficiency, 183
      - on engine power available, 184
      - on speed, 181
      - on take-off, 184
    - use, as brake, 188
      - with supercharger, 187
  - Velocity of sound, 119
  - Vibration, 244
  - Vortex blade-element theory, 64
    - limitations of, 72
- W
- Wake, 65
  - Wall effect, wind tunnel, 27
  - Walnut, 215
  - Warping, of wood, 213
  - Weave, 243
  - Weight, standard metal propellers 274
  - Whirling tests, 247
  - Wide-tip plan form, 117